

FINAL REPORT

DEVELOPMENT OF A LONG LIFE THERMAL CELL

By

J. R. Moser
R. L. Blucher
D. Crouch

Prepared For

NATIONAL AERONAUTICS AND SPACE ADMINISTRATION

November 15, 1969

CONTRACT NAS 3-10932

TECHNICAL MANAGEMENT
NASA-LEWIS RESEARCH CENTER
CLEVELAND, OHIO
SPACE POWER SYSTEMS
WILLIAM NAGLE

CASE FILE
COPY

CATALYST RESEARCH CORPORATION
6101 Falls Road
Baltimore, Maryland 21209

FINAL REPORT

DEVELOPMENT OF A LONG LIFE THERMAL CELL

By

J. R. Moser
R. L. Blucher
D. Crouch

Prepared For

NATIONAL AERONAUTICS AND SPACE ADMINISTRATION

November 15, 1969

CONTRACT NAS 3-10932

TECHNICAL MANAGEMENT
NASA-LEWIS RESEARCH CENTER
CLEVELAND, OHIO
SPACE POWER SYSTEMS
WILLIAM NAGLE

CATALYST RESEARCH CORPORATION
6101 Falls Road
Baltimore, Maryland 21209

SUMMARY

This report is basically divided into two sections. That is, a section containing the experimental procedures and results, and another section containing the appendices. The first appendix shows typical performance curves resulting from the testing of many different parameters. In addition this appendix shows schematic diagrams and figures of the experimental apparatus used during this work. Appendix II presents a number of sample calculations indicating the mathematical procedure by which some of the results have been calculated. Appendix III gives a complete flow chart by which this long life thermal cell can be constructed and also gives complete instructions on the routing of materials. The quality control procedures and specifications for each component is given along with the proper sequence for applying the QC procedures.

The work described in this report was preceded by a more fundamental study under NASA Contract NAS 3-8517. That work concentrated on selecting the best composition of cupric oxide and/or cuprous oxide cathode material. In addition, cathode fabrication techniques were studied and experiments were conducted to arrive at an appropriate separator for this cell. The successful conclusions to that work indicated the use of cupric oxide in the form of a sintered needle compaction, and the use of a bulk Vitron E separator. The work described herein was initiated using the recommendations from the NASA Contract NAS 3-8517.

Initially this report describes the scale-up from the 14 ampere-hour cell used in NASA Contract NAS 3-8517 to a 50 ampere-hour capacity unit. This design described a cell using a magnesium anode, lithium chloride-potassium chloride eutectic electrolyte, and cupric oxide cathode. The design operating conditions for this cell consisted of an operating temperature of 427°C, a cyclic discharge of 278 milliamps for 54 minutes and 833 milliamps for 6 minutes repeated each hour. The desired nominal operating life was 150 hours.

The initial studies concentrated chiefly on the optimization of the cathode structure and its consequent electrochemical performance. Cathodes were fabricated with three copper needle sizes. The copper needle is in all cases 1/8" long, but 3 diameters were studied, namely 3 mil, 5 mil, and 10 mil diameters. It was found that 10 mil copper needles could not be thermally oxidized to 100% cupric oxide. In consequence only 3 mil and 5 mil copper needles could be used in fabricating the cathodes used for this subsequent electrochemical testing. Analysis of the electrochemical results indicated that the 3 mil copper needle electrodes gave a utilization of 72.8% while the 5 mil cathodes only gave a utilization of 66.1%. In addition to this, the 3 mil copper needle electrodes could be oxidized to cupric oxide significantly faster than those constructed with 5 mil copper needles. From that data, the 3 mil copper wire cathodes were selected to be used in further studies.

Cathodes were fabricated in three capacities to determine the input capacity necessary to give an output of 50 ampere-hours. The three capacities investigated were: 62.5, 71.5 and 83.5 ampere-hours. When the electrochemical results were plotted as input vs output capacity, a linear relationship was obtained but not in a 1:1 ratio. The results indicated that the higher capacity electrodes produced a lower utilization of materials. Considering the average deviations of these tests it was accepted that a 61 ampere-hour capacity electrode was required to produce the 50 ampere-hour output.

Since the fabrication technique and the capacity needed in the electrode have been determined and accepted, this electrode was studied further to apply appropriate quality control techniques for its controlled fabrication. Five quality control parameters were studied. These parameters were (a) bulk density, (b) BET surface area, (c) pore size distribution, (d) modulus of rupture, and (e) compression strength. Bulk density was the only non-destructive test considered, and consequently correlation between the other parameters and bulk density was desirable. The pore volume between 1 and 30 microns gave a good correlation with bulk density. The other three parameters showed little cor-

relation with bulk density. The BET surface area measurements gave very ill defined results due to their low surface area. From these studies it was determined that a bulk density of 3.18 to 3.38 grams per cubic centimeter was an acceptable cathode.

Separator studies were essentially of two types: Electrical testing and the effect of the separator on the cell discharge performance. Four different thicknesses of the separator were studied. The electrical testing essentially indicated that the resistance contributed by the separator was insignificantly low. On the basis of self discharge current and average life of the cells, the 1.5 centimeter thickness separator was accepted for further use.

Studies concerning the terminal seal used in this cell indicated that a ceramic insulator was necessary. In addition, a copper braze was necessary between the ceramic and the metal components of the seal. Nickel was used for all metal parts since it was inert in the electrolyte and easily welded to the nickel can. The terminal-to-case resistance over the operating temperature range of the cell was greater than 10^{14} ohms. By using the method of helium leak detection it was observed that thermal shock did not cause the seals to leak. Exposure of these seals to the cell components at its operating temperature for a period of 200 hours did not have any deteriorating effect on the seal. The Alite B50-1 terminal seal was selected to be used on the final design of these cells, since it was expected that this seal would offer more mechanical stability in future environmental conditions.

Twenty cells were constructed and subjected to various conditions of shock, vibration and acceleration. These tests resulted in having 70% of the anode connectors broken. Modifications were made to this cell to prevent this failure mode. Environmental tests with the modifications resulted in no mechanical failures in the cell. Subsequent electrochemical testing resulted in approximately 30% loss of the cell's normal life.

At this point in the work it could not be logically reasoned that the environmental testing caused this 30% loss of life. Two other possible efficiency loss modes could be envisioned. These consisted of possible high resistance shorting across the terminal seal causing a higher cell discharge rate or separator failure which would result in lost efficiency of the electrode materials. Cells were constructed and discharged utilizing three radically different seal constructions. The largest of three seals could not be evaluated in terms of the cell discharge characteristics since mechanical failures in the seal limited the length of the test. The discharge results that were obtained involving the other two seals showed no difference in the electrochemical performance. These results indicated that high resistance shorting across the terminal seal was not a significant problem and would not result in the decreased lives observed. Hesgon B woven glass cloth was selected as an alternate separator material. Five cells were constructed using this alternate separator material and the electrochemical discharge indicated an average deviation of 2.5 hours life. Due to the encouraging results from the 427°C tests, ten additional units were constructed. Five of these units were discharged at 371°C and the other five were discharged at 481°C. Reproducibility was good in all tests. The performance of the cells at 427°C and 481°C were essentially the same. The cells discharged at 371°C gave somewhat inferior performance as compared to the higher temperature test. Interpolation and minor extrapolation of the data indicates that these cells will operate efficiently between 400°C and 480°C.

The goals of the work statement having been successfully completed, 20 complete cells were constructed for delivery to NASA. Fifteen of these units were delivered to NASA and at NASA's instruction, five units were discharged at CRC. This data was sent to the NASA contract manager to serve as typical performance data for the other units delivered.

This final report presents in detail the work performed for NASA-Lewis during the past 28 months towards the successful development of a long life thermal cell.

TABLE OF CONTENTS

Summary -----	ii
Table of Contents -----	vi
Contract Objectives -----	vii
1.0 Introduction -----	1
2.0 Quality Control Program -----	2
3.0 Experimental and Design Studies -----	3
3.1 Design of Fifty Ampere Hour Cell -----	3
3.2 Cell Component Fabrication, Tests and Evaluation -----	5
4.0 Environmental Cell Tests -----	39
4.1 Control Cells -----	39
4.2 Environmental Tests -----	41
4.3 Environmental Cell Test Conclusions -----	43
5.0 Modifications for Solving Shorting and Environmental Problems -----	44
5.1 Preliminary Modifications to Eliminate Shorting -----	44
5.2 Work Alternate Flow Chart -----	45
6.0 Final Cell Design -----	53
7.0 Delivery -----	53
8.0 Summary of Accomplishments and Conclusions -----	53
9.0 Recommendations -----	55
10.0 Distribution -----	56
11.0 Appendices -----	65
Appendix I - Figures and Table of Cell Test Data -----	66
Appendix II - Sample Calculations -----	120
Appendix III - Quality Control, Flow Chart, Fabrication and Testing Procedures -----	123

CONTRACT OBJECTIVES

The research under Contract NAS 3-10932 is directed toward the development of a long life thermal battery using a magnesium anode, cupric oxide cathode, a separator and fused eutectic salt, 59 mole % LiCl and 41 mole % KCl, operating at 427°C. Component optimization and quality control characterization was to be determined to provide an easily constructed and high performance cell. The performance goal was to provide a cell that would operate for 150 hours at 278 ma for 54 minutes and 833 ma for 6 minutes each hour while maintaining a low current voltage no less than 0.5 volts.

1.0 Introduction

The objective of this program was to design, build and test a reliable fifty ampere-hour thermal cell. Cells were to be subjected to environmental and electrochemical performance tests to evaluate their capability and reproducibility. Components were to be evaluated singly and then incorporated into complete cells for further testing. Most cell tests were scheduled for evaluation at 427°C but a limited number were examined at 371°C, 481°C and 538°C to more fully explore the temperature capability of the cell. Finally, after the design weaknesses were corrected, a final design specification was prepared and twenty cells were delivered to NASA for evaluation.

Particular emphasis was placed on quality control procedures, tests, and inspection before as well as after building of components and during final testing.

2.0 Quality Control Program

Appendix III gives a complete quality control program for all steps developed simultaneously with experimental investigation of the cell components. The quality control complement is divided into three sections: Section A shows a flow chart for constructing the finished cell beginning with the raw materials and progressing through each assembly and inspection step to the finished unit; Section B gives the dimensional drawings of each component along with the inspection procedure for that piece; Section C sets forth the vendors, raw materials, chemical compositions and purity.

An original quality control program was submitted to NASA at the commencement of the program, which served to provide quality control at that stage of technology. Revisions and additions were made to the original program as they became defined and evident from the progressive experimentation.

Throughout this program CRC has inspected each cell component and completed cell to determine its compliance with the quality control specifications as developed at that time. Variable data were recorded for each cell where such data were necessary to determine the degree of reproducibility and uniformity from cell to cell.

All inspections were recorded and identified to each cell with serial numbers.

3.0 Experimental and Design Studies

3.1 Design of Fifty (50) Ampere-Hour Cell

3.1.1 Design Specifications

The basic design of the cell used in this work was to be taken from the 50 ampere-hour cell designed under NASA Contract NAS 3-8517. Each of the components used in the cell is shown in detail in the quality control plan in Appendix III. A cross-sectioned view, showing the parts location, is given in Figure 1.

The significant operating characteristics desired for a cell operating at 427°C were:

- (A) Nominal operating life --- 150 hours
- (B) Capacity --- 50 ampere-hours delivered over a 150 hour life
- (C) Initial open-circuit voltage --- 1.5 volt, minimum
- (D) Nominal duty cycle --- 0.278 ±0.5% amps for 54 minutes, followed by 0.833 amps ±0.5% for 6 minutes, with the cycle repeated each hour.
- (E) Peak voltage under load, nominal --- 1.2 volt, minimum
- (F) Current density --- 10-30 ma/cm²
- (G) Operating temperature --- 427°C design point, 371°C - 538°C service range
- (H) Construction type --- sealed.

As will be shown later, the proposed design has met all these specifications during static testing.

3.1.2 Discussion of Cell Design

Throughout this discussion refer to Figure I and to the appropriate figures in the quality control section in Appendix III.

The cell case used for all the cell tests is made of 0.050" grade A nickel. Nickel, as reported in literature and shown by our experimental tests, is essentially inert in a moisture-free LiCl-KCl environment. It has a high tensile

strength and is easily welded. Several hundred individual cell tests have demonstrated this material to be satisfactory for the cell case.

Vycor and ceramic terminal seals were studied and the ceramic seals show overwhelming superiority, primarily because of thermal shock resistance. Only one terminal seal is used on each cell. This seal provides electrical connection to the anode while providing electrical insulation between the anode and cathode. The cathode, being internally mounted against the cell case, is connected electrically by a nickel terminal which is electron-beam welded to the cell case.

The magnesium anode communicates with the terminal seal through a nickel connector. Past experimentation has shown that a reliable connection between the connector and anode can be made by threading the connector and screwing the anode onto it. The connector is also made from grade A nickel for the reasons mentioned earlier.

In the initial tests the separator was constructed from "Vitron-E", 1.5 cm thick. This thickness was optimum, as shown experimentally in a later section. It will also be shown that a glass tape separator is superior to the Vitron E material. The separator encases the anode and is retained by a nickel ring clamped into place. This method of separator connection is simple, convenient in construction and trouble-free in performance.

The most satisfactory method for adding electrolyte to the cell has proven to be a two-step method. The anode assembly is positioned and molded into a block of electrolyte. While the electrolyte is molten, sufficient time is allowed so that the separator is saturated and then the salt is cooled, molding the anode assembly into the salt block. The salt block is molded in a nickel can of such dimensions that the molded salt block will easily fit into the final cell case. If the separator is saturated without the support of the salt block, a network of fine cracks develops in the Vitron E material which substantially increases the average self-discharge current of the cell and shortens the cell life. After positioning the salt block and anode assembly into the cell case, the anode connector is hermetically fused to the terminal by electron-beam

welding. Electron-beam welding must be used on this cell since all the other welding methods examined produce enough heat to vaporize the electrolyte and prevent total sealing of the unit.

A grade A nickel cathode retainer ring is used to immobilize the cathode and to cause the cathode to fit snugly against the cell case. The final construction operation is to electron-beam weld the bottom on the case.

Electron-beam welding must be performed in a high vacuum and consequently the fully constructed thermal cell is evacuated. The quantity of electrolyte used is accurately weighed (tolerance ± 0.5 grams) to assure the complete filling of the cell in the molten state. The combination of evacuation and exact salt content results in an omni-positional operating cell.

3.2 Cell Component Fabrication, Tests and Evaluation

3.2.1 Electrodes

Anode

The anode used in the cell design is that specified by NASA in both composition and purity. The anode is composed of magnesium of the following purity specifications:

Mg	99.80% or greater
Total Al, Cu, Fe, Mn, Si, Ni	<0.20%
Cu	<0.05%
Ni	0.01%

Magnesium is purchased from the Dow Chemical Company as 12 inch rods, 1.54 inches in diameter.

As given in the contract directives, no development work was performed on the magnesium anode.

Cathode

Based on the results of NASA Contract NAS 3-8517, the cathode composition has been standardized at 99.8% cupric oxide, or better. The remainder of the cathode would be <0.2% cuprous oxide. The experimental evidence and discussion of this selection is given in NASA Final Report NASA CR-72361.

Cathode Fabrication Technique

This discussion describes cathode fabrication. Exact tolerances, purities and quality control are given in Appendix III, quality control.

The initial step in the fabrication of the cathode involves the cutting of pure copper wire into 1/8" lengths, using an automatic cutting machine. These cut needles are placed in a one piece glassrock mold (previously constructed) which has been lined with mica to provide a quick release. The assembly is placed in a furnace at 650°C for two hours to sinter the individual wires into a porous, sturdy structure. The sintered electrode is removed from the oven, cooled and extracted from the mold. The electrode structure is then placed back into the oven at 650°C, under a forced air stream at four liters per minute, for five days. The quantity of copper needles placed in the mold originally was weighed and the weight of the final resulting cupric oxide can be calculated. At the end of five days of heating, the electrodes are cooled and weighed. If the electrode weighs 99.8% or greater than the calculated figure, it is accepted for further quality control measurements. If the weight is too low, it is returned to the furnace for further oxidation. After the electrode has reached an acceptable weight, the thickness and diameter are measured at several spots on the electrode and its density is calculated. The decision to accept or reject the cathode is made at this point before the electrode is further considered for testing in a cell.

Copper Needle Size

The effect of the copper needle size on the ease of fabrication and on the physical and electrochemical properties of the cathode was studied.

Three different needle sizes were examined: 0.0032, 0.0055 and 0.010 inch diameters. Certain considerations were restrictive in deciding the range of needle diameters to be tested. The lack of commercial availability of copper wire less than 0.0032" diameter determined this as the lower limit. Experimental testing (see NASA report NASA CR-72361) has demonstrated that copper wire greater than 0.010" in diameter is extremely difficult to completely oxidize to cupric oxide. Consequently, these two practical limitations set the range of study. The 0.0055" diameter was selected as an intermediate size and because it is a commercially available stock item.

Five tests were run on each of the three needle sizes in normal laboratory cells of the same configuration as shown in Figure 1. All electrodes prepared in this study had a nominal capacity of 71.5 ampere hours. The cells were discharged at the nominal duty cycle specified in Section 3.1.1 in a 100% nitrogen environment at 427°C. The minimum desired life of a cell was 150 hours. Tests were terminated when the cell voltage declined to 0.5 volts under the low current load. All tests were run at a constant current and not a constant external load.

A number of possible variables were kept constant throughout these tests and are specified below.

- (A) Container material --- grade A nickel
- (B) Diameter of cathode --- 2.330 inches
- (C) Height of cathode --- 0.394 inches
- (D) Diameter of anode --- 1.540 inches
- (E) Height of anode --- 0.633 inches
- (F) Spacing between electrodes --- 1.23 inches
- (G) Thickness of Vitron-E separator --- 0.59 inches
- (H) Total volume of electrolyte at 427°C --- 217.2 cm³
- (I) Anode connector material --- grade A nickel
- (J) Terminal seal --- ceramic, Alite D-312

Before and after each test the cells were examined by X-ray to determine the proper placement of parts and to aid in solving problems that became evident during the electrochemical tests. In several cases the X-ray analysis technique provided the only information that indicated the necessary modifications to improve the cell performance.

The analysis of the electrochemical data for the three needle sizes is given in Table 1, Appendix I. The cell test numbers using the 3 mil wire in the cathode are 258, 259, 270, 271 and 272; using the 5 mil wire they are 262, 274, 281, 286 and 282; and using the 10 mil wire they are 268, 275, 276, 278 and 279. Figures 2-4 show the voltage versus time traces for these cathodes. The three needle sizes examined are conveniently referred to as 3, 5 and 10 mil diameters, but the actual diameters were 3.2, 5.5 and 10 mils, respectively.

The 10 mil needles are very difficult, if not impossible, to completely oxidize to cupric oxide by a heating process. The extent of the oxidation appears to be sensitive to the manner in which the needles are positioned in the mold. The non-uniform oxidation of the needles makes any quality control procedure most difficult to be applied meaningfully. In all cases the 10 mil needles had still not been converted to >99.8% CuO after heating for over 300 hours. Additional heating did not cause the electrodes to gain any further weight. Analysis of these electrodes also indicated that no residual metallic copper remained in the electrode structure. Consequently, it would be safely assumed that the electrode was composed of a mixture of cupric and cuprous oxides. On the basis of the initial weight of copper in the electrode and the final weight of the oxidized electrode, the percent composition of each specie in the electrode and its coulombic capacity could be calculated. The results of these calculations are shown in Table 1 for the five 10 mil cathodes tested.

Table 1

Capacity and Percent of CuO and Cu₂O in 10 mil Cathodes

<u>Test Number</u>	<u>% CuO</u>	<u>% Cu₂O</u>	<u>Cathode Capacity (Amp-Hrs)</u>
268	78.3	21.7	62.9
275	45.7	54.3	51.1
276	38.0	62.0	47.9
278	69.3	30.7	59.6
279	64.9	35.1	58.0

Due to their overall poor qualities in electrochemical performance, poor reproducibility and incomplete oxidation to cupric oxide, this needle size (10 mil) was eliminated as a material for fabricating cathodes. The voltage vs time traces at constant current are shown in Figure 4.

Table 2 shows a comparison of the average values for the five runs for each of the three needle sizes and the average deviation from the mean.

Table 2

Average Data Comparison for Different Needle Sizes

Needle Size (Mils)	Avg. Life (Hrs)	Avg. Cathode Utilization %	Avg. Self- Discharge (ma)
3	153.4 ±23.1	72.8 ±10.4	51.7 ±29.9
5	142.6 ± 8.9	66.1 ± 5.0	87.7 ±22.6
10	103.0 ±13.7	64.1 ± 3.3	21.0 ± 6.2

The 3 mil and 5 mil needle cathodes are similar in electrochemical performance as is seen in Figures 2 and 3 respectively. The 3 mil needle cathodes indicate a slight superiority over the 5 mil needle electrodes. In addition the fabrication of the 3 mil needle cathodes is quicker since it requires only about 75% of the time necessary for the 5 mil needles to oxidize to an acceptable cupric oxide composition.

Table 2 shows the relative performance of the three needle sized cathodes. Overall, the electrochemical performance favors the choice of 3 mil needle cathodes. The average deviations show that no statistical advantage is present in electrochemical performance for either the 3 or 5 mil needle sizes. However, examination of the individual tests shows that three of the 3 mil tests ran for over 150 hours, whereas only one of the 5 mil tests exceeded this life. Similarly these three 3 mil tests had cathode utilizations greater than 70%, but only one 5 mil test exceeded this utilization. Individual tests for the 3 mil needle cathodes shows three tests where the average self-discharge current (I.s.d.) are <35 ma while for the 5 mil needle cathodes they do not show any tests less than 35 ma for the same factor. The self-discharge current, however, is probably more dependent upon the reproducible application of the separator than on the needle size used in the cathode.

Considering the electrochemical performance and ease and reproducibility of construction, the 3 mil copper needles were selected to be used in the succeeding experiments.

Cathode Capacity Study

The object of this testing was to determine the cathode capacity required to deliver fifty (50) ampere-hours at 427°C over a 150 hour period when discharged at the nominal duty cycle specified in Section 3.1.1.

For these tests, cells were fabricated as shown in Figure 1, using 3 mil copper needles in fabricating the cathodes. The data from the 3 mil needle cathodes were reviewed to determine the approximate input cathode capacity needed to deliver 50 ampere-hours output. Table 2 indicates an average cathode utilization of approximately 68 ampere-hours would be necessary. By invoking the average deviation, a range of cathode input between approximately 61 to 80 ampere-hours appeared appropriate for testing. The two capacities selected for further testing were 62.5 and 83.0 ampere-hours.

The anode capacity used had a capacity 20% greater than that of the cathode so that the cell would necessarily be limited by the cathode.

Ten cells of acceptable performance were tested in two series of five cells. One series of tests used a 62.5 ampere-hour capacity cathode; the other used 83.5 ampere-hour cathodes.

Table 1, Appendix I gives the collected and calculated data for the 62.5 A-Hr electrodes. These tests are numbered 300, 301, 304, 309 and 316. Similarly, for the 83.5 A-Hr electrodes, they are numbered 294, 296, 297, 306, and 307. The voltage vs. time curves for the 62.5 ampere-hour cathodes are shown in Figure 5 and for the 83.5 ampere-hour cathodes in Figure 6.

After considering the reproducibility and average of the results for the 71.5 ampere-hour cathodes, it became apparent that these quantities were much higher than expected. Several additional cells of this capacity (71.5 A-hrs) were constructed and tested. These tests were numbered 317 and 319 and the results are given in Table 1, Appendix I. The voltage vs time curves for these two tests are shown in Figure 7.

In each cathode-capacity series it can be observed that one run stands out as not being part of the main group of data. Each of these tests were dropped when calculating the group averages and average deviations. On this basis the data for each cathode capacity series were calculated and are shown in Table 3.

Table 3*

<u>Average Data Comparison for Different Cathode Capacities</u>			
<u>Avg. Cathode Capacity (Amp-Hrs)</u>	<u>Avg. Cell Life (Hrs)</u>	<u>Avg. Cathode Utilization (%)</u>	<u>Avg. Cell Output (Amp-Hrs)</u>
62.47 ±0.15	157.7 ± 3.2	84.37 ±1.73	52.7 ±1.1
71.55 ±0.10	169.3 ±12.9	79.09 ±6.11	56.7 ±4.6
82.87 ±0.05	188.2 ± 2.8	75.86 ±1.16	62.9 ±0.9

*Average of four cells in each cathode capacity series.

If the average cathode input capacity is plotted against the actual cell output in ampere-hours, it is seen in Figure 8 that a straight line relationship exists. The design point for the cathode was a 50 ampere-hour output. The testing did not encompass this value but the lowest cathode output capacity was only greater by 2.7 ampere-hours. Extrapolation of the curve to the design point (50 ampere-hours output) indicates that a 57.1 ampere-hour cathode input is required. However, considering also the average deviations experienced on these tests, a cathode input capacity greater than 57.1 ampere-hours would be required to guarantee a 150 hour life at the nominal duty cycle. To meet this running time specification of the cell reliably a nominal 61.0 ampere-hour cathode capacity input was chosen.

It is instructive to note in Figure 9, where the cathode input capacity is plotted against the percent cathode utilization, that the percent utilization decreases markedly as the cathode capacity increases. The only variable allowed to fluctuate during the preparation of the cathodes is its height. That is to say that the height of a higher capacity cathode will be greater than lower capacity cathodes. In view of this, the trend in Figure 9 is quite reasonable for at least two reasons:

- (A) Reaction products, such as Li_2O , are trapped in the cathode pores and cannot diffuse to the bulk electrolyte rapidly enough to prevent freezing of the electrolyte in the electrode.
- (B) Electrolyte diffusion into a thick cathode is too slow and the deeper parts of the cathode become electrolyte starved.

Both of these reasons may be ramifications of the same principle. This data indicates that the thinnest possible cathode structure would be most desirable to attain high cathode utilizations resulting in a lighter weight cell.

Physical Properties of Cathodes

At this stage of the work, the most advantageous copper needle size (3 mil) had been selected for the cathode fabrication and the proper cathode input capacity had been determined (61.0 ampere-hours) to deliver a 50 ampere-hour cell output. Definition of the physical properties of the cathode was begun so that a quality control procedure could be applied to the cathode fabrication. As shown in the quality control program in Appendix III, the diameter of the cathodes was controlled in all tests. The height, and consequently the bulk density, was allowed to vary according to the normal fabrication method. Every cathode manufactured, however, had its thickness and density measured and recorded as standard practice. The physical property testing discussed below is an attempt to define appropriate parameters that will result in reproducible cathode fabrication.

Five different physical properties were selected for study:

- (A) Bulk density
- (B) B. E. T. true surface area by N_2 adsorption
- (C) Pore size distribution by Hg intrusion
- (D) Modulus of rupture
- (E) Compression strength.

Each of these tests is discussed more fully below.

Bulk Density

Ten (10) cathodes of a nominal 61.0 ampere-hour capacity were constructed by the normal fabrication technique described earlier and in Appendix III. No extraordinary precautions were taken during fabrication since these tests were meant to define the normal fabrication limits during the construction. The maximum and minimum diameters and heights of each electrode were measured with caliper and micrometer and an average height and diameter was recorded. The electrode was weighed on an analytical balance to ± 1 mg. The calipers used are able to measure to 0.001". The numbers were used to calculate the bulk density of each cathode. The results of these calculations are shown in Table 4.

Table 4

Density Variation of 61 Ampere-Hour Cathodes

<u>Electrode Number</u>	<u>Cathode Capacity (Amp-Hrs)</u>	<u>Density (GMS/cc)</u>
1	61.27	3.26
2	61.11	3.37
3	61.13	3.47
4	61.13	3.28
5	61.27	3.18
6	61.33	3.20
7	61.06	3.37
8	61.27	3.14
9	61.13	3.23
10	61.06	3.29

The average density and average deviation calculated from Table 4 is, respectively, 3.28 ± 0.08 g/cc. Probably a more acceptable measure of precision is the standard deviation of a single point (σ), defined as $\sigma = (\sum D_i^2 / (N-1))^{1/2}$, where D_i is the deviation of the point from the arithmetical mean and N is the number of samples measured. On this basis ± 1 sigma will encompass

approximately two-thirds of the measured samples. One sigma for this set of measurements is 0.10 grams/cc indicating that any electrodes fabricated with densities outside the range 3.18-3.38 should be rejected.

B. E. T. Surface Area

The second technique examined to define quality control tolerances for the CuO cathode was to measure their surface area by the Brunauer, Emmet and Teller gas adsorption (B. E. T.) method. The same ten samples that were used for the bulk density determination were sent to the Coors Spectrochemical Laboratory in Golden, Colorado for this study. Approximately 2-3 gram samples were taken from the electrode and de-gassed under a high vacuum at room temperature for 24 hours. The adsorbed gas used was nitrogen. After the pre-treatment, the surface area determination was conducted and the results are shown in Table 5. The electrode numbers correspond directly to those in Table 4.

Table 5

B. E. T. Surface Areas of Cathodes

<u>Electrode Number</u>	<u>Surface Area Meters²/GM</u>
1	0.03
2	0.03
3	0.02
4	0.04
5	0.03
6	0.01
7	0.04
8	0.01
9	0.05
10	0.03

Comparison of the data of Tables 4 and 5 indicates that a rough correlation exists between these two parameters. However, the data are so scattered that a quality control measure cannot be derived from it. The surface

areas of the CuO cathodes are so low that they approach the minimum sensitivity of the B. E. T. method. This method was useful in determining the magnitude of the electrode surface area but appears to be a poor criterion for quality control of the electrode fabrication.

Pore Size Distribution

Since the cathodes are fabricated from thin copper wires sintered together, the resulting CuO electrode is very porous, approximately 47-50 percent of the cathode volume being due to pore volume. The method of fabrication would also suggest that a range of pore sizes would exist but that a predominant range of pore sizes would be experienced in which the majority of the pore volume would reside. On a physical basis, it would seem that an electrode composed of relatively large pore sizes would perform well since diffusion of reaction products away from the electrode and free electrolyte into the electrode would be faster.

To define our cathode more closely in this respect, ten (10) cathodes of a nominal 61 ampere-hour capacity were supplied to the American Instrument Company, Silver Spring, Md. to determine their pore size distribution by mercury intrusion. Several preliminary pore-size distribution tests were made to determine whether the mercury would amalgamate with the CuO. These tests showed no evidence of the Hg affecting the CuO through the duration of the measurement. The samples for these tests were taken out of the exact center of the electrode and weighed 1.3 to 1.5 grams. A typical result of these tests is shown in Figure 10 and some data calculated from these curves are given in Table 6.

Table 6

<u>Percent Pore Volume Between 1 and 30 μ</u>		
<u>Electrode Number</u>	<u>% Pore Volume 1-30 μ, (cc)</u>	<u>Bulk Density (GMS/CC)</u>
27	54.3	3.22
23	56.6	3.00
29	66.8	3.21
24	68.6	3.22
33	72.3	3.27
34	72.3	3.43
22	74.3	3.29
31	74.6	3.38
32	79.4	3.20
30	81.0	3.18

The calculated average of the pore volume between 1 and 30 microns is 70.0% of the total pore volume. One standard deviation (σ) for an individual determination is 5.9%. Accepting the deviation of $\pm\sigma$ as a usable cathode, this sets the quality control range of cathode acceptance between 64.1 and 75.9% of the total pore volume existing between 1 and 30 μ pore diameters.

In previous discussion it was seen that good correlation is present between acceptable bulk density range and the pore volume between 1 and 30 μ . Table 6 shows that electrodes 27, 32 and 30 would be rejected on the basis of bulk density. These same electrodes plus number 23 would be rejected on the basis of pore volume. Electrode 23 is at the lowest limit of acceptance on the bulk density basis. It appears that electrodes being accepted from bulk density tests will also be acceptable from the pore size measurement determinations.

Referring to the typical curve in Figure 10 it can generally be observed that steep sloping sections are present for each pore size determination. The slope at any point on the curve, i.e., the change of pore volume per decade of pressure, is directly related to the number of pores of a specific diameter. A plot of the slope vs the pore diameter, shown in

Figure 11, for electrode number 24 indicates two maxima. This analysis indicates that two predominant pore size regions are present. For this particular electrode the maxima occur at 3 μ and 30 μ . This is not too surprising since the copper needles are horizontally distributed randomly, thus contributing one predominant pore size. It has also been observed that after the 3 mil copper wires have been oxidized to cupric oxide, they are invariably hollow, i.e., a tube of CuO is produced from a rod of copper. This phenomenon supports the theory that the copper must migrate from the center to the surface to be oxidized. In this way a second major pore size is expected to appear in the pore size distribution trace.

The diameters of the two major pore sizes support the selection of the range 1-30 μ for the quality control region.

Modulus of Rupture

The previous quality control tests have been chiefly designed to describe properties other than structural. In order to establish a reproducible and dynamically strong electrode, the following two tests were applied.

The "modulus of rupture" tests were performed to ascertain the region in which the electrode could be expected to break. A fixture was designed for this purpose and is shown in Figure 12. The electrode was supported at two pivot edges being 1.400 inches apart. The center of the electrode was positioned equi-distant between the two pivots. Three different shaped pivots were examined: (A) wedge, (B) semi-circular, 0.188" radius and (C) semi-circular, 0.376" radius. The criterion of acceptability for the pivots was whether the pivot caused any crushing of the electrode under the force required to break the electrode. The rupture-plunger used in all cases was a wedge that was positioned parallel to the pivots and intersecting the center of the electrode. A number of "blank" tests were conducted to evaluate the applicability of the pivots. Testing was begun with the wedge shaped pivots. A hand-operated press, previously calibrated with an accurate Dillon gage, was used to apply a force to the rupture-plunger. Force was applied until the electrode ruptured, at which time the rupture force was noted. The electrodes were then examined to determine whether the pivots

caused any degradation of the electrode at their point of contact. The wedge pivot caused a very definite ridge on the electrode, resulting in some compression and crumbling. The test was repeated using the smaller semi-circular wedge. No deleterious effects were observed with this pivot. Further testing with the larger semi-circular pivot caused some crumbling of the cathode at its point of contact; but more important, the rupture of the electrode did not occur along the line of the rupture-plunger wedge. The electrode invariably ruptured to give more than two pieces. This indicates that strain forces are radiating in directions other than along the wedge of the rupture-plunger. This can be traced back to slight irregularities in the surface (bottom) of the cathode and the pivot radius is large enough to support the force over a number of these irregularities causing a strain in these directions.

Of the three pivots examined, the wedge and large semi-circle was eliminated from further use. The small semi-circle pivot was accepted for further use, not necessarily as a process of elimination, but rather that the initial tests indicated it to be a very satisfactory pivot.

The fixture was completely constructed from steel parts. The spring, used to keep the rupture-plunger from striking the base plate, was calibrated at the electrode height and corrected for in the final force readings.

Six electrodes were subjected to this test. All electrodes were of a nominal 61 ampere-hour capacity. The modulus of rupture data is collected below in Table 7. The average of the rupture forces gives 478 pounds with an average deviation of ± 57 pounds. Using 1.5 times the average deviation as a rejection factor, electrodes number 25 and 35 should be rejected since they don't represent a good precision. Recalculating the average after eliminating electrodes 25 and 35 gives an average of 505 pounds as the average rupture force.

Table 7

Modulus of Rupture Data

<u>Electrode Number</u>	<u>Modulus of Rupture (LBS)</u>	<u>Density (GMS/CC)</u>
25	570	3.30
26	490	3.26
35	280	3.13
36	540	3.20
37	460	3.00
38	530	3.03

On the basis of the four accepted tests, a standard deviation of 37 lbs. is calculated. Again applying the standard deviation of $\pm\sigma$ as an acceptable rupture test, the range of acceptability is 468-542 lbs. Since this is a destructive test, it becomes impossible to apply the test to the actual electrode to be used in the thermal cell. The test does define a desirable rupture range but its usefulness and application are seriously hindered (except for random sampling procedures). To make this test useful, it would have to be related to a non-destructive test, such as bulk density. The bulk density of each electrode is also given in Table 7. No definite correlation appears to exist between the modulus of rupture and the density. It might reasonably be expected that such a correlation would exist and more intensive testing might show this trend.

Compression Tests

The cathode compression tests are again tests to study the stability of the cathode structure. The test, being a destructive one, is meant to establish the degree of compression an electrode can tolerate and still be a usable electrode.

The compression tests were performed with the same fixture as that used for the modulus of rupture except that the wedge shaped rupture plunger

was replaced by a compression plunger as described in Figure 13. The compression head that seats against the electrode is a rod 1/4" in diameter with a machined flat face. In this test the electrode is set flat on the fixture base during the test.

Two conditions were examined in this test. In the first case the plunger was very carefully placed on the electrode surface and pressure was applied slowly. At the first visible evidence of surface fracture, the force was noted. For the second condition, force was applied to the plunger until it had been pushed 0.063 inches into the electrode surface. The results of these tests on six cathodes of a 61 ampere-hour capacity are given below in Table 8.

Table 8

Results of Compression Tests

<u>Electrode Number</u>	<u>Surface Fracture Force (LBS)</u>	<u>Force at 0.063" Depth (LBS)</u>	<u>Density (G/CC)</u>
39	480	930	3.12
40	580	980	3.23
41	580	880 (Fracture)	3.30
42	580	980	3.15
43	480	490 (Fracture)	3.10
44	530	980	3.10

The results show that these electrodes are very sturdy. No visual evidence of compression occurs until 500 pounds of force is applied and nearly twice this force is required to cause a 0.063" depression.

In a general way, a correlation exists between the surface fracture force and the bulk density. The three lowest bulk density cathodes had the three lowest surface fracture force while the three most dense electrodes all indicated a surface fracture force of 580 pounds.

Summary of Physical Property Tests

Only two of the five physical property tests examined can be considered non-destructive. A non-destructive test is a powerful quality control measure because it can be applied to the actual components being used. The two tests mentioned above are (A) bulk density and (B) B. E. T. surface area measurement. The bulk density measurement is the most applicable test that can easily be applied to each electrode. In general, it appears that if an electrode is accepted on the bulk density test, it will be acceptable in pore size distribution, modulus of rupture and compression. B. E. T. determination of true surface area is too insensitive for these small areas to be a good non-destructive quality control method.

The three destructive tests, i.e., pore size distribution, modulus of rupture and compression, cannot be used as a 100% sampling quality control method but could be used as an acceptance test on a batch basis. If a batch is first quality controlled by bulk density tests and the resulting electrodes considered as a batch, then the destructive tests could be applied to a random sampling, e.g., 10% sampling of a batch. Observing the acceptability of an electrode if it falls within one σ of the mean, then the range of acceptance will be as summarized below.

Bulk density	---	3.18 to 3.38 G/CC
Percent pore volume between 1-30 μ	---	64.1 to 75.9%
Modulus of rupture	---	468 to 542 pounds
Compression force	---	489 to 587 pounds

It can be reasoned further that cathodes having densities ranging from 2.0 to 4.3 GMS/CC have not shown an average poorer performance than cathodes having tightly controlled bulk densities. The major reason for maintaining a close tolerance on the bulk density is to control the height of the cathode. Since the cathode retainer ring is welded into the case before the cathode is assembled on the ring, it considerably facilitates fabrication if the cathode retainer ring can be located at a standard distance from the

cell bottom. Otherwise each cathode must be matched to a particular case so that a tight fitting cathode connection is achieved. From this standpoint it is beneficial to control the cathode bulk density rather closely. No true experimental correlation has been made between cell performance and any of the destructive tests.

Based on these considerations, bulk density will be controlled to the tolerance mentioned but no attempt will be made to measure the other physical properties as a quality control specification.

3.2.2 Anode Connectors

In a cell that must operate for a period of 150 hours it is particularly important that the internal electrical connection of the electrodes to their terminals remain intact. The main concern deals with the anode since the cathode connection is made directly to the cell case. The anode is insulated from the case by using a ceramic terminal seal. A connector must be provided through which the anode is connected to the terminal.

All cell tests conducted for the first 15 months had been made using a nickel 200 anode connector material. This encompassed about 250 individual tests. No visible evidence has been observed during these tests that the nickel is attacked by the cell components.

The joining method used during this time has been a screw connection. The magnesium anode is tap-drilled and threaded. In a similar manner the nickel connecting rod is threaded. By tightly screwing the nickel connector rod into the magnesium, a reliable, trouble-free joint is made. Over the period of use of this connector material and joining method, not one cell failure could be attributed to an anode disconnect or any other reason related with the material or joining method.

To complete the connector study, three complete cells were constructed using nickel 200 anode connectors and the anode joined to the connector by the screw technique described above. After these cells had been electrochemically discharged according to the specification given in Section 3.1.1,

electrolyte samples were taken from each and analyzed quantitatively for dissolved nickel. The results of these analyses are given in Table 9.

Table 9

Anode Connector Study-Electrolyte Analysis for Ni

<u>Test Number</u>	<u>Ni (%)</u>	<u>Ni (GMS Total)</u>	<u>Avg. Rate of Dissolution (GMS/HR)</u>
272	0.09	0.305	0.00237
273	0.05	0.169	0.00231
274	0.08	0.271	0.00166

The cell life, and consequently the time the cells were in the molten state, were: Test 272 - 117 hrs, test 273 -- 73.4 hrs, and test 274 -- 163.2 hrs. From the first two tests it is seen that the average rate of solution of nickel is about the same while test 274 shows a decreased rate. This can be interpreted to mean that the electrolyte becomes saturated with nickel corrosion product some time between 117 hrs. and 163 hrs. Judging from the percent Ni found in the electrolyte, saturation occurs near the 117 hr. mark. It appears reasonable to accept the dissolution rate of the nickel to be 0.0023 gms. Ni/Hr. at times less than the time of saturation. It is important to note that the three tests were conducted in a cell case constructed from nickel 200. If it is assumed that the dissolution rate of the nickel is directly proportional to its area exposed to the electrolyte, then it can be calculated that only 52.2 μ gms/Hr is lost from the anode connector with the progressive loss of nickel from the connector terminating at the saturation time of 117 hrs. The total weight loss from the nickel anode connector would be 0.0061 gms. The above calculations show that an insignificant quantity of nickel is lost from the anode connector and therefore that nickel makes a very satisfactory connector material. For the second point of investigation, the method of joining the anode to the connector is very satisfactory based on the large number of anode assemblies built in this manner without the slightest difficulty. The joining method is shown in a diagram in the Quality Control Section, Appendix III.

3.2.3 Separator Study

Under NASA Contract NAS 3-8517 it was shown that "Vitron-E" was the most stable and effective separator to be used in a long life thermal cell. In that contract it was also demonstrated that a separator was necessary in all the cell tests conducted under the present contract. The bulk density of the "Vitron-E" has previously been determined to be 0.01 gms/cc.

There are several properties of a separator that should be known so that an optimum separator design can be achieved. The thickness of the separator to be used in a cell to give optimum performance is a basic parameter. In terms of separator resistance, it is desirable to keep the separator as thin as possible to keep the resistance contribution small. On the other hand the separator must be thick enough to significantly retard the flow of oxidants to the anode surface. Another point in favor of maintaining a thin separator is that the reaction product from the anode ($MgCl_2$) should be allowed to easily diffuse to the electrolyte bulk to prevent an increase in the electrolyte melting point. The following sections present data to facilitate the selection of an optimum separator thickness.

Separator Resistance vs Thickness

Four thicknesses of bulk "Vitron-E" were studied to determine the resistance contributed to an operating cell due to the separator. The four thicknesses examined were: (A) 0.50 cm, (B) 1.00 cm, (C) 1.50 cm and (D) 2.00 cm. All tests in this section were performed in duplicate.

The most applicable method to examine the extent of resistance contribution was to use a cell structure of the same dimensions as used in an actual cell. These tests were performed in a cell structure the same as shown in Figure 1. The magnesium anode was replaced by a nickel (grade 200) slug of exactly the same dimensions as the magnesium anode. The separator was applied around the nickel slug in the same manner as described in the Quality Control Section, Appendix III for the magnesium anode. The same quantity of electrolyte was used in all tests and amounted to 360.5 grams.

Each test cell was heated to 800^oF and one-half hour was allowed to reach equilibrium temperature. The tests were conducted in a 100% nitrogen atmosphere and resistance measurements were made with a General Radio, Model 1650A, conductivity bridge. No cathode was used in the case but rather the resistance was measured between the nickel slug and the case.

Two units were constructed using no separator material. These resistance values were intended to serve as a calibration and base upon which the resistance values with separators could be compared. In all cases the resistance values were recorded manually each hour through the work day for a period of 150 hours.

Figure 14 shows the results of these tests as compared to the standard units without separators. As can be seen from the figure, no conclusions are evident from these results. All the measurements fell within a range of +0.02 to -0.03 ohms of the cells without separators. One fact that is obvious from these results is that the separator contributes very little resistance to the overall cell assembly. If one ampere were drawn from the cell, only 50 mv. of the operating cell voltage would be lost due to separator resistance (assuming the worst possible case of 0.05Ω separator thickness of "Vitron-E" separator up to 2.0 cm thick could be used without exceeding a reasonable resistance limit.

Cell Tests with Various Separator Thicknesses

In order to optimize separator thickness, three complete cells were constructed for each thickness of separator mentioned in the last section i.e., 12 cells. The cells were constructed according to the procedure given in Appendix III. The cells were then tested according to the standard test specifications given in Section 3.1.1.

Typical discharge curves are shown in Figures 15-17 for each series of tests with the various thicknesses of separator. The numerical data are given for tests 333-344 in Table 1, Appendix I.

Table 10

Average Calculations for Separator Thickness Study

<u>Separator Thickness (cm)</u>	<u>Cathode Util. (%)</u>	<u>Is.d. (mA)</u>	<u>Cell Life (Hrs)</u>	<u>Output Energy (Watt-Hrs)</u>
0.50	78.9	14.7	144.7	39.58
1.00*	82.2	15.1	150.0	42.28
1.50	87.9	9.4	160.7	49.82
2.00	80.2	16.7	146.8	43.79

*Average of two best tests.

In each of the categories in Table 10, the 1.5 cm separator thickness shows superior results, and further cells were constructed with this thickness separator.

Prevention of Separator Cracking

Each cell test that is conducted is post-mortemed to recover the anode remains and to generally inspect the conditions of the "spent" cell. One disturbing factor that was present in most cases was that the separator was cracked. The degree of cracking varied from fine hairline cracks to catastrophic failure. Various methods have been examined to eliminate this phenomenon but one difficulty or another has precluded use of method tried.

The major reason for the cracking is that once the separator has been saturated with molten electrolyte, 20% contraction occurs upon cooling to room temperature. One technique attempted was to do no pre-saturation of the separator but this invariably resulted in the anode being isolated from the electrolyte by a gas bubble, seriously shortening the cell life. Pre-saturation of the separator appears necessary but in most cases the cracking causes high self-discharge currents and decreased cathode utilizations (decreased cell life).

Another technique attempted was to pre-saturate the separator and cool it very slowly with a subsequent annealing stage for 16 hours. This helped considerably but still 40% of the post-mortems indicated separator cracking.

The most successful method to be found has been to use a blank can (nickel 200) in which the proper amount of salt has been melted, the anode/separator assembly is properly located in the molten salt, a vacuum is drawn to remove the air bubbles from the separator and finally the whole unit is allowed to cool to room temperature. The salt block formed around the separator and apparently distributed any strain throughout the total block. The result is a crack-free salt block containing 360.5 gms of electrolyte with the anode/separator assembly embedded in it.

The twelve cell tests conducted in the separator study were constructed in this manner. Post-mortem of the cells indicated that none of the separators had cracked. It appears that future use of this technique will give more reliable cells with longer lives and low average self-discharge currents.

3.2.4 Electrolyte

The composition of the electrolyte used throughout this study was 59 mole % LiCl - 41 mole % KCl. The electrolyte was obtained from the Anderson's Physics Laboratory, Champaign, Ill. and was of a comparable quality as reported in the Final Report of Contract NAS 3-8517 (CR-72361). The electrolyte was prepared in accordance with the method of H. A. Laitinen described in the Journal of the Electrochemical Society, 104, 8, pp 516-519. Effectiveness of this preparation was confirmed by observation of the characteristic polarographic residual current using a platinum microelectrode. The LiCl-KCl melt used had no polarographic wave less than -2.6 volts vs. a 0.1 M Pt(II)/Pt reference electrode, and had a residual current less than six microamperes at -2.5 volts. Each batch of electrolyte was examined by the Anderson Physics Laboratories and certified to meet these quality control specifications.

3.2.5 Cell Case

Cell Case Material Selection

All enclosed full cell tests conducted under NASA Contract NAS 3-8517 were performed in copper No. 122 cases. This material contained 0.02% phosphorous with an undetermined quantity of oxygen. Copper was initially selected as an acceptable material since the reaction product of the cathodic reaction was also copper, i.e., $\text{CuO} + 2\text{e}^- \rightarrow \text{Cu} \downarrow + \text{O}^-$. It was reasoned that this material could have no greater detrimental effect on the cell performance than would the natural reaction product. Copper was also known to have a low reactivity with the LiCl-KCl molten electrolyte at 800°C. The greatest difficulties experienced with this case material, however, manifest themselves in welding to create a hermetically sealed cell. A relatively cold weld was required so that the electrolyte remained solid during the sealing procedure. Electron-beam welding provided the appropriate method but much difficulty was experienced in forming hermetic seals. The smallest traces of oxygen or phosphorous in the copper were vaporized during welding with resulting porous weld joints. It became obvious that extremely pure copper was required and that very rigorous control had to be observed during the welding process.

Electron-beam welding experts at NASA-Lewis, Fusion Laboratories and Atlas Chemicals were consulted as to what materials were conveniently welded by the electron-beam technique. Of the materials recommended, a second criterion was required and that was that the material must be essentially inert in molten LiCl-KCl at 427°C for periods up to 200 hours. The one material that suggested itself above all others was commercial grade A nickel. Nickel has a greater tensile strength and is less malleable than copper which is advantageous in cell case construction. Nickel is more noble than copper and resists oxidation much more readily at high temperatures in an oxidizing atmosphere. Upon initial tests it was found that grade A nickel welded reliably and hermetically by the electron-beam welding technique.

Grade A nickel was recommended as the material to be used for the cell case for the reasons mentioned above. Construction of over 200 cells using grade A nickel for the cell case has proven the choice to be a good one. No experimental problems exist that can be attributed to the use of this material for the cell case.

Cell Case Fabrication and Assembly Method

The basic cylindrical cell case used in all previous cell tests on the previous NASA Contract NAS 3-8517 was accepted as the configuration to be used in this work. A review was made concerning all components and welds that were to be made on the external surface of the cell case. Particular attention was given to ease and reliability of the fabrication technique. The areas that were considered were:

- (A) Cell case thickness
- (B) Terminal seal
- (C) Connection of anode connector to the terminal seal
- (D) Cathode terminal pin
- (E) Case bottom.

For the laboratory type cells ease of fabrication was facilitated by using 0.050 inch thick nickel cases. This thickness was selected primarily so that counterbores could easily be machined to accept a press fit of the terminal seal flange and the case bottom. This type of component fitting was recommended by the electron-beam welding company so that the best possible conditions existed for this type of welding. By using a 0.050" cell case thickness up to 0.030" counterbore depths could easily be machined.

Ceramic terminal seals with nickel collars appeared most suitable for this particular cell design. As shown in the drawings of Appendix III the terminal seal collar was matched in dimensions to a hole and counterbore set in the center of the cell case top. Collar-counterbore matching provided a press fit of the two components to facilitate and provide a reliable

electron-beam weld. Nickel collars were recommended on the seals so that the welds could be made between like metals and because the nickel is unaffected by chemical attack by the cell electrolyte.

Since nickel provides a material that is chemically inert in the LiCl-KCl salt system, practically all of the metal cell components (except the anode and cathode) utilized this material. The anode connector, again being constructed of nickel, was machined to snugly fit through the central nickel pin of the terminal seal. In all cases the connector was closely matched to the hole in the terminal seal to provide easier and more reliable electron-beam welds.

The cathode connection was merely a nickel terminal pin electron-beam welded to the case. Since the cathode was placed against the internal surface of the case, this method of terminal connection was convenient and easily fabricated.

The case bottom was also constructed of 0.050" nickel sheet. A counterbore was placed in the bottom rim of the cylindrical cell case to accept the cell bottom. When assembled, the case bottom fit flush with the bottom edge of the cell walls and typically showed less than 0.001" gap between the cell bottom edge and the walls of the cell case. This arrangement was accepted by the electron-beam welding company as a very satisfactory assembly and welding technique.

In summary, electron-beam welding is utilized on the outside surface of the cell case at the following locations: (A) terminal seal flange to the cell case top (B) anode connector pin to the central pin of the ceramic seal (C) cathode output terminal pin to the cell case top (D) cell case bottom to the bottom of the cell case. At this point the cell case has been hermetically sealed.

Several methods for making the cell case were reviewed. Three methods were studied on the basis of (A) ability to hold an acceptable tolerance (B) case fabrication and delivery time and (C) cost. The three methods of cell case fabrication studied were (A) hydroforming, (B) die cast forming and (C) metal spinning. Very few hydroforming manufacturers exist in the

United States. In general the price was high and the companies were reluctant to make our cell cases in the small quantities we needed. The die-cast technique could not form cases as tall as our cell case construction demanded.

Metal spinning provided a good technique able to meet our specifications. Metal-spinning techniques could form the cases to the proper dimensions and within acceptable tolerances. Fabrication and delivery time was acceptable since the manufacturer was local. Cost was appreciably lower by this technique than by the other two fabrication methods considered. Metal-spinning was accepted as the method for fabricating the cell cases.

According to the above discussion five (5) cell case assemblies were constructed consisting of: (A) cell case (B) ceramic terminal seal (C) anode connector pin (D) cathode terminal pin (E) case bottom. A 1/4" O.D. copper tube was welded into the case bottom to provide access to the inside of the case to apply pressure or vacuum. The cases were then submitted to tests at 427°C and at several pressure conditions to determine whether the cases were hermetically tight under the various temperature/pressure environments. Figure 19 shows a cell case constructed for these tests and Figure 20 shows the experimental set-up used for the testing. A CEC Model 24-120 helium leak detector was used throughout these studies.

The cell case was placed in the pressure chamber (located in a temperature regulated furnace) and connections made to a helium pressure line, a vacuum line and the helium leak detector. The cell case and pressure chamber were thoroughly flushed with helium and the temperature brought to 427 ±2°C. The inside of the cell was flushed with nitrogen and evacuated ten times to remove all traces of helium from the inside of the cell case, and finally the cell case was evacuated. This provided a 15 psi pressure on the external surface of the cell case. This condition was allowed to stand 30 minutes while monitoring the leak rate gage of the helium leak detector.

The same procedure was followed to determine whether any leakage occurred from the cell interior to the outside of the cell case. In this situation the pressure chamber was flushed with nitrogen and finally evacuated

while the cell case interior was filled with helium at 15 psi pressure. The helium leak detector in this case monitored the pressure chamber volume to detect any helium leakage from the cell case interior.

The data obtained from these tests at 427°C are given below in Table 11.

Table 11

Results of Cell Case Leak-Rate Tests

Case No.	*Leak Rate at 15 psi Internal (cc/sec)	*Leak Rate at 15 psi External (cc/sec)
1	3.3×10^{-10}	3.3×10^{-10}
2	3.1×10^{-10}	3.3×10^{-10}
3	3.3×10^{-10}	3.1×10^{-10}
4	3.1×10^{-10}	3.1×10^{-10}
5	3.5×10^{-10}	3.5×10^{-10}

*These leak rate figures represent the maximum calibrated leak sensitivity of the instrument at 800°F and at the time of measurement. Consequently, any leakage occurring was less than the rates given in the table.

From Table 11 it can be seen that no detectable leakage occurred in any of the five tests at 427°C and under ±1 atm. pressure. Based on these results this fabrication and assembly method was accepted for use on any subsequent cell case fabrication.

3.2.6 Terminal Seals

With the current design of the NASA long life thermal cell, a terminal seal is required to provide an electrical connection to the anode while providing electrical insulation from the cell case, which acts as the cathode electrical connection. Basic preliminary specifications which the terminal seal must meet were the following:

- (A) Provide low electrical losses for current flow up to 2.0 amperes, continuous.
- (B) Withstand "flash" currents of 20 ampere for a few seconds.
- (C) Provide a hermetic seal for the electrode lead through the cell case.

Vycor glass seals were briefly examined but it was found that a fine network of cracks developed in the Vycor during the welding of the seal to the case. Since a hermetic seal could not be made under these conditions, further consideration of this seal type was dropped.

Based upon a knowledge of the chemical components used in this cell and upon our background in thermal battery manufacture, it was felt that a ceramic seal would be required. Three different ceramic seals were selected for evaluation and are shown in Figure 21. A description of the selected seals follows:

Type I -- Alite 1-2-IG, 42% Ni-58% Fe, Silver braze, Al_2O_3 ceramic

Type II -- Alite B50-1, Grade A nickel, OFHC copper braze, Al_2O_3 ceramic

Type III --- Alite D-312, Grade A nickel, OFHC copper braze, Al_2O_3 ceramic

Each of the seals were supplied with an anode connector pin which fit snugly into the center seal pin. The seal pin and anode connector were welded together. For the three types of seals tested, it was found that 5 mv. was lost due to IR while passing a continuous 2.0 ampere current. All seals withstood a 20 ampere pulse for five seconds without any noticeable heating. These three seals were accepted on a preliminary basis and subjected to more vigorous testing.

Terminal Seal Evaluation

Tests were conducted to determine the resistance between the center pin of the seal and the cell case. This resistance must be high to prevent any leakage current to flow resulting in decreased useful capacity and wasted energy.

A sample of each candidate terminal seal was electron-beam welded to the case in a manner similar to actual cell construction. The electrical resistance between the terminal and case was measured at room temperature. The resistance was again measured at 800^oF in one hour. The measurements ,

were performed with a Keithly electrometer able to measure up to 10^{16} ohms. All tests were conducted in triplicate and the data are shown in Table 12 below.

Table 12

Terminal-to-Case Resistance of Terminal Seals

<u>Seal Type</u>	<u>Room Temperature</u> Ω	<u>At 427°C</u> Ω
I	3.6×10^{15}	4.1×10^{14}
	3.9×10^{15}	4.3×10^{14}
	4.2×10^{15}	4.7×10^{14}
II	2.6×10^{15}	2.9×10^{14}
	1.6×10^{15}	2.1×10^{14}
	2.4×10^{15}	2.0×10^{14}
III	2.8×10^{15}	3.3×10^{14}
	2.2×10^{15}	1.9×10^{14}
	3.1×10^{15}	2.3×10^{14}

In all cases the terminal-to-case resistance shows a favorably high value, representing a leakage current no larger than 5×10^{-15} amperes per volt.

It is noted that an order of magnitude decrease in resistance occurs when heating to 427°C. Since this phenomenon is observed in all the seals, the cause of the resistance loss must be due to a common factor. The ceramic in all cases is glazed and it is well known that the conductivity of glasses increase as temperature increases. The overall resistance loss can reasonably be attributed to the increased conductivity of the glass at 427°C.

Tests were required to determine whether the seals could withstand a thermal shock without causing a resultant leak or a substantial reduction in the terminal-to-case resistance. A case similar to the one used in the electrical resistance tests was inserted into a pre-heated furnace at 427°C for 10 minutes and then cooled to room temperature in ambient air. Leak rate and electrical resistance (terminal-to-case) of each sample was measured at 427°C and at room temperature before and after the heating cycle. The tests were run in triplicate. The results of these tests are given in Table 13 for the three candidate seals.

Table 13

Thermal Shock Results on Terminal Seals

<u>Seal Type</u>	<u>L.R. (Initial) cc/sec, 25°C</u>	<u>L.R. (Heated) cc/sec, 427°C</u>	<u>L.R. (Final) cc/sec, 25°C</u>
I	2.6×10^{-10}	8.6×10^{-10}	2.7×10^{-10}
	2.6	9.2	1.5
	2.6	8.7	3.4
II	2.6	7.8	3.6
	2.6	8.1	4.4
	2.6	9.2	3.6
III	3.3	8.3	4.2
	3.1	9.3	3.1
	3.2	8.8	3.5

The above measurements were made by Glass Blowing Enterprise, Inc. At the time of each test the leak test equipment was calibrated with a standard leak. All the numbers reported in Table 13 represent the limit of sensitivity of the instrument at the conditions of measurement. In other words, none of the seals gave any indication of leaking within the capability of the instrument sensitivity.

Resistance measurements between the terminal seal and the case fell in the range of 1.5×10^{15} to 4.0×10^{15} Ω at room temperature before and after heating. The resistance values at 427°C fell in the range of 1.9×10^{14} to 4.4×10^{14} Ω . Comparing these values to Table 12 indicates that no detrimental effect occurred to the resistance values caused by the thermal shock.

Evaluation of the data to this point indicates that all the terminal seal candidates are satisfactory. Consequently, further testing will include the three types of seals.

Compatibility Tests

Tests were extended to determine whether the internal chemical components of the cell would affect the quality of the seal at 427°C over a period of 200 hours.

Cell cases were constructed similar to those used in 3.2.5 and shown in Figure 19. Again in these tests each candidate seal was examined in triplicate. The cell case was loaded with 200 grams of LiCl-KCl eutectic electrolyte and 50 gms. of cupric oxide powder. The cupric oxide was included to simulate a quantity of dissolved cathode material that might be expected in an actual operating cell, i.e., the electrolyte would be saturated with dissolved cupric oxide. If any reduction would spontaneously occur to cause metallic bridging between the terminal and case, one would expect this to be due to the reduction of the copper ions. After loading the internal components the cell bottom was electron-beam welded to the case and the whole unit was heated to 427°C in one hour. The cell was then inverted so the electrolyte contacted the terminal seal. The cell was maintained in this attitude for 200 hours. During the 200 hour stand, the external pressure on the seal was cycled between 0 psia and 30 psia every ten hours. At the conclusion of the test the cell was inverted to an upright position, cooled to room temperature in one hour and the terminal seals examined for:

- (A) Helium leak rate
- (B) Terminal-to-case electrical resistance
- (C) Physical deterioration due to chemical attack.

In all nine tests, no helium leak rate was observed after the tests that was within the limit of sensitivity of the helium leak detector at room temperature, i.e., no leakage occurred in excess of 3.5×10^{-10} cc He/sec.

Electrical resistance measurements between the terminal seal and the case were in the 10^{14} - 10^{15} Ω range. Obviously no bridging occurred between the terminal seal and case due to the reduction of copper ions.

All the seal flanges indicated a slight tarnishing effect, but no chemical attack was evident to the extent that it would cause any performance loss in the cell.

In some respects the result obtained for the Type I, Alite 1-2-IC terminal seal was surprising. The metal parts of this seal was an alloy of 42% Ni and 58% Fe. In previous electrochemical discharge tests, a seal of this metallic composition invariably was corroded and caused the cell to leak copiously. In the cell tests that were electrochemically discharged, the potential field on the seal could have caused the electrochemical oxidation of the iron from the alloy while in the static tests conducted in this section might have an insignificant effect on the alloy material. Since this effect has been observed previously on Type I terminal seals, they were eliminated from any further consideration for use on the final cell.

Selection of a Terminal Seal

Based upon the previous testing, terminal seal Types II and III appear equally acceptable for reliable use. Therefore, the choice of seals must depend on convenience of use or that one seal can contribute to a structurally more reliable final cell.

Using these additional considerations, it becomes evident that Type II, Alite B50-1 is the preferred design. The Type II seal has a considerably larger hole in the ceramic into which an enlarged section of the anode connector can rest. Since the anode connector can have this larger shank with this seal, less chance of bending will occur during conditions of shock, acceleration and vibration. It is also much easier to machine the anode connector if it has the enlarged shank. Ease in fabrication and assembly of the anode connector-terminal seal joint and greater structural integrity supports the use of the Type II seal in preference to the Type III seal.

3.2.7 Cell Assembly Tests

As a final test of the components assembled into a completed cell, tests were conducted to ascertain that no unforeseen interactions would occur that would be detrimental to the hermetic seal or the intended placement of the components.

Five complete cells were constructed according to the construction details given in Appendix III. These cells were a culmination to and inclusive of all the testing done up to this point. The completed cells were inserted into a helium pressure chamber at 30 psia for 24 hours after which the chamber was cleansed of He with a N₂ flush and evacuated. A helium leak detector was attached to the chamber to determine whether any helium was diffusing from the cells. This procedure was conducted at room temperature. No leaks were detectable during these tests. The five cells were then placed in an oven and heated to 427°C in one hour and maintained at that temperature for 10 hours. The leak tests were performed at 427°C after the ten hours and the data again shows that no leakage was evident. The cells were cooled to room temperature in one hour and examined again for tightness. Throughout these tests no helium leakage could be detected. This testing indicates that all components mounted on the external surface of the case are compatible and weld joint integrity is wholly satisfactory.

After the leak testing was completed, the cells were X-rayed to determine the distribution of the electrolyte and any possible displacement of the components. A print of the X-ray is shown in Figure 22. The X-ray does not indicate any improper parts displacement or unusual displacement of the electrolyte. X-rays were taken of the cells since uncertainties could arise if the internal components were disrupted during the disassembly of the cell. Finally, the top of the cell was removed with a band saw and the cell was bisected through its vertical axis. Visual inspection showed no sign of anything unusual or unexpected. Electrolyte had saturated the porous structure of the cathode and no internal parts had been displaced from their initially intended location.

The collected results lead us to believe that these techniques and materials will yield a sturdy and reliable long-life thermal cell.

4.0 Environmental Cell Tests

The objective of this section is to determine the effect of shock, vibration and acceleration on the performance of the cells. This work is divided into two sections: the first section is the testing of control cells at three temperatures to act as our standard reference performance. The second section involves the environmental testing with subsequent electrochemical testing of units to determine the effect of the environmental testing on electrochemical performance.

4.1 Control Cells

The construction of these cells is exactly the same as previously used except for one change--that being the terminal seal. Previous cells were constructed using the Alite D312 seal, where in this case the Alite B50-1 seal has been used. Figure 21 shows this seal design. The reason for selecting this terminal seal in preference to the other one used was based on the fact that it would be more mechanically stable and would withstand the environmental testing with more success. In conjunction with this seal, the anode connector was made larger to fit snugly into the larger diameter ceramic of the seal. In this fashion, the anode connector would have a larger shank and would rest more snugly against the seal, creating a lesser chance of failure due to the anode connector breaking.

Twenty cells were constructed and were tested at three different temperatures. Ten of these cells were tested at 427°C, five cells were tested at 481°C, and the remaining five cells were tested at 538°C. All of the test conditions for these cells except for the various temperatures, were the same as given in Section 3.1.1. The results of these individual tests are shown in Table 1 of Appendix I and are summarized in Table 14. The results shown in this table are an average of the runs at that particular temperature showing the average and the deviations experienced.

Table 14

Average Data for Control Cells

Temperature (°C)	Life (hrs.)	Cathode Utilization (%)	Self-Discharge Current (ma)	Number of Replicates Averaged
427	151.3 ± 3.3	82.6 ± 2.2	21.4 ± 6.8	10:10
481	132.8 ± 12.2	72.4 ± 6.5	60.2 ± 24.3	4:5
538	48.9 ± 10.8	26.7 ± 6.2	247.7 ± 73.8	5:5

Figures 23, 24 and 25 represent the typical shape of the voltage versus time traces. These figures also reflect the average deviation of the data given in Table 14. If the lives of the cells at the different temperatures are considered to be dependent upon the self-discharge rate, then it might be expected that the loss of life would occur exponentially as the temperature is increased. Using the 427 degree average test as the standard, the percentage of this life that the other cells ran at the other temperatures can be calculated. If the logarithm of this quantity is plotted versus $\frac{1}{t}$, where t is the absolute temperature, then one might expect a linear plot. A graph showing this analysis is given in Figure 26. It can be noted that the result for the 538° tests was 247.7 ma. From Figure 26 it was found by extrapolation that a maximum life of 80 hours would be expected for the cell running at 538°C. This being the case, the total capacity lost over this running time due to self-discharge would be .2477 multiplied by 80 giving 21.9 ampere-hours due to the self-discharge. Also the cells would have been running at the nominal duty cycle with an average current of .333 amps for the 80 hours. This would account for 26.6 ampere-hours of capacity used in the electrochemical discharge of the cell. By adding these two capacities together, a total of 48.5 ampere-hours can be accounted for. A similar analysis done on the 427° test would give a total used capacity of 53.5 ampere-hours. When comparing these two bits of information it would appear that the self-discharge rate is the controlling factor as the temperature is increased, and consequently decreases the lives of the cells. In any case, the tests made at 538°C failed due to the disconnect of the anode from the anode connector. Even if the anode had not disconnected from the connector, this analysis shows that considerably decreased life could be expected from the cells.

The results given in Table 14 are accepted as the results of the control cells at the three temperatures. These results acted as our standard against which the electrochemical performance of cells that were environmentally tested were compared.

4.2 Environmental Tests

Ten cells were constructed identically to the control cells discussed in Section 4.1. These ten units were shocked, accelerated, and vibrated. The conditions under which these cells were environmentally tested are given below:

Shock - Each cell was subjected to three shocks of 18 g's in each direction along three mutually perpendicular axes (total 18 shocks). The input pulse was a half-sine pulse with a time duration of eight milliseconds.

Vibration - A resonant survey test was run on each cell to determine the resident modes of the cell structure. A sweep was made from 5 to 16 Hz at 0.368" displacement amplitude, from 16 to 2,000 Hz at 5 g peaks on each of three mutually perpendicular axes. Measurement was made at the point of coupling between the exciting mechanism and the cell. All resonances in each direction were noted. When a resonance occurred, the cell was vibrated at one half the resonant frequency for 30 minutes.

Acceleration - The cells were accelerated as follows: 7 g's acceleration for five minutes along the longitudinal axis in a direction which simulated lift-off; 3 g's acceleration in the opposite direction for five minutes; 4.5 g's acceleration in both directions along mutually perpendicular axes for five minutes. After each test the cells were examined for cracks, dents, and other exterior damage. Table 15 below shows the results for the ten cells tested according to the specifications given above.

Table 15

Results of Vibration Testing

Test No.	Resonant Frequencies (H z)			Resulting Damage Shown by X-Ray
	<u>X Axis</u>	<u>Y Axis</u>	<u>Z Axis</u>	
383	2000-60g peaks	NONE	NONE	Anode Connector Broken
384	122-60g peaks 1779-60g peaks	120-60g peaks 1920-60g peaks	20-60g peaks	Anode Connector Broken
385	NONE	160-60g peaks	2000-60g peaks	Anode Connector Broken
386	NONE	NONE	NONE	
387	1837-58g peaks	NONE	NONE	Anode Connector Broken
388	90-80g peaks 1912-minor	100-40g peaks 16-minor	16-minor	Anode Connector Broken
389	130-minor	130-minor	130-minor	
390	27-40g peaks	100-80g peaks 2000-minor	100-minor	Anode Connector Broken
391	NONE	NONE	NONE	
392	NONE	200-minor	NONE	Anode Connector Broken

As is shown in the table, eight of the ten cells showed a resonant frequency. In addition, it was noted that five of the ten cells had resonance in the Z-axis. A resonance can occur from two different sources. The salt block in the cell could contribute to an x-y resonant frequency, while the cathode would also contribute to resonance in these axes. In the Z-axis, however, it appears that only the cathode could contribute to a resonant frequency. Since resonant frequencies were observed in all three axes, it can be expected that both the salt block and the cathode were involved in causing the resonances.

In addition to the visual observations of cracking or denting of the units after the environmental testing, X-rays were also taken to observe the internal components of the cell. The X-rays showed that seven of the ten cells had broken anode connectors. Two of the cells were cut open to confirm the evidence shown on the X-ray. The anode connectors broke at the base of the terminal seal cap. In addition, the cathodes of both cells were broken. The salt blocks were covered with powdered copper oxide, which came from the cathode wearing against the side of the can, the case cover, and the retainer ring.

The salt block contracts away from the cold wall of the case mold when it is cast. This leaves a space of about five mils in which the salt block can vibrate, suspended only by the 0.062" portion of the anode connector. This movement probably caused the connector breakage during resonance vibration.

Since the cathode is not a machined part, it is difficult to achieve contact over the entire surface of the retainer ring and case cover. Our support mechanism depends solely on friction to hold the cathode in place. In addition, the support given by the retainer ring is only on the edge of the cathode. The upper surface must be opened to the electrolyte in order to allow for impregnation and diffusion to take place during discharge. If any of this cathode edge is ground away during any of the environmental testing, the cathode is free to move in any of the three axes.

Since seven out of ten cells tested environmentally had broken anode connectors, it became impossible to test these electrochemically. Since the remaining three tests would not be representative of the ten constructed, no discharge tests were made on these cells.

4.3 Environmental Cell Test Conclusions

After collecting the data and evaluating both the environmental and control units, three problems became evident. These problems are listed below with recommended methods for solving the problems. One of the most serious problems that was noted was the breaking of the anode connector. As was described earlier, enough space was present between the salt block and the can so that the salt block could act as a pendulum swinging from the narrow portion of the anode connector. A suggested solution for this problem would be to stabilize the salt block by forcing material between the salt block and the can. Such a material as mica would be chemically inert and serve as a wedge between the salt block and the can. The second problem noted was the abrasion and cracking of the cathode. Since the cathode could move in any of three directions, it becomes evident that wedging must occur for all the directions. Glass tape could be wrapped around the cathode to prevent movement in the x-y direction. On top of the cathode could be placed a thin, asbestos washer to provide a cushion between the cathode retainer ring and the cathode. This also would prevent abrasion between the two metal surfaces.

Since this would isolate the cathode electrically from the can, except for possibly sitting on the bottom of the can, it would be required to have a connection between the cathode and the retainer ring.

During the post-mortem examination of the control cells as a routine measurement, the resistance between the anode connector pin and the case was determined. This resistance should, theoretically, be infinite. In most cases we found that a considerably lower resistance was present--ranging from 50 ohms to 400,000 ohms. Due to this internal high-resistance shorting, it is possible that some of the capacity of the cell could be used in this manner, thus reducing the life of the cells. Close examination of the area between the anode connector pin and the cell case indicated that some metallic copper was imbedded on the surface of the ceramic terminal seal. This high resistance shorting could probably be eliminated by wrapping the anode connector with an insulator material.

5.0 Modifications for Solving Shorting and Environmental Problems

The objective of this phase of the work was two-fold--modifications to the cell design were to be made to determine whether the shorting and environmental problems could be eliminated. In addition, the effect of these modifications on discharge performance was to be determined.

5.1 Preliminary Modifications to Eliminate Shorting

All of the cells constructed in this section are the same as used in Section 4.1. The only change concerns the anode connector and its immediate surroundings. The heavy shank of the anode connector, which is normally seated in the ceramic of the terminal seal, was reduced from 0.250" to 0.155". Three insulator materials were used to enclose the anode connector shank. These materials were: lava rod, isomica and ceramic tubing. The purpose of these insulators was to diminish the possibility of having an electronically conductive path between the anode connector and the cell case. Five cells were constructed using the isomica insulator; three cells were constructed using the ceramic insulator; and one cell was constructed using the lava insulator. In addition, two cells were constructed having no insulator material.

The results of these tests indicated that no significant difference occurred. For example, the tests that were run without any insulator material, gave lives of 116 hours and 148 hours; the three cells with ceramic insulators gave lives of 117 hours, 142 hours and 152 hours. The scatter of results in the two circumstances does not allow for any conclusion to be drawn.

5.2 Work Alternate Flow Chart

A NASA briefing was held concerning our work at this stage of development. In this discussion it was realized that two major problems existed, i.e. electrical problems and environmental problems. Based on the recommendations of our previous testing, it was concluded that these recommendations should be incorporated into cells and examined to determine if it did solve either or both of these problems. The modifications were made on ten cells; five of these cells were to be used as control units, and five were to be tested environmentally and subsequently, discharged electrically. The results obtained from the tests on these ten cells would lead to one of four different approaches. These alternatives are given in the Work Alternative Flow Chart in Figure 27. The four legs of this chart are based upon the four conditions that could exist resulting from the tests of the ten cells. If the results of the ten cells indicate an electrical problem, then the chart indicates that three terminal seals should be studied to determine if this solves the problem. If an environmental problem still exists after these tests, all environmental testing will be eliminated from further study.

During this NASA briefing, it was concluded that further testing at 538°C should be eliminated due to the extremely poor performance reported earlier. In lieu of this temperature, it was decided that further testing should be continued at 371°C. Consequently, the three temperatures that will be studied henceforth are 371°C, 427°C and 481°C.

5.2.1 Preliminary Testing of Modified Cells

This section deals strictly with the flow chart shown in Figure 27. The flow chart indicates that the first testing that should be done involves the

ten cells that have all the previously recommended modifications. These modifications are described in Section 4.3. These tests were preliminary tests to indicate whether continued environmental or electrical problems existed. Consequently, the ten cells were divided into two groups, five cells being control units and five cells being examined environmentally and subsequently being discharged electrically.

The five control cells were discharged at a constant temperature of 427°C at the nominal duty cycle given in Section 3.1.1. The results of the individual control tests are shown in Table 1, Appendix 1, and are labeled test numbers 409 to 413. A summary of these data is given in Table 16. A typical discharge curve for these control units is shown in Figure 28.

Table 16

<u>Average Data for Modified Cells</u>				
Temperature (°C)	Life (hrs.)	Cathode Utilization (%)	Self-Discharge Current (ma)	Tests Averaged: Tests Run
427	126.0 ± 3.4	68.8 ± 1.7	23.8 ± 3.8	5:5
427 (ENV)	87.6 ± 22.6	47.7 ± 12.2	51.8 ± 44.1	4:5

If the average results from Table 16 are compared to those control units shown in Table 15, it is seen that a considerably decreased life exists in our present units. This can most probably be attributed to a restricted lateral volume for cathode expansion. As may be recalled, the cathode in this case was wrapped with glass tape so it would fit snugly against the walls of the cell case. Because of this, lateral volume expansion of the cathode was considerably restricted and the expansion was required to take place in the vertical direction. As was noted on the post-mortems of these units, the cathode swelling in the vertical direction was considerably greater than that found for those units listed in Table 14. The vertical growth rate of the cathode in these latter tests was calculated to be 0.20 mm/hr. In the control tests of Table 14, a similar calculation shows that a growth rate of 0.17 mm/hr existed. This is a difference of approximately 15% in the growth rate. The average lives of the units in Table 16 compared to those in Table 14 also indicated an approximate 15% difference. This in turn would indicate that the cell life is dependent on how much cathode reaction product exists on top of the active cathode material. There are two possible explanations that become apparent.

One explanation would involve the production of lithium oxide as one of the products of the cathode reaction. In this case the freezing point of the electrolyte in the cathode will be affected in such a way that after running for a certain period of time the electrolyte in the cathode would freeze. The phase diagram for KCl-LiCl eutectic shows that if the mixture is 7% deficient in LiCl it will freeze at 427°C.

The second possible explanation would involve the possibility that the cathode has become electrolyte starved during the cell operation. As the copper reaction product is built up on the active copper oxide cathode, it is possible that diffusion of the electrolyte into the remainder of the copper oxide is very slow. In this case the cathode reaction will discontinue due to lack of sufficient quantity of electrolyte.

The remaining five cells were subjected to environmental testing as described in Section 4.2. The results of the environmental testing are given in Table 17. After the environmental tests, X-rays were taken of the cells and the results observed are also shown in Table 17. The cells were then discharged at 427°C under the nominal duty cycle given earlier.

Table 17

Results of Vibration Testing

<u>Test No.</u>	<u>Resonant Frequencies (Hz)</u>			<u>Resulting Damage Shown By X-Ray</u>
	<u>X Axis</u>	<u>Y Axis</u>	<u>Z Axis</u>	
415	None	None	None	None
416	1800 @ 32g peaks	None	680 @ 16g peaks 1611 @ 22.5g peaks 1700 @ 27g peaks	None
417	None	None	None	None
418	None	None	None	None
419	None	None	1640 @ 26g peaks 1950 @ 42g peaks	None

The average data for these tests are shown in Table 16. The individual tests are given in Table 1, Appendix 1, as tests numbers 415 to 419, inclusive. A typical discharge curve is also given in Figure 28.

As indicated in Table 17, three units had no resonant frequencies. Two of the five cells had resonance on the Z-axis and one of these same two units had resonance in the X-axis. Comparing the data in Table 17 to the data in Table 15, it can be seen that the latter resonant frequencies were considerably increased in frequency and the g-peaks have been considerably decreased. It must also be noted that 60% of the units had no resonant frequencies at all. X-ray analysis also indicated no internal problems were evident.

The average results of the electrochemical discharge as shown in Table 16 show that a decreased life existed after the environmental testing. Analysis of the environmental test results and the electrochemical discharge results give no clear indication that the decreased lives were due to the environmental testing. If the environmental testing were of substantial bearing on the electrochemical performance, it might be suspected that the units having resonance would give the poorest performance. However, it is instructive to note that the longest and the shortest runs were those cells having no resonant frequencies. The two units having resonance ran as mediocre units. Consequently, no direct relationship can be made between cells having resonance and their length of electrochemical discharge lives.

The instructions given according to Figure 27 indicate that if any decrease in lives results after the environmental testing it is to be assumed that environmental testing had an affect on these lives and that further environmental studies should be discontinued.

5.2.2 Electrical Problems

As mentioned in the previous section, it was assumed that the environmental problems caused a decrease in the cell lives and consequently it must be assumed that the environmental testing had an effect on the performance of the cells. In a like manner, since the average cell test in all cases were less than 150 hours (the projected life), it must also be assumed that an electrical problem existed. Referring again to Figure 27, it is indicated

that if electrical and environmental problems exist, then the work shall progress according to leg D of the work schedule. Along this leg no further environmental studies are indicated.

The prime emphasis at this point then will be to produce a cell with the desired 150 hour life. This approach will strictly emphasize the solving of any electrical problems.

Referring to Section 5.1 it is seen that the insulators around the anode connector did not solve the terminal seal high resistance shorting problem. By mutual agreement between NASA and CRC it was decided to investigate whether various shapes and sizes of terminal seals would circumvent this problem. Three terminal seals were selected to be studied. These seals are shown in Figure 30. Anode connector pins were dimensionally designed to uniquely fit each of these seals. These anode connector dimensions are shown in Figure 31. In all other respects the cells were constructed as indicated in Section 4.0. In the case of the B-50-1 terminal seal Varglas sleeving was placed around the anode connector to inhibit the flow of copper particles to the ceramic surface.

These fifteen cells were tested at 427°C at the nominal duty cycle. The individual test results for these fifteen cells are given in Appendix 1, Table 1 as test numbers 423 to 438 inclusive except for test number 433. Table 19 gives the test results of the terminal seals studied. Cells constructed from one of the terminal seals (B-75-1) had data so scattered that it was impossible to include the results as a summary in Table 18. Typical discharge curves for the two seals reported in the table are given in Figures 32 and 33.

Table 18

Alternate Terminal Seal Testing
All Cells Discharged at 800°F (427°C)

Terminal Seal	Life (hrs.)	Cathode Utilization (%)	Self-Discharge Current (ma)	Number of Replicates Averaged
D-312	137.8 ± 15.4	75.0 ± 8.3	79.6 ± 34.7	5:5
B50-1 W/Varglas	138.5 ± 16.0	75.6 ± 8.8	41.1 ± 29.5	4:5

The average life of the cells with the Alite D-312 terminal seals was 137.8 hours. This is not significantly different from the results with the B-50-1 terminal seals which had an average life of 138.5 hours. None of the cells leaked and no shorting was observed across the terminal seals.

The lives of the cells with the Alite B-75-1 terminal seals were widely scattered. Tests 435 and 437 leaked where the anode connector is welded to the terminal cap. These leaks occurred because the welds had to be made without disturbing the threads on the terminal seal cap. Therefore, no excess metal could flow over the sides of the terminal cap. In addition, post-mortems of tests 444, 435 and 437 had heavy copper deposits on the anode indicating separator failure. None of the tests exhibited terminal seal shorting.

This testing completed the study of the three terminal seal designs as a possible method for eliminating the shorting problem. When the Varglas sleeving was first used, with the B-50-1 terminal seal, the shorting problem was eliminated. The other two designs were investigated to investigate the effect of different sizes and configurations on terminal seal shorting.

The results show that all the seals are capable of yielding a 150 hour life. There was no terminal seal shorting in any of the cells. Therefore, it is difficult to choose the best terminal seal design on the basis of the electrochemical performance of the cell on which the seal was used. However, one design shows definite superiority on a constructional basis.

The B-50-1 seal has 0.031 inches of ceramic extending below the flange (see Figure 30). On the other hand, the D-312 seal has 0.25 inches and the B-75-1 seal has 0.375 inches. If the molten salt freezes against a large ceramic mass during block casting, it is very difficult to remove the block from the mold. When casting salt blocks for D-312 seals, or B-75-1 seals, the ceramic portion which extends into the case mold must be covered to prevent the molten salt from wetting the ceramic surface. This precaution is unnecessary with the B-50-1 terminal seal. Therefore, the B-50-1 terminal seal was adopted for the remaining tests. In addition, they had Varglas sleeving around the anode connector.

During the course of this project, post-mortems have shown that the separator had broken in many tests during the discharge cycle causing the cell to die prematurely. In an effort to achieve better reproducibility, CRC sponsored the fabrication and testing of two cells using a glass tape separator in place of the Vitron. The glass tape was Hessgon B from the Hess Goldsmith Company and was 5 mils thick. The cells were discharged under the same conditions as the other cells in this section. The results of the tests on these cells are given in Table 19 and Figure 34.

Table 19

Test Results of Cells With Glass Tape Separators

Test No.	Cell Life (hrs.)	Cathode Utilization (%)	Self-Discharge Current (ma)
433	156.5	85.2	26.1
439	159.0	86.4	24.0

The lives and self-discharge currents are quite reproducible. Post-mortems of the cells showed three beneficial results from the use of this separator. First, neither separator broke during block casting or during discharge. Second, both separators retained their original shape and dimensions during the entire life of the cell. Third, the glass tape allowed diffusion of electrolyte into the anode chamber as the anode was oxidized, yet it kept copper particles from reaching the anode surface. Fabrication is also easier because the glass tape is not as easily altered by handling as is the Vitron.

The results of this work were reported to the NASA Contract Manager. By NASA directive the glass tape replaced the Vitron as our separator material.

5.2.3 Standard Cell Design Tests at Three Temperatures

The objective of this phase of the work was to characterize the performance of the cells at three temperatures, namely, 371, 427 and 481°C.

These cells were constructed as described in Section 4.0 except that Varglas sleeving was used around the anode connector and the glass tape separator was used in place of the Vitron separator. Five cells were tested at each of the three above-mentioned temperatures. The results of these tests are shown in Table 1, Appendix 1 as test numbers 440 to 455 except for test number 445. In addition the results of these tests are summarized in Table 20 and typical curves are shown in Figures 35, 36 and 37 for each of the three temperatures.

Table 20

Cells With Glass Tape Separators

Temperature (°E)	Life (hrs.)	Cathode Utilization (%)	Self-Discharge Current (ma)	Tests Averaged: Tests Run
427	159.4 ± 2.5	86.7 ± 1.4	25.8 ± 2.4	5:5
371	76.2 ± 17.4	41.4 ± 9.6	15.9 ± 3.7	5:5
481	155.5 ± 4.7	84.7 ± 2.4	39.0 ± 6.9	4:5

The results of the testing at 371°C show short life and low self-discharge currents. The salt was much closer to its melting point during these tests than it is normally. Lithium chloride-potassium chloride eutectic melts at 352.5°C. This lower temperature increases the resistance and density of the electrolyte. Hence, lower voltages and self-discharge currents were expected. In addition these cells show a sharp decline in voltage after 10-15 hours life. This probably is an effect related to the increased concentration of magnesium chloride in the anolyte or lithium oxide in the catholyte. The addition of these reaction products cause an elevation in the electrolyte freezing point.

The tests run at 481°C did not indicate any significant decrease in life as compared to the tests at the design point, i.e. 427°C. Self-discharge rate, however, was slightly higher. As might be expected, the diffusion rate of the copper oxide to the magnesium anode was dependent upon temperature, i.e. the self-discharge rate was dependent on the temperature. At 371°C the self-discharge rate lower while at 481°C the self-discharge rate was the highest. The 427°C tests showed a self-discharge rate that was intermediate to the other two temperatures.

It appears from these results that highly efficient operation of this cell could take place at a temperature as low as 400°C. The reasonable upper limit of temperature is dictated by extremely high self-discharge rates.

6.0 Final Cell Design

A final cell design is given in Appendix III. This appendix gives a breakdown of design, construction and quality control of the cell. This appendix includes the following:

1. Engineering drawings
2. Fabrication flow chart
3. Operation sequences
4. Testing procedures
5. Inspection sequences
6. Material specifications
7. List of vendors

7.0 Delivery

Twenty cells were constructed according to the final design specifications given in Appendix III. Fifteen of these units were delivered to NASA and five were tested for NASA at the CRC facility. The results of these five were delivered as part of the final delivery items. The individual results of these tests are given in Table 1, Appendix I as test numbers 440 to 444 inclusive.

8.0 Summary of Accomplishments and Conclusions

All objectives of the program were successfully achieved. A summary of the conclusions are given below.

1. A complete quality control program and cell construction flow chart was formulated based on the successful experimental fabrication and testing of components and cells.
2. Fabrication techniques have been defined to produce cathodes with reproducible bulk densities.
3. Three mil copper needles produced cathodes with the best electrochemical performance.
4. Ten mil copper needles cannot be oxidized to 100% CuO by thermal oxidation.

5. A 61 ampere-hour cathode input capacity is required to reliably deliver 50 ampere-hours.
6. Cathode bulk densities can be controlled between 3.18 and 3.38 gms/cc and bulk density was accepted as a quality control measure.
7. Cathode surface areas are too low to be used as a quality control measure.
8. Within one sigma of the average, the pore volumes of the cathodes between 1 and 30 μ pore diameter fall in the range of 64.1 to 75.9% of the total volume.
9. Modulus of rupture tests on the cathode gives insufficient meaningful data to be used as a reliable quality control test.
10. Compression tests of the cathode show a one sigma range of 489 to 587 pounds using a 1/4" dia. plunger.
11. A nickel anode connector can be successfully used and joined to the anode by a threaded screw connection.
12. A double layer of 5 mil thick glass tape, square weave, separator gave the best performance in electrochemical testing.
13. Grade A nickel was found to be an effective cell case material.
14. Cell cases with ceramic terminal seals and electron-beam welded joints were shown to be hermetically sealed at room temperature and 800^oF.
15. Alite B-50-1 ceramic terminal seals was the most satisfactory terminal examined.
16. Weld joints and terminal seals were shown to be unaffected during thermal shock as determined by helium leak tests.
17. The terminal seals and weld joints remain unaffected at 800^oF in the presence of electrolyte and CuO over a 200 hour period as determined by actual runs and helium leak tests.
18. Fully assembled cells were found to be leak free and unaffected by heating to 800^oF. The components maintained their original position throughout the test, as determined by X-ray monitoring and post mortem examinations.

19. The use of Varglas sleeving around the anode connector prevents any significant terminal seal shorting.

20. The glass tape separator results in more reproducible performance than is possible with bulk Vitron "E".

21. The operating temperature range of this cell is approximately 400-480°C.

9.0 Recommendations

This section is designed to mention recommendations that are not specifically noted throughout the text. The following recommendations are aimed at the improvement of construction techniques and output performance of the cell. The following features are of particular importance in future use of this cell.

1. Reduction of electrolyte volume.
2. Reduce the case wall thickness from 50 mils to 10 mils.
3. Use reagent grade chemicals in preparing the electrolyte.
4. Keep the cathode thickness to a minimum and expand the cathode projected surface as much as possible.
5. Reduce the interelectrode spacing to decrease the internal resistance of the cell.
6. It is imperative to have a hermetic seal in this cell. Electrolyte creeps through the smallest holes causing corrosion. In addition, loss of electrolyte will eventually cause the cell to fail.

10.0 Distribution

National Aeronautics & Space Administration
Lewis Research Center
21000 Brookpark Road
Cleveland, Ohio 44135

Attn: Dr. L. Rosenblum (MS 302-1)
H. J. Schwartz (MS 309-1)
Dr. J. S. Fordyce (MS 6-1)
J. E. Dilley (MS 500-309)
Technology Utilization Office (MS 3-19)
W. J. Nagle (MS 309-1)
D. G. Soltis (MS 309-1)
V. Hlavin (MS 3-14)
Library (MS 60-3)
Report Control (MS 5-5)
Dr. B. Lubarsky, (MS 3-3)
W. A. Robertson (MS 309-1)
J. Toma (MS 302-1)

National Aeronautics & Space Administration
Scientific & Technical Information Division
Washington, D. C. 20546

Attn: RNW/E. M. Cohn
RNW/Arvin Smith
FC/A. M. Greg Andrus
RN/William H. Woodward
UT/Dr. S. J. Glassman

National Aeronautics & Space Administration
Goddard Space Flight Center
Greenbelt, Maryland 20771

Attn: Thomas Hennigan, Code 716.2
Gerald Halpert, Code 735
Joseph Sherfey, Code 735
Louis Wilson, Code 450

National Aeronautics & Space Administration
Langley Research Center
Instrument Research Division
Hampton, Virginia 23365

Attn: John L. Patterson, MS 472
M. B. Seyffert, MS 112

National Aeronautics & Space Administration
Geo C. Marshall Space Flight Center
Huntsville, Alabama 35812

Attn: Philip Youngblood
Richard Boehme (R-ASTR-EP)
C. B. Graff (S&E-ASTR-EP)

National Aeronautics & Space Admin.
Manned Spacecraft Center
Houston, Texas 77058
Attn: William R. Dusenbury (EP-5)

Attn: W. E. Rice (EP-5)
Attn: Robert Cohen
Gemini Project Office
Attn: Forrest E. Eastman (EE-4)

National Aeronautics & Space Admin.
Washington, D. C. 20546
Attn: Office of Technology Utilization

National Aeronautics & Space Admin.
Langley Research Center
Langley Station
Hampton, Virginia 23365
Attn: S. T. Pererson/Harry Ricker

National Aeronautics & Space Admin.
Scientific & Technical Information
Center: Input
P. O. Box 33
College Park, Maryland 20740
(2 copies plus 1 reproducible)

National Aeronautics & Space Admin.
Ames Research Center
Pioneer Project
Moffett Field, California 94035
Attn: Arthur Wilber/A. S. Hertzog

National Aeronautics & Space Admin.
Ames Research Center
Moffett Field, California 94035
Attn: Jon Rubenzer
Code PBS, MS 244-2

National Aeronautics & Space Admin.
Electronics Research Center
575 Technology Square
Cambridge, Massachusetts 02139
Attn: Dr. Sol Gilman, Code GPE

Jet Propulsion Laboratory
4800 Grove Drive
Pasadena, California 91103
Attn: Mr. Paul Goldsmith (MS 198-223)
Dr. R. Lutwack (MS 190-220)

Department of the Army

U. S. Army Mobility Equipment R&D Center
MERDC
Fort Belvoir, Virginia 22060
Electro Technology Lab
Energy Conversion Research Division

Commanding General
U. S. Army Weapons Command
Attn: AMSWE-RDR, Mr. G. Reinsmith
Rock Island Arsenal
Rock Island, Illinois 61201

U. S. Army Research Office
Box CM Duke Station
Durham, North Carolina 27706
Attn: Dr. Wilhelm Jorgensen

U. S. Army Research Office
Chief, R&D
Department of the Army
3D442, The Pentagon
Washington, D. C. 20546

U. S. Army Natick Laboratories
Clothing and Organic Materials Div.
Natick, Massachusetts 01762
Attn: L. A. Spano

Commanding Officer
U. S. Army Electronics R&D Labs
Fort Monmouth, New Jersey 07703
Attn: Power Sources Division (SELRA/PS)

Army Materiel Command
Research Division
AMCRD-RSCM-T-7
Washington, D. C. 20315
Attn: John W. Crellin

Army Materiel Command
Development Division
AMCRD-DE-MO-P
Washington, D. C. 20315
Attn: Marshall D. Aiken

U. S. Army TREGOM
Fort Eustis, Virginia 23604
Attn: Leonard M. Bartone (SMOFE-ASE)
Dr. R. L. Eshols (SMOFE-PSG)

U. S. Army Mobility Command
Research Division
Warren, Michigan 48090
Attn: O. Renius (AMSMO-RR)

Harry Diamond Laboratories
Room 300, Building 92
Conn. Ave & Van Ness St., N. W.
Washington, D. C. 20438
Attn: Nathan Kaplan

Department of the Navy

Office of Naval Research
Washington, D. C. 20360
Attn: Director, Power Program
Code 473

Office of Naval Research
Department of the Navy
Washington, D. C. 20460
Attn: H. W. Fox (Code 472)

Naval Research Laboratory
Washington, D. C. 20390
Attn: Dr. J. C. White, Code 6160

Naval Ship R&D Center
Annapolis, Maryland 21402
Attn: J. H. Harrison, Code M760

U. S. Naval Observatory
Attn: Robt. E. Trumbule
STIC, Bldg. 52
Washington, D. C. 20390

Naval Air Systems Command
Department of the Navy
Washington, D. C. 20360
Attn: Milton Knight (Code AIR-340C)

Commanding Officer
(Code QEWE, E. Bruess/H. Schultz)
U. S. Naval Ammunition Depot
Crane, Indiana 47522
Attn: D. Miley, Code QEWE

Naval Weapons Center
Corona Laboratories
Corona, California 91720
Attn: William C. Spindler (Code 441)

U. S. Naval Observatory
Washington, D. C. 20390
Attn: R. E. Trumbule (STIC)
Bldg. 52

Naval Ordnance Laboratory
Silver Spring, Maryland 20910
Attn: Philip D. Cole (Doce 232)

Naval Ship Engineering Center
Washington, D. C. 20360
Attn: C. F. Viglotti (Code 6157D)

Bureau of Naval Weapons
Department of the Navy
Washington, D. C. 20360
Attn: Whitewall T. Beatson
(Code RAAE-52)

Naval Ship Systems Command
Washington, D. C. 20360
Attn: Bernard B. Rosenbaum
Code 03422

Department of the Air Force

Aero Propulsion Laboratory
Wright-Patterson AFB, Ohio 45433
Attn: James E. Cooper, APIP-1

AF Cambridge Research Lab
Attn: CRFE
L. G. Hanscom Field
Bedford, Massachusetts 01731
Attn: Dr. R. Payne

AF Cambridge Research Lab
L. G. Hanscom Field
Bedford, Massachusetts 01731
Attn: Francis X. Doherty, CRE
Edward Raskind (Wing F)

Headquarters, U. S. Air Force (AFRDR-AS)
Washington, D. C. 20325
Attn: Major G. Starkey

Headquarters, U. W. Air Force (AFRDR-AS)
Washington, D. C. 20325
Attn: Lt. Col. William G. Alexander

Rome Air Development Center, ESD
Attn: Frank J. Mollura (EMEAM)
Griffis AFB, New York 13442

Space Systems Division
Los Angeles Air Force Station
Los Angeles, California 90045
Attn: SSSD

Other Government Agencies

National Bureau of Standards
Washington, D. C. 20234
Attn: Dr. W. J. Hamer

National Bureau of Standards
Washington, D. C. 20234
Attn: Dr. A. Brenner

Office, Sea Warfare System
The Pentagon
Washington, D. C. 20310
Attn: G. B. Wareham

U. S. Atomic Energy Commission
Auxiliary Power Branch (SNAP)
Division of Reactor Development
Washington, D. C. 20325
Attn: Lt. Col. George H. Ogburn, Jr.

Lt. Col. John H. Anderson
Advanced Space Reactor Branch
Division of Reactor Development
U. S. Atomic Energy Commission
Washington, D. C. 20325

Mr. Donald A. Hoatson
Army Reactors, DRD
U. S. Atomic Energy Commission
Washington, D. C. 20545

Bureau of Mines
4800 Forbes Avenue
Pittsburgh, Pa. 15213
Attn: Dr. Irving Wender

Clearing House for Scientific &
Technical Information
5285 Port Royal Road
Springfield, Virginia 22151

Private Organizations

Aerojet-General Corporation
Chemical Products Division
Azusa, California 91702
Attn: William H. Johnson

Aerojet-General Corporation
Von Karman Center
Bldg. 312, Dept. 3111
Azusa, California 91703
Attn: Mr. Russ Fogle

Allis Chalmers Mfg. Co.
Advanced Electrochem Products Division
P. O. Box 540
Green Dale, Wisconsin 53129
Attn: Dr. H. J. Seim

Aeronutronic Division of Philco Corp.
Technical Information Services
Ford Road
Newport Beach, California 92663

Aerospace Corporation
P. O. Box 95085
Los Angeles, California 90045
Attn: Library Acquisition Group

Aerospace Corporation
Systems Design Division
2350 East El Segundo Boulevard
El Segundo, California 90246
Attn: John G. Krisilas

Allis-Chalmers Mfg. Co.
1100 South 70th Street
Milwaukee, Wisconsin 53201
Attn: Dr. P. Joyner

A.M.F.
Attn: R. J. Mosny/M. S. Mintz
689 Hope Street
Stamford, Connecticut 06907

American University
Mass. & Nebraska Avenue, N.W.
Washington, D. C. 20016
Attn: Dr. R. T. Foley
Chemistry Department

Arthur D. Little, Inc.
Acorn Park
Cambridge, Massachusetts 02140
Attn: Dr. James D. Birkett

Atomics International Division
North American Aviation, Inc.
8900 DeSota Avenue
Canoga Park, California 91304
Attn: Dr. H. L. Recht

Battelle Memorial Institute
505 King Avenue
Columbus, Ohio 43201
Attn: Dr. C. L. Faust

Bell Laboratories
Murray Hill, New Jersey 07974
Attn: U. B. Thomas/D.O. Feder

American Cyanamid Company
1937 W. Main Street
Stamford, Connecticut 06902
Attn: Dr. R. A. Haldeman

The Boeing Company
P. O. Box 3999
Seattle, Washington 98124
Attn: Sid Gross, MS 85-86, 2-7814

Borden Chemical Company
Central Research Lab.
P. O. Box 9524
Philadelphia, Pennsylvania 19124

Burgess Battery Company
Foot of Exchange Street
Freeport, Illinois 61032
Attn: Dr. Howard J. Strauss

C & D Batteries
Division of Electric Autolite Co.
Conshohocken, Pennsylvania 19428
Attn. Dr. Eugene Willihnganz

Calvin College, Science Bldg.
3175 Burton St., S.E.
Grand Rapids, Michigan 49506
Attn: Prof. T. P. Dirkse

Communications Satellite Corporation
1835 K Street, N.W.
Washington, D. C. 20036
Attn: Mr. Robt. Strauss

Catalyst Research Corporation
6101 Falls Road
Baltimore, Maryland 21209
Attn: Frederick Tepper

ChemCell Inc.
150 Dey Road
Wayne, New Jersey 07470

Cubic Corporation
9233 Balboa Avenue
San Diego, California 92123
Attn: Librarian

Delco Remy Division
General Motors Corporation
2401 Columbus Avenue
Anderson, Indiana 46011
Attn: J. A. Keralla

Bellcomm, Inc.
955 Lenfant Plaza North, S.W.
Washington, D. C. 20024
Attn: B. W. Moss
McDonnell-Douglas Corporation
Astropower Laboratory
2121 Campus Drive
Newport Beach, California 92663
Attn: Dr. George Moe

Dynatech Corporation
17 Tudor Street
Cambridge, Massachusetts 02139
Attn: R. L. Wentworth

Bellcomm
1100-17th Street, N.W.
Washington, D. C. 20036
Attn: B. W. Moss

Eagle-Picher Company
Post Office Box 47
Joplin, Missouri 64801
Attn: E. P. Broglio

ESB Inc.
P. O. Box 11097
Raleigh, North Carolina 27604
Attn: Director of Engineering

Electromite Corporation
2117 South Anne Street
Santa Ana, California 92704
Attn: R. H. Sparks

ESB Inc.
Research Center
19 West College Avenue
Yardley, Pennsylvania 19067
Attn: Librarian

Electrochemical & Water Desalination
Technology
13401 Kootenay Drive
Santa Ana, California 92705
Attn: Dr. Carl Berger

Electrochimica Corporation
1140 O'Brien Drive
Menlo Park, California 94025
Attn: Dr. Morris Eisenberg

Electro-Optical Systems, Inc.
300 North Halstead
Pasadena, California 91107
Attn: Martin Klein

E. I. DuPont Nemours & Co.
Engineering Materials Laboratory
Wilmington, Delaware 19898
Attn: J. M. Williams
Bldg. 304

Energetics Science, Inc.
4461 Bronx Blvd.
New York, New York 10470
Attn: Dr. H. G. Oswin

Elgin National Watch Company
107 National Street
Elgin, Illinois 60120
Attn: T. Boswell

Emhard Corporation
Box 1620
Hartford, Connecticut 06102
Attn: Dr. W. P. Cadogan

Engelhard Industries, Inc.
497 Delancy Street
Newark, New Jersey 07105
Attn: Dr. J. G. Cohn

Dr. Arthur Fleischer
466 South Center Street
Orange, New Jersey 07050

General Electric Company
P. O. Box 43
Schenectady, New York 12301
Attn: Dr. R. P. Hamlen

General Electric Company
Missile & Space Division
Spacecraft Department
P. O. Box 8555
Philadelphia, Pennsylvania 19101
Attn: K. L. Hanson, Room M-2614

General Electric Company
Battery Business Section
P. O. Box 114
Gainesville, Florida 32601
Attn: W. H. Roberts
Dr. R. L. Hadley

General Electric Company
Research & Development Center
P. O. Box 8
Schenectady, New York 12301
Attn: Whitney Library

Dr. P. L. Howard
Centreville, Maryland 21617

General Telephone & Electronics Labs
Bayside, New York 11352
Attn: Dr. Paul Goldberg

Gould Ionics, Inc.
P. O. Box 1377
Canoga Park, California 91304
Attn: Dr. J. E. Oxley

Globe-Union, Inc.
P. O. Box 591
Milwaukee, Wisconsin 53201
Attn: John R. Thomas

Gould-National Batteries, Inc.
Engineering & Research Center
2630 University Avenue, S.E.
Minneapolis, Minnesota 55418
Attn: D. L. Douglas

Gulton Industries
Alkaline Battery Division
1 Gulton Street
Metuchen, New Jersey 08840
Attn: Dr. H. N. Seiger

Grumman Aircraft
Plant 35, OAAP Project
Bethpage, Long Island, N.Y. 11714
Attn: J. S. Caraceni

Hughes Aircraft Corporation
Centinda Ave. & Teale Street
Culver City, California 90230
Attn: T. V. Carvey

G. & W. H. Corson, Inc.
Plymouth Meeting
Pennsylvania 19462
Attn: Dr. L. J. Minnick

Hughes Aircraft Corporation
Bldg. 366, M.S. 524
El Segundo, California 90245
Attn: M. E. Ellison

Hughes Research Labs. Corp.
3011 Malibu, California 90265
Attn: T. M. Hahn

ITT Federal Laboratories
500 Washington Avenue
Nutley, New Jersey 07110
Attn: Dr. P. E. Lighty

ITT Research Institute
10 West 35th Street
Chicago, Illinois 60616
Attn: Dr. H. T. Francis

Institute for Defense Analyses
R&E Support Division
400 Army-Navy Drive
Arlington, Virginia 22202
Attn: Mr. R. Hamilton

Institute for Defense Analyses
R&E Support Division
400 Army-Navy Drive
Arlington, Virginia 22202
Attn: Dr. R. Briceland

Idaho State University
Department of Chemistry
Pocatello, Idaho 83201
Attn: Dr. G. Myron Arcand

Institute of Gas Technology
State and 34th Street
Chicago, Illinois 60616
Attn: B. S. Baker

International Nickel Co.
1000-16th St., N.W.
Washington, D. C. 20036
Attn: Wm. G. Mearns

Johns Hopkins University
Applied Physics Laboratory
8621 Georgia Avenue
Silver Spring, Maryland 20910
Attn: Richard E. Evans

Johns-Manville R&E Center
P. O. Box 159
Manville, New Jersey 08835
Attn: J. S. Parkinson

Leesona Moos Laboratories
Lake Success Park, Community Drive
Great Neck, New York 11021
Attn: Dr. A. Moos

Honeywell Inc.
Livingston Electronic Laboratory
Route 309
Montgomeryville, Pennsylvania 18936
Attn: Library

Lockheed Missiles & Space Company
P. O. Box 504
Sunnyvale, California
Attn: R. E. Corbett
Dept. 62-14, Bldg. 154

Lockheed Missiles & Space Company
Dept. 62-30
3251 Hanover Street
Palo Alto, California 94304
Attn: J. E. Chilton

Mallory Battery Company
South Broadway & Sunnyside Lane
Tarrytown, New York 10591
Attn: R. R. Clune

P. R. Mallory & Co., Inc.
Northwest Industrial Park
Burlington, Massachusetts 01803

P. R. Mallory & Company, Inc.
Technical Services Laboratory
Indianapolis, Indiana 46206
Attn: Technical Librarian

Marquardt Corporation
16555 Saticoy Street
Van Nuys, California 91406
Attn: Dr. H. G. Krull

Martin Company
Electronics Research Department
P. O. Box 179
Denver, Colorado 80201
Attn: William B. Collins, MS 1620
Attn: M. S. Imanura, MS 8840

Material Research Corporation
Orangeburg, New York 10962
Attn: V. E. Adler

Mauchly Systems, Inc.
Montgomeryville Industrial Park
Pennsylvania 18936
Attn: John H. Waite

Melpar
Technical Information Center
7700 Arlington Boulevard
Falls Church, Virginia 22046

McDonnell Douglas Corp.
3000 Ocean Park Blvd.
Santa Monica, California 90406
Attn: A. D. Tonelli, MS-7C

North American Rockwell
Autonetics Division
P. O. Box 4181
Anaheim, California 92803
Attn: R. F. Fogle GFIG

Metals and Controls Division
Texas Instruments, Inc.
34 Forrest Street
Attleboro, Massachusetts 02703
Attn: Dr. E. M. Jost/Dr. J. W. Ross

Midwest Research Institute
425 Volker Boulevard
Kansas City, Missouri 64110
Attn: Physican Science Laboratory

North American Aviation, Inc.
12214 Lakewood Boulevard
Downey, California 90241
Attn: Burton M. Otzinger

North American Aviation, Inc.
Rocketdyne Division
6633 Canoga Avenue
Canoga Park, California 91303
Attn: Library

North American Aviation Co.
S&ID Division
Downey, California 90241
Attn: Dr. James Nash

Oklahoma State University
Stillwater, Oklahoma 74075
Attn: Prof. William L. Hughes
School of Electrical Engineering

Dr. John Owen
P. O. Box 87
Bloomfield, New Jersey 07003

Power Information Center
University City Science Institute
3401 Market St., Rm. 2107
Philadelphia, Pennsylvania 19104

Prime Battery Corporation
15600 Cornet Street
Santa Fe Springs, Calif., 90670
Attn: David Roller

Portable Power Sources Corp.
122 East 42nd Street
New York, New York 10017
Attn: L. Schulman

RAI Research Corporation
36-40 37th Street
Long Island City, New York 11101

Philco Corporation
Division of the Ford Motor Company
Blue Bell, Pennsylvania 19422
Attn: Dr. Phillip Colet

Radio Corporation of America
Astro Corporation
P. O. Box 800
Hightstown, New Jersey 08540
Attn: Seymour Winkler

Philco-Ford Corporation
Space Power & Prop. Dept, MS W-49
3825 Fabian Way
Palo Alto, California 94303
Attn: Mr. D. G. Briggs

Radio Corporation of America
415 South Fifth Street
Harrison, New Jersey 07029
Attn: Dr. G. S. Lozier
Bldg. 18-2

Southwest Research Institute
8500 Culebra Road
San Antonio, Texas 78206
Attn: Library

Thomas A. Edison Research Laboratory
McGraw Edison Company
Watchung Avenue
West Orange, New Jersey 07052
Attn: Dr. P. F. Greiger

Texas Instruments, Inc.
P. O. Box 5936
Dallas, Texas 75222
Attn: Dr. Isaac Trachtenberg

Stanford Research Institute
820 Mission Street
South Pasadena, California 91030
Attn: Dr. F. R. Kalhammer

TRW Systems Inc.
One Space Park
Redondo Beach, California 90278
Attn: Dr. A. Krausz,
Bldg. 60, Rm. 1047

TRW Systems Inc.
One Space Park
Redondo Beach, California 90278
Attn: Dr. Herbert P. Silverman (R-1/2094)
Dr. W. R. Scott (M-2/2154)

TRW, Inc.
2355 Euclid Avenue
Cleveland, Ohio 44117
Attn: Librarian

Tyco Laboratories, Inc.
Bear Hill
Hickory Drive
Waltham, Massachusetts 02154
Attn: Dr. A. C. Makrides

Unified Sciences Associates, Inc.
2925 E. Foothill Blvd.
Pasadena, California 91107
Attn: Dr. S. Naiditch

Union Carbide Corporation
Development Laboratory Library
P. O. Box 6056
Cleveland, Ohio 44101

Union Carbide Corporation
Parma Laboratory
P. O. Box 6116
Parma, Ohio 44130
Attn: Dr. Robert Powers

University of California
Space Science Laboratory
Berkeley, California 94720
Attn: Dr. C. W. Tobias

University of Pennsylvania
Electrochemistry Laboratory
Philadelphia, Pennsylvania 19104
Attn: Prof. John O'M. Bockris

University of Toledo
Toledo, Ohio 43606
Attn: Dr. Albertine Krohn

Westinghouse Electric Corporation
Research and Development Center
Churchill Borough
Pittsburgh, Pennsylvania 15235
Attn: Dr. C. C. Hein

Whittaker Corporation
Narmco R&D Division
3540 Aero Court
San Diego, California 92123
Attn: Dr. M. Shaw

Yardney Electric Corporation
40 Leonard Street
New York, New York 10013
Attn: Dr. Geo. Dalin

Whittaker Corporation
3850 Olive Street
Denver, Colorado 80237
Attn: J. W. Reiter/Borch Wendir

Western Electric Company
Suite 802, RCA Building
Washington, D. C. 20006
Attn: R. T. Fiske

Westinghouse Electric Corporation
Research & Development Center
Churchill Borough
Pittsburgh, Pennsylvania 15235
Attn: Dr. A. Langer

11.0 Appendices

Appendix I - Figures and Table of Cell Test Data

Appendix II - Sample Calculations

Appendix III - Quality Control, Flow Chart, Fabrication and
Testing Procedures

Appendix I - Figures and Table of Cell Test Data

Table 1 - Cell Test Data -----	66
Figure 1 - Cross Section of 50 A-Hr Cell -----	73
Figure 2 - E vs. T - Typical Curves - 3 mil Needle Cathodes -----	74
Figure 3 - E vs. T - Typical Curves - 5 mil Needle Cathodes -----	75
Figure 4 - E vs. T - Typical Curves - 10 mil Needle Cathodes -----	76
Figure 5 - E vs. T - Typical Curves - 62.5 A-Hr Cathodes -----	77
Figure 6 - E vs. T - Typical Curves - 83.5 A-Hr Cathodes -----	78
Figure 7 - E vs. T - Two Additional Tests - 71.5 A-Hr Cathodes -----	79
Figure 8 - E vs. T - Cathode Input vs. Cathode Output -----	80
Figure 9 - Cathode Input Capacity vs. Percent Cathode Utilization -----	81
Figure 10 - Pore Volume vs. Pore Diameter for a Typical Electrode -----	82
Figure 11 - Pore Volume per Decade vs. Log of Pore Diameter for Electrode No. 24 -----	83
Figure 12A - Fixture Base -----	84
Figure 12B - Top Plate -----	85
Figure 12C - Spring -----	86
Figure 12D - Spring Retainer Pin -----	87
Figure 12E - Spring Retainer Washer -----	87
Figure 12F - Modulus of Rupture Plunger -----	88
Figure 12G - Small Half-Moon Surface -----	89
Figure 12H - Large Half-Moon Surface -----	90
Figure 12I - Knife Edge Surface -----	91
Figure 12J - Assembled Fixture -----	92
Figure 13 - Compression Plunger -----	93
Figure 14 - Separator Resistance vs. Time -----	94
Figure 15 - E vs. T - Test No.'s - 342, 343, 344 -----	95
Figure 16 - E vs. T - Test No.'s - 339, 340, 341 -----	96
Figure 17 - E vs. T - Test No.'s - 333, 334, 335 -----	97
Figure 18 - E vs. T - Test No.'s - 336, 337, 338 -----	98
Figure 19 - Cell Case Assembly -----	99
Figure 20 - High Temperature Leak Testing Apparatus -----	100

Figure 21 - Ceramic Terminal Seals -----	101
Figure 22 - X-Ray Positive of Cells After Heating -----	102
Figure 23 - E vs. T - Typical Curves - Control Cells at 427°C -----	103
Figure 24 - E vs. T - Typical Curves - Control Cells at 481°C -----	104
Figure 25 - E vs. T - Typical Curves - Control Cells at 538°C -----	105
Figure 26 - Log of Percent Loss of Life vs. $\frac{1}{T}$ -----	106
Figure 27 - Work Alternate Flow Chart -----	107
Figure 28 - E vs. T - Typical Curves - Control Cells with Modifications ---	108
Figure 29 - E vs. T - Typical Curves - Environmentally Tested -----	109
Figure 30A - Ceramic Terminal Seal - Alite D-312 -----	110
Figure 30B - Ceramic Terminal Seal - Alite B-50-1 -----	110
Figure 30C - Ceramic Terminal Seal - Alite B-75-1 -----	111
Figure 31A - Anode Connector - Alite D-312 Seal -----	112
Figure 31B - Anode Connector - Alite B-50-1 Seal -----	113
Figure 31C - Anode Connector - Alite B-75-1 Seal -----	114
Figure 32 - E vs. T - Typical Curves - Alite - D-312 Seal -----	115
Figure 33 - E vs. T - Typical Curves - Alite B-50-1 Seal -----	116
Figure 34 - E vs. T - Tests 433 and 439 -----	117
Figure 35 - E vs. T - Typical Curves - Glass Tape -427°C -----	118
Figure 36 - E vs. T - Typical Curves - Glass Tape -481°C -----	119
Figure 37 - E vs. T - Typical Curves - Glass Tape -371°C -----	120

The Figures denoted "E vs. T - Typical Curves" reflect the average deviation in life of a set of duplicate tests. The dashed lines show the upper end of the deviation and the solid lines the lower end. The upper lines are the voltages of each cell at 278 ma. current drain for 54 minutes out of each hour. The corresponding lower lines are the voltages at 833 ma. for 6 minutes out of each hour.

Table 1 - Cell Test Data

Test No.	Cathode Capacity (A-Hrs)	Anode Capacity (A-Hrs)	Cathode Efficiency (%)	Anode Efficiency (%)	Cell Life (Hrs)	I _{s.d.} (ma)	Output (A-Hrs)	Diameter (in)
<u>Copper Needle Size</u>								
258	71.3	86.8	64.0	80.1	136.7	83.1	45.7	0.003
259	71.4	86.9	73.9	77.9	158.5	94.3	52.7	0.003
270	71.6	86.9	81.8	90.3	175.5	34.4	59.6	0.003
271	71.7	86.9	88.6	92.4	188.9	28.1	63.0	0.003
272	71.5	86.7	55.5	94.9	117.8	17.5	39.4	0.003
262	70.2	86.9	64.4	84.2	135.5	62.4	45.3	0.005
274	71.2	87.0	77.1	95.8	163.2	56.4	54.6	0.005
281	71.3	86.9	67.6	76.9	144.3	89.2	48.2	0.005
284	71.2	87.4	64.7	76.0	138.0	89.7	46.1	0.005
286	71.1	87.5	56.7	63.9	132.0	146.7	40.4	0.005
268	62.9	86.8	59.8	--	84.9	--	37.6	0.010
275	56.5	86.8	45.9	95.6	77.5	15.3	25.9	0.010
276	47.9	86.9	60.2	96.1	86.4	13.1	28.8	0.010
278	59.6	87.0	67.0	93.6	127.5	20.0	40.0	0.010
279	58.0	86.4	68.3	95.0	117.8	17.4	39.4	0.010
<u>Cathode Capacity</u>								
300	62.3	77.7	86.1	93.2	160.5	23.7	53.6	
301	62.4	77.8	84.1	89.7	157.0	36.7	52.4	
304	62.6	77.9	86.1	94.8	161.4	17.4	53.9	
309	62.6	77.9	81.2	83.5	152.0	57.2	50.8	
316	62.2	77.6	70.9	80.3	132.0	78.2	44.1	
259	71.4	86.9	73.9	77.9	158.5	94.3	52.7	0.003
270	71.6	86.9	81.8	90.3	175.5	34.4	59.6	0.003
271	71.7	86.9	88.6	92.4	188.9	28.1	63.0	0.003
317	71.7	86.8	67.6	80.3	145.0	82.2	48.4	
319	71.5	87.4	72.1	92.7	154.3	25.2	51.5	
294	82.8	100.8	76.9	79.0	190.5	88.3	63.6	
296	82.9	100.6	77.2	92.3	191.5	27.6	64.0	
297	82.9	100.6	73.9	86.4	183.5	49.8	61.3	
306	83.0	100.6	65.0	83.2	161.4	45.0	53.9	
307	82.9	100.1	75.5	94.9	187.3	13.9	62.6	

Table 1 - Cell Test Data

Test No.	Cathode Capacity (A-Hrs)	Anode Capacity (A-Hrs)	Cathode Efficiency (%)	Anode Efficiency (%)	Cell Life (Hrs)	I _{s.d.} (ma)	Output (A-Hrs)	Separator Thickness (cm)
<u>Separator Thickness</u>								
342	61.2	73.6	79.4	94.8	145.5	16.7	48.6	0.5
343	61.3	73.5	75.2	96.5	138.0	12.1	46.1	0.5
344	61.1	73.6	82.2	95.3	150.5	15.3	50.3	0.5
339	61.1	73.7	82.8	95.3	151.5	15.6	50.6	1.0
340	61.2	73.7	27.3	91.8	50.0	23.1	16.7	1.0
341	61.2	73.7	81.6	95.5	149.5	14.8	49.9	1.0
333	61.1	73.6	88.1	97.9	161.0	7.0	53.8	1.5
334	61.1	73.5	85.6	95.9	156.5	13.4	52.3	1.5
335	61.1	73.4	90.0	97.6	164.5	8.0	54.9	1.5
336	61.1	73.8	90.0	96.7	164.5	11.3	54.9	2.0
337	61.1	73.6	78.4	94.6	143.5	19.2	47.9	2.0
338	61.3	73.2	72.2	94.3	132.5	18.5	44.3	2.0
<u>Control Cells</u>								
								<u>Temperature (°F)</u>
357	61.1	73.5	81.2	94.8	148.5	18.0	49.6	800
366	61.1	72.9	79.3	95.1	146.0	15.4	48.8	800
375	61.1	73.5	85.6	95.9	156.5	13.3	52.3	800
376	61.1	73.8	90.0	96.7	164.5	12.2	54.9	800
377	61.1	73.3	82.8	95.3	151.5	16.6	50.6	800
378	61.2	73.3	81.6	94.5	149.5	14.1	49.9	800
379	61.3	73.6	79.4	94.8	145.5	16.7	48.6	800
380	61.1	73.7	82.2	95.3	150.5	15.3	50.3	800
381	61.1	73.2	83.2	91.6	152.0	27.2	50.8	800
382	61.3	73.3	80.7	90.7	148.0	34.0	49.9	800
393	61.1	72.8	60.2	75.5	110.0	102.7	36.7	900
394	61.3	73.2	37.6	69.8	69.0	103.1	23.1	900
395	61.3	73.2	79.0	92.3	45.0	27.6	48.4	900
396	61.3	73.3	79.0	88.3	145.0	44.2	48.4	900
397	61.1	73.5	71.7	82.5	131.0	66.4	43.8	900

Table 1 - Cell Test Data

Test No.	Cathode Capacity (A-Hrs)	Anode Capacity (A-Hrs)	Cathode Efficiency (%)	Anode Efficiency (%)	Cell Life (Hrs)	I _{s.d.} (ma)	Output (A-Hrs)	Temperature (°F)
398	61.1	73.3	40.2	59.9	73.5	181.7	24.6	1000
399	61.3	72.9	24.5	71.0	45.0	129.1	15.0	1000
400	61.1	73.2	26.0	49.1	47.5	335.6	15.9	1000
401	61.2	73.2	28.1	40.8	51.5	339.3	17.2	1000
402	61.4	73.3	14.7	42.9	27.0	252.6	9.0	1000
<u>Control Cells With Modifications</u>								
403	61.1	72.7	73.6	91.9	134.5	27.8	44.9	800
404	61.2	73.4	54.6	93.8	100.5	22.1	33.6	800
405	61.4	73.2	67.2	92.6	123.5	26.5	41.3	800
406	61.3	72.8	54.0	94.0	114.5	20.4	38.1	800
407	61.4	72.6	74.3	93.9	136.5	20.9	46.6	800
409	61.3	72.8	67.9	93.0	124.5	22.9	41.6	800
410	61.1	73.0	68.7	90.4	125.5	32.3	41.9	800
411	61.1	73.1	65.9	93.2	120.5	21.3	40.2	800
412	61.1	73.1	68.7	94.3	125.5	18.3	41.9	800
413	61.4	73.3	72.9	93.1	134.0	24.2	44.8	800
<u>Environmental Cells With Modifications</u>								
415	61.5	73.1	70.6	91.2	130.0	29.7	43.4	800
416	61.1	73.2	39.6	99.3	72.5	2.2	24.2	800
417	61.3	73.3	31.3	71.3	57.5	140	19.2	800
418	61.1	73.2	9.6	26.9	17.5	647	5.8	800
419	61.5	73.2	49.2	90.2	90.5	35.1	30.2	800
<u>Cells With Alternate Terminal Seals</u>								
428	61.5	73.0	71.4	76.4	131.5	91.7	43.9	D-312
429	61.5	73.1	81.0	84.6	149.0	54.7	49.8	D-312
430	61.3	73.5	67.9	71.8	124.5	110	41.6	D-312
431	61.5	73.0	89.7	94.9	165.0	17.9	55.1	D-312
432	61.3	73.0	64.8	72.6	119.0	124	39.8	D-312
423	61.1	73.7	84.2	92.9	154.0	24.5	51.4	B-50-1
424	61.1	72.7	66.1	99.1	121.0	2.6	40.4	B-50-1
425	61.5	73.2	42.4	97.0	78.0	8.5	26.1	B-50-1
426	61.3	73.1	67.6	76.6	124.0	87.2	41.4	B-50-1
427	61.2	73.2	84.6	98.5	155.0	5.0	51.8	B-50-1

Table 1 - Cell Test Data

Test No.	Cathode Capacity (A-Hrs)	Anode Capacity (A-Hrs)	Cathode Efficiency (%)	Anode Efficiency (%)	Cell Life (Hrs)	I _{s.d.} (ma)	Output (A-Hrs)	Terminal Seal
434	61.3	73.1	1.1	63.8	2.0	22.4	0.7	B-75-1
435	61.5	73.2	37.8	90.8	69.5	33.6	23.2	B-75-1
436	61.4	72.8	84.3	93.7	155.0	21.8	51.8	B-75-1
437	61.5	73.1	8.1	89.3	15.0	35.3	5.0	B-75-1
438	61.3	72.9	87.1	91.4	160.0	31.3	53.4	B-75-1
<u>Cells With Glass Tape Separators</u>								<u>Temperature</u> (°F)
440	61.5	73.0	85.6	91.8	158.0	28.8	52.8	800
441	61.4	73.1	87.6	93.6	161.0	22.2	53.8	800
442	61.3	73.8	84.4	93.1	155.0	23.2	51.8	800
443	61.4	73.0	86.5	92.0	159.0	28.0	53.1	800
444	61.5	73.0	89.1	92.6	164.0	26.6	54.8	800
446	61.3	73.2	46.3	94.9	85.0	12.6	28.4	700
447	61.5	73.5	24.1	93.2	45.0	23.2	15.0	700
448	61.5	73.1	34.8	94.7	64.0	17.9	21.4	700
449	61.3	73.2	50.1	95.2	92.0	12.9	30.7	700
450	61.5	73.1	51.7	95.3	95.0	12.9	31.7	700
451	61.3	73.0	14.4	89.2	26.5	33.4	8.9	900
452	61.5	73.1	88.6	91.4	163.0	30.5	54.4	900
453	61.3	73.3	89.5	90.2	155.0	33.8	51.8	900
454	61.4	73.2	80.0	85.3	147.0	50.5	49.1	900
455	61.3	73.0	85.6	88.4	157.0	41.3	52.4	900

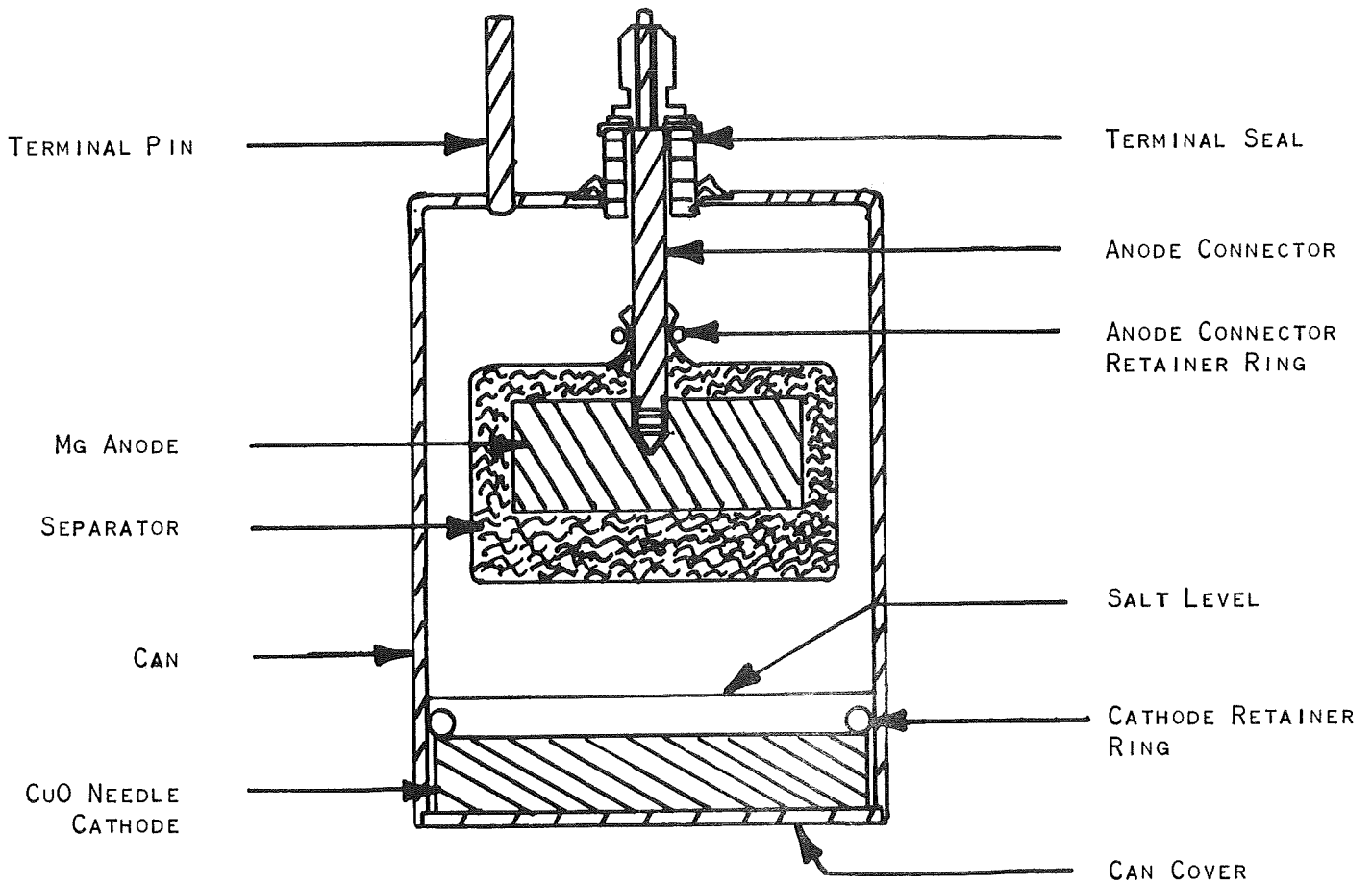


FIGURE 1. CROSS-SECTION OF 50 A-HR. CELL

Figure 2 - Cathode Needle Size
Needle Size = 0.003"
Test No. 270 Test No. 258

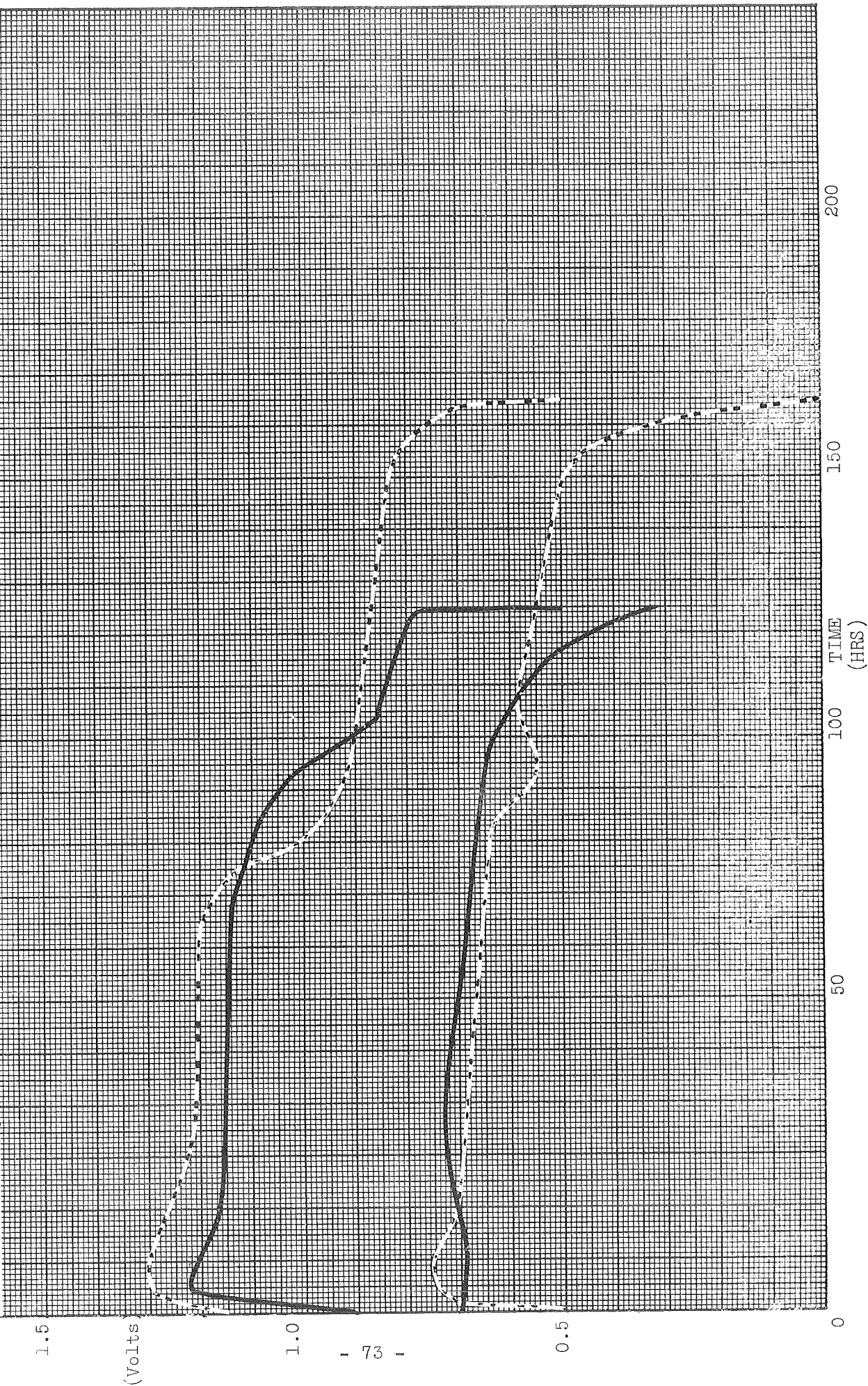


Figure 3 - Cathode Needle Size
Needle Size = 0.005"
Test No. 274 Test No. 262

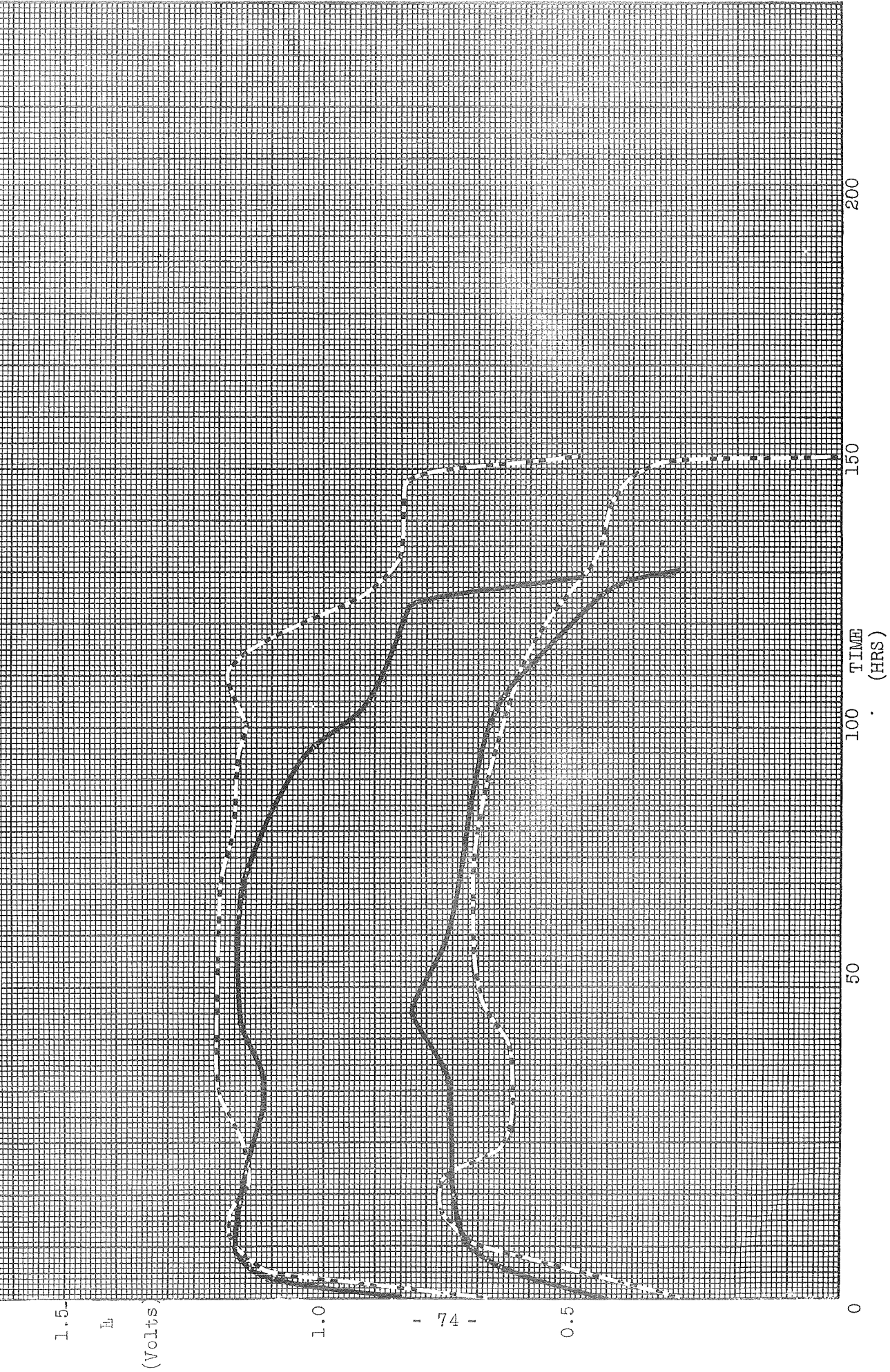


Figure 4 - Cathode Needle Size
Needle Size = 0.010"
Test No. 279 Test No. 276

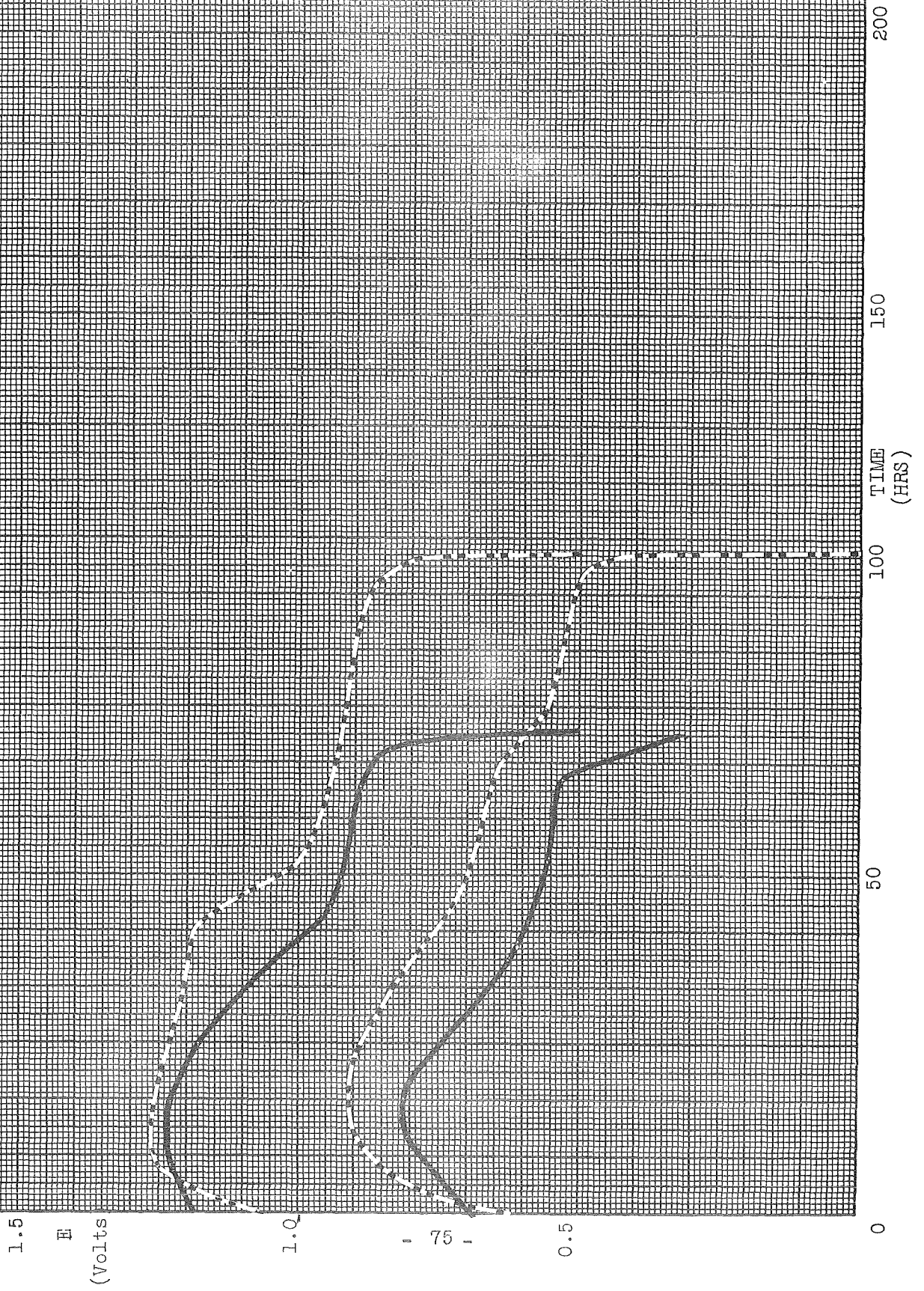


Figure 5 - Cathode Capacity
62.5 Ampere - Hours
Test No. 304 Test No. 309

1.5
E
(Volts)

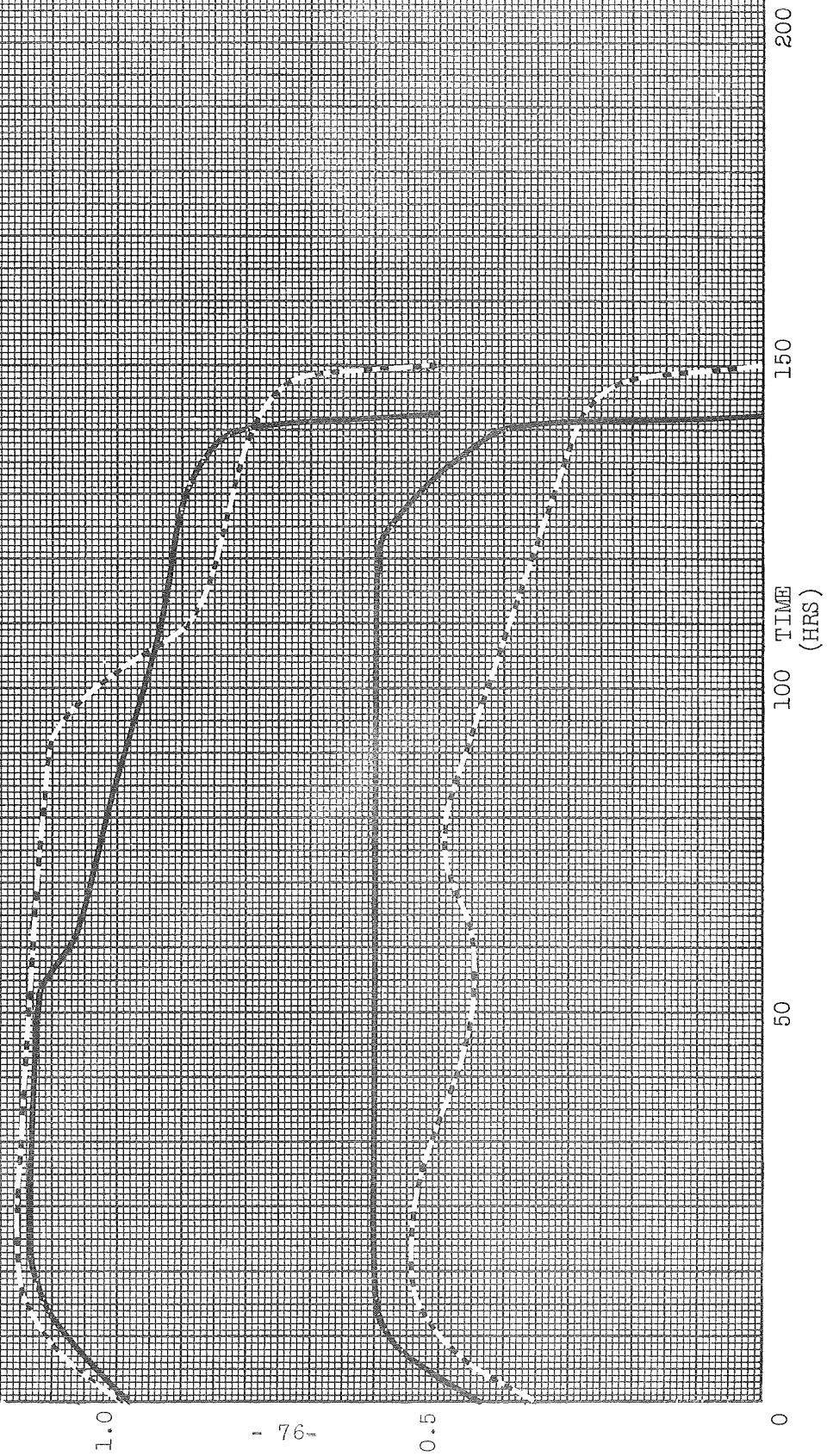


Figure 6 - Cathode Capacity
83.5 Ampere - Hours
Test No. 296 Test No. 297

1.5
E
(Volts)

1.0

- 77 -

0.5

0

200
150
100
50
TIME
(HRS)

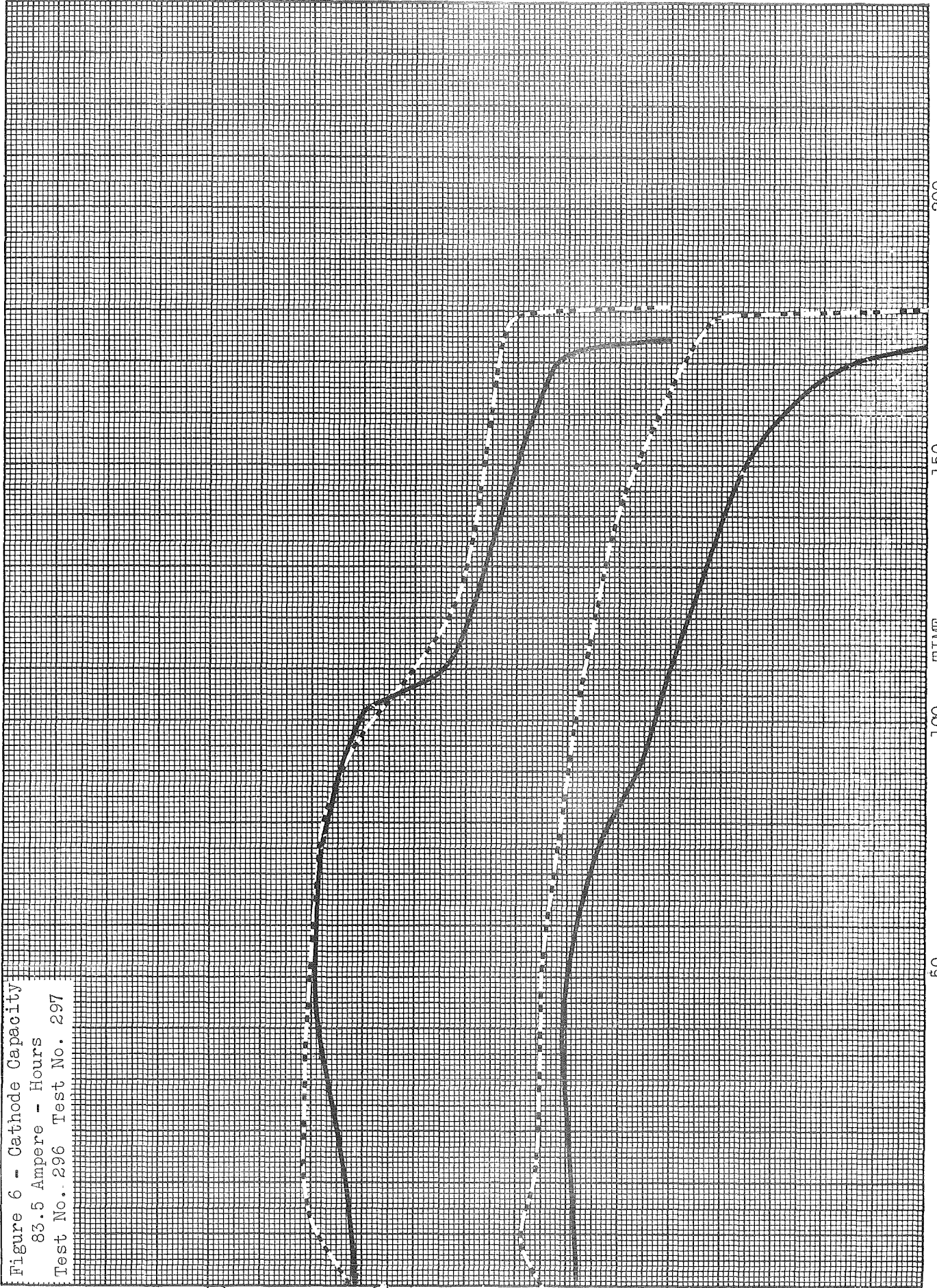


Figure 7 - Cathode Capacity
71.5 Ampere - Hours
2 additional cells
Test No. 317 Test No. 319

1.5

E

(Volts)

1.0

- 78 -

0.5

0

200

150

100

50

0

TIME
(HRS)

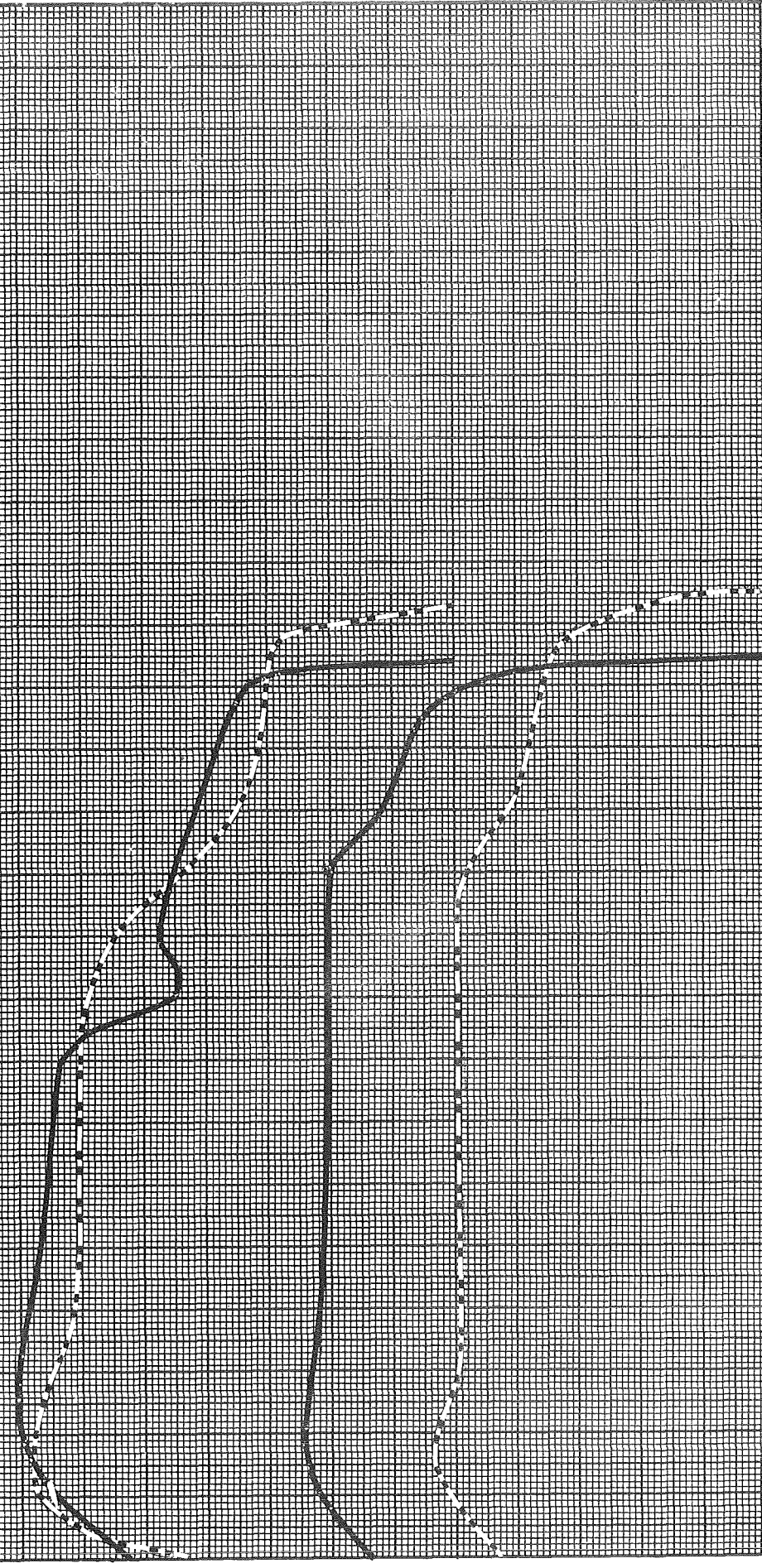


FIGURE 8
CATHODE INPUT CAPACITY VS.
CATHODE OUTPUT CAPACITY

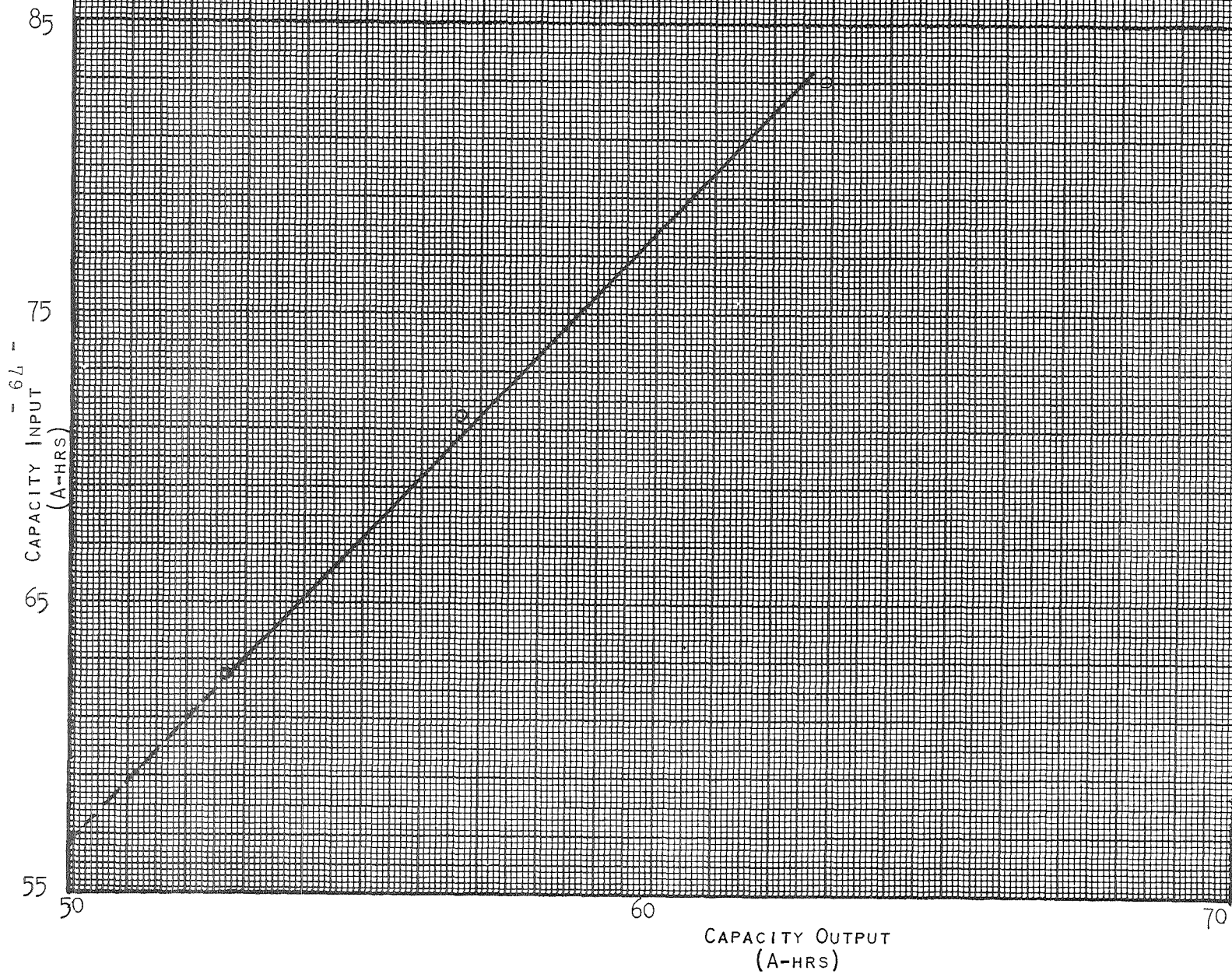


FIGURE 9
CATHODE INPUT CAPACITY VS.
CATHODE PERCENT UTILIZATION

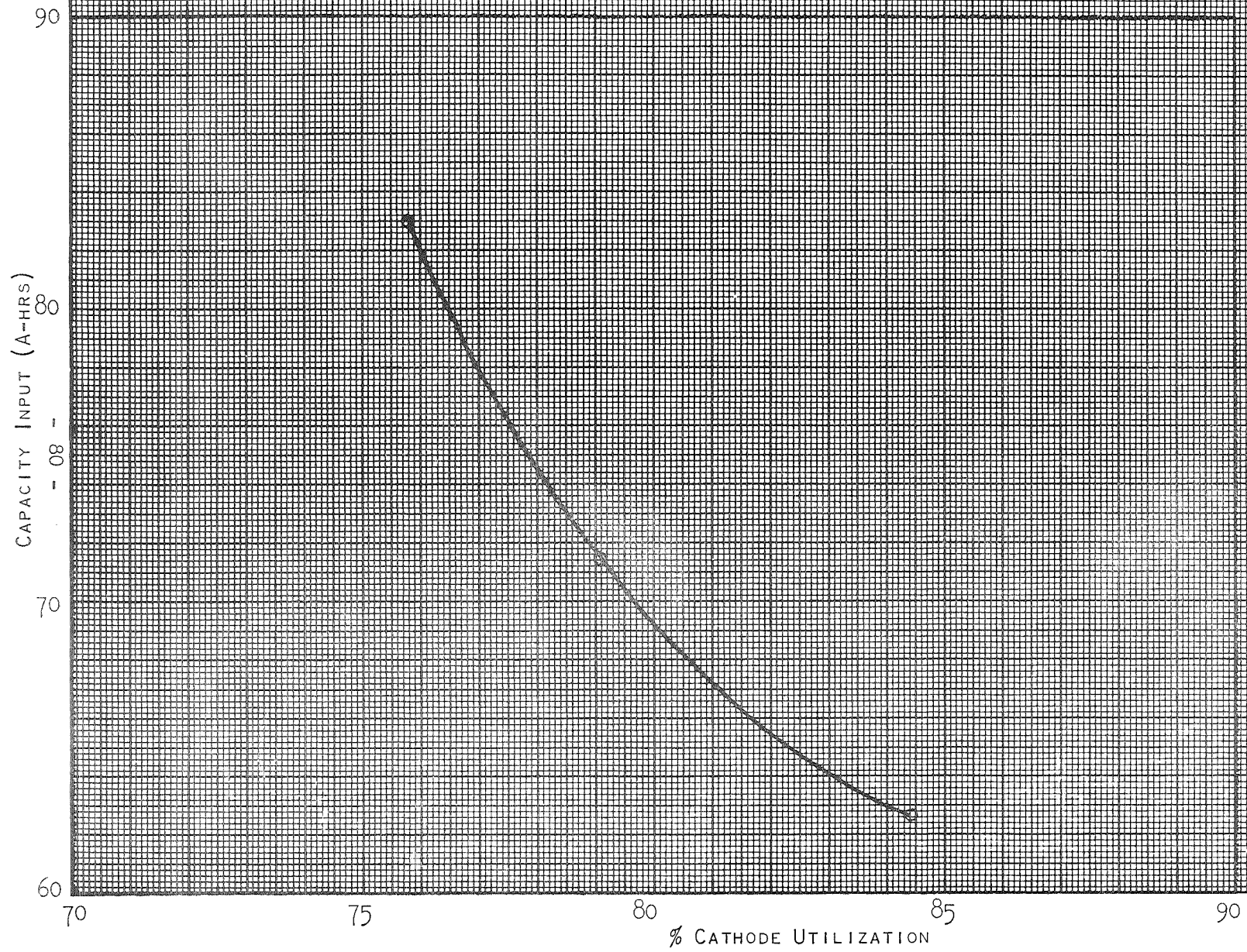


FIGURE 10
 PORE VOLUME VS. PORE DIAMETER
 FOR ELECTRODE No. 22

Cat. No. 5-7135

POROSITY DETERMINATION

(By 5-7107 or 5-7108 Aminco—Winslow Porosimeter)

DATE November 7, 1968

SAMPLE Electrode Assembly #22 Measured Pore Volume: 0.12 cc/g.

WT. OF SAMPLE, G. 1.2980

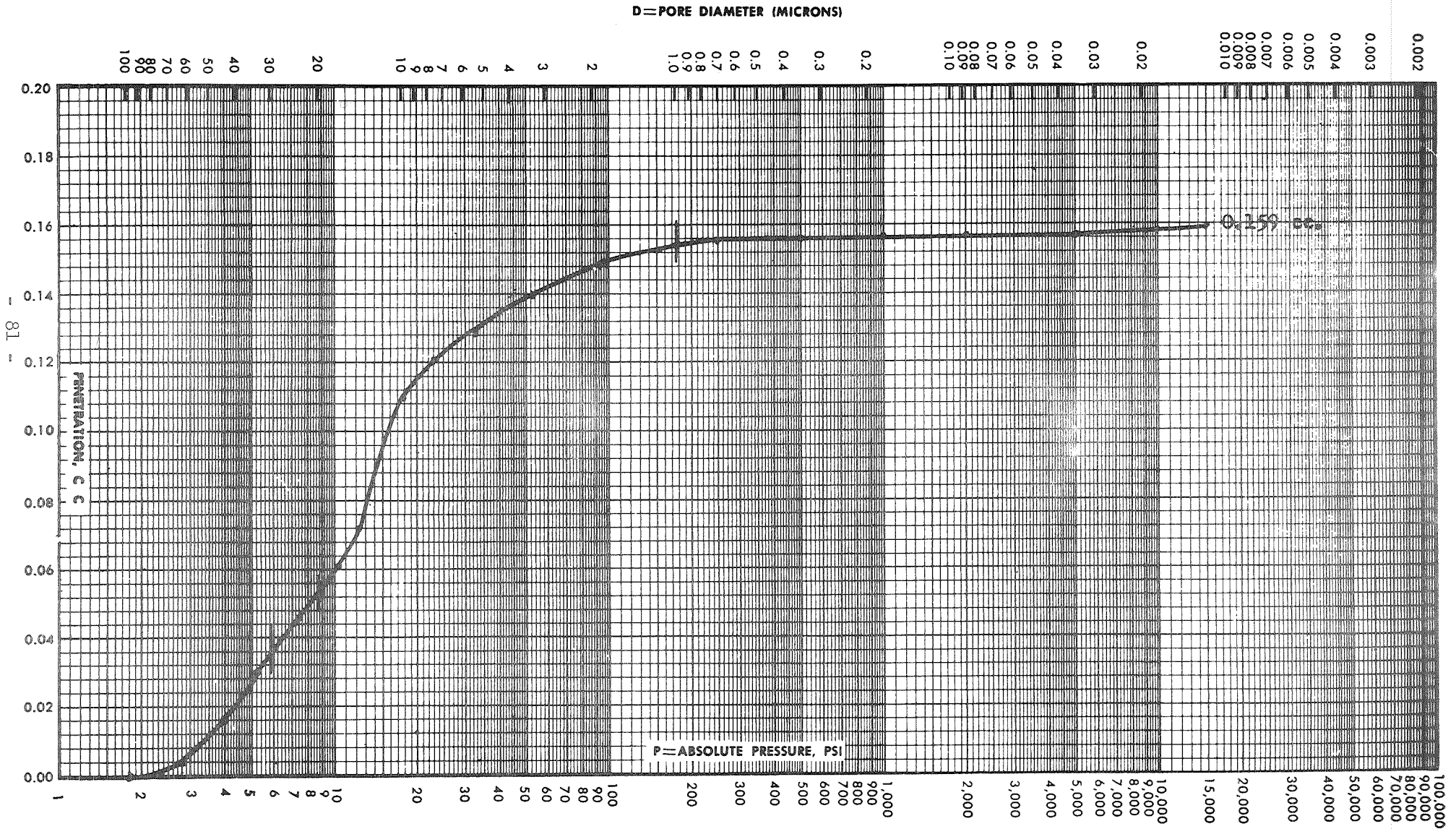
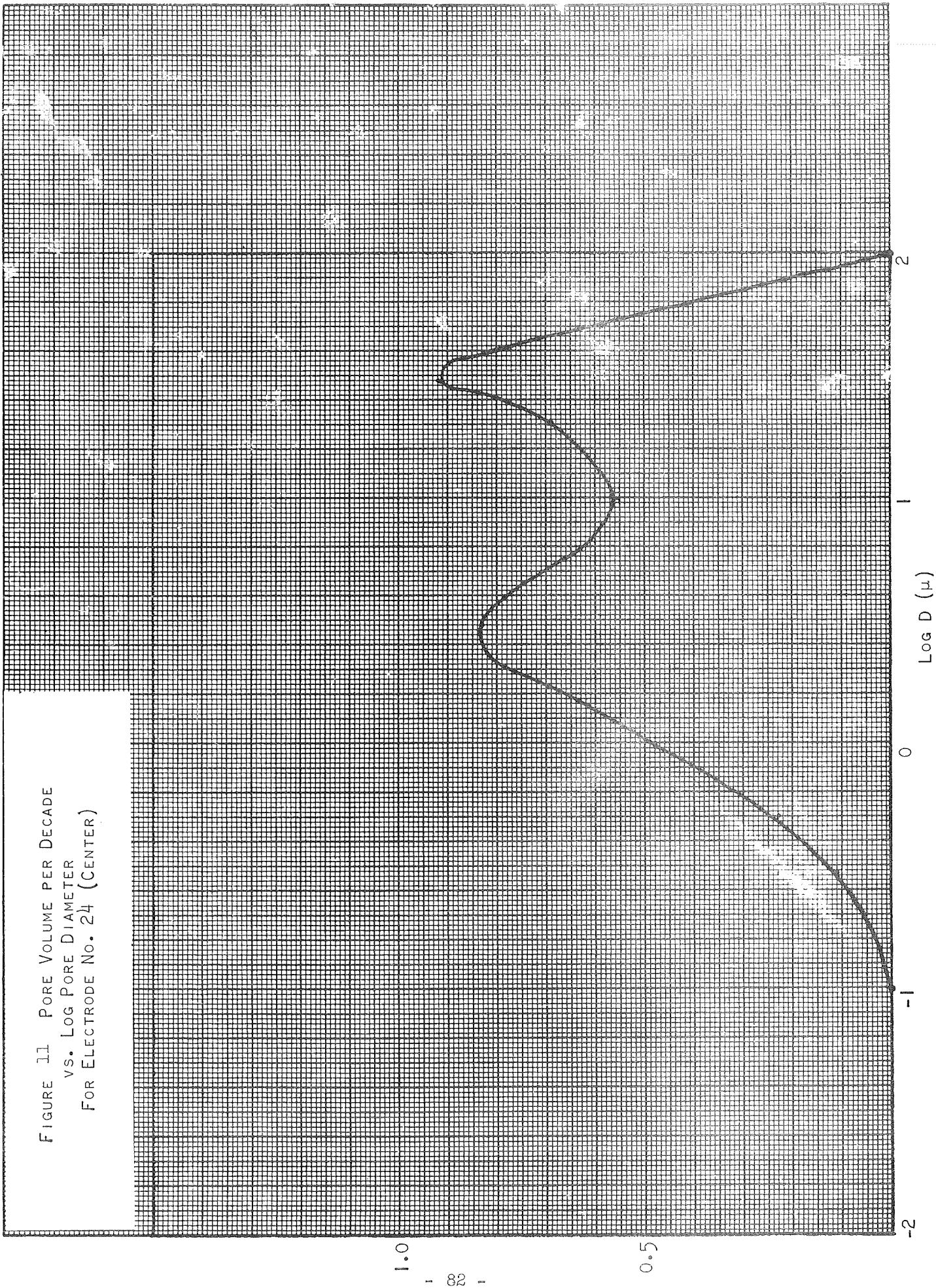
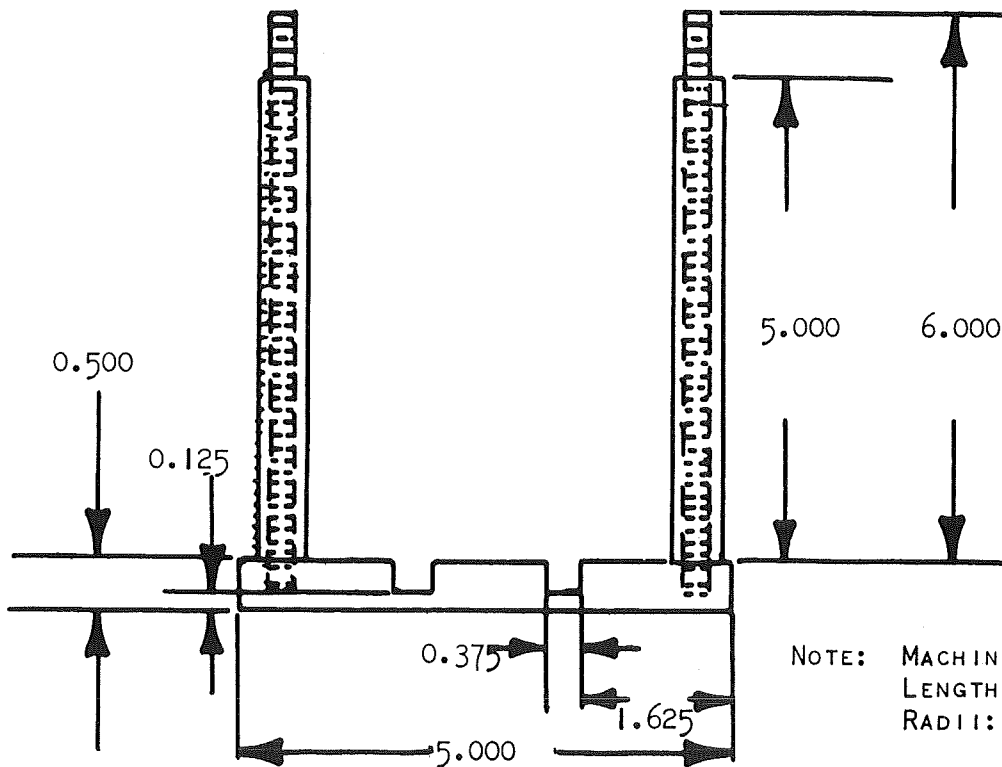
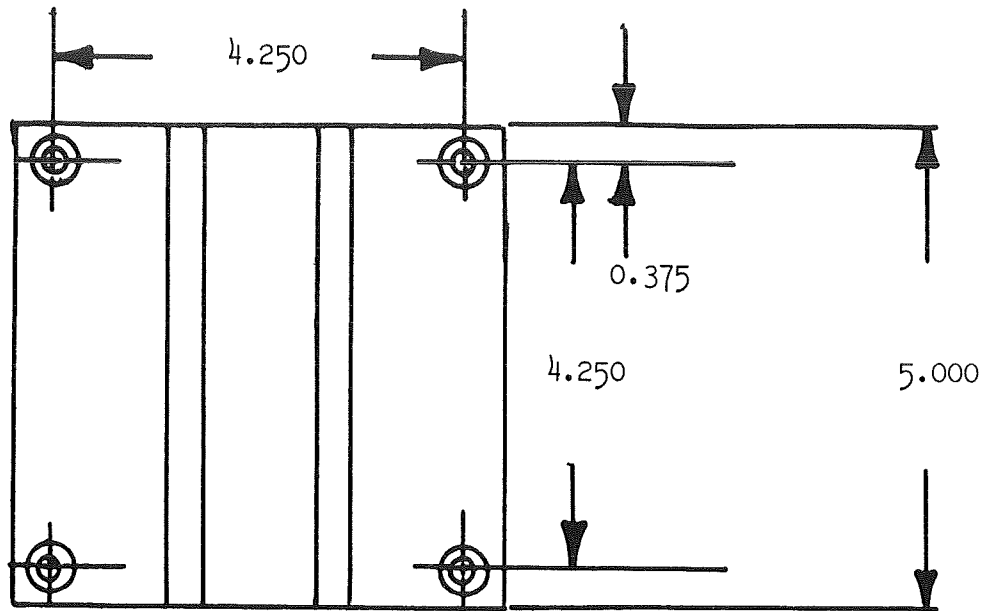


FIGURE 11 PORE VOLUME PER DECADE
VS. LOG PORE DIAMETER
FOR ELECTRODE No. 24 (CENTER)





NOTE: MACHINE SHOP TOLERANCES:
 LENGTHS: ± 0.003
 RADII: ± 0.001

FIGURE 12A FIXTURE BASE. ALL DIMENSIONS IN INCHES.

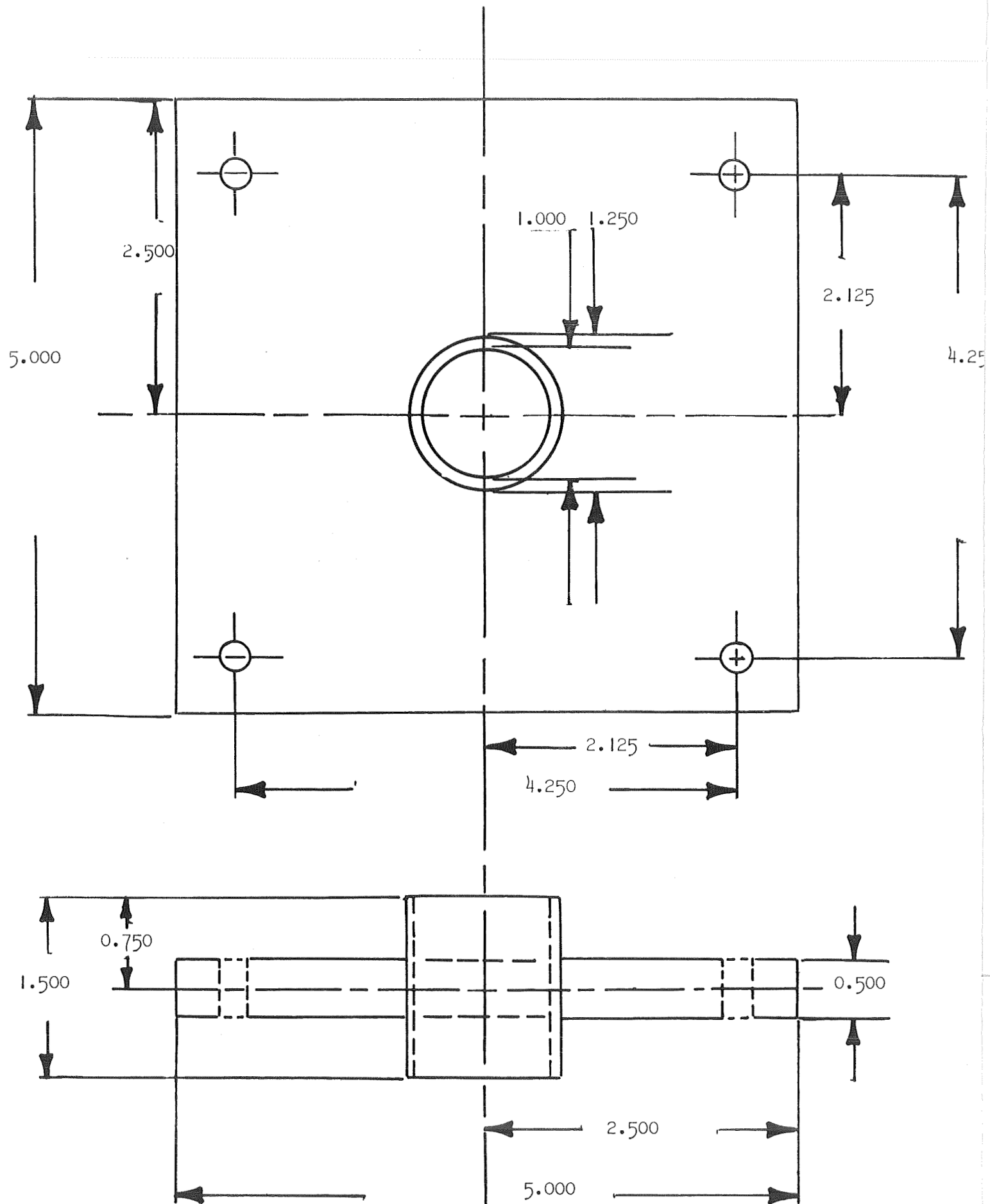


FIGURE 12B TOP PLATE OF FIXTURE.

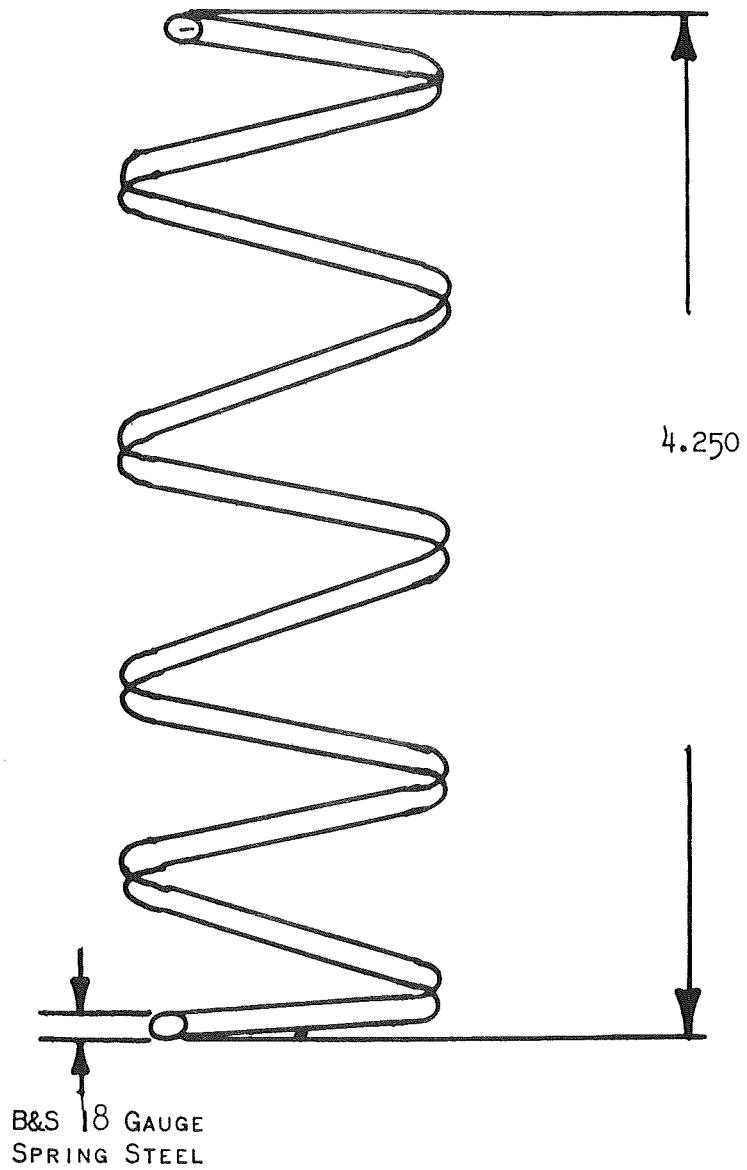


FIGURE 120 SPRING.

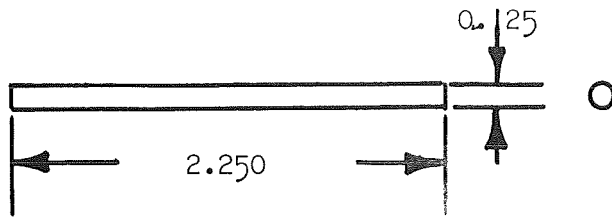


FIGURE 12D SPRING RETAINER PIN.

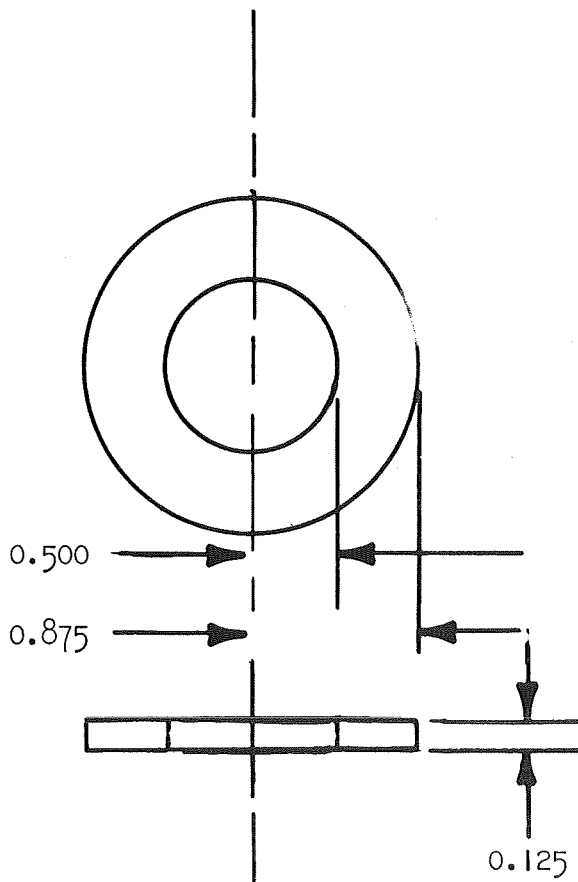


FIGURE 12E SPRING RETAINER WASHER.

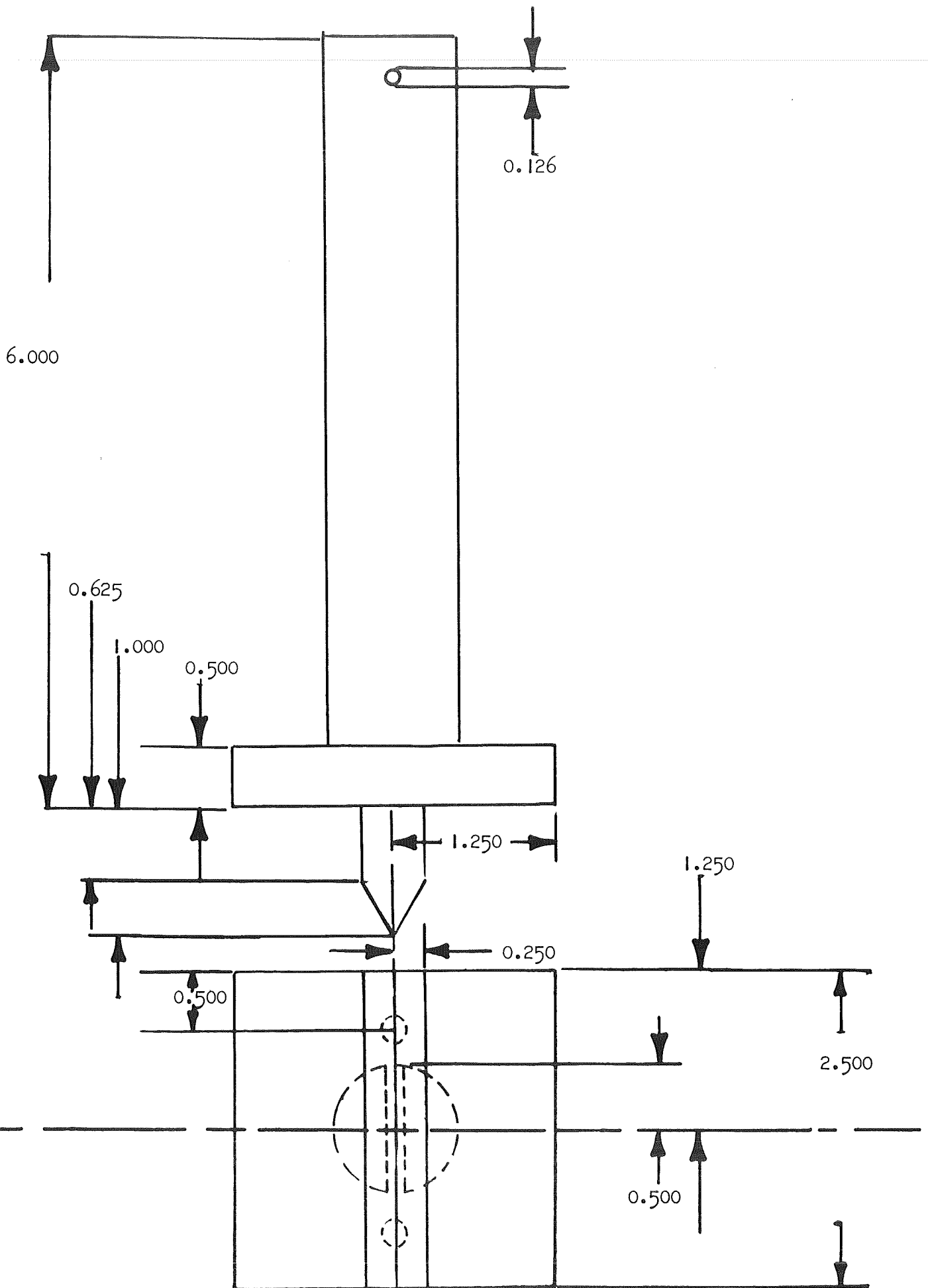


FIGURE 12F MODULUS OF RUPTURE PLUNGER. - 87 -

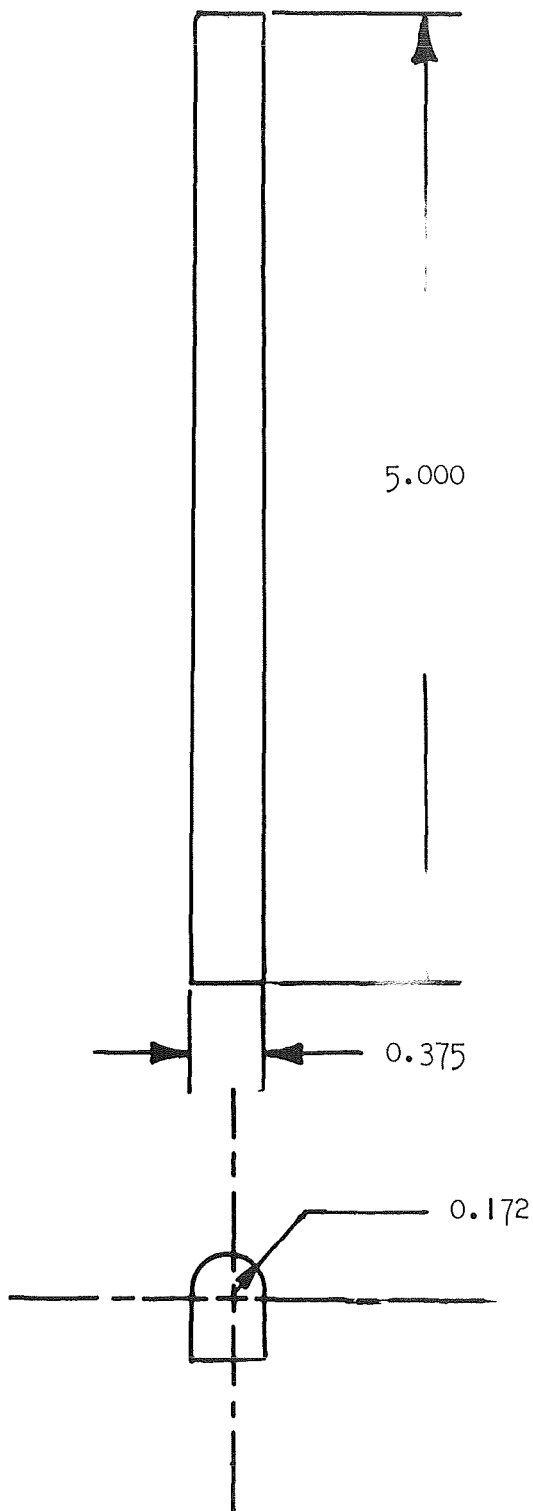


FIGURE 12G SMALL HALF-MOON SURFACE.

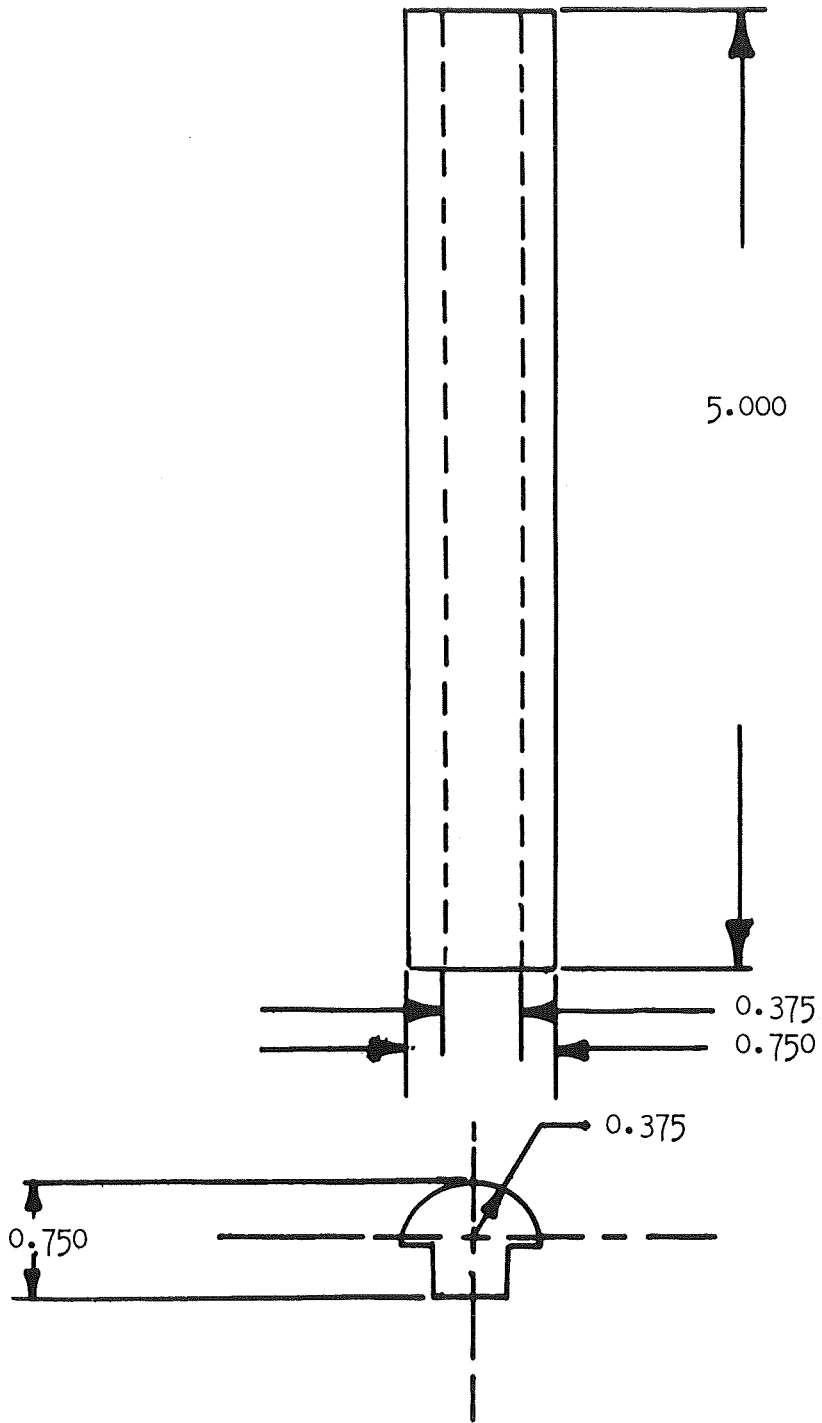


FIGURE 12H LARGE HALF-MOON SURFACE.

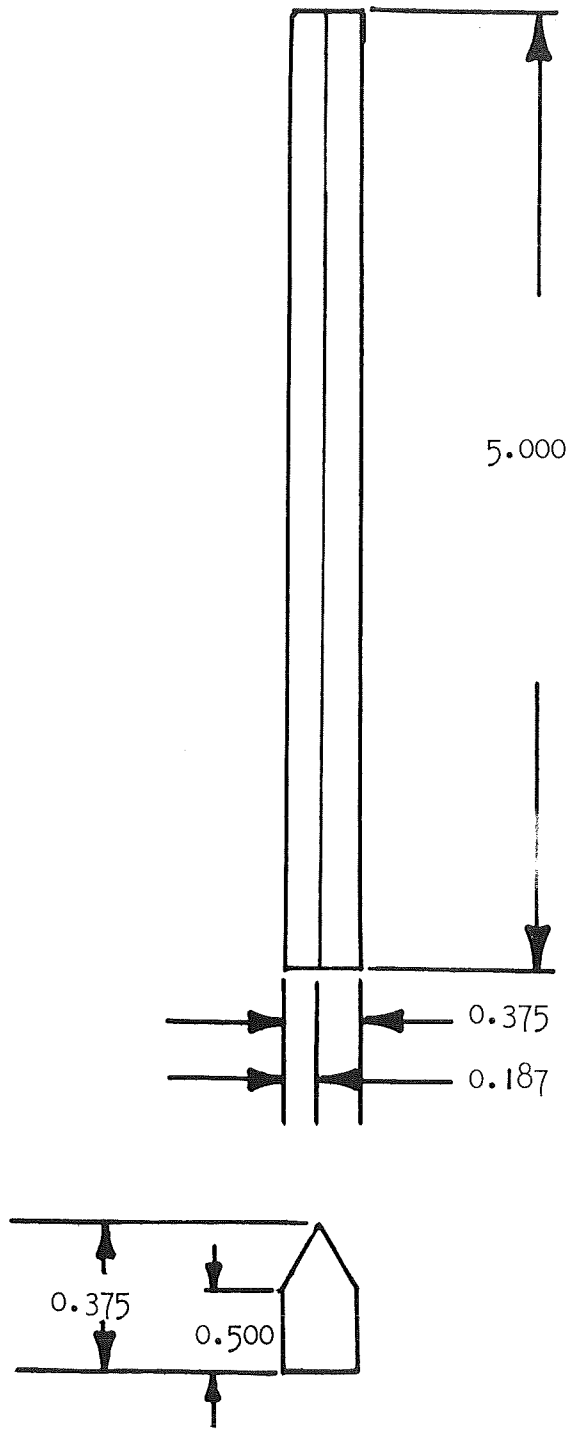
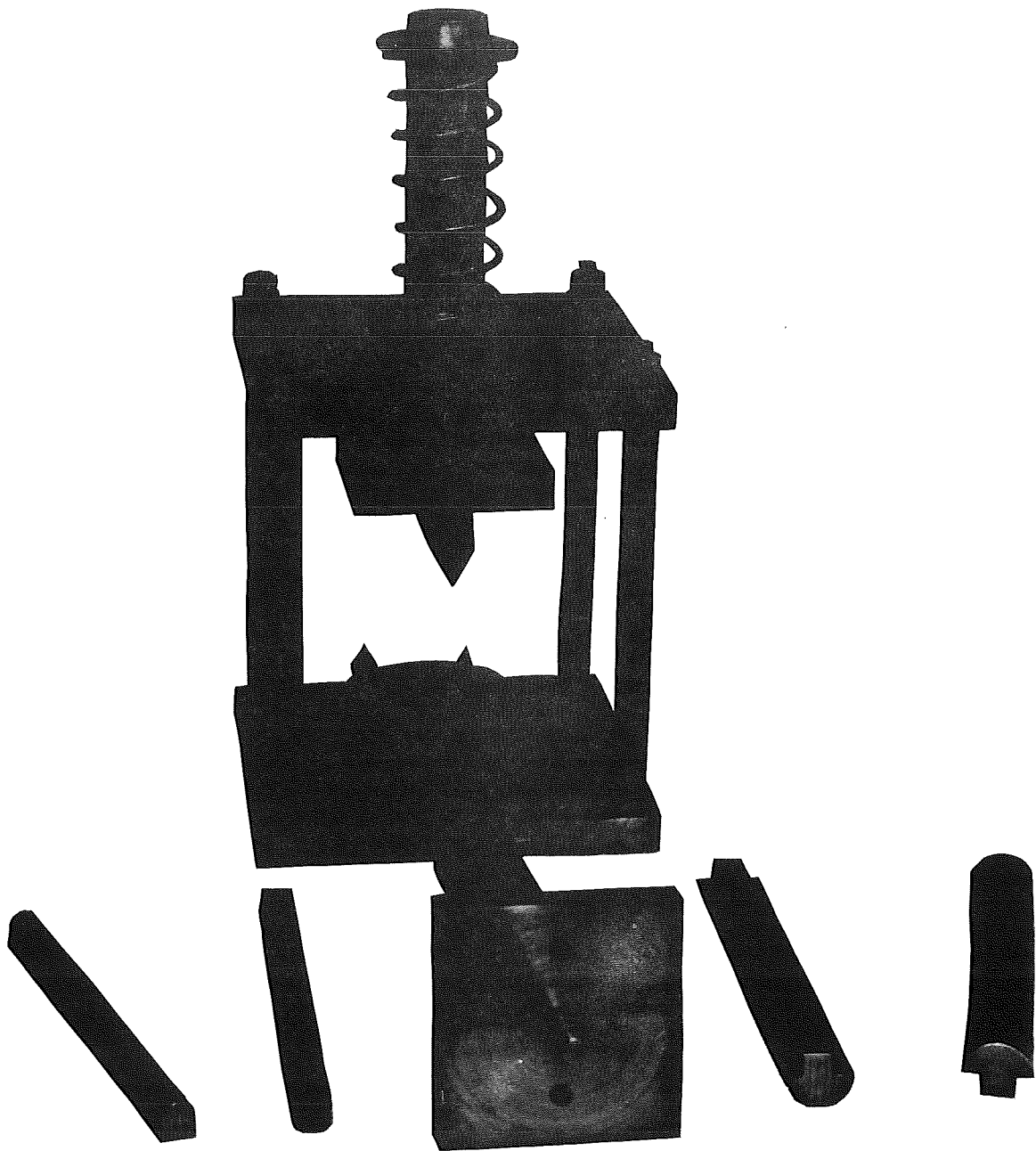


FIGURE 12I KNIFE EDGE SURFACE.



A - Fixture Base
B - Top Plate
C - Spring Retainer Pin
D - Spring Retainer Washer
E - Spring

F - Modulus of Rupture Plunger
G - Knife-Edge Surface
H - Cathode
I - Small Half-Moon Surface
J - Compression Plunger
K - Large Half-Moon Surface

Figure 12J

Assembled Fixture

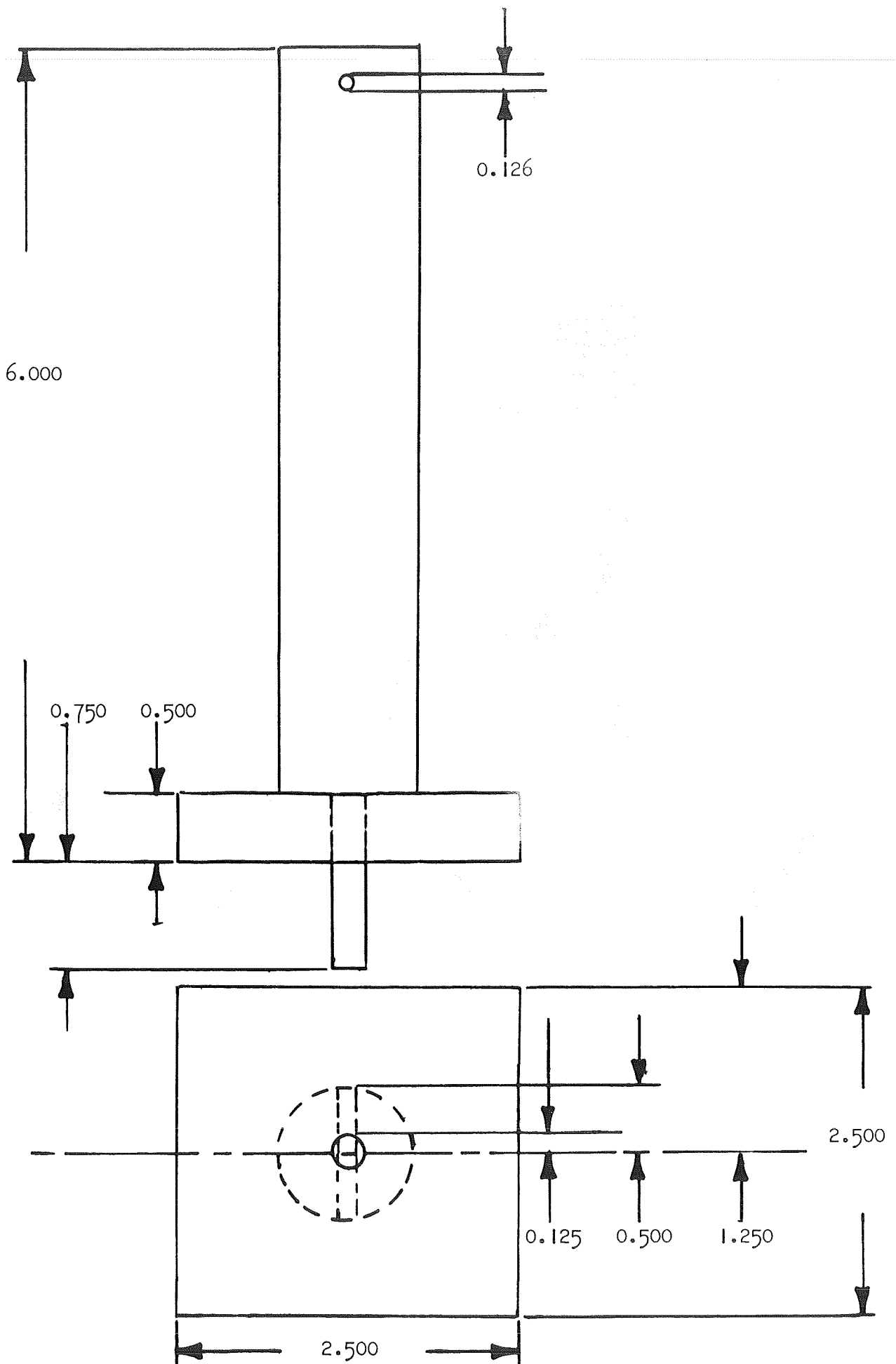


FIGURE 13 COMPRESSION PLUNGER. ALL DIMENSIONS IN INCHES. - 92 -

FIGURE 14 Separator Resistance vs. Time

. - Std.
 O - 0.5
 X - 1.0
 Δ - 1.5
 □ - 2.0

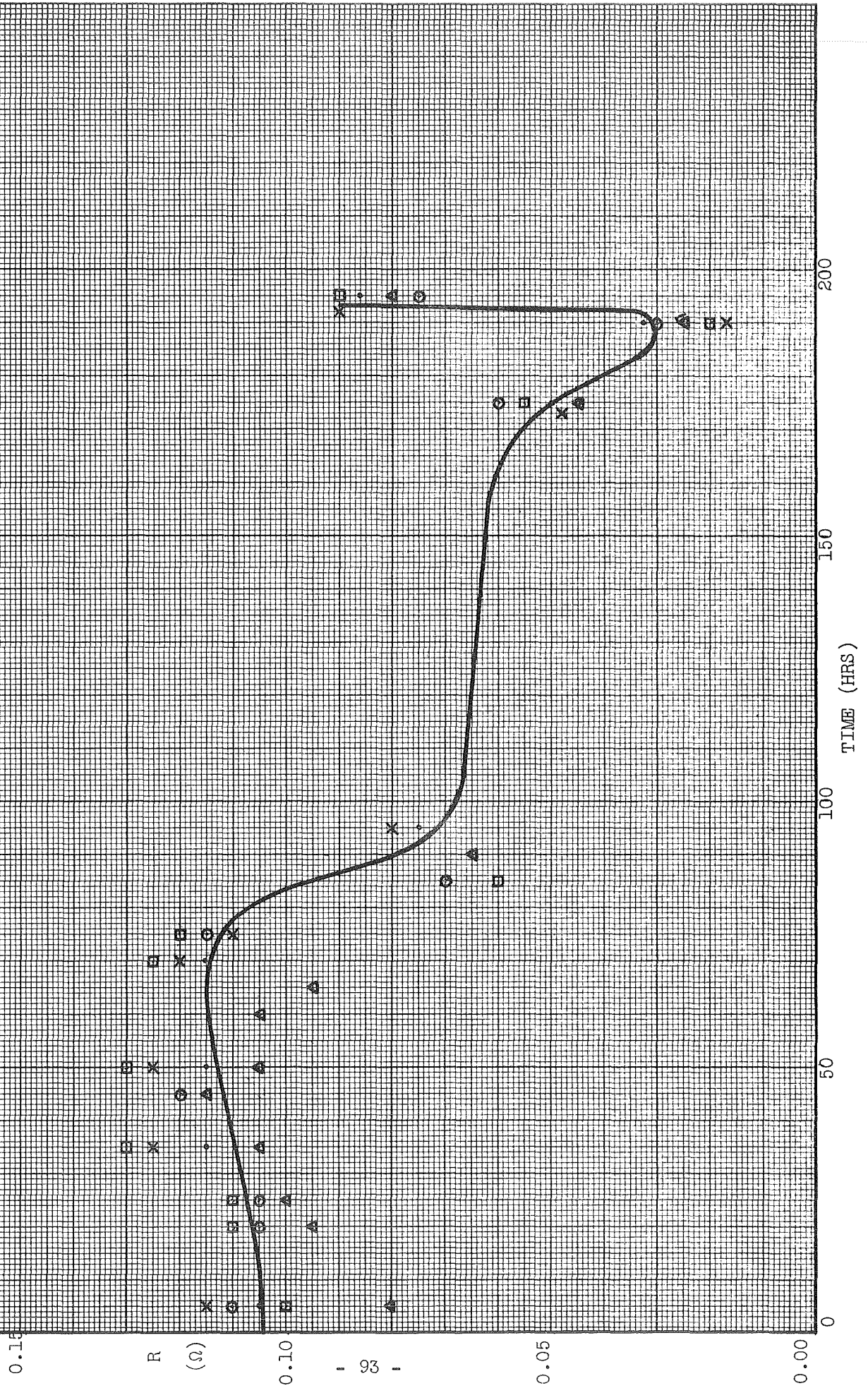


FIGURE 15 Test Nos. 342, 343, 344
Separator Thickness
Separator Thickness = 0.5 cm
O Test #344; □ Test #343; Δ Test #342

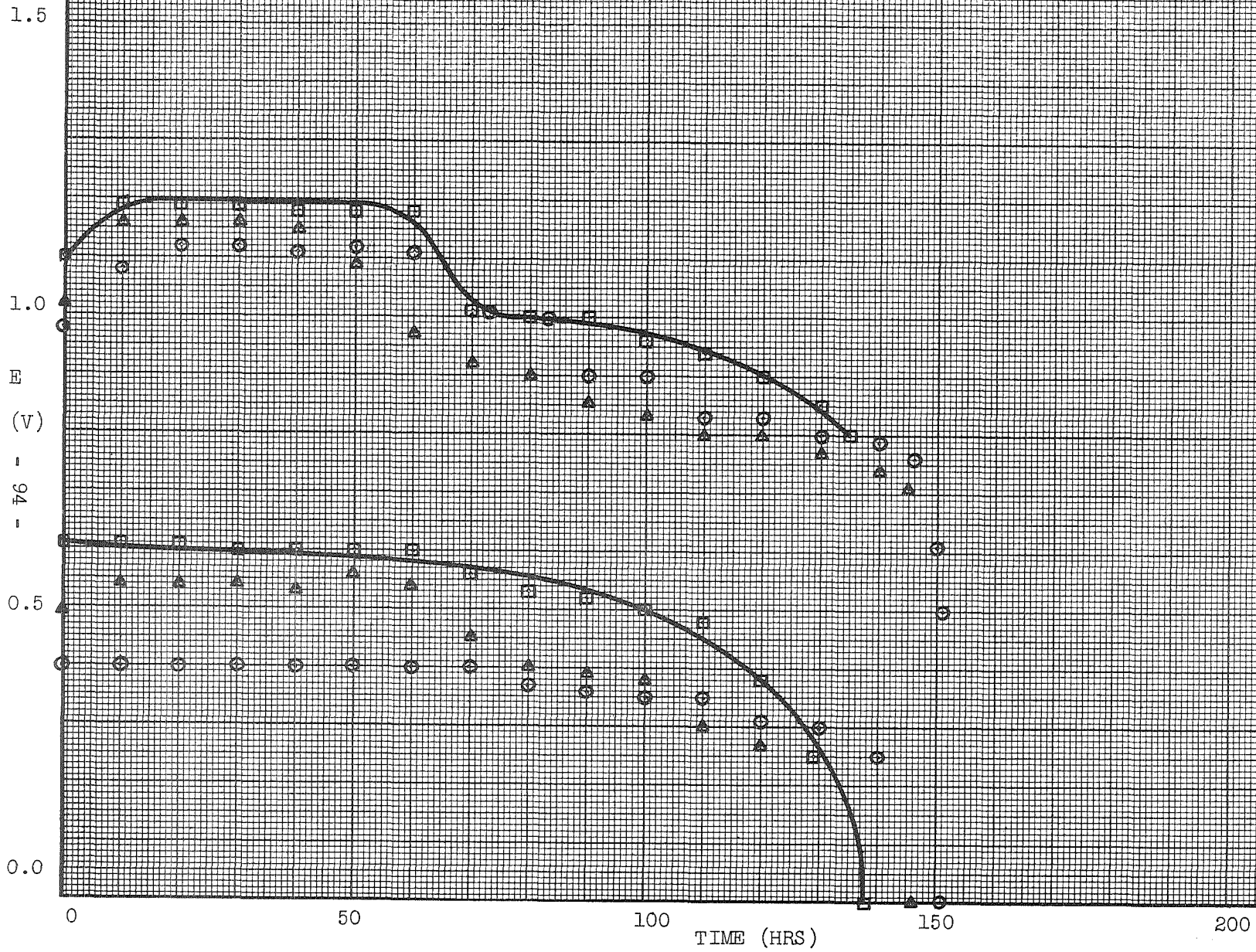


FIGURE 16 Test Nos. 339, 340, 341
 SEPARATOR THICKNESS
 Separator Thickness = 1.0 cm
 O Test #341; □ Test #340; Δ Test #339

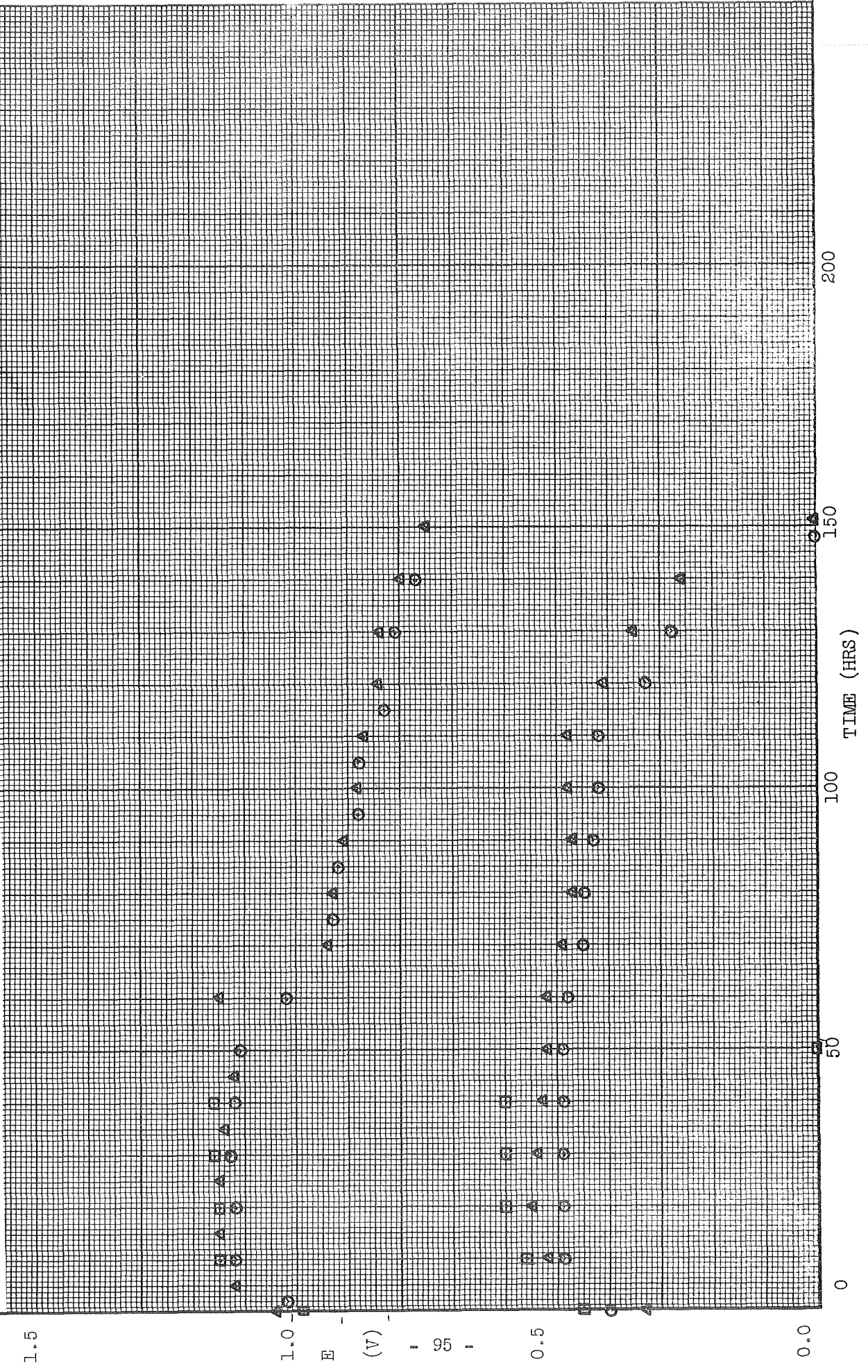


FIGURE 17 Test Nos. 333, 334, 335
 Separator Thickness = 1.5 cm
 0 Test #333; □ Test #335; Δ Test #334

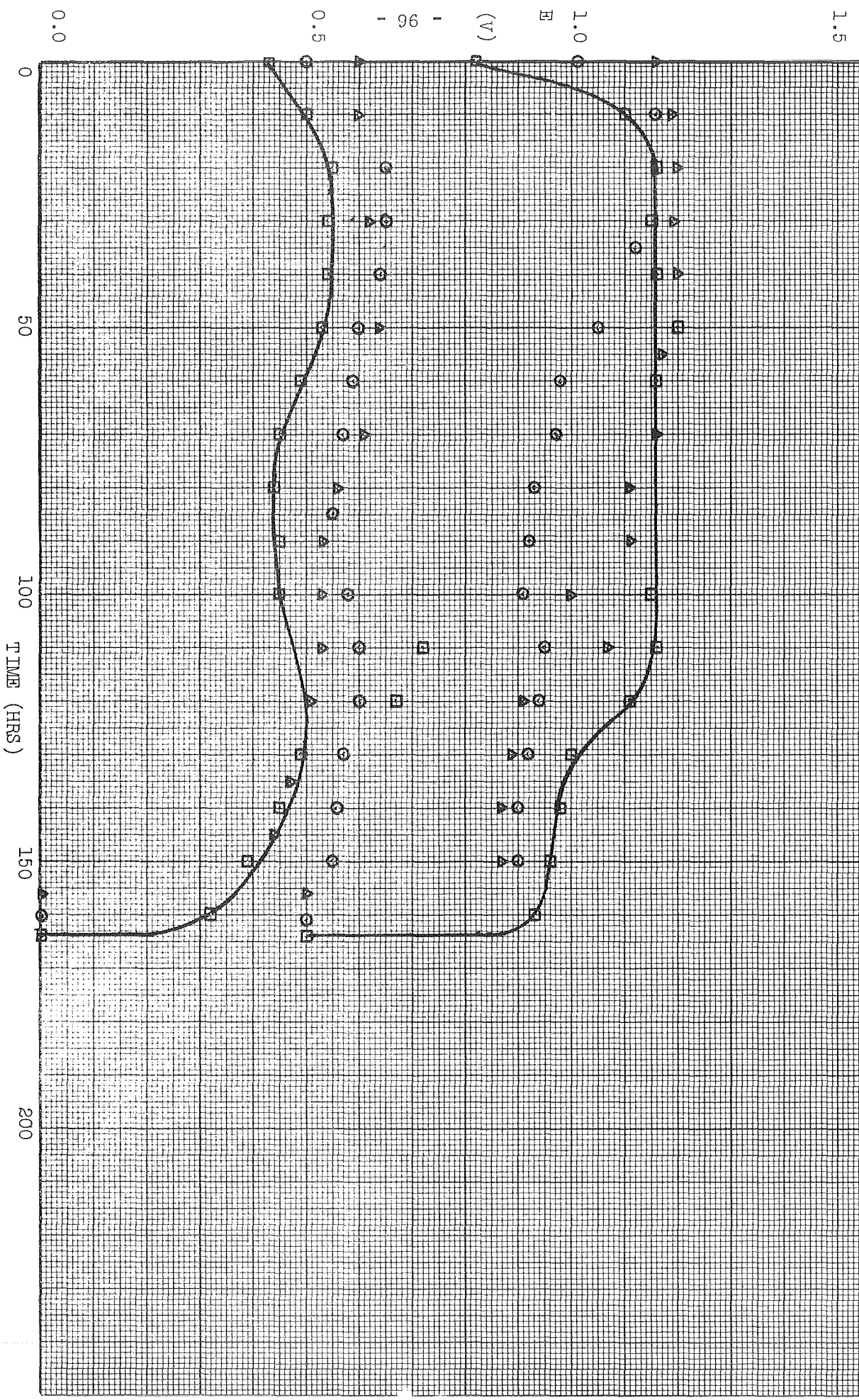
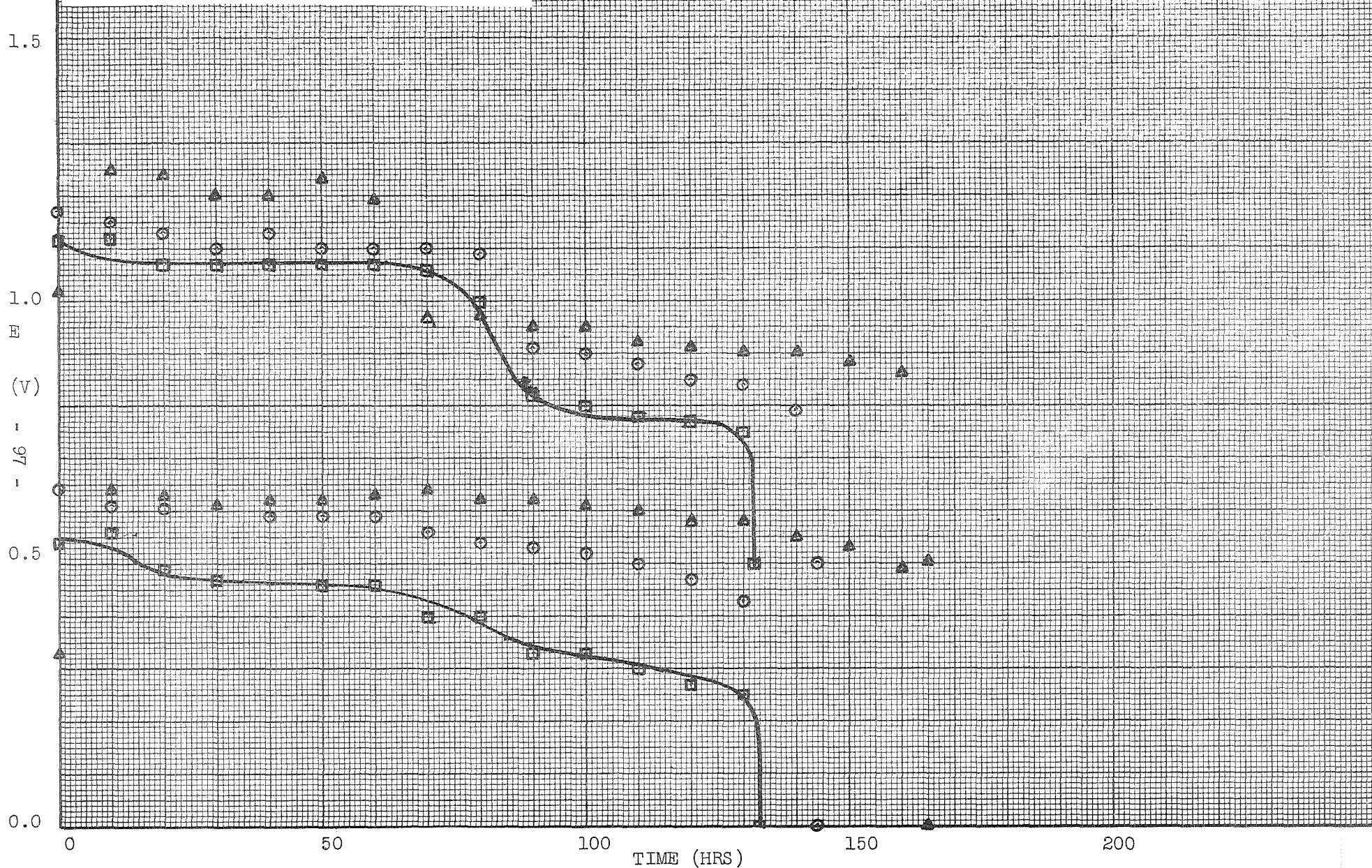


FIGURE 18 Test Nos. 336, 337, 338
Separator Thickness
Separator Thickness = 2.0 cm
○ Test #337; □ Test #338; △ Test #336



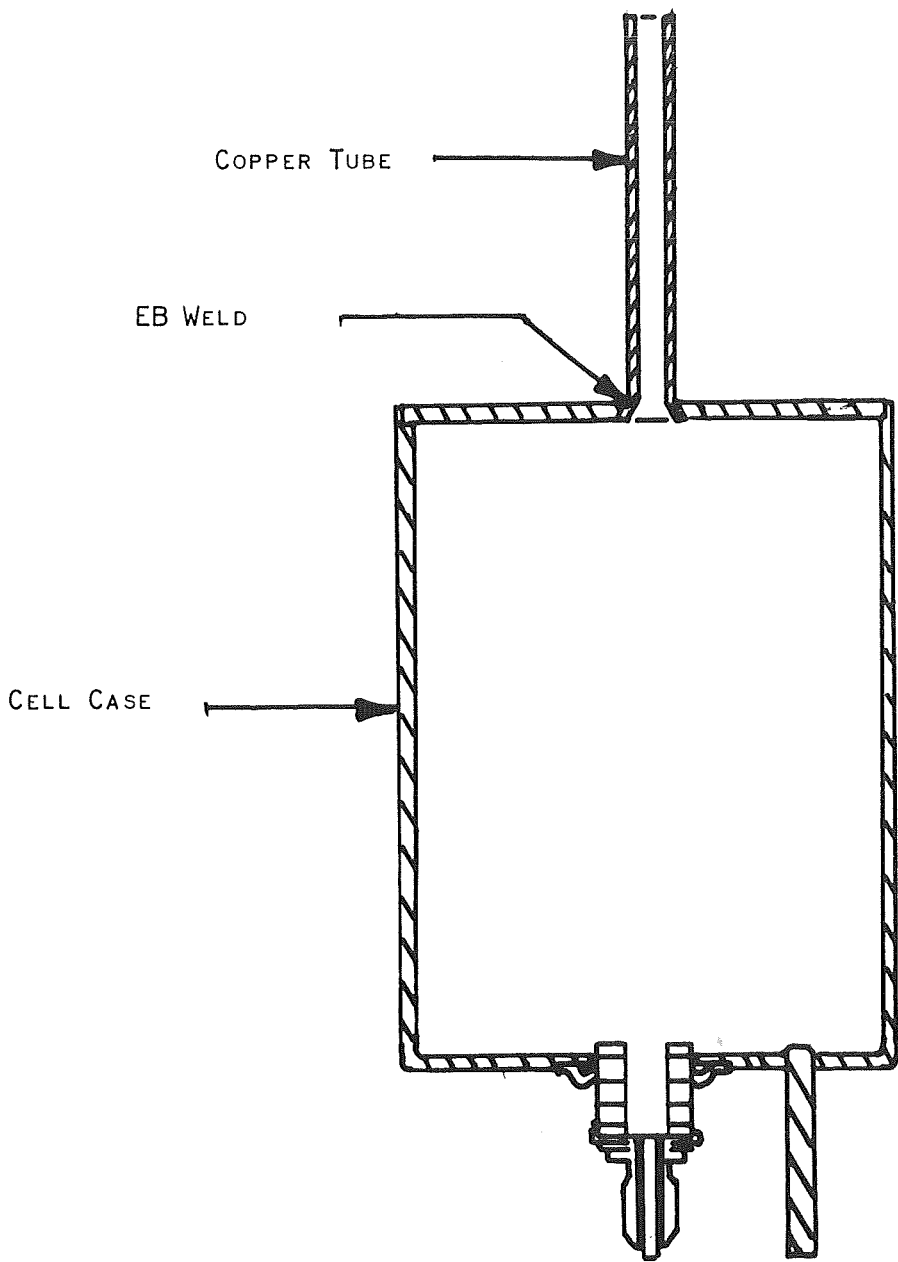


FIGURE 19 CELL CASE ASSEMBLY.

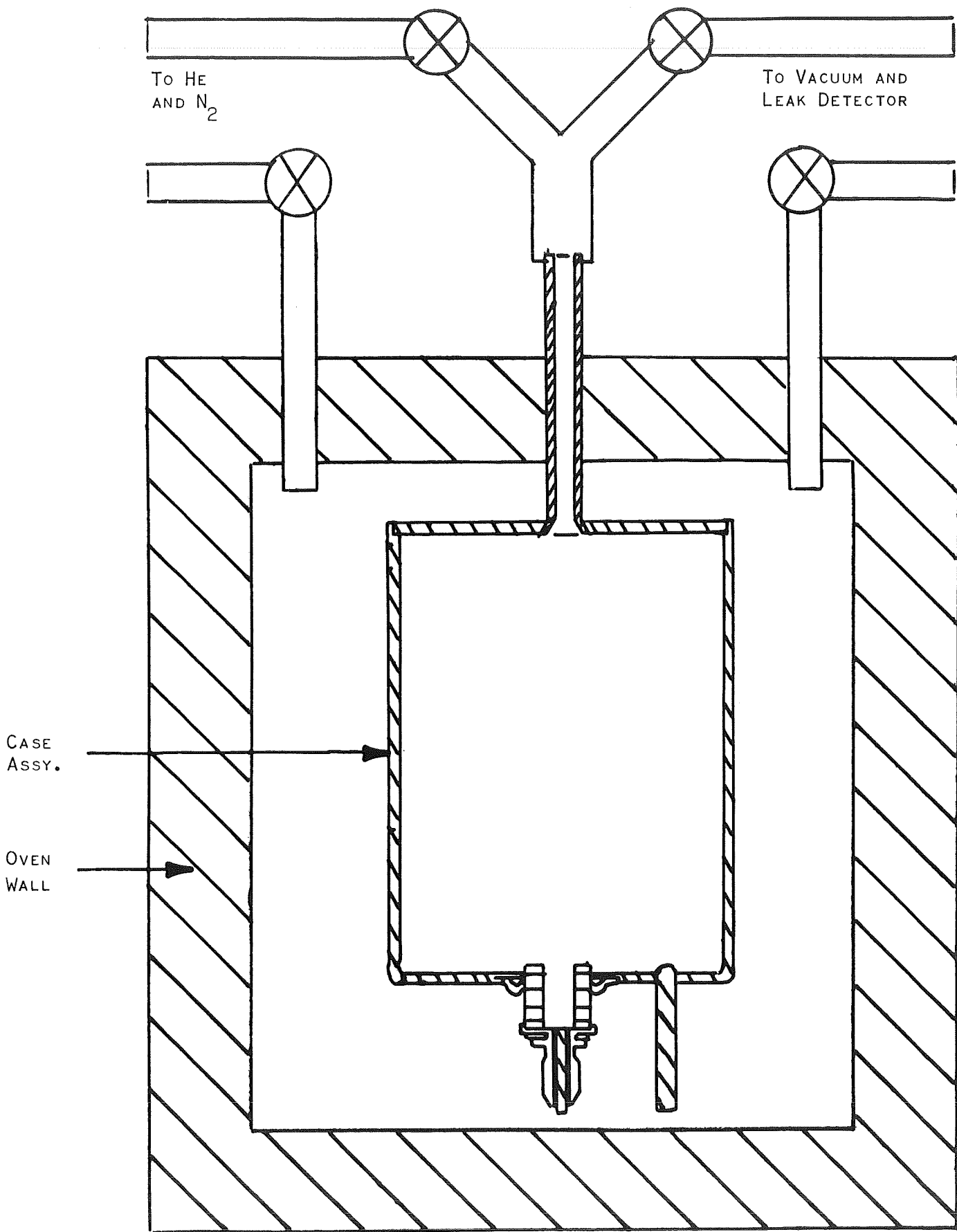
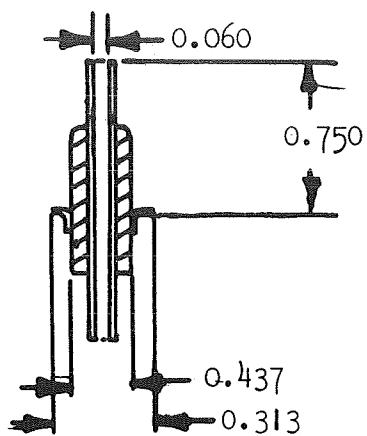
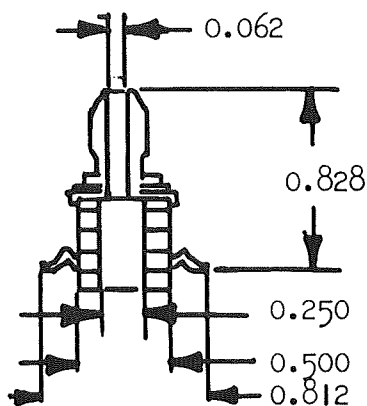


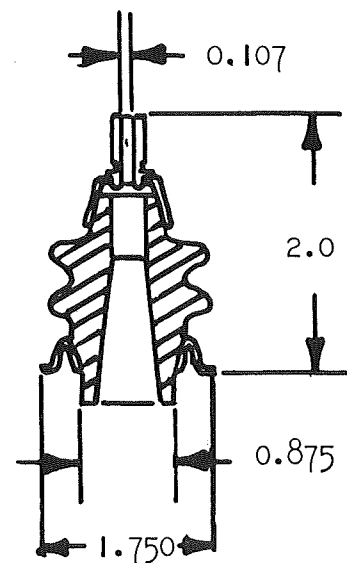
FIGURE 20 HIGH TEMPERATURE LEAK TESTING APPARATUS.



ALITE D-312
 METAL PARTS: GRADE A NICKEL
 BRAZE: OFHC COPPER
 CERAMIC: AL_2O_3



ALITE B50-1
 METAL PARTS: GRADE A NICKEL
 BRAZE: OFHC COPPER
 CERAMIC: AL_2O_3



ALITE 1-2-1C
 METAL PARTS: NICKEL-IRON (42% NI)
 BRAZE: SILVER
 CERAMIC: AL_2O_3

FIGURE 21 CERAMIC TERMINAL SEALS EVALUATED AT 800°F.

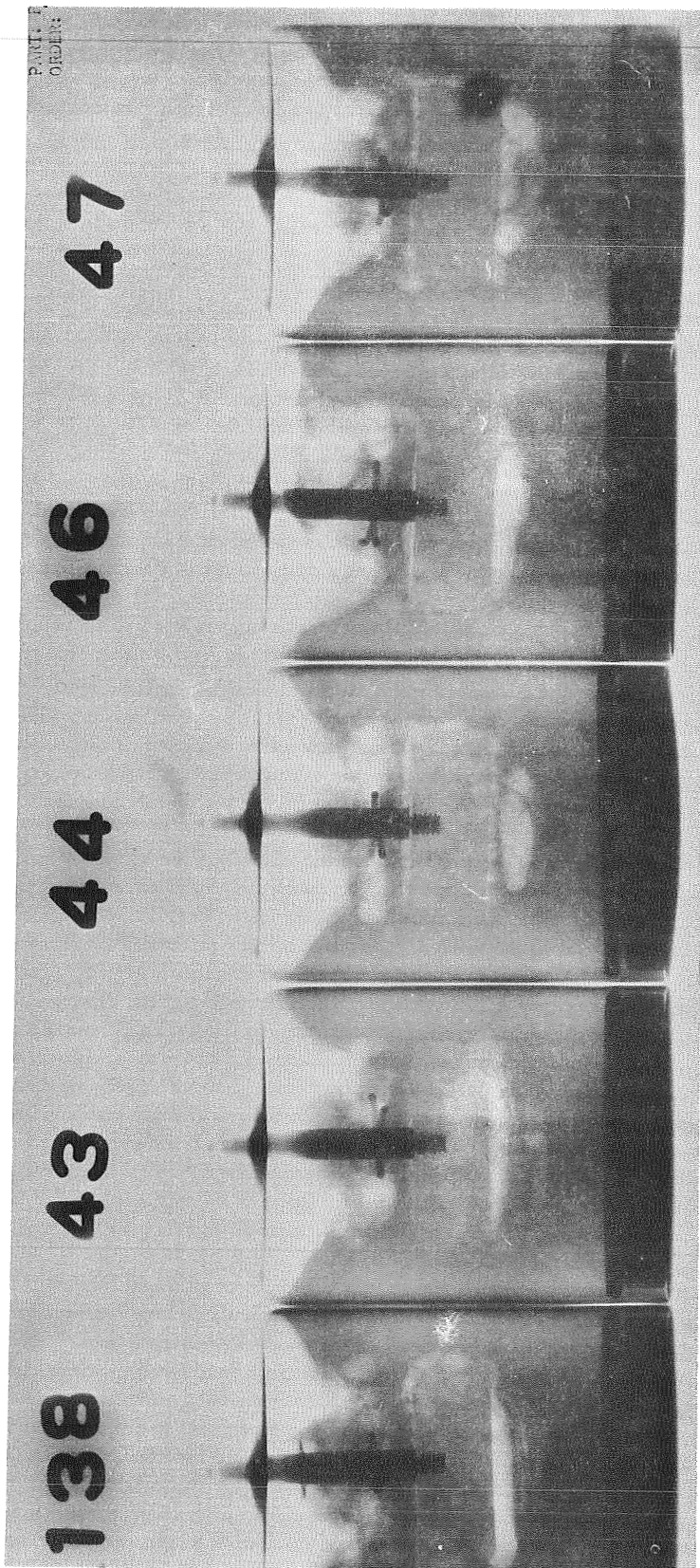


FIGURE 22

X-Ray Positive of Cells After Heating At 800°F

Figure 23 - E vs T
Control Cells at 427°C
Test No. 375 Test No. 382

1.5

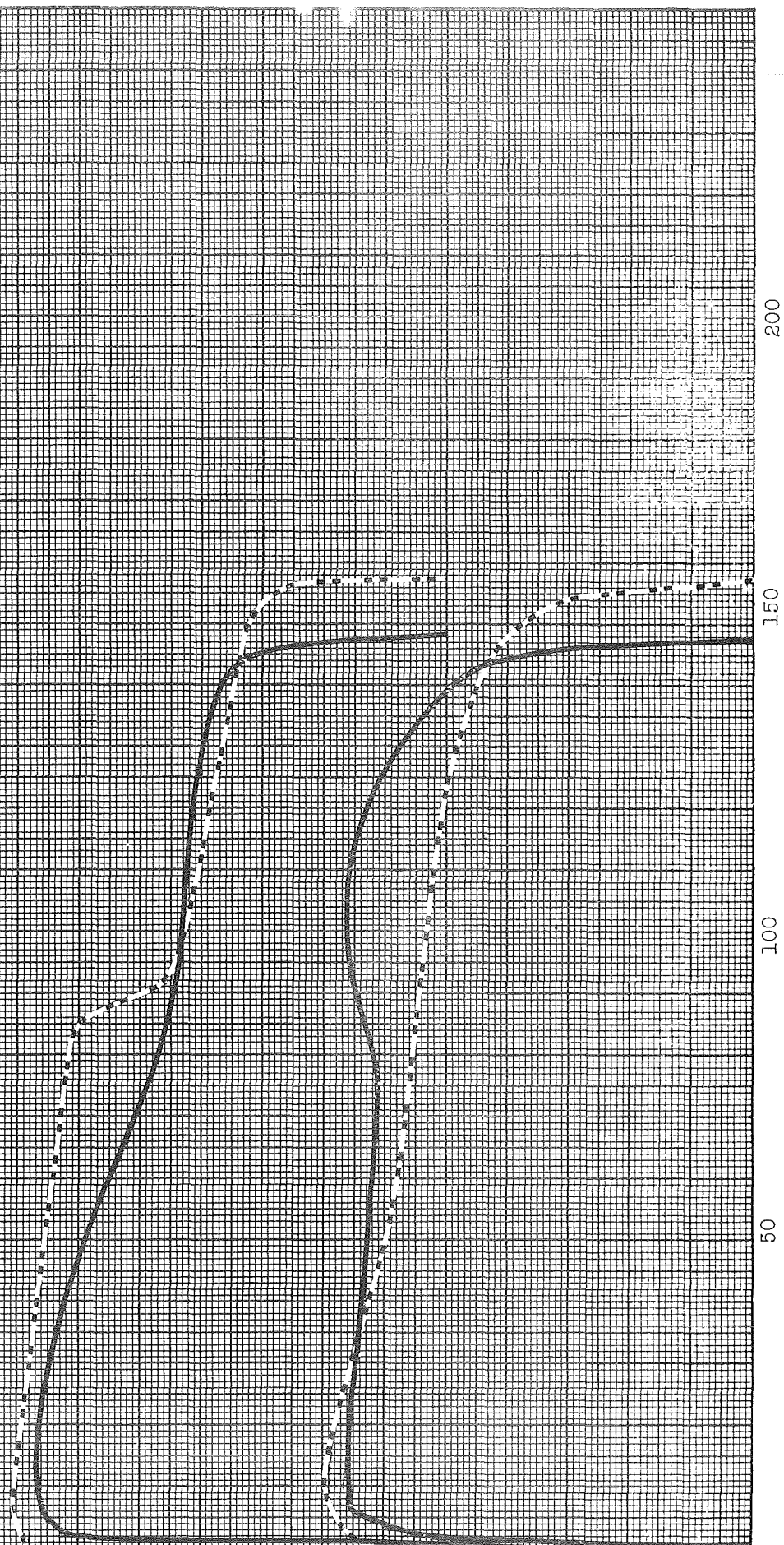
1.0

E

(Volts)

0.5

0



- 102 -

Figure 24 - E vs T
Control Cells at 481°C
Test No. 396 Test No. 393

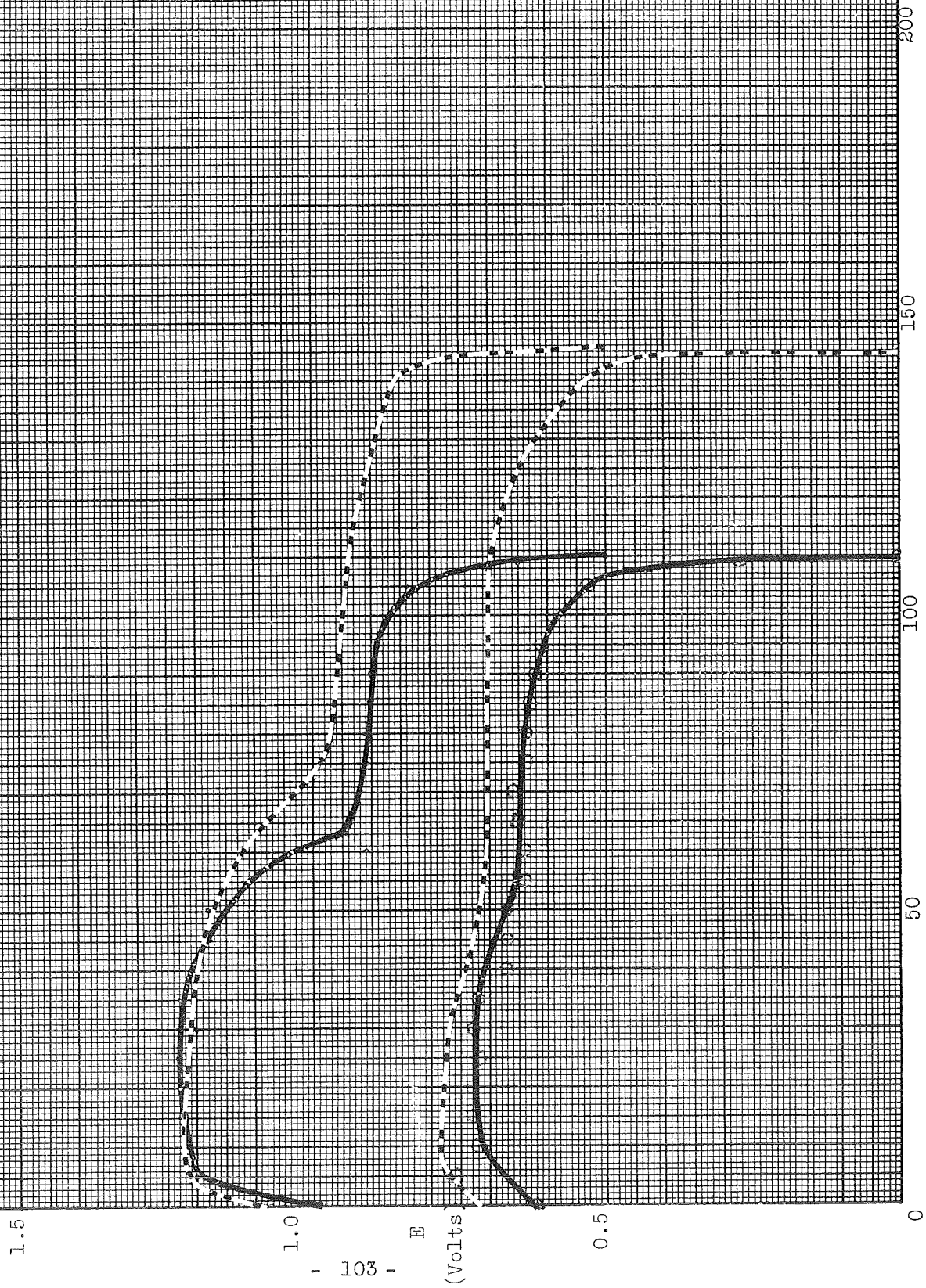


Figure 25 - E vs T
Control Cells at 538°C
Test No. 398 Test No. 402

1.5

1.0

E

(Volts)

0.5

0

104

200

150

100

50

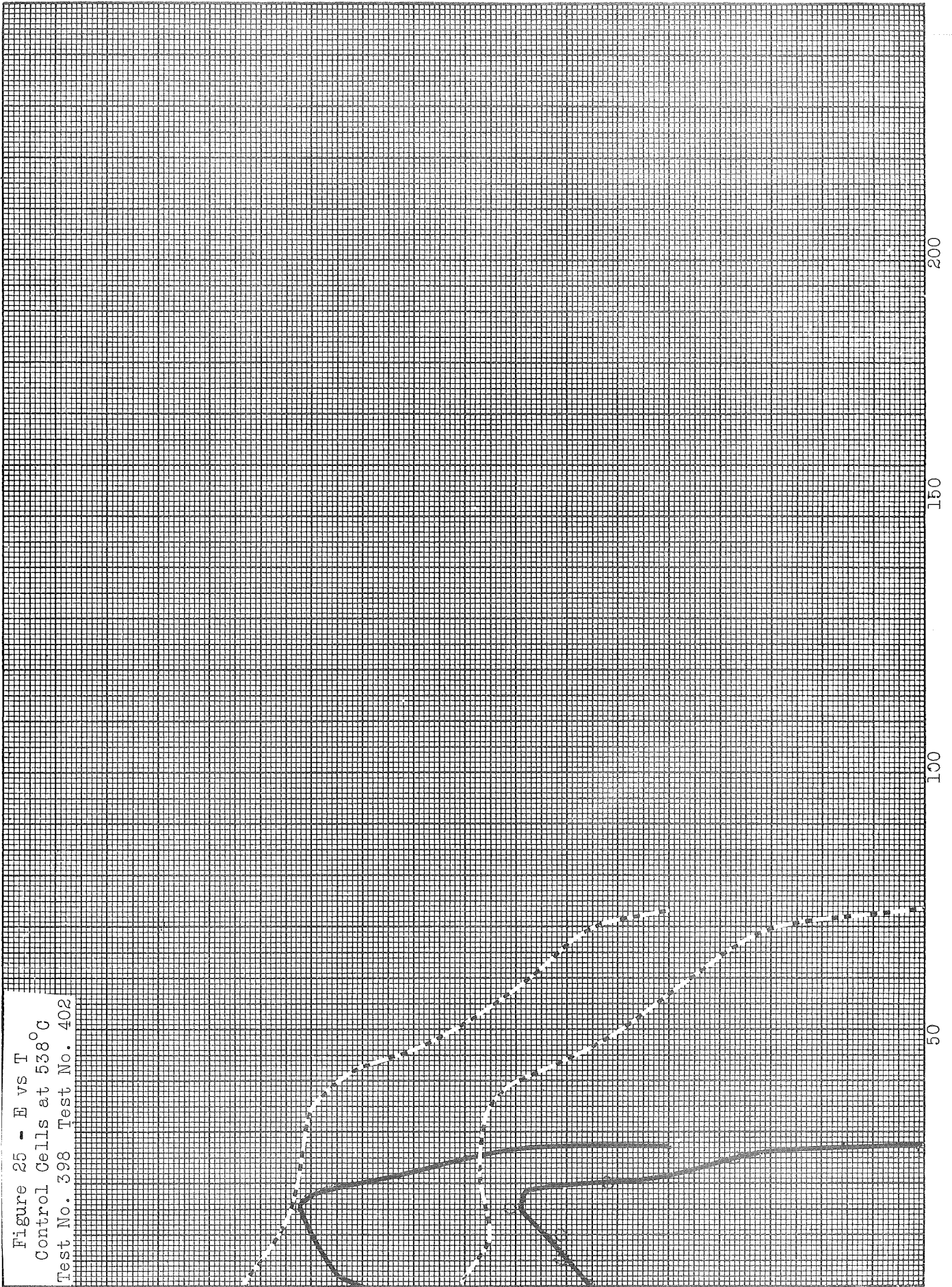


Figure 26 - Log of Percent
Loss of Life
vs $\frac{1}{T}$

Log
%
Loss
of
Life

2.0

1.5

1.0

0.5

0

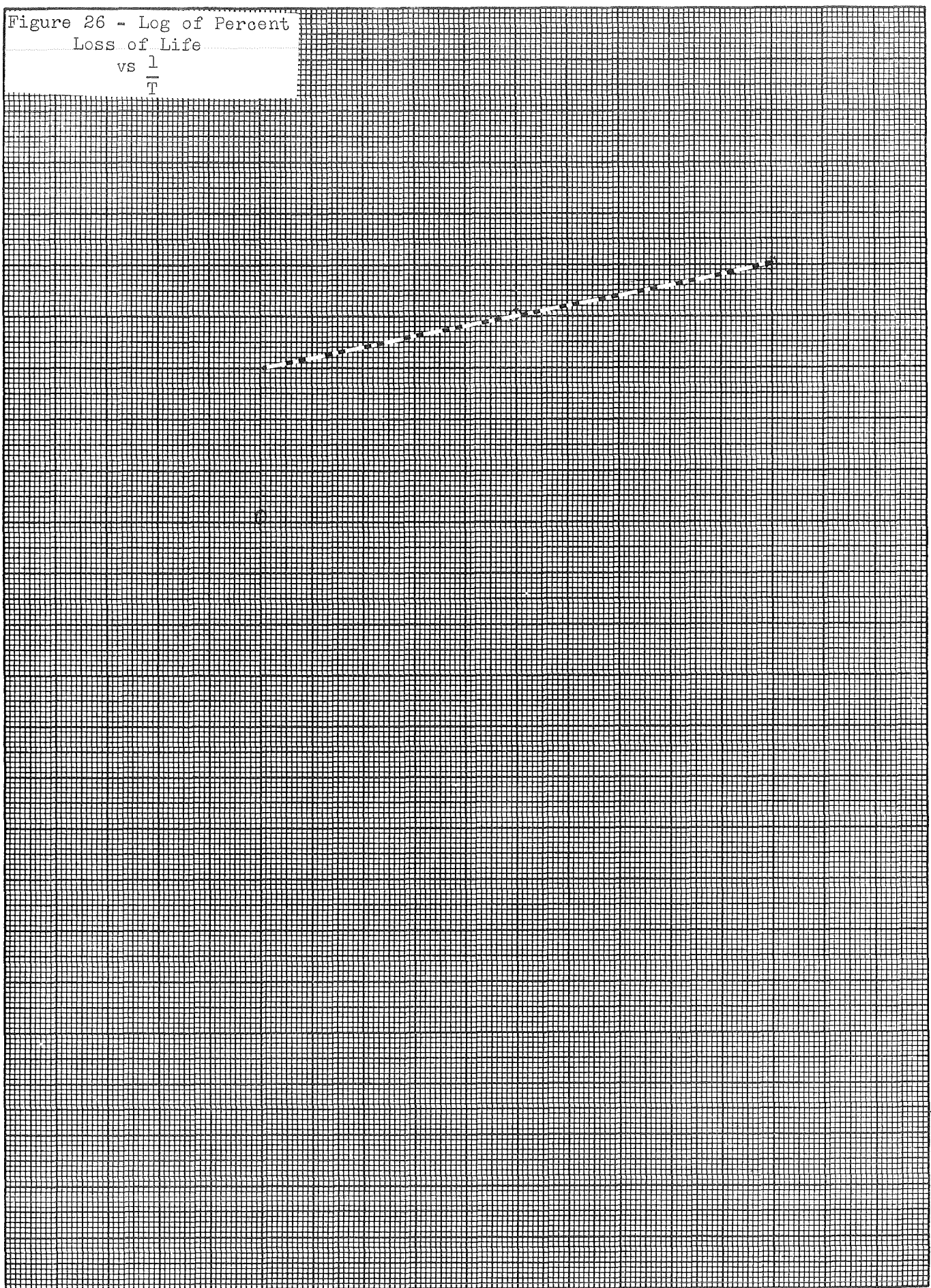
1.1

1.2

1.3

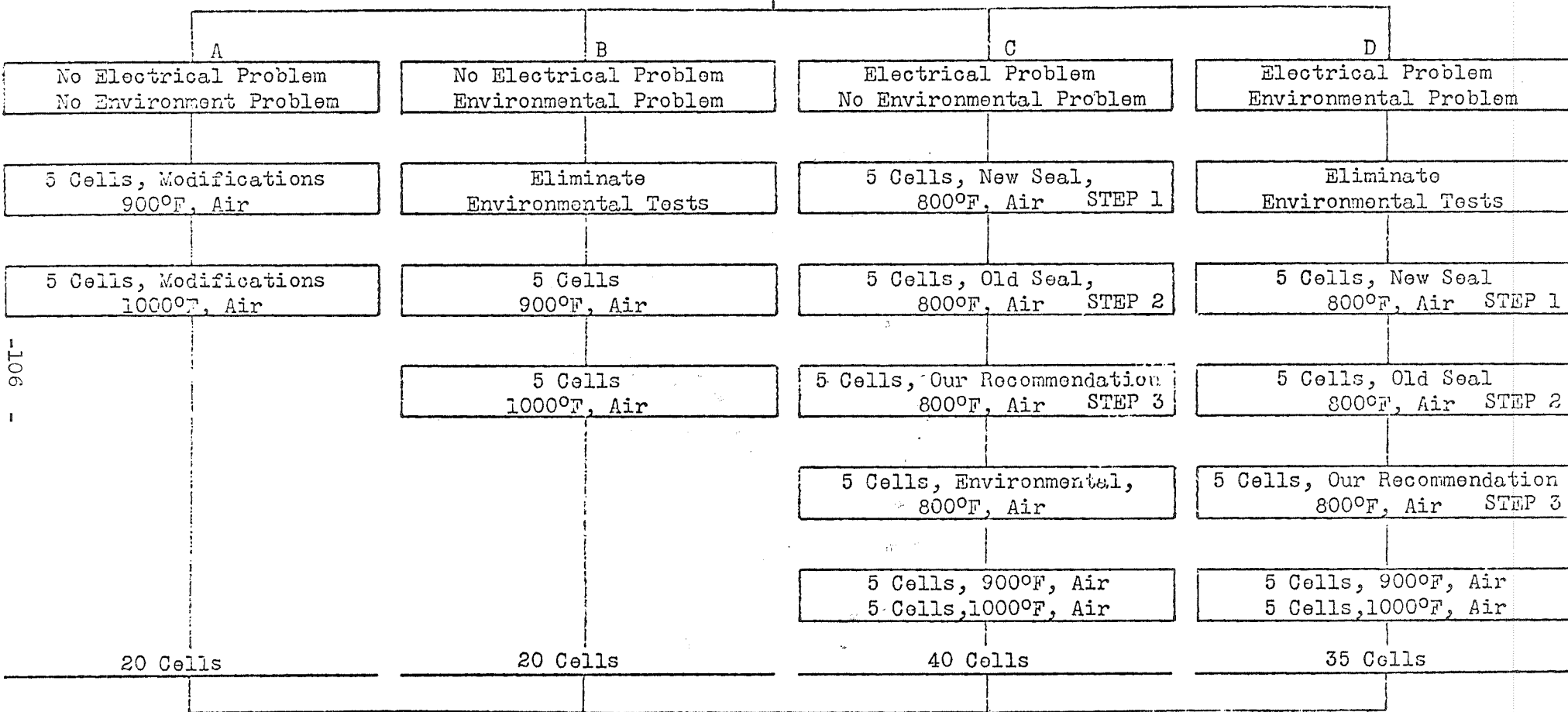
1.4

$\frac{1}{T} \times 10^3 (^{\circ}K)$



Work Alternative Flow Chart

5 Cells, Control, Modifications, 800°F, Air
5 Cells, Environmental Modifications, 800°F, Air



20 Delivered Cells

Detailed Final Cell
Specifications

Final Report

If step 1 is successful, omit
Steps 2 and 3

If step 2 is successful, omit
Step 3

-106

Figure 28 - E vs T
Modified Control Cells
Test No. 413 Test No. 411

1.5

1.0

107

E (V)

0.5

0

200

150

100

50

T (hrs.)

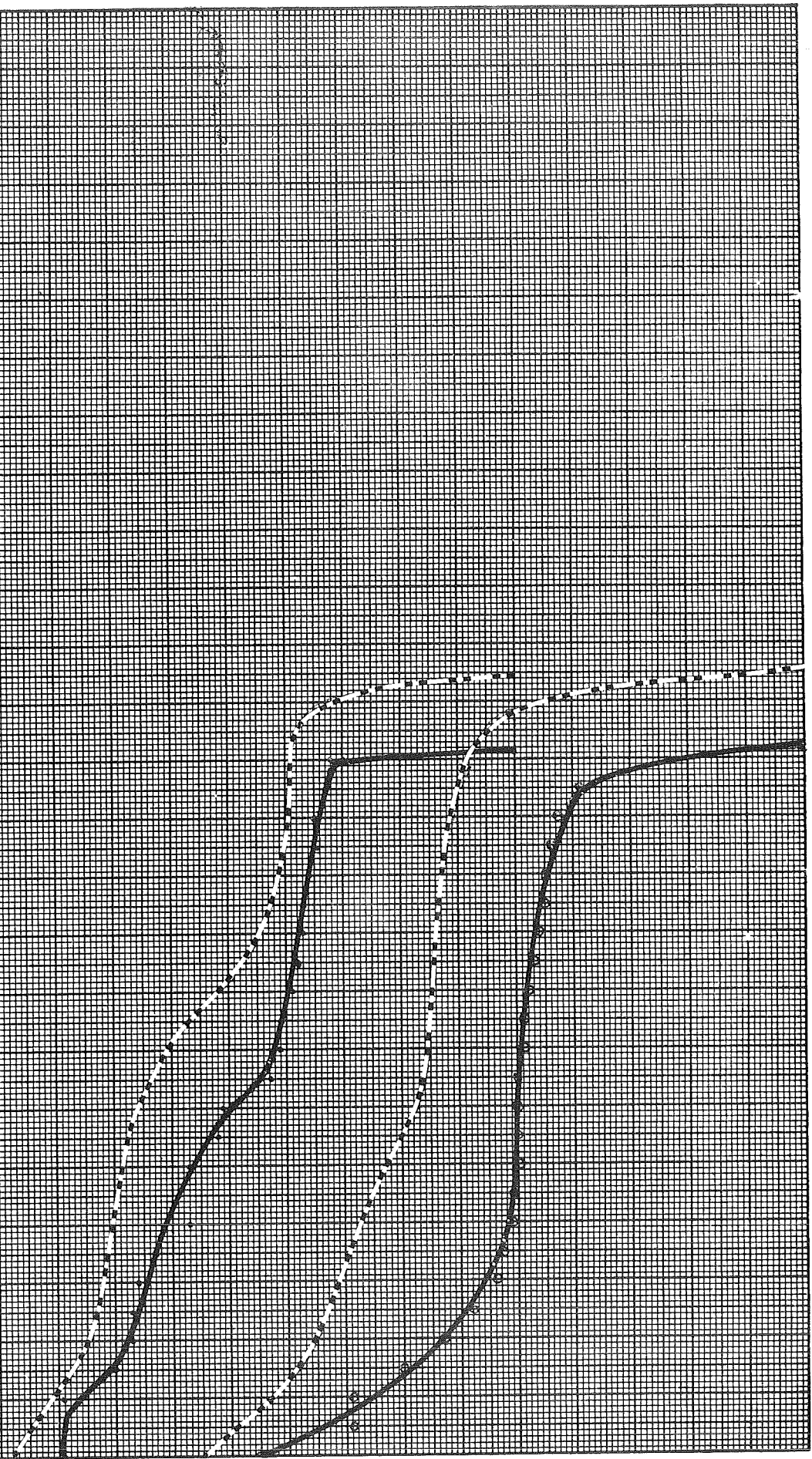


Figure 29 - E vs T
Environmentally Tested Cells
Test No. 416 Test No. 417

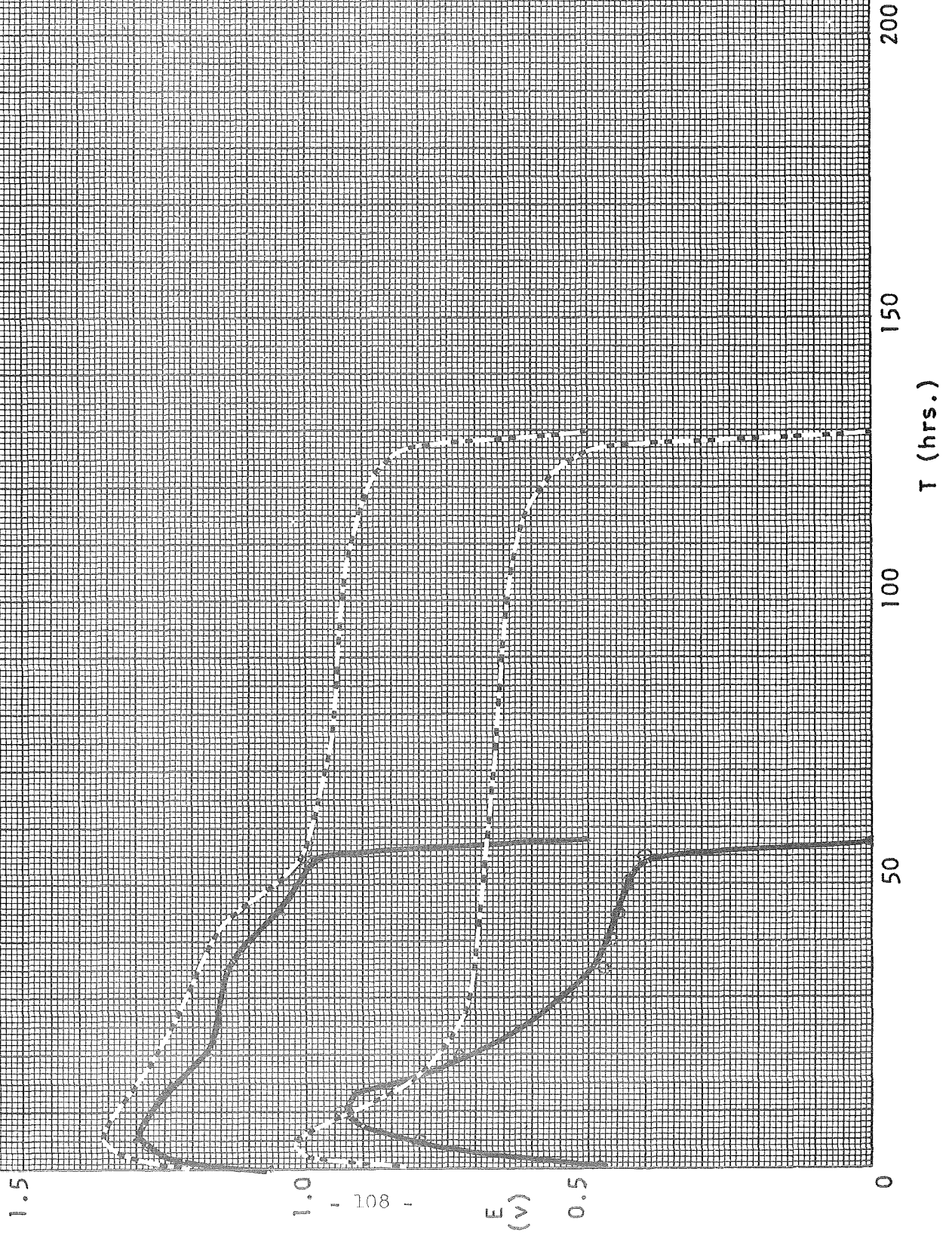
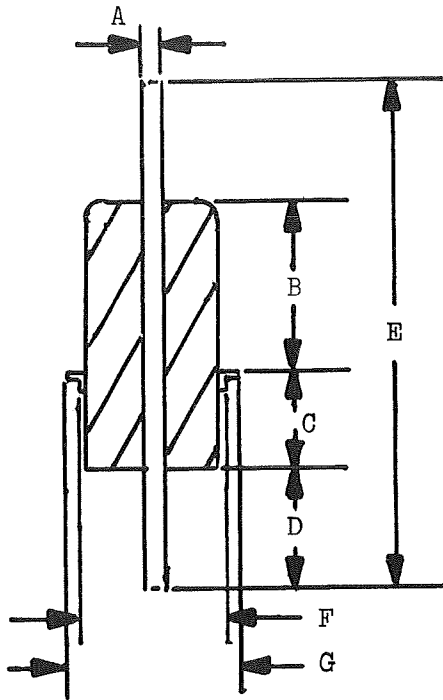


Figure 30A

Alite D-312



A = 0.060 I.D.

B = 0.437

C = 0.250

D = 0.313

E = 1.313

F = 0.313 O.D.

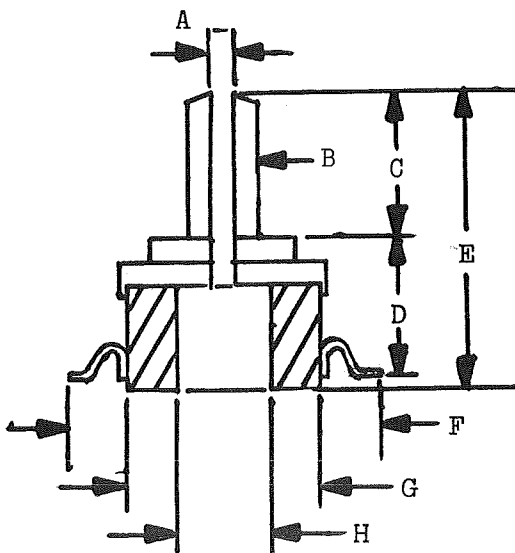
G = 0.437 O.D.

All dimensions in inches.

Scale = 2:1

Shaded portion = Ceramic

Figure 30B
Alite B50-1



A = 0.062 I.D.

B = 10-32 TH'D

C = 0.375

D = 0.453

E = 0.859

F = 0.813

G = 0.500

H = 0.250

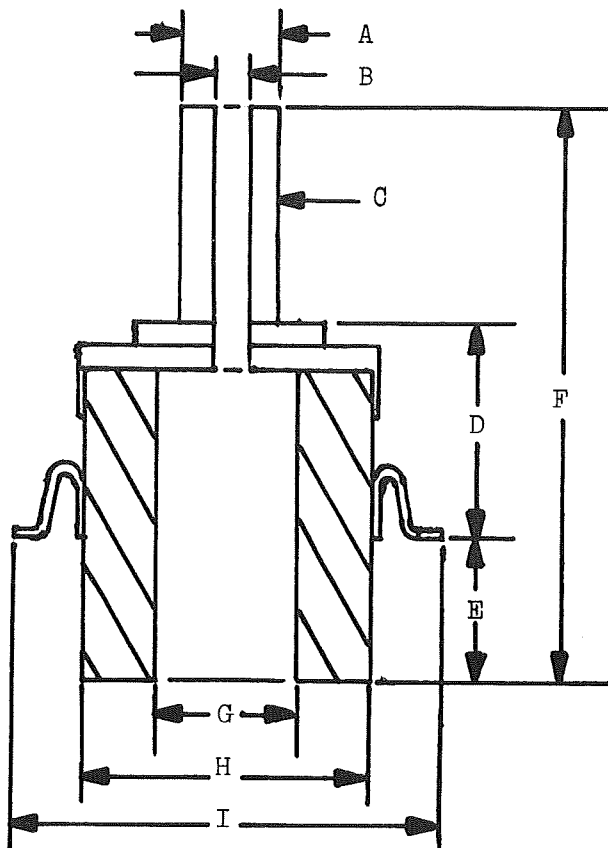
All dimensions in inches.

Scale = 2:1

Shaded Portion = Ceramic

Figure 30C

Alite B75-1



A = 0.250

B = 0.107

C = 0.250 - 28 TH'D

D = 0.687

E = 0.375

F = 1.5

G = 0.375 I. D.

H = 0.750 O.D.

I = 1.125 O.D.

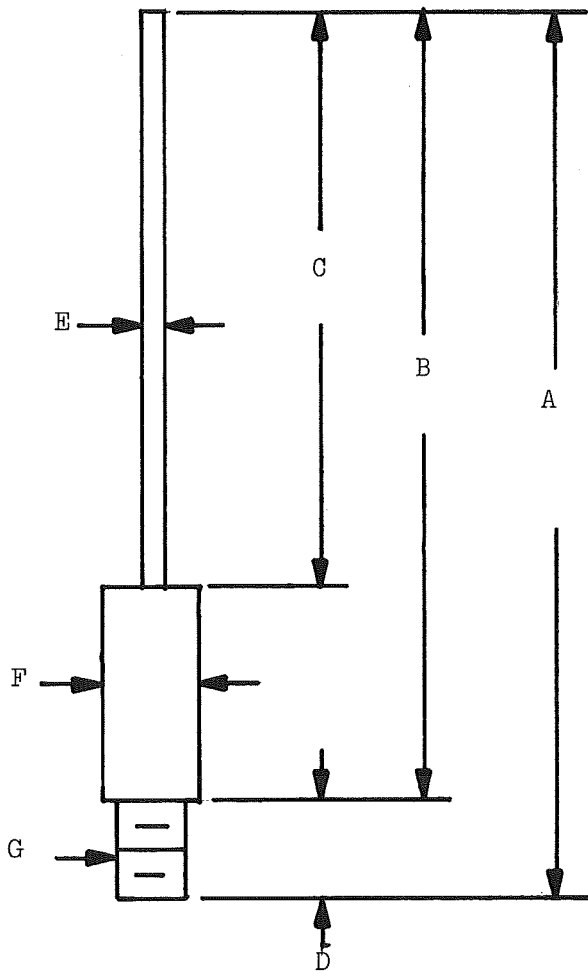
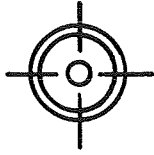
All dimension in inches.

Scale = 2:1

Shaded Portion = Ceramic

Figure 31A - Anode Connector

Alite D-312 Seal



A = 2.321

B = 2.071

C = 1.50

D = 0.250

E = 0.062

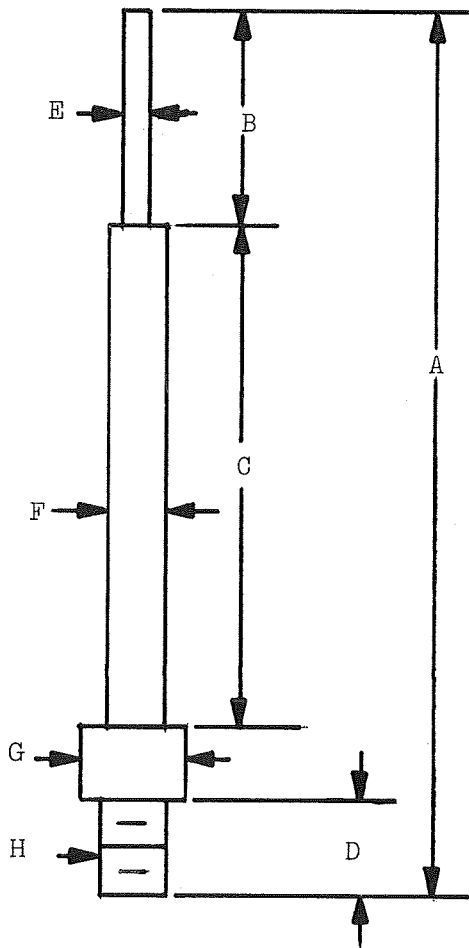
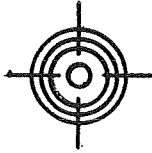
F = 0.250

G = 10-24 NC Thread

Scale - 2:1

All dimensions in inches

Figure 31B - Anode Connector for
B-50-1 Seal

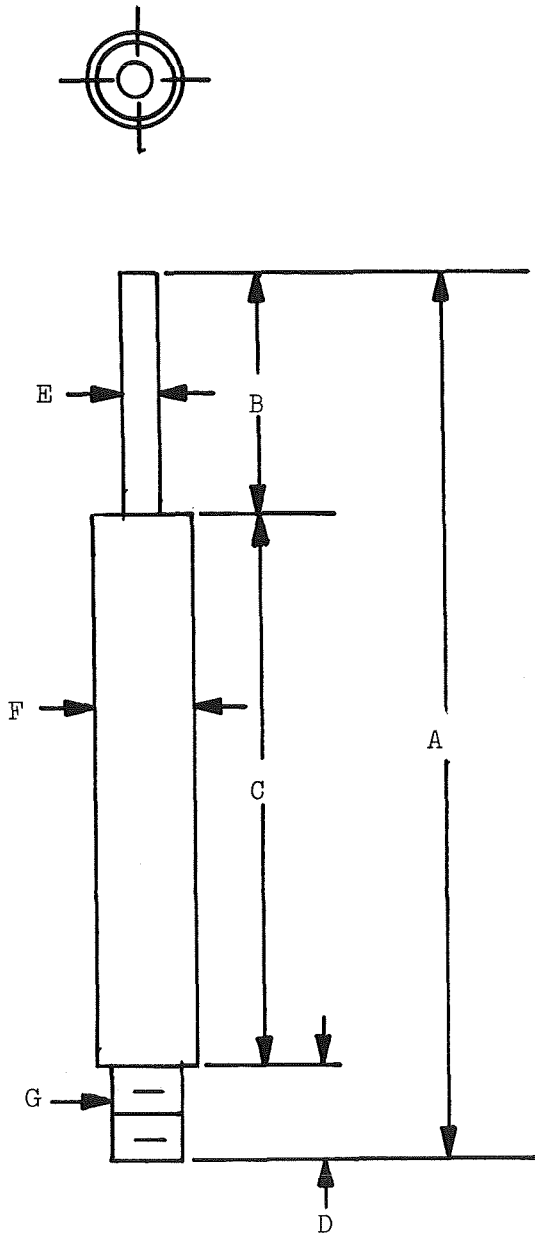


- A = 2.321
- B = 0.600
- C = 1.25
- D = 0.250
- E = 0.061
- F = 0.155
- G = 0.250
- H = 10-24 NC Threads

Scale = 2:1

All dimensions in inches

Figure 31C - Anode Connector for
B-75-1 Seal



A = 2.321

B = 0.625

C = 1.346

D = 0.250

E = 0.100

F = 0.250

G = 10-24 NC Threads

Scale = 2:1

All dimensions in inches

Figure 32 - E vs T
Alite D-312 Seal
Test No. 429 Test No. 430

1.5

1.0

E
(v)

1114

0.5

0.0

50

100

150

200

Life (hours)

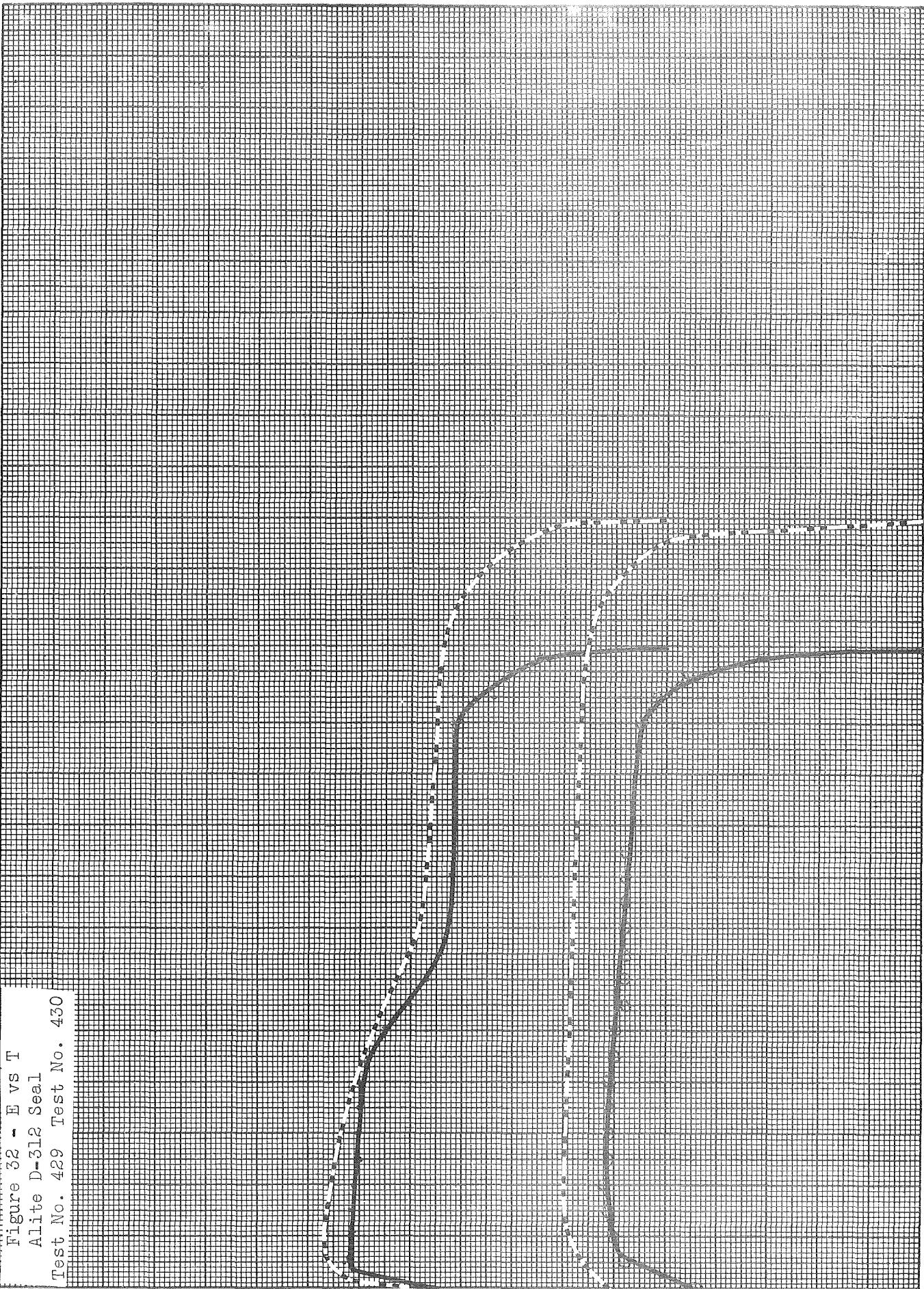


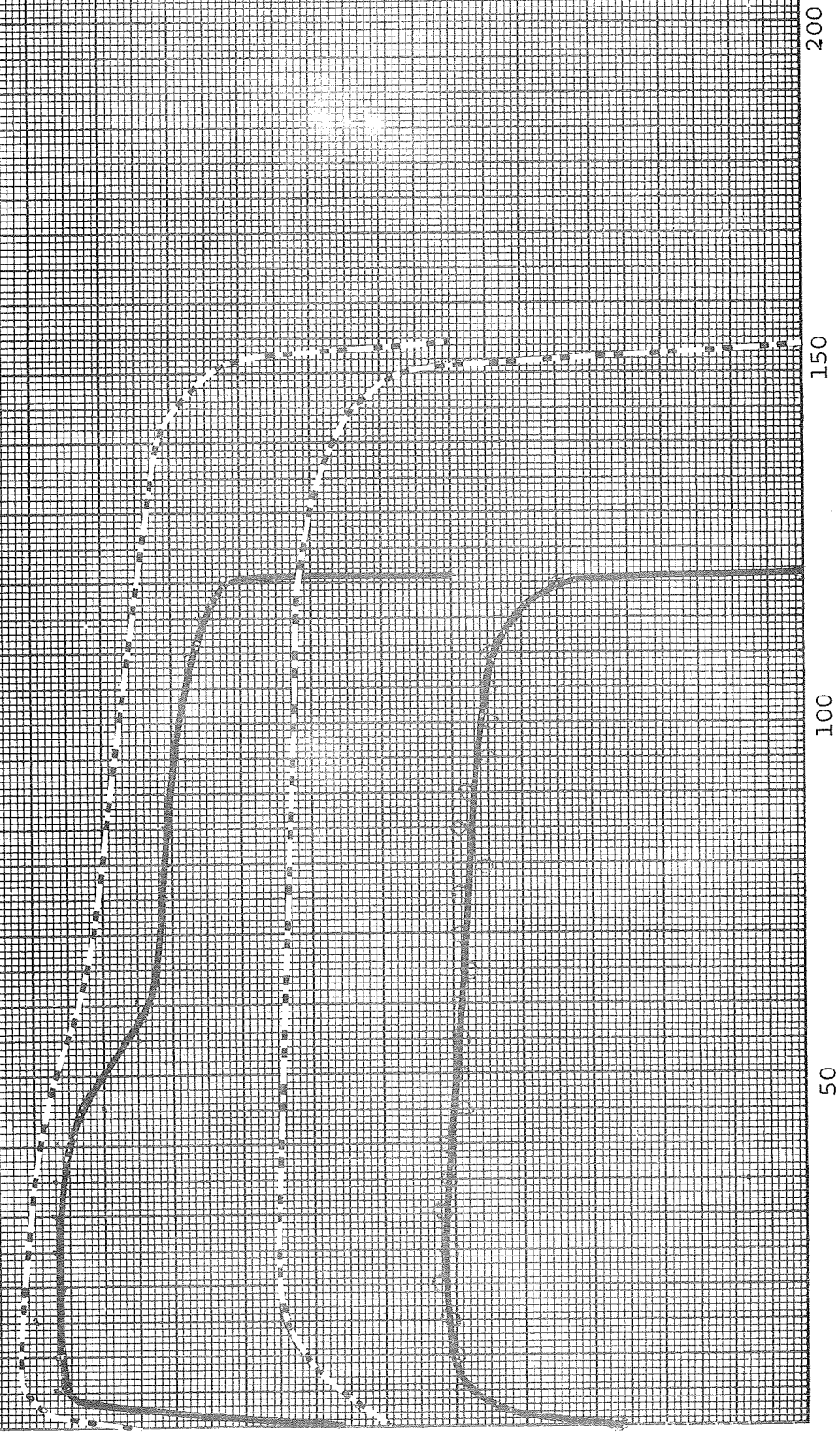
Figure 33 - E vs T
Alite B-50-1 Seal
Test No. 423 Test No. 424

1.5

1.0
115
E:
(v)

0.5

0.0



Life (hours)

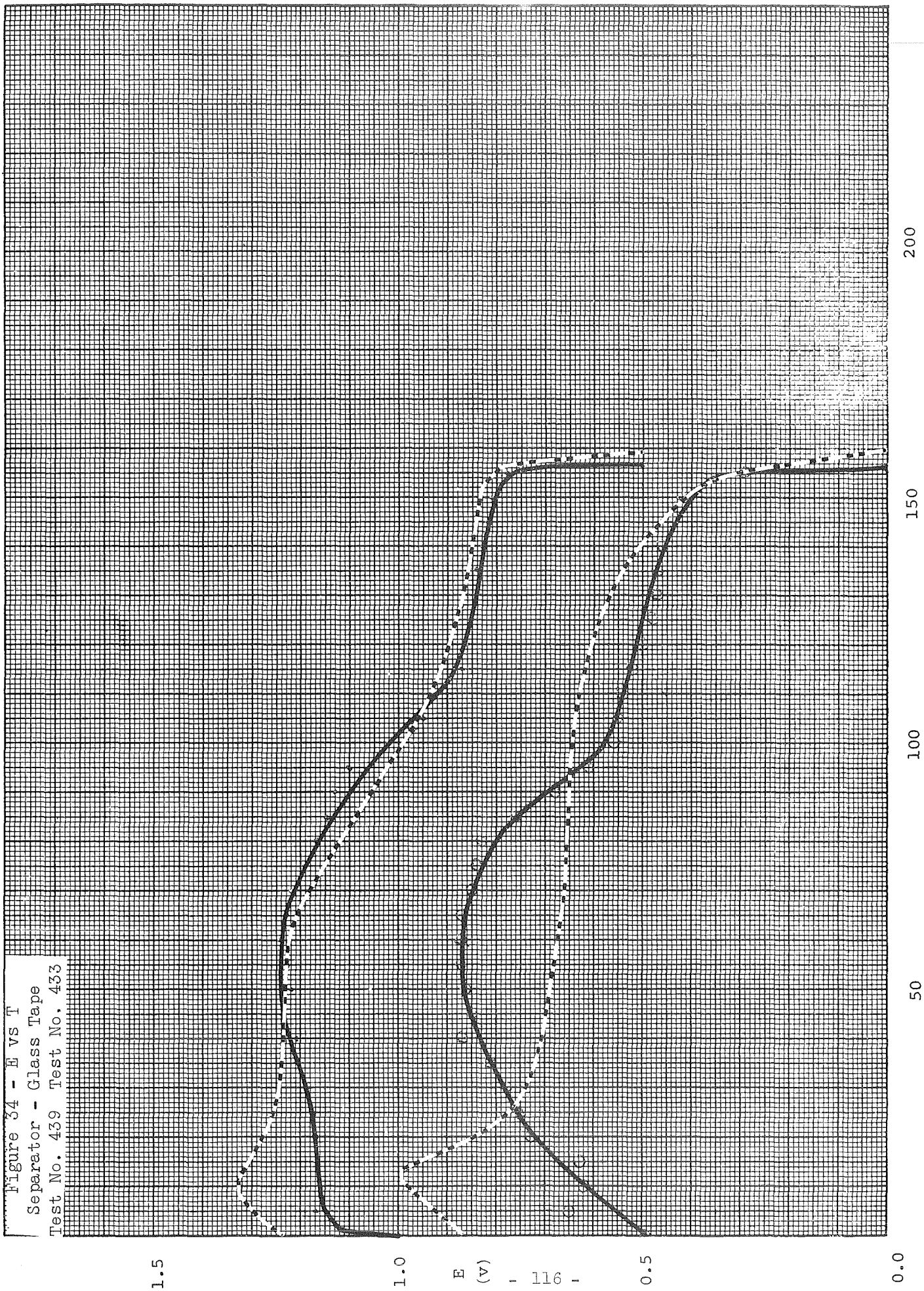
200

150

100

50

Figure 34 - E vs T
Separator - Glass Tape
Test No. 439 Test No. 433



1.5

1.0

E (v)

116

0.5

0.0

50

100

150

200

Figure 35 - E vs T
Glass Tape - 427°C
Test No. 441 Test No. 442

1.5

1.0

E (v) - 117 -

0.5

0.0

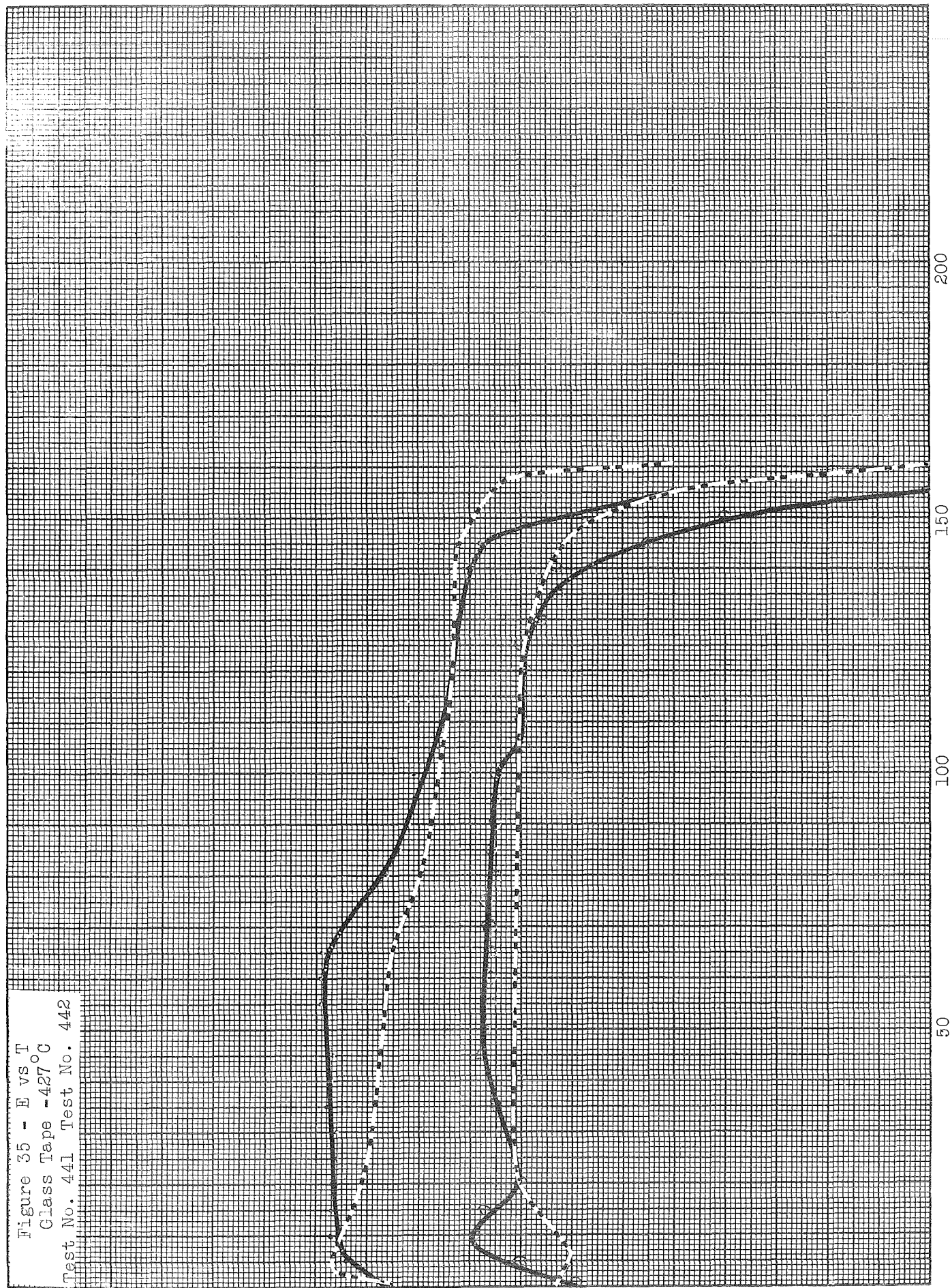


Figure 36 - E vs T
Glass Tape -481°C
Test No. 452 Test No. 454

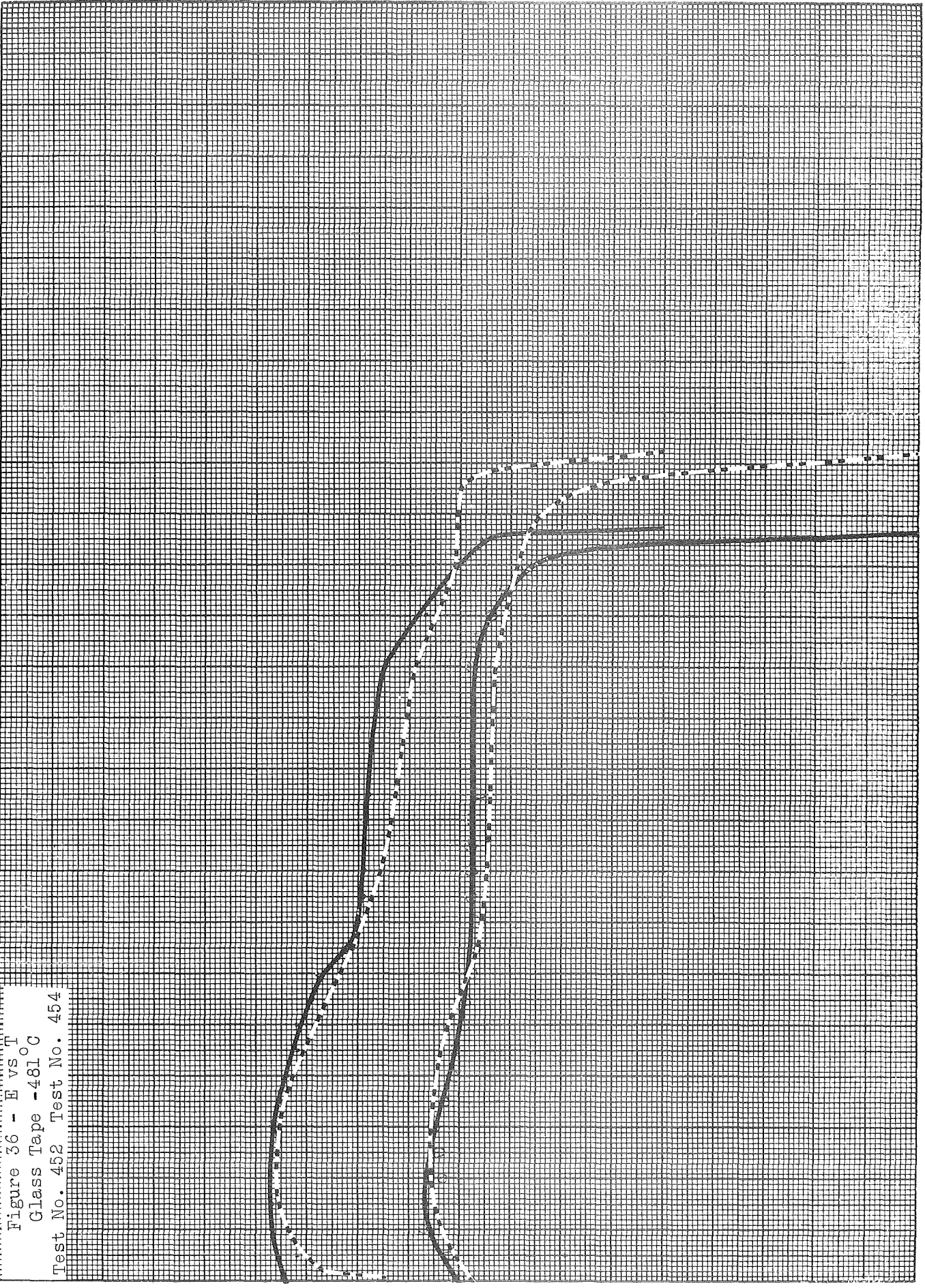
1.5

1.0

E (v)

0.5

0.0



200

150

100

50

Figure 37 - E vs T
Glass Tape -371°C
Test No. 449 Test No. 448

1.5

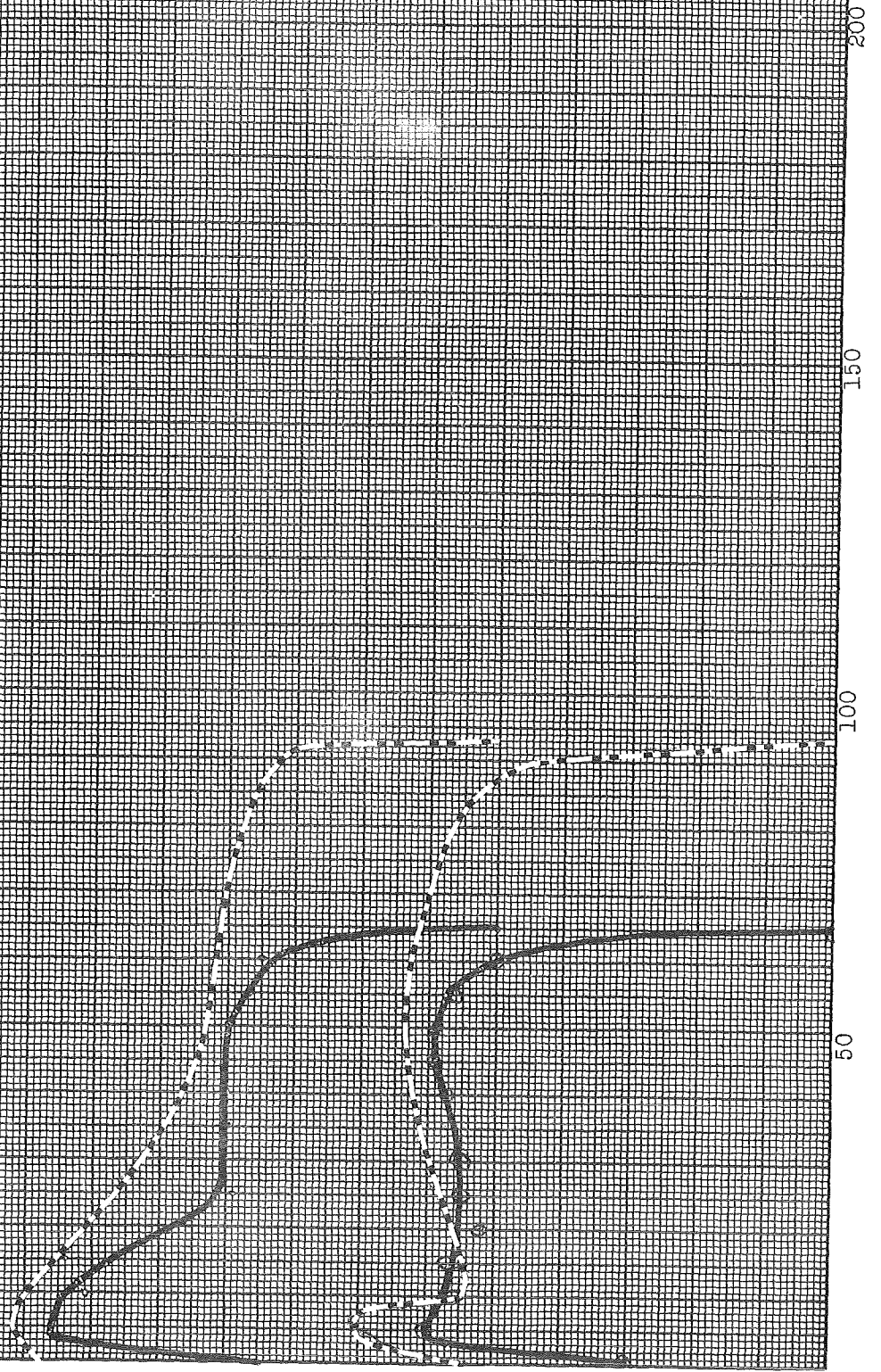
1.0

E (v)

119

0.5

0.0



Appendix II - Sample Calculations

- (1) Cathode Capacity
- (2) Output
- (3) Cathode Utilization
- (4) Anode Capacity Used
- (5) Anode Utilization
- (6) Average Self-Discharge Current
- (7) Anode Capacity - Initial

Sample Calculation for NASA Thermal Cells

(1) Cathode Capacity

* If electrodes reach the predicted theoretical weight, it can be assumed that the oxide is 100% CuO. If the weight is light, the relative percentages of CuO and Cu₂O must be computed.

In the case where the proper weight is attained:

$$\begin{aligned} \text{A-hr Capacity} &= \frac{(\text{cath. weight, gms})(\text{Faraday Constant, coul/eq})}{(\text{eq wt. of CuO, gms/equiv})(\text{Time Conv, sec/hr})} \\ &= \frac{(\text{cath. weight, gms})(96,500 \text{ coul/eq})}{(39.79 \text{ gms/eq})(3600 \text{ secs/hr})} \\ &= (\text{cath. weight, gms})(0.674) \end{aligned}$$

(2) Output

The time used in calculating output must refer only to the time in which current was being passed.

$$\begin{aligned} \text{A-hr Output} &= \frac{(1201 \text{ coul/hr})(\text{active running time, hrs})}{(3600 \text{ secs/hr})} \\ &= (\text{active running time, hrs})(0.334) \end{aligned}$$

(3) Cathode Utilization

This value represents the relative amount of the cathode that was useful output.

$$\text{Cath. Effic. \%} = \frac{(\text{Output, A-hrs})}{(\text{Cath. Capacity, A-hrs})} \times 100\%$$

(4) Anode Capacity Used

$$\begin{aligned} \text{Total Anode Used, A-hrs} &= \frac{(\text{initial anode wt, gms} - \text{final anode wt, gms})(F, \text{ coul/eq})}{(\text{eq. wt. Mg})(\text{Time Conversion, sec/hr})} \\ &= \frac{(w_i - w_f, \text{ gms})(96,500 \text{ coul/eq})}{(12.16 \text{ gms/eq})(3600 \text{ sec/hr.})} \\ &= (\Delta W)(2.205) \end{aligned}$$

(5) Anode Utilization

This value represents the quantity of the anode used in practical cell output.

$$\text{Anode Effic. \%} = \frac{(\text{Output, A-hrs})}{(\Sigma \text{It, A-hrs})} \times 100\%$$

(6) Average Self-Discharge Current

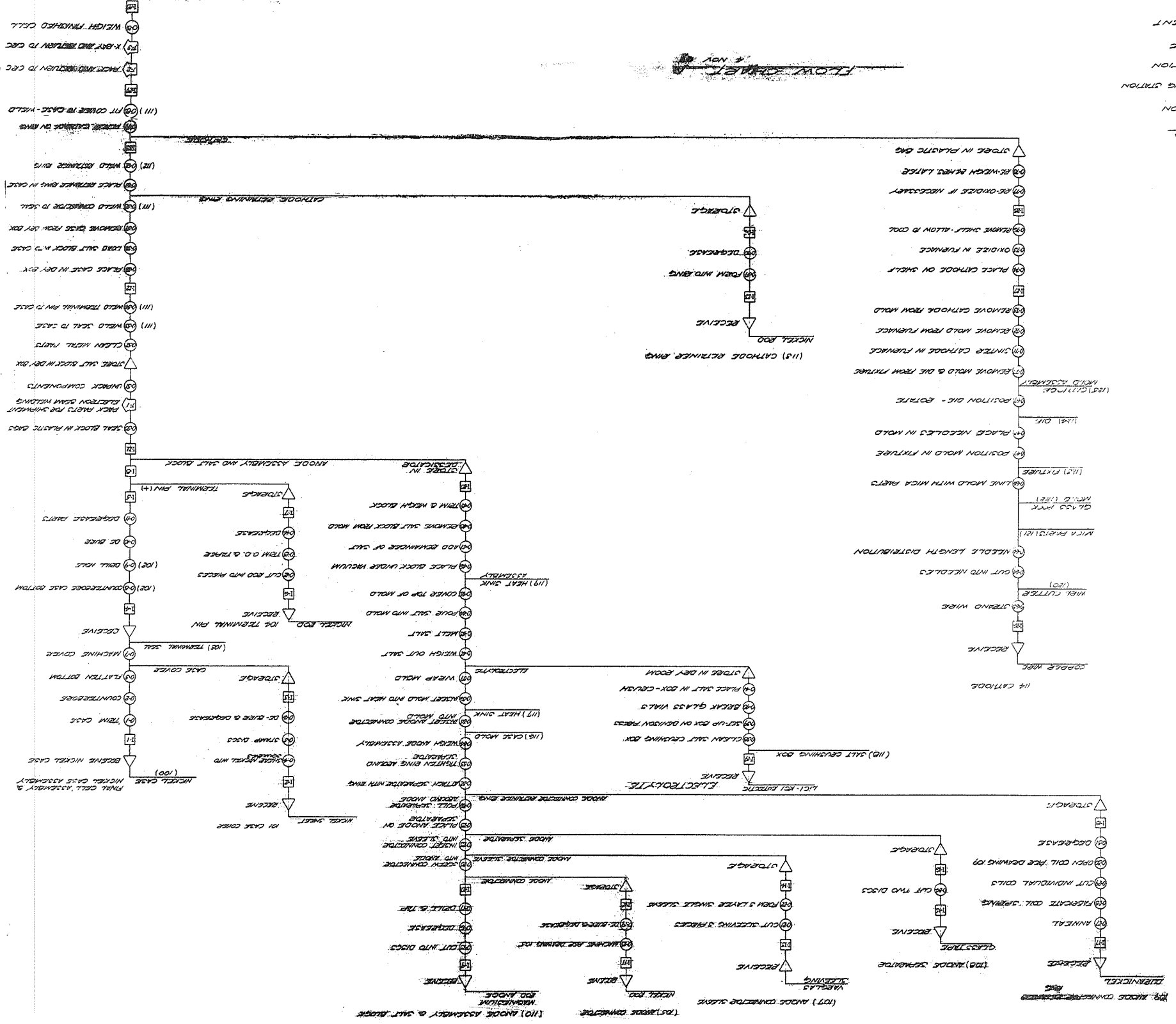
Whenever the cell is in a molten state, self-discharge will be occurring. Consequently, the time used in this calculation must reflect this situation.

$$I_{\text{s.d.}}, \text{ ma} = \frac{(\text{Anode Capacity Used, A-hrs} - \text{Output, A-hrs})}{(\text{Time in molten state, hrs})} \cdot 1000 \text{ ma/A}$$

(7) Anode Capacity - Initial

$$\begin{aligned} \text{Anode Cap., A-hrs.} &= \frac{(\text{initial wt Mg, gms})(F)}{(\text{eq wt Mg, 2/eq})(\text{Time Conversion, secs/hr})} \\ &= (\text{Initial wt. Mg, gms})(2.205) \end{aligned}$$

- LEGEND**
- ◻ SHIPMENT
 - △ STORAGE
 - INSPECTION
 - ▽ RECEIVING STATION
 - OPERATION



APPENDIX III

QUALITY CONTROL

AND

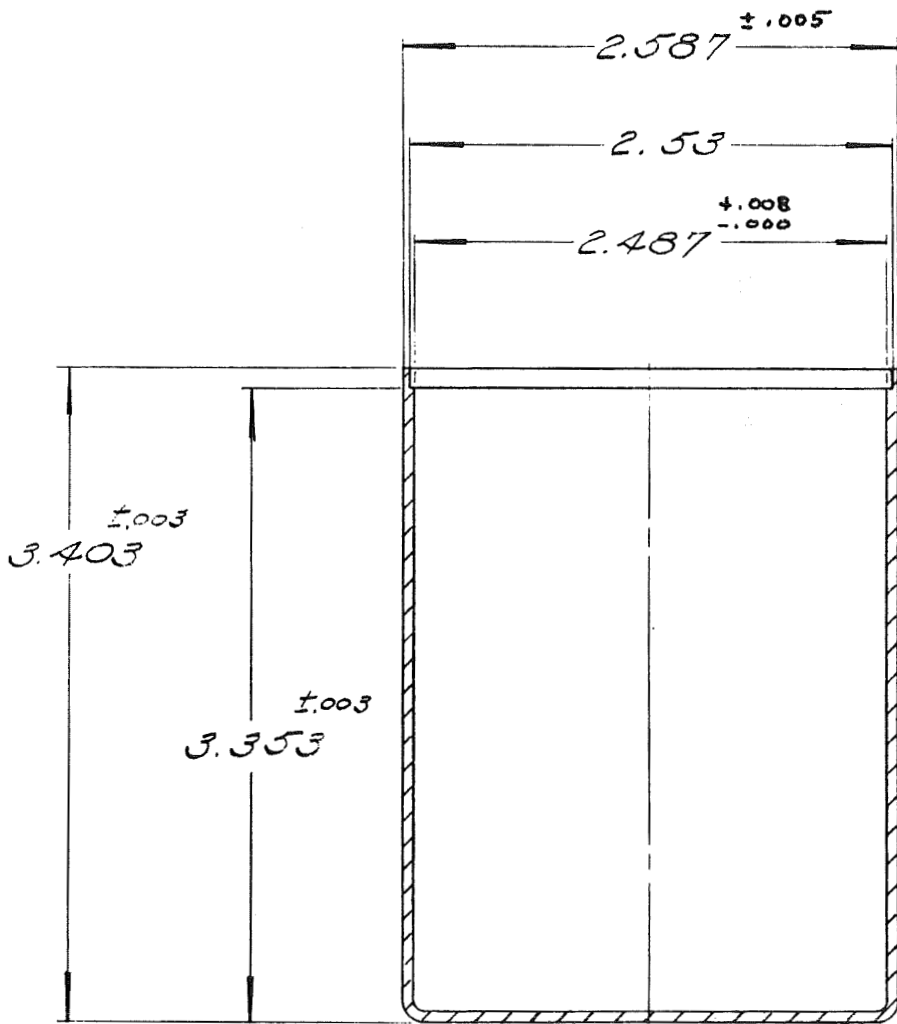
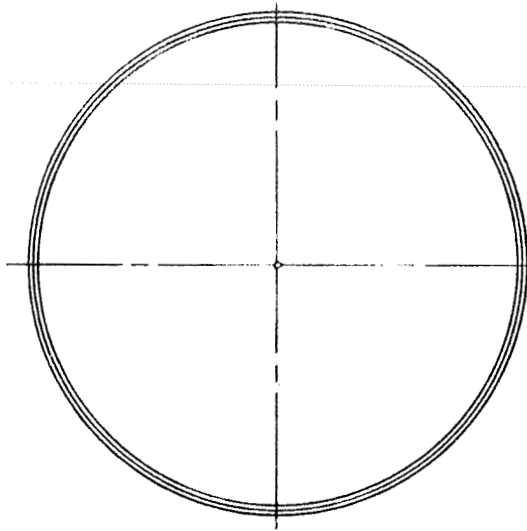
CONSTRUCTION PROGRAM

Section 1

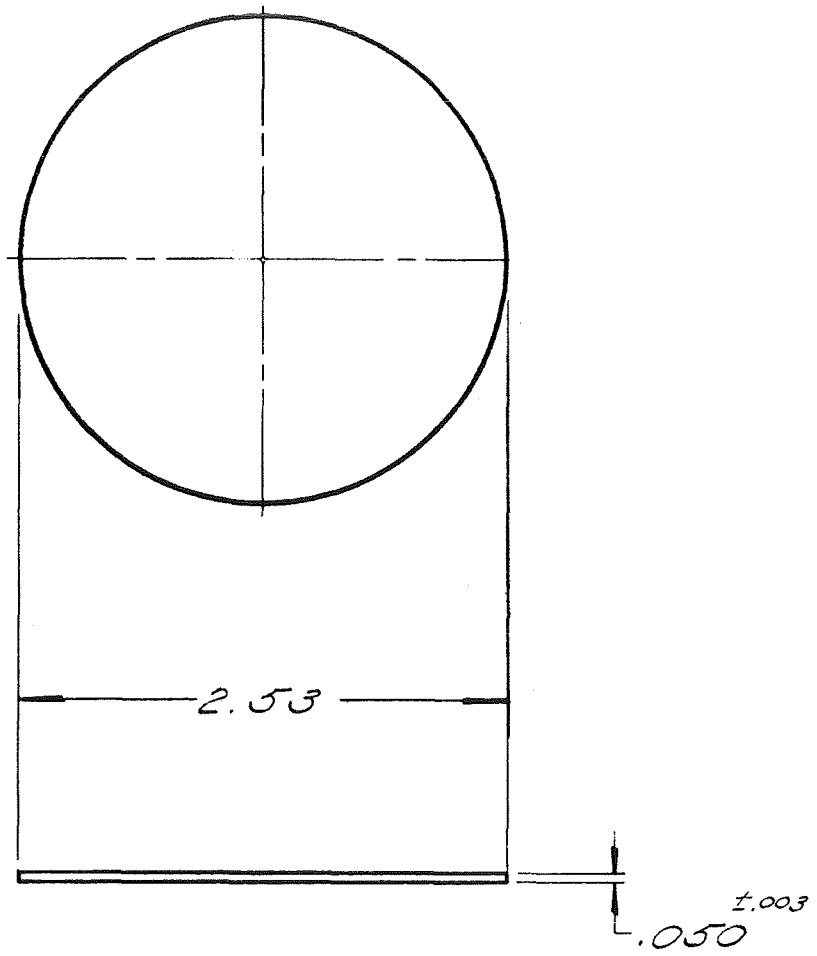
Cell Fabrication and Testing

Drawings

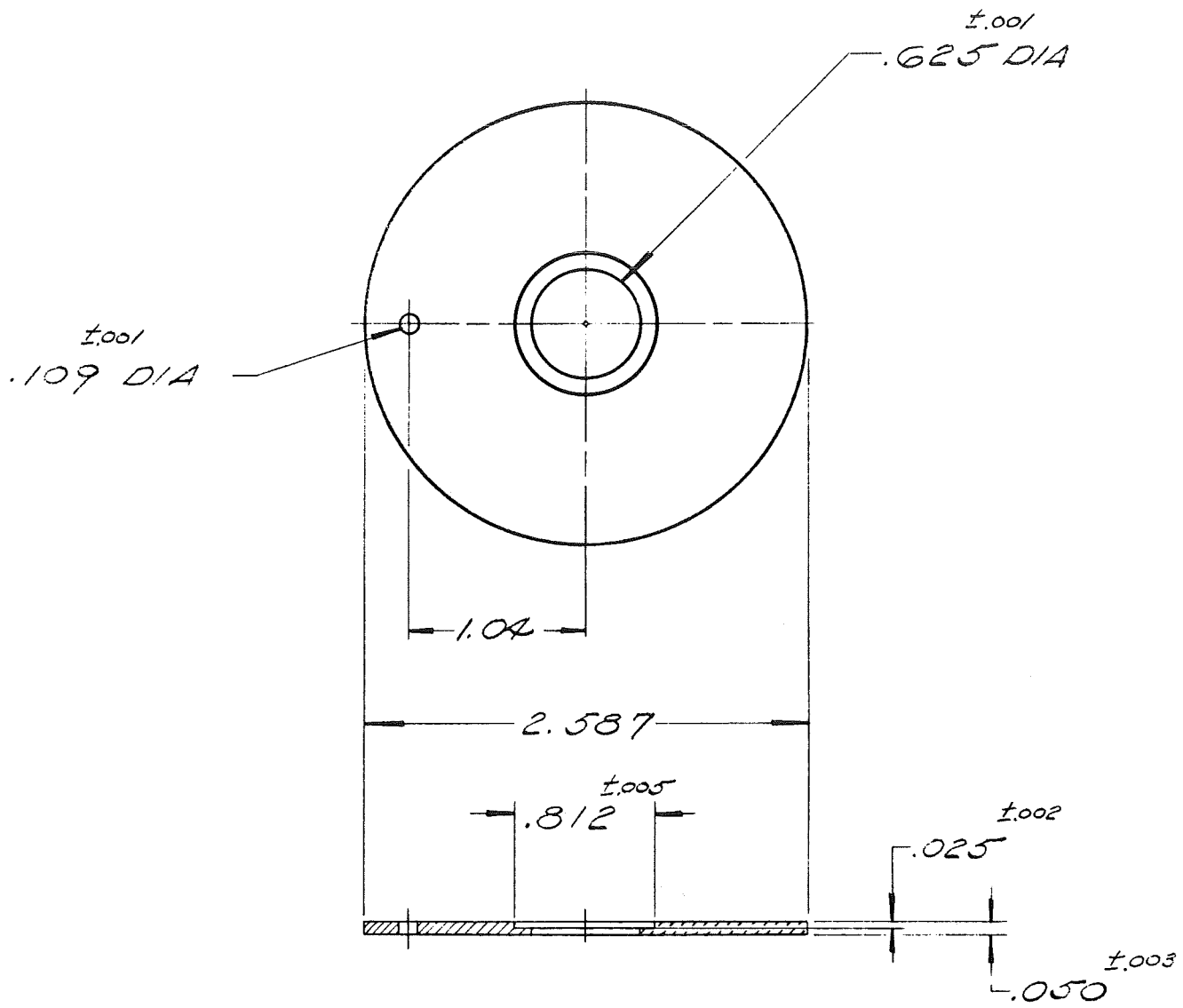
1. All drawings are according to standards set forth in MIL-D-1000, Category A, Form 2.
2. All dimensions are in inches.



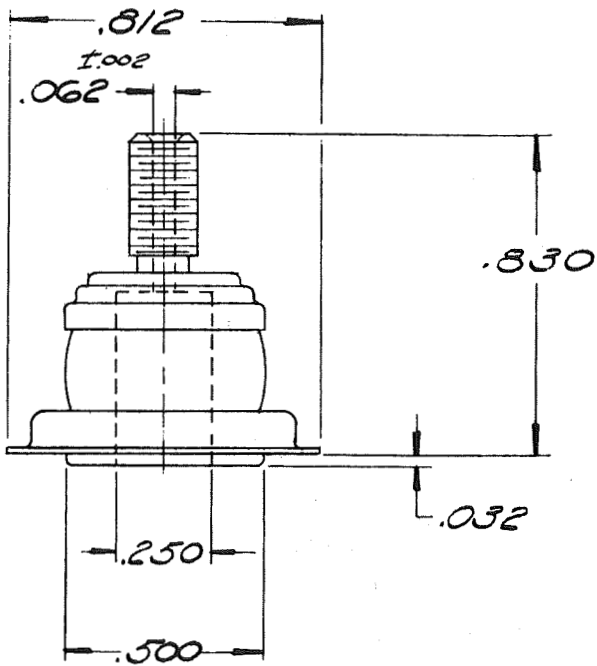
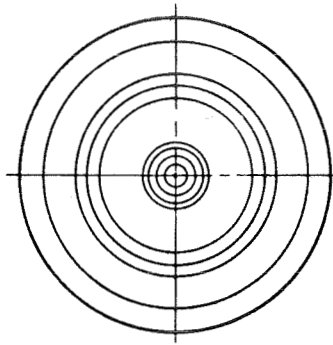
100 - Cell Case, Nickel 200



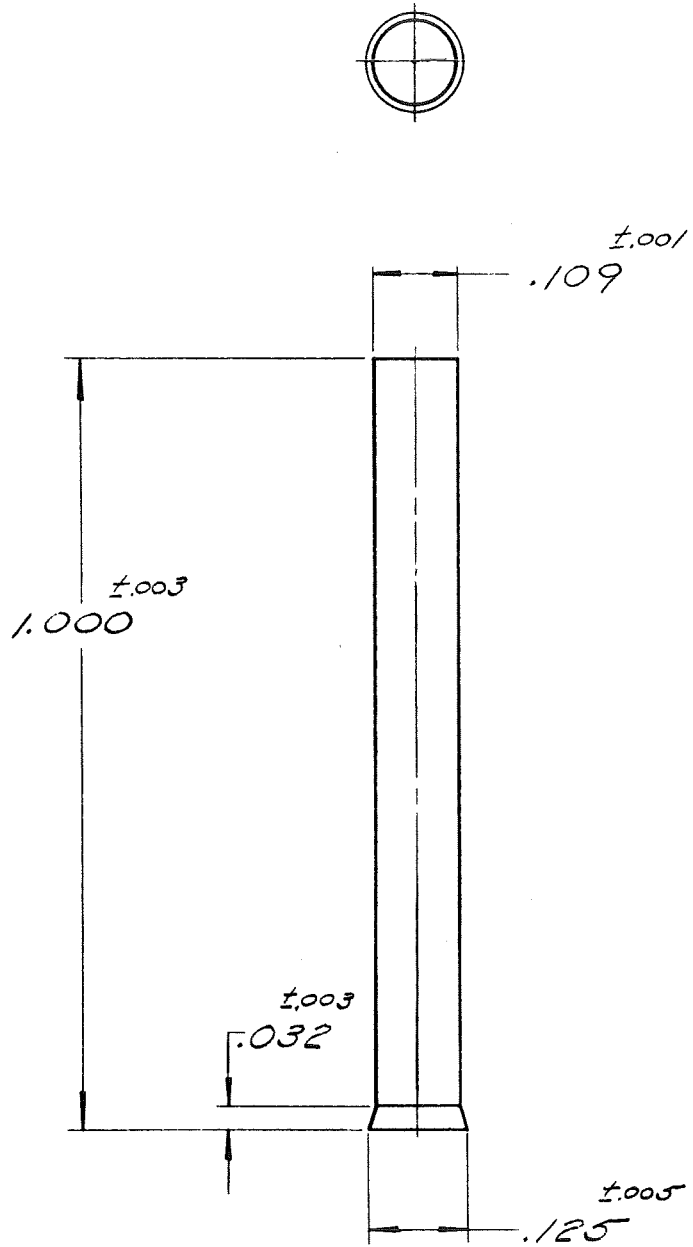
101 - Case Cover, Nickel 200



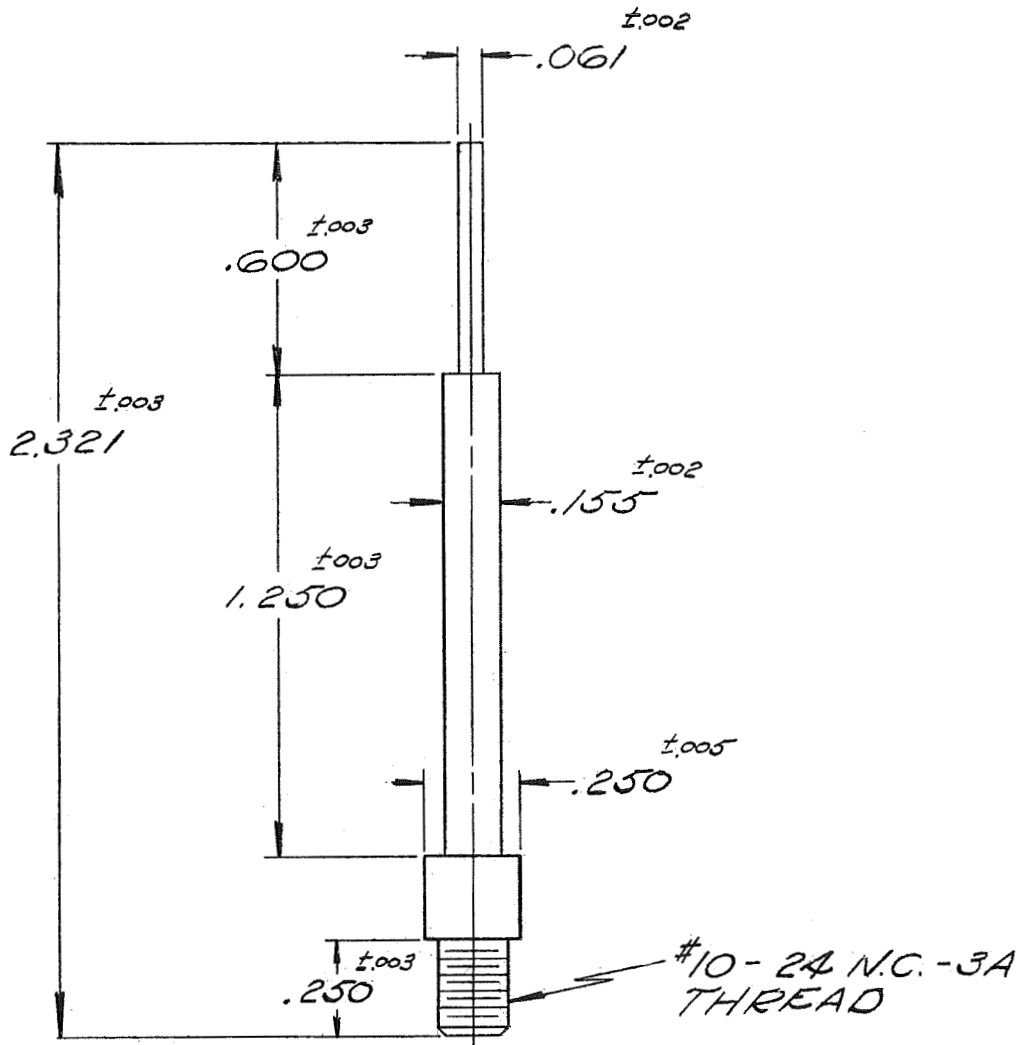
102 - Case Bottom Preparation



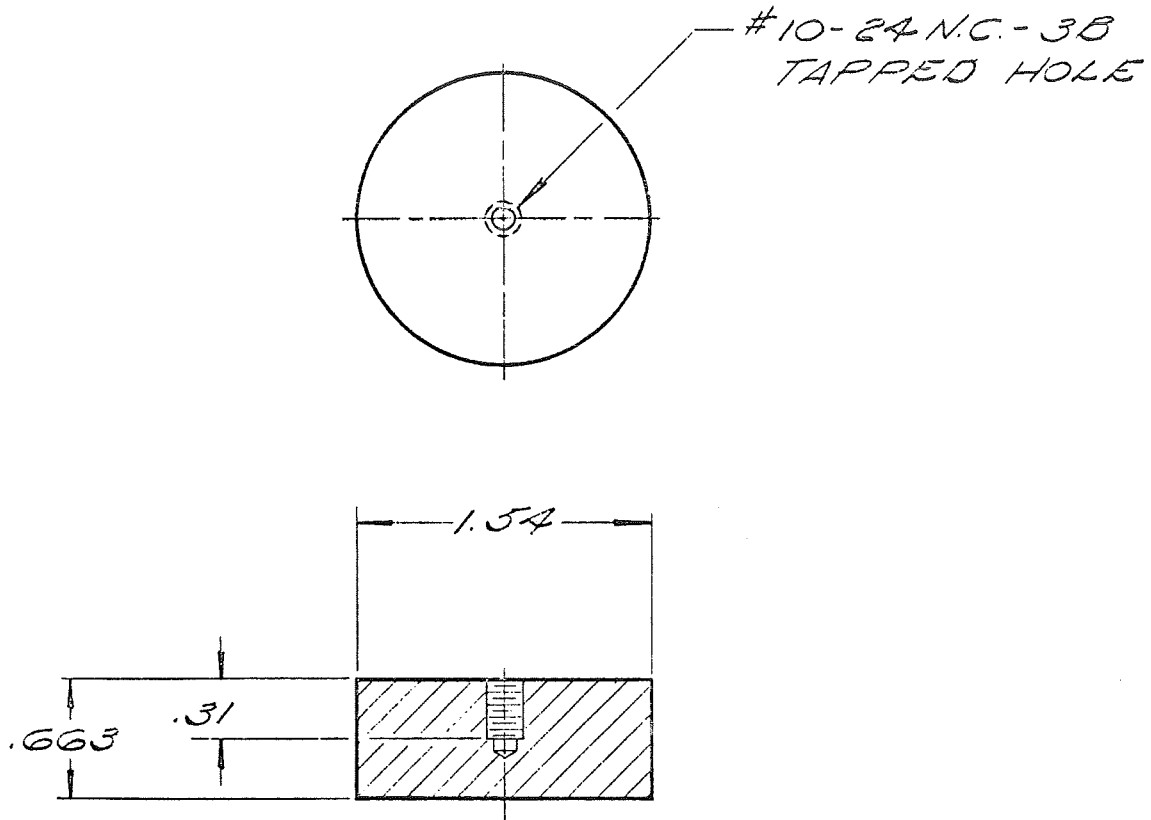
103 - Terminal Seal Alite B50-1
Manufacturer's Tolerances \pm 0.005 unless Otherwise Stated



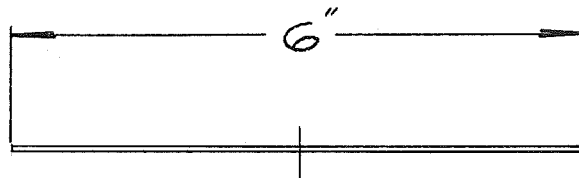
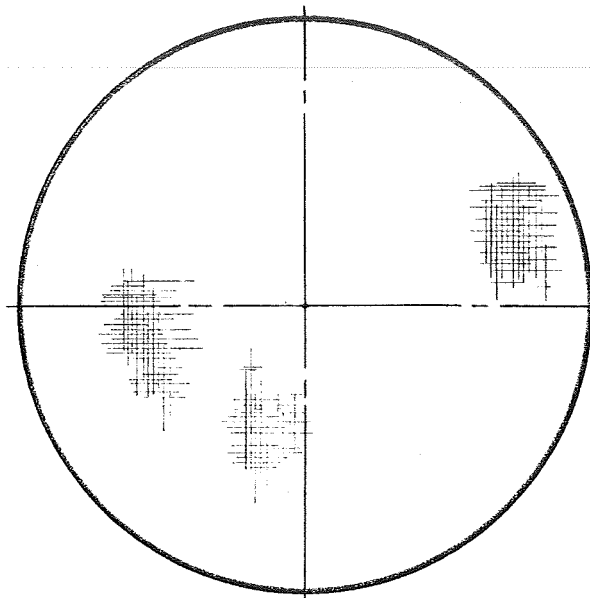
104 - Terminal Pin, Nickel 200



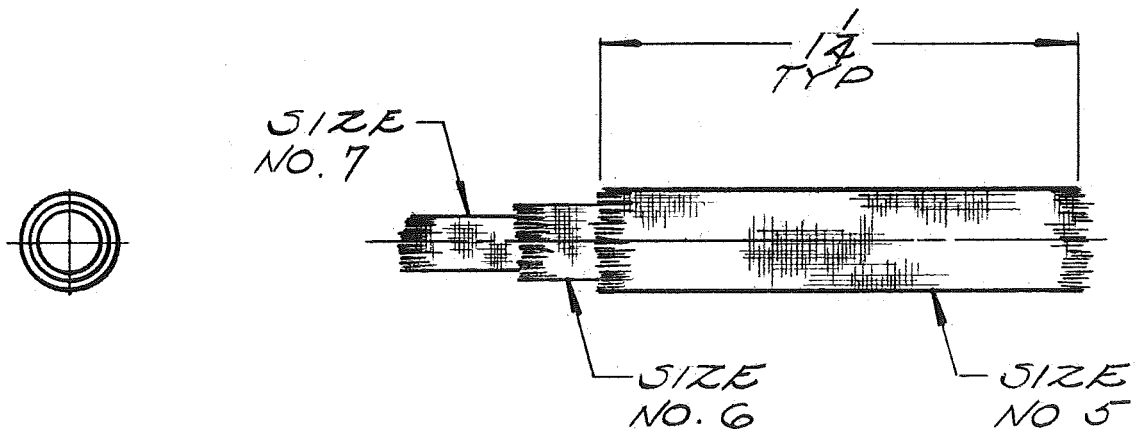
105 - Anode Connector Nickel 200



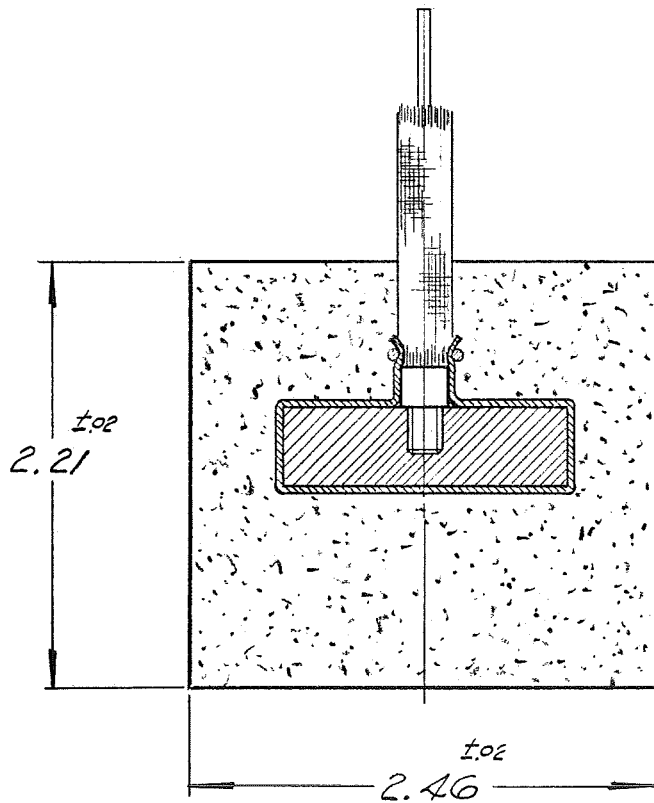
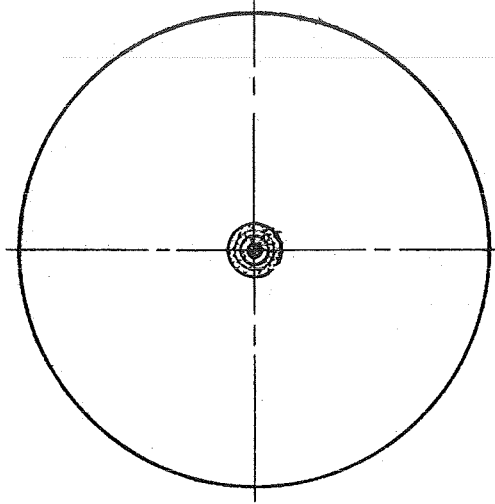
106 - Anode Magnesium, Wt. 33.320 ± 0.250 g.



108 - Anode Separator
 Hesgon "B" Glass Tape - 5 mils thick
 2 discs per part

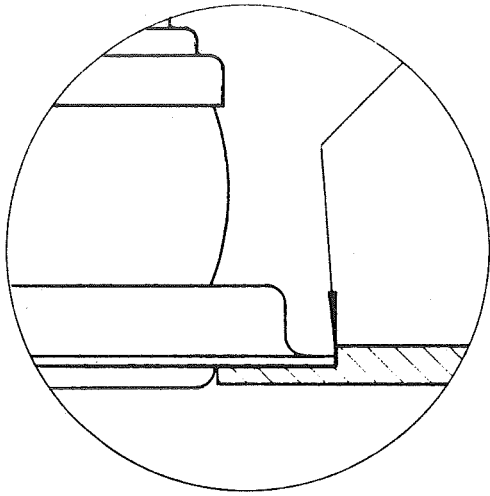


107 - Anode Connector Sleeve
 Varglas Type "H"

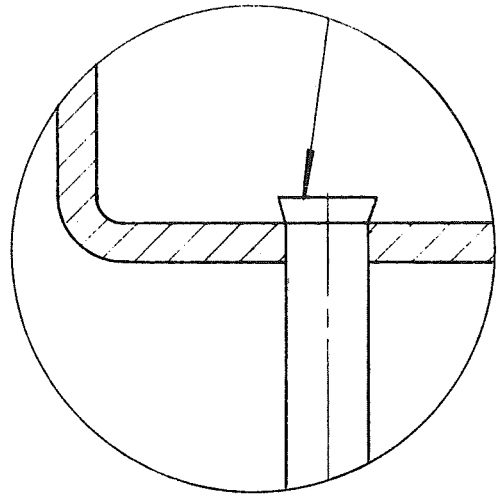


110 - Salt Block Assembly

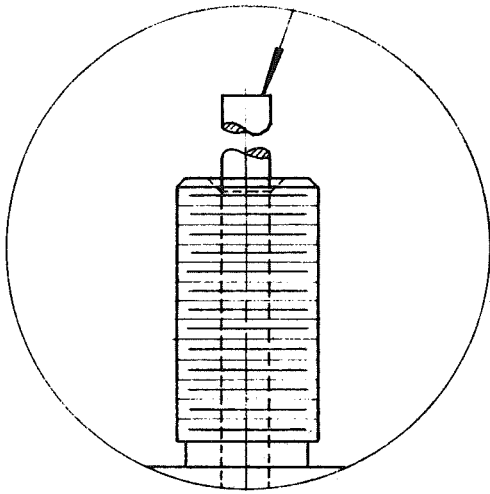
111 - Electron Beam Welding, Allowable
Weld Joint Tolerance = +0.000,
-0.002



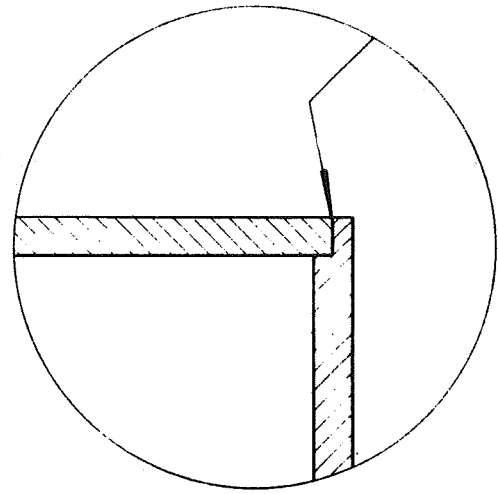
Operation 51



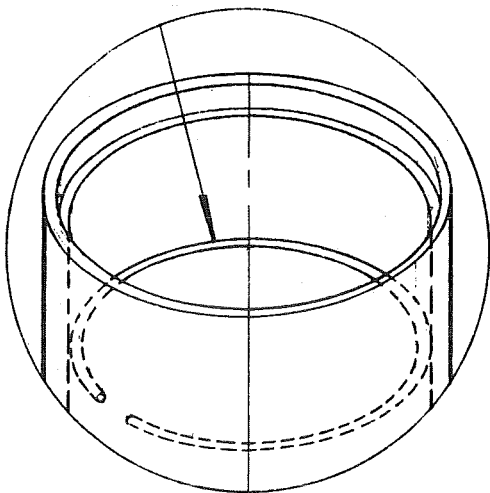
Operation 52



Operation 56

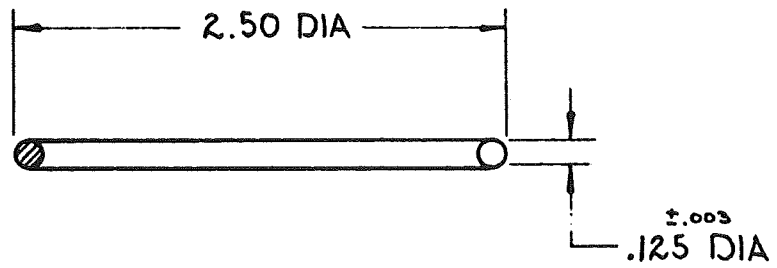
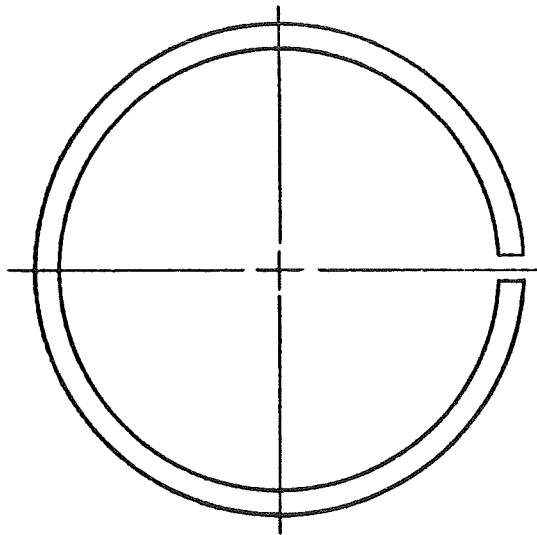


Operation 78

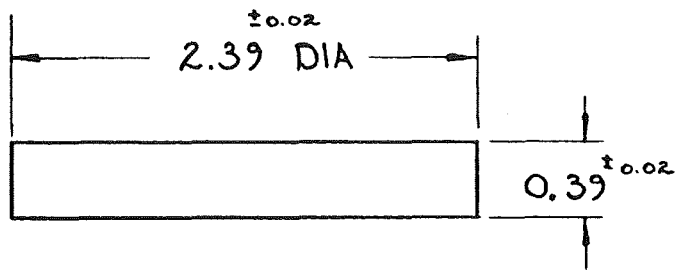
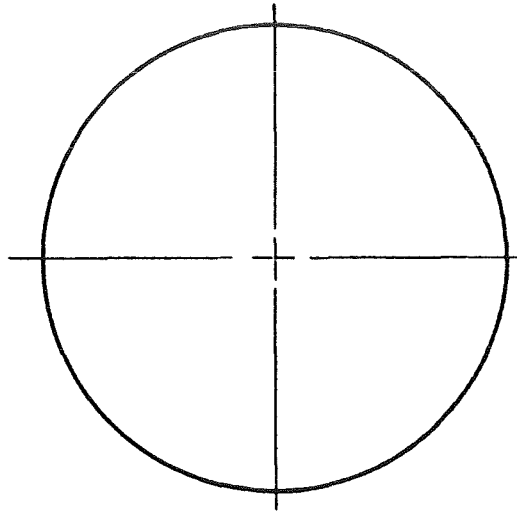


Operation 60

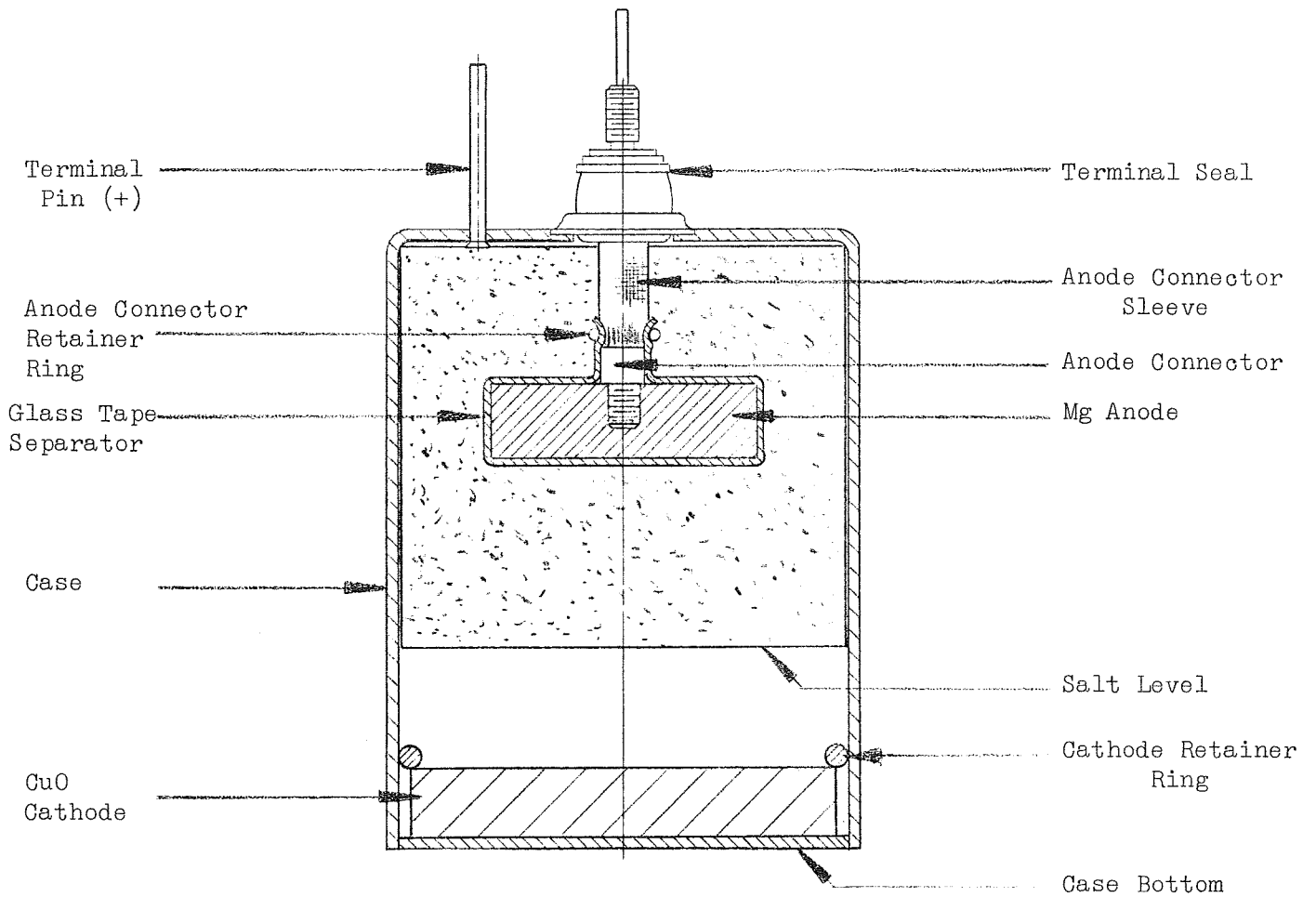
112 - Cathode Retainer Ring Weld



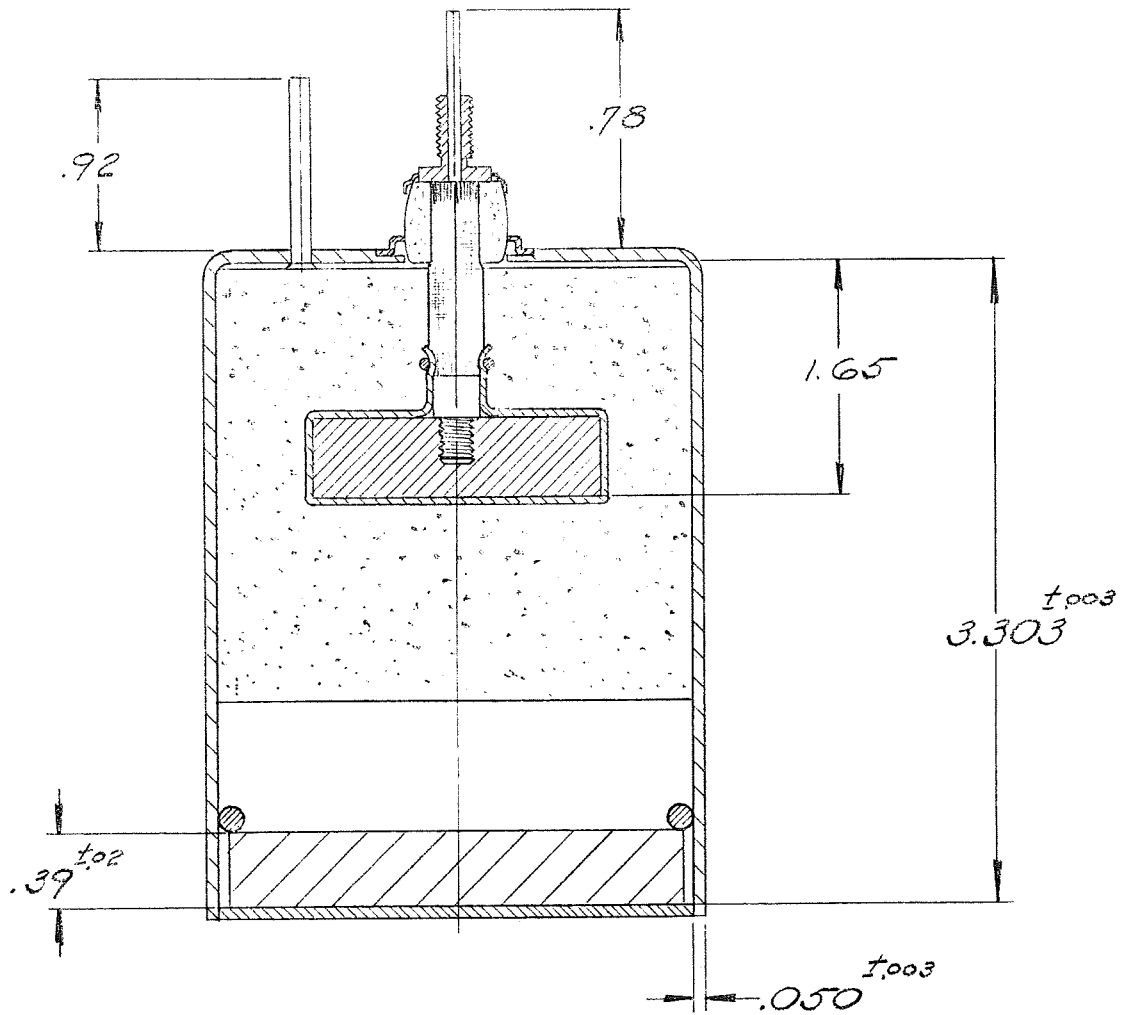
113 - Cathode Retainer Ring, Nickel 200



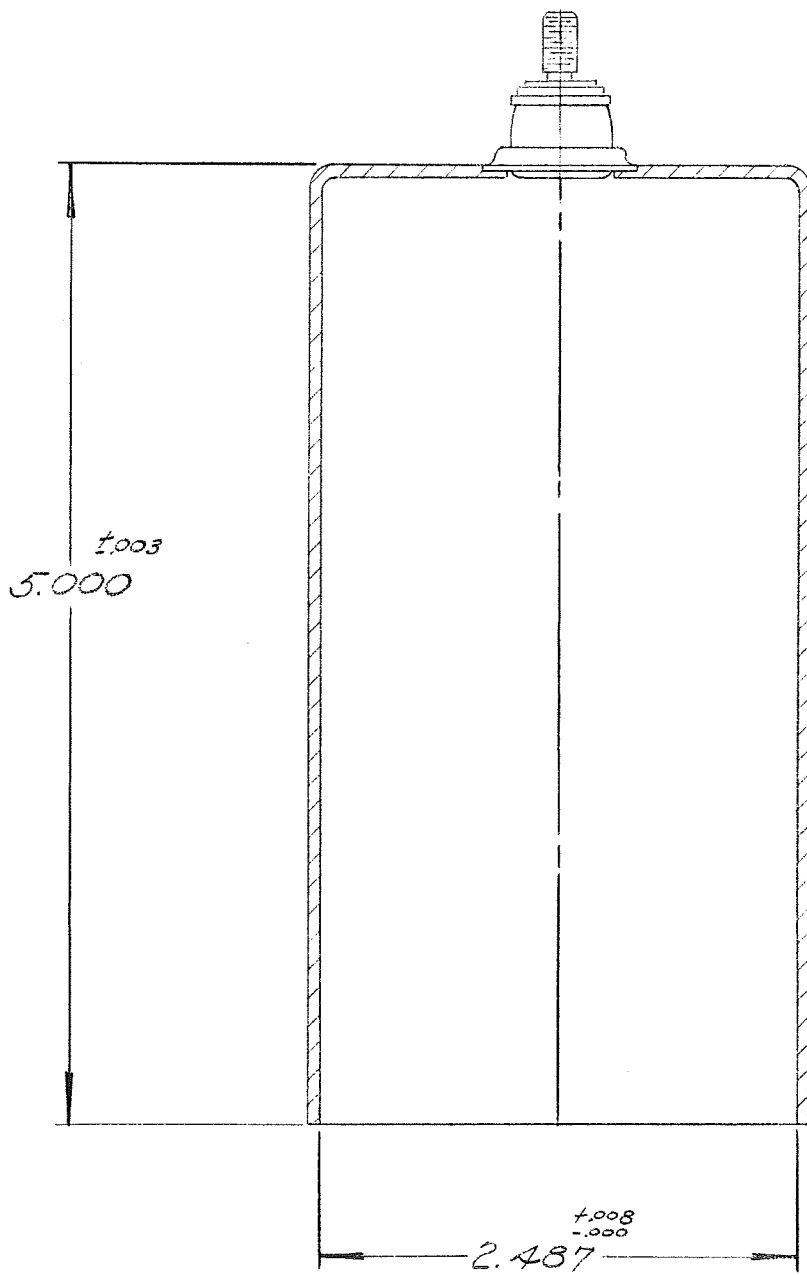
114 - Cathode CuO Needles
Weight = 90.6 - 91.2 g.
Density = 3.18 - 3.38 g/cc



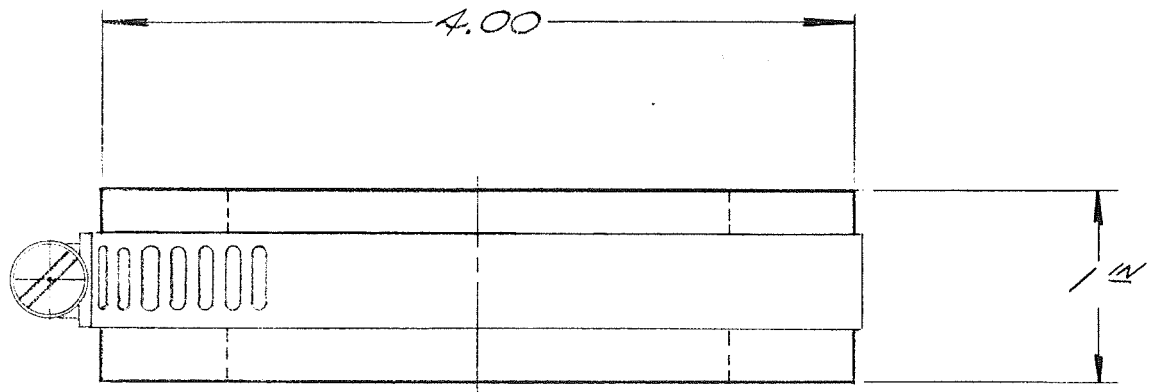
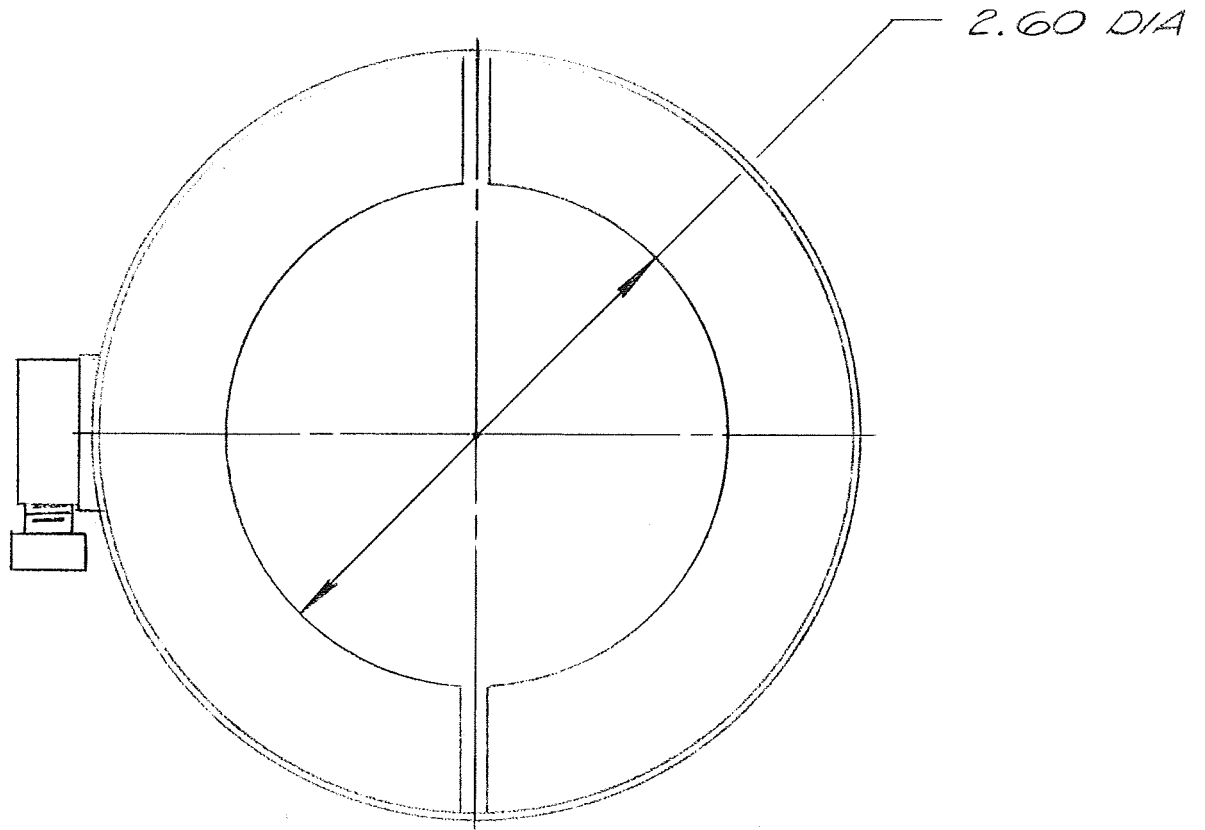
115A - Thermal Cell



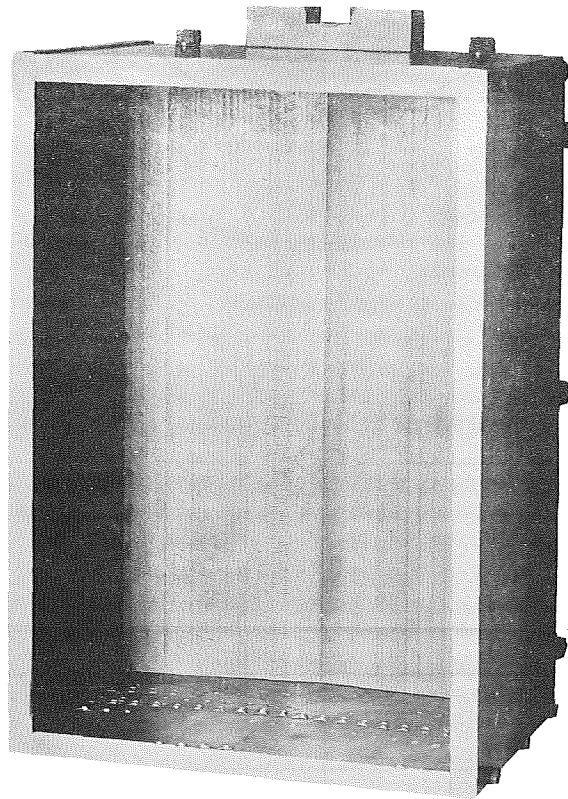
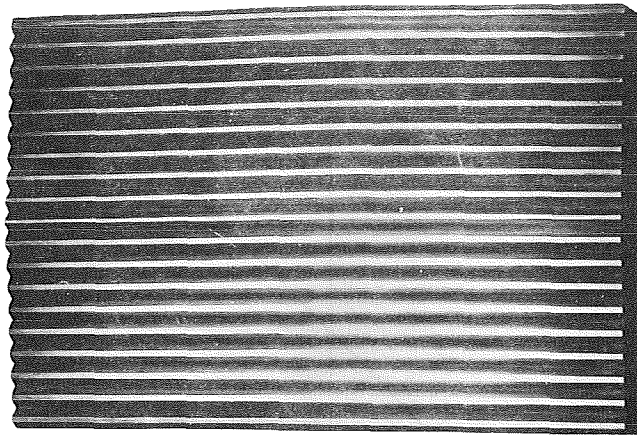
115B - Thermal Cell



116 - Case Mold Nickel 200



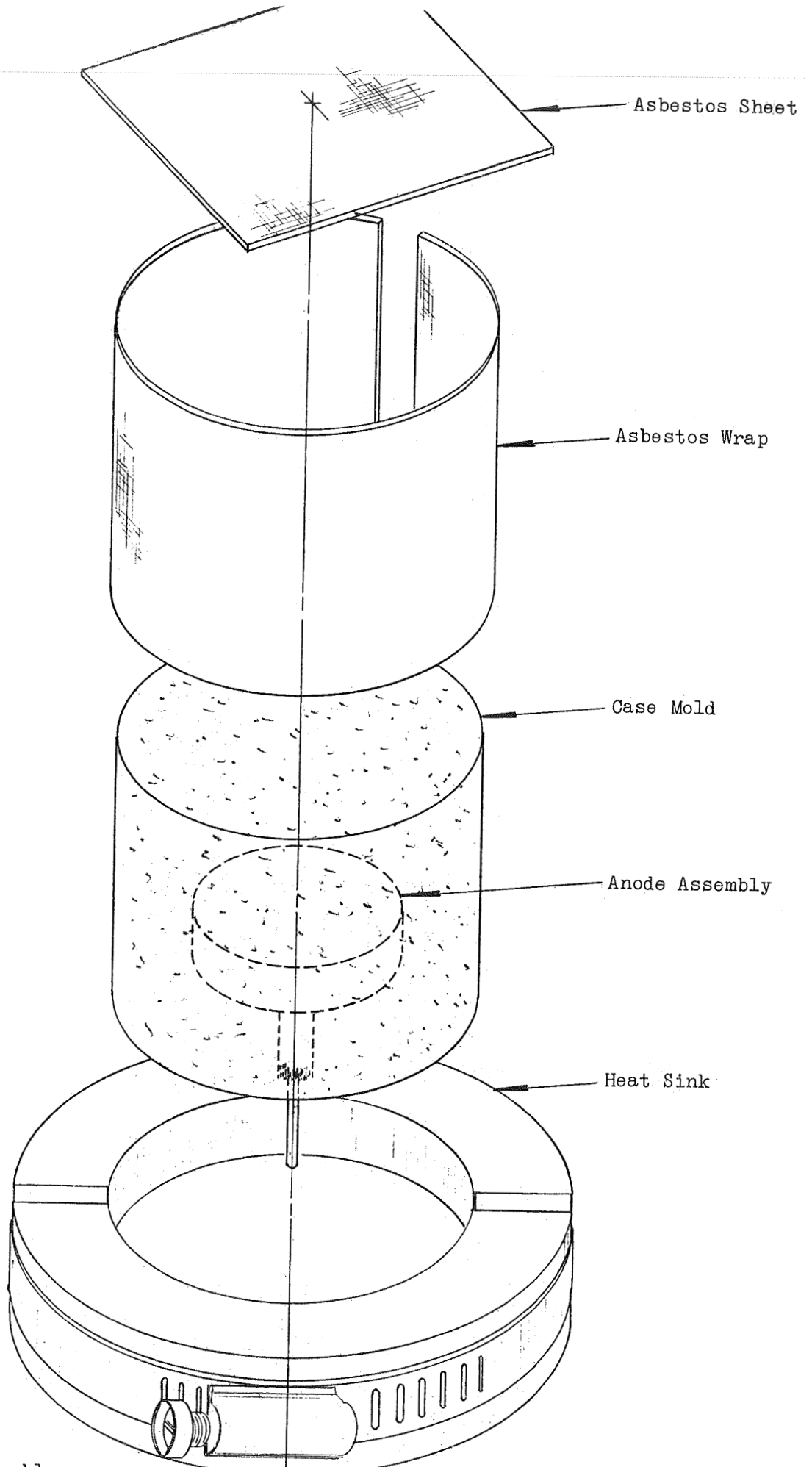
117 - Heat Sink - Aluminum



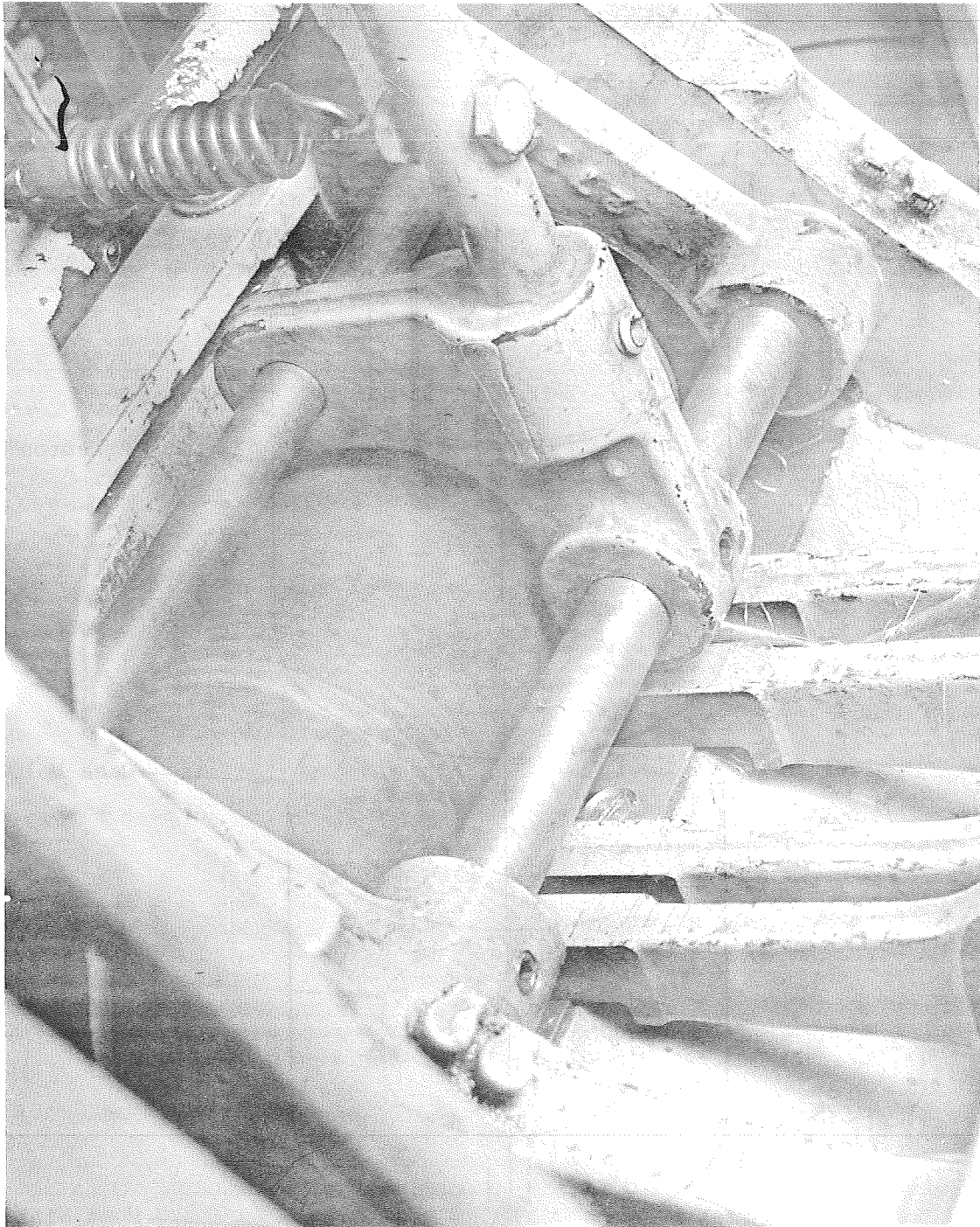
Photograph 118

Salt Crushing Box

Hampton Oil Hardening Steel



119 Heat Sink Assembly

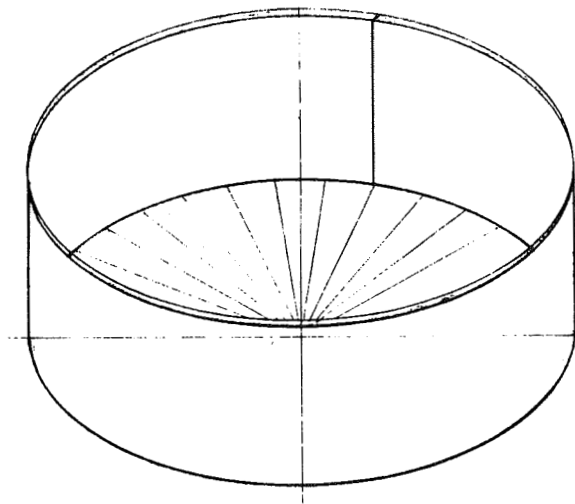
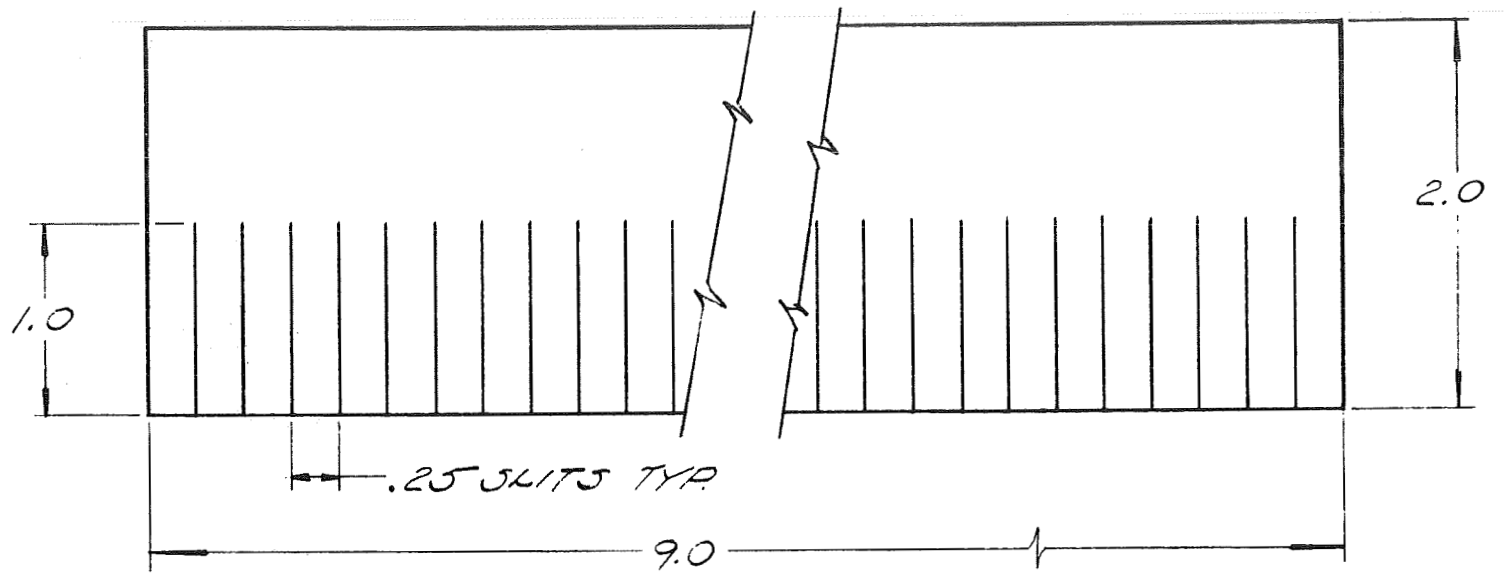


A - Copper Wire
B - Wire Guide
C - Roller

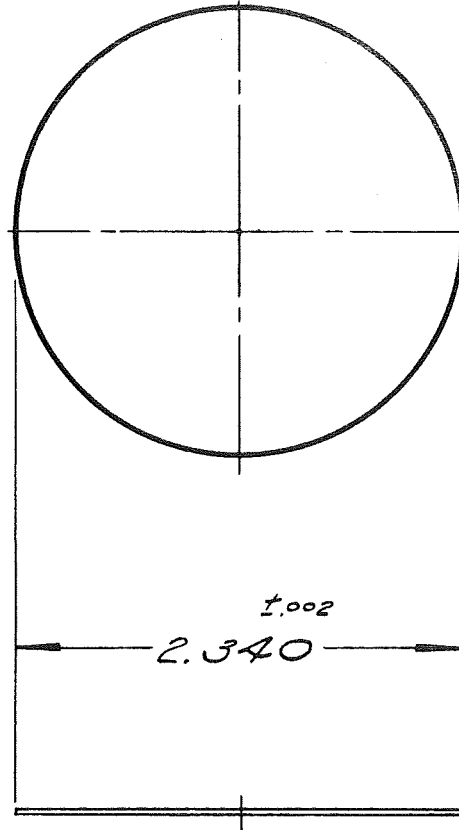
D - Roller Tension
Adjustment
E - Cutting Blade

Photograph 120

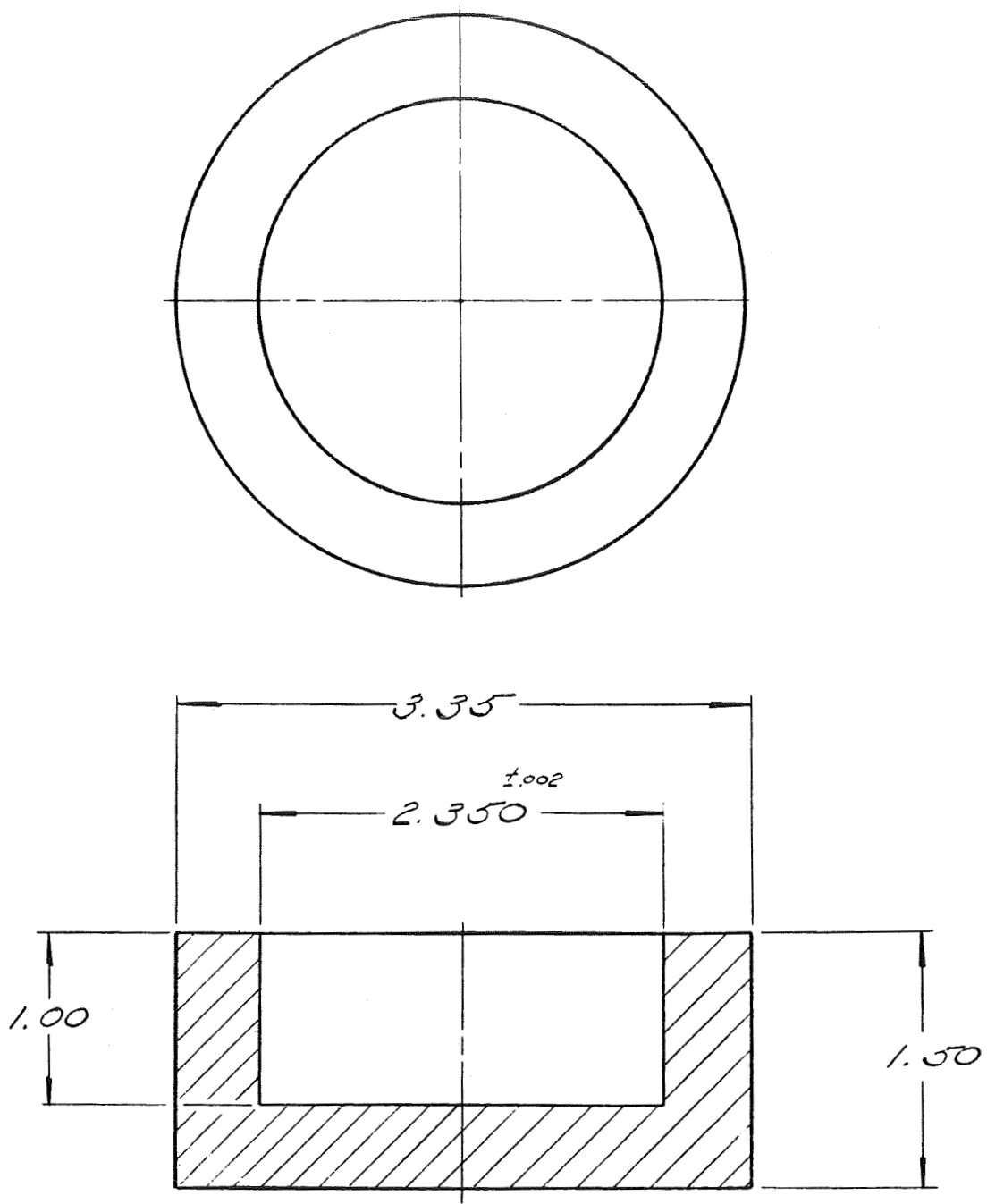
Artos Model M Wire Cutter



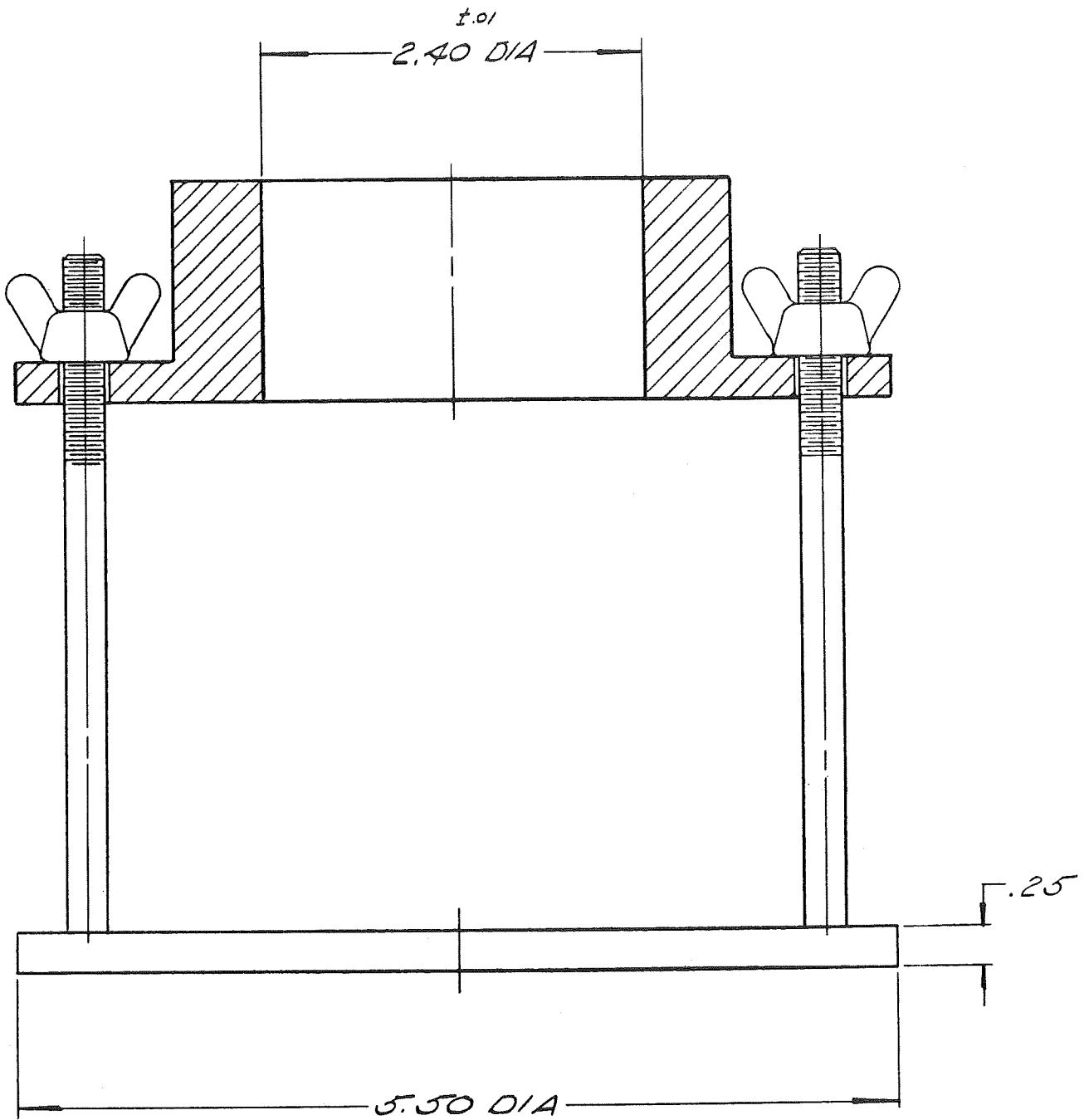
121 - Mica Sleeve - Mica
Thickness 0.003 +0, -0.001



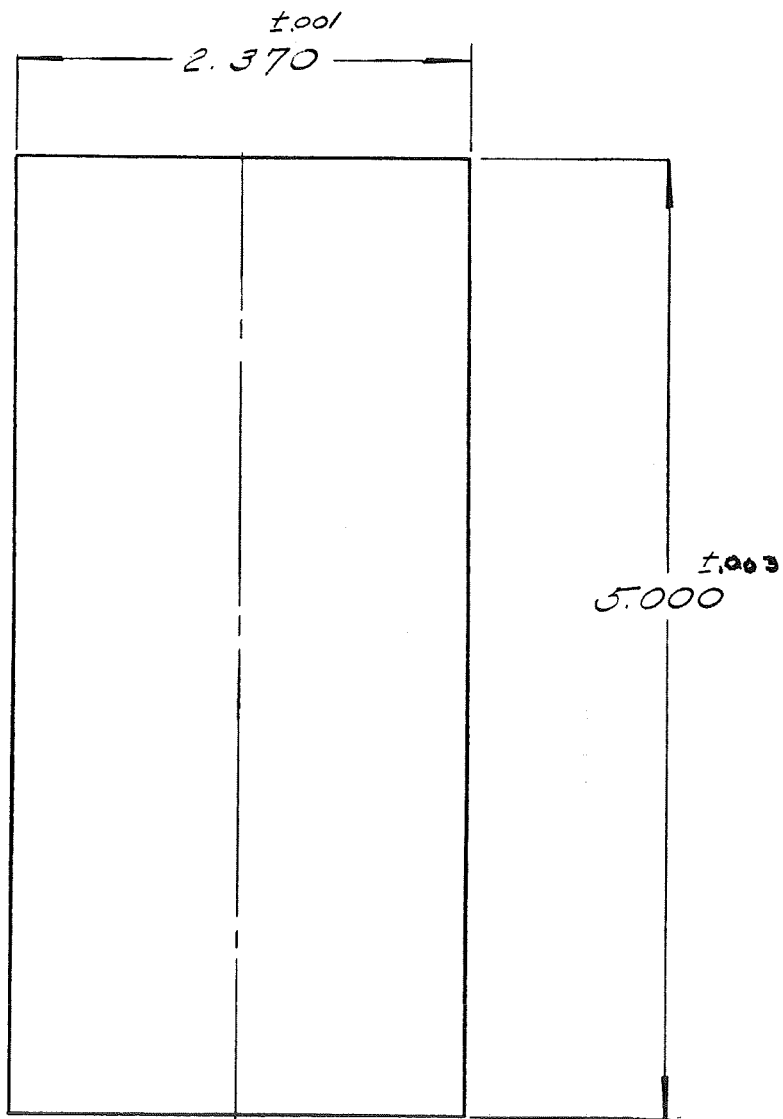
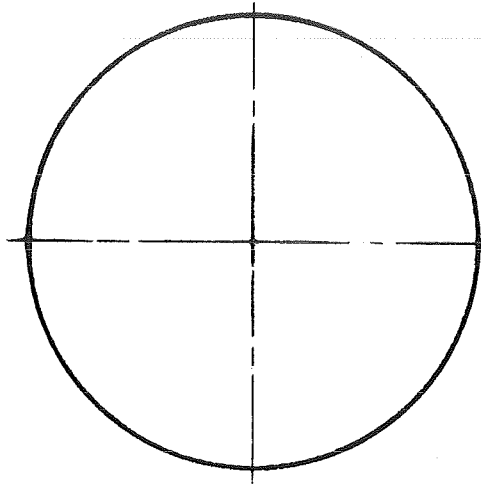
122 - Mica Disc - Mica Thickness
0.003 +0, -0.001



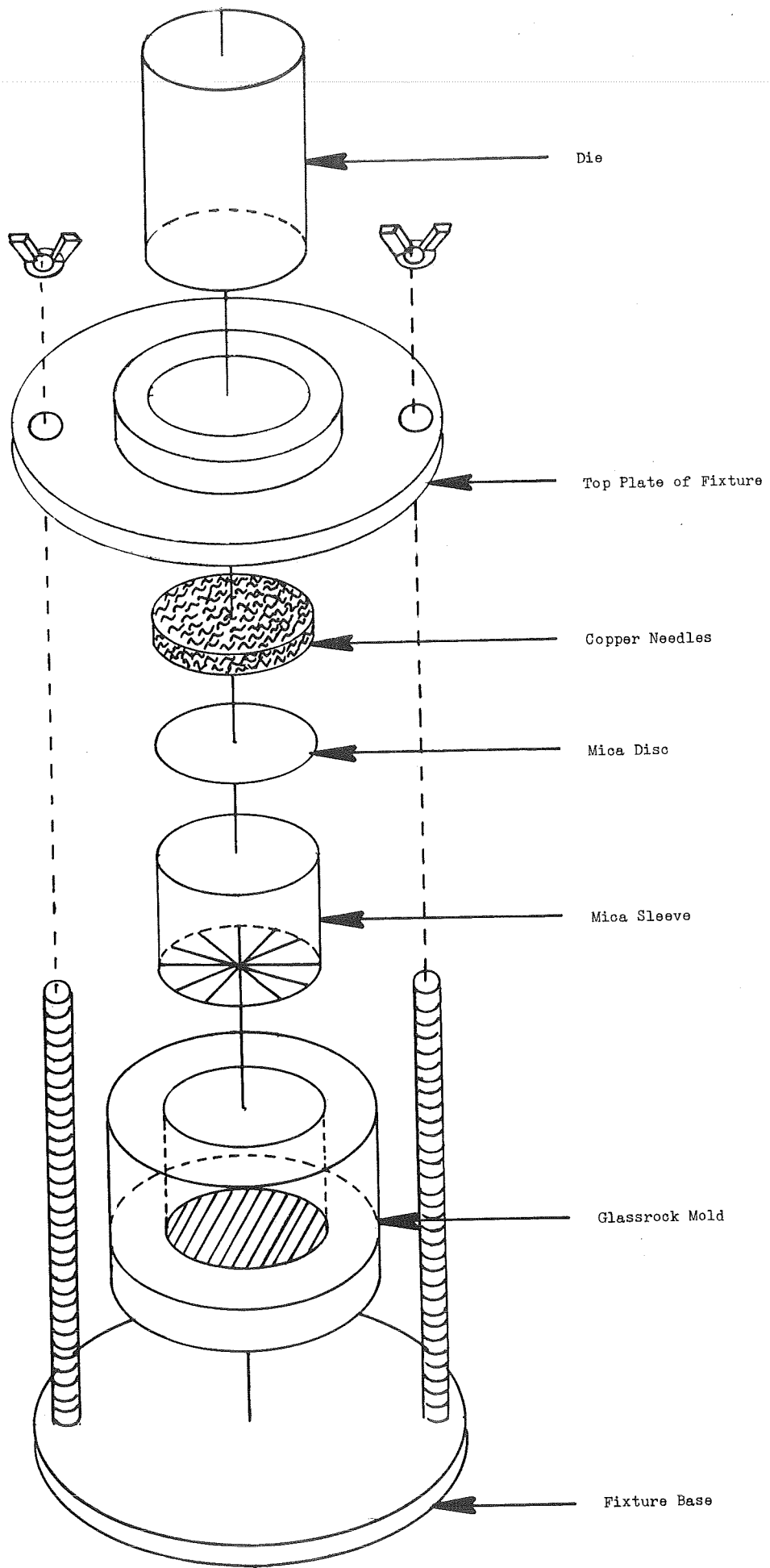
123 - Glass Rock Mold

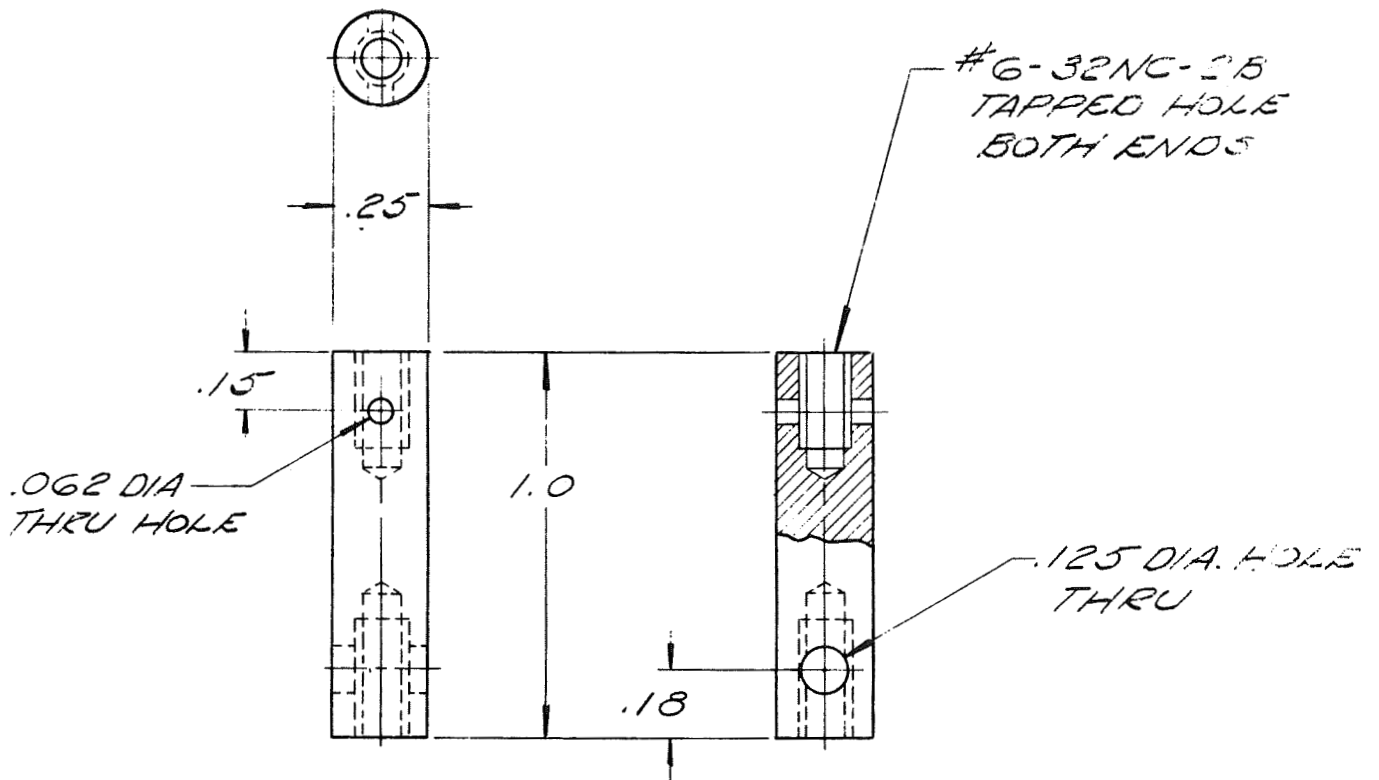


124 - Fixture, Aluminum

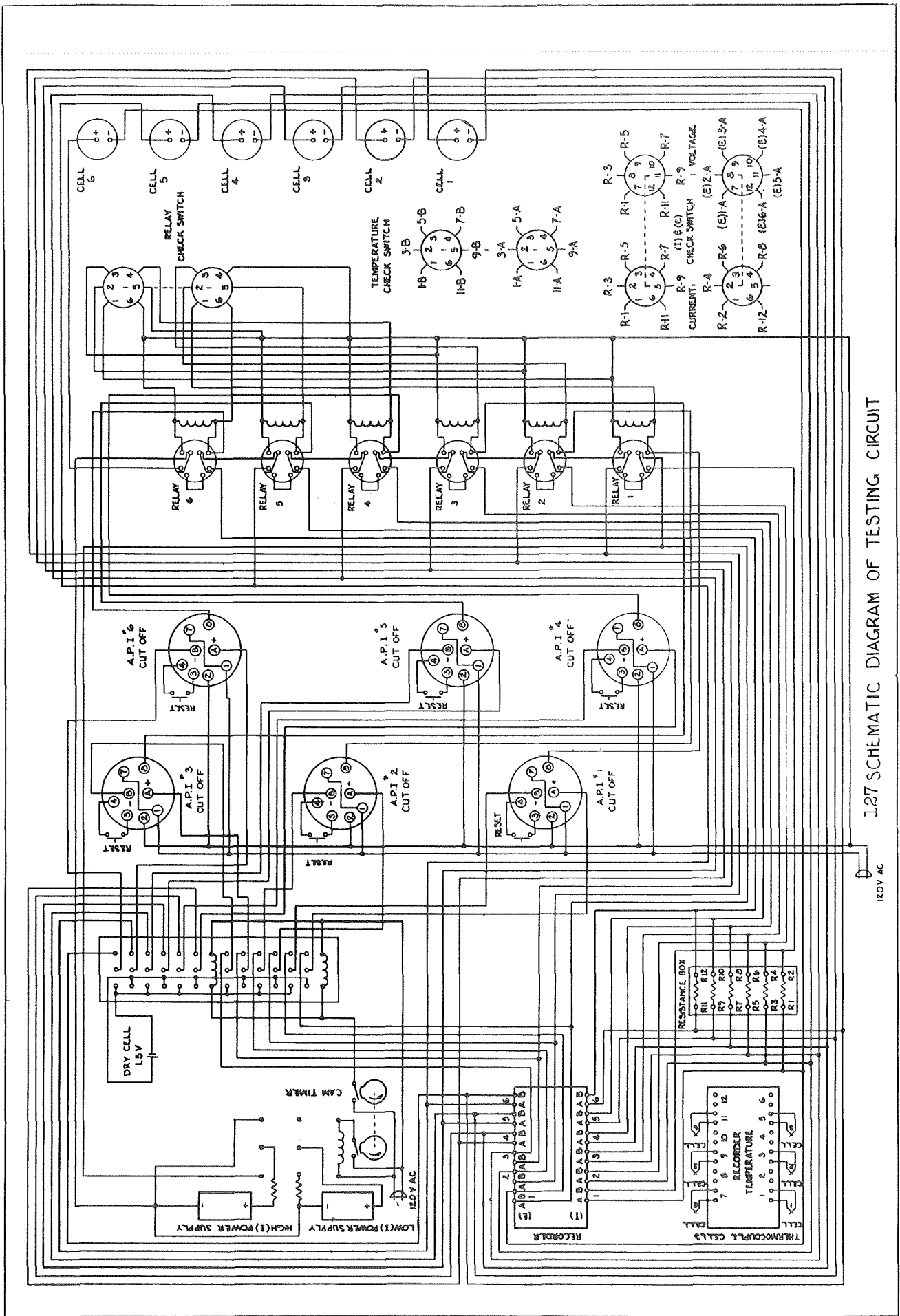


125 - Die, Aluminum





127 - Terminal Connector, Nickel 200 Rod



1.27 SCHEMATIC DIAGRAM OF TESTING CIRCUIT

120V AC

OPERATION SEQUENCES

- 0-1 Trim the height of the case to 3.403 inches per drawing 100.
- 0-2 Counterbore the open end of the case as shown in drawing 100.
- 0-3 Flatten the bottom of the case using an Arbor Press. This is done to insure a flat surface for the counterbore which accepts the terminal seal. If the counterbore is not flat, the terminal seal will not fit properly.
- 0-4 Shear the nickel sheet into 2.750 inch squares.
- 0-5 Stamp out a 2.60 inch disc from each square.
- 0-6 Deburr the cover. Degrease the cover in vapors of hot trichloroethylene.
- 0-7 Machine the case cover so that it is a press fit in the counterbore.
- 0-8 Counterbore the case bottom to match the terminal seal (see drawings 102 and 103). Make the edges of the counterbores as sharp as possible to facilitate welding the seal to the case bottom. Match the seal to the counterbore.
- 0-9 Drill a 0.109 inch hole in the case bottom as shown in drawing 102.
- 0-10 Deburr the counterbore, hole, and cover.
- 0-11 Degrease the can, cover, and seal in vapors of hot trichloroethylene. Etch number on matched case and case cover.
- 0-12 Cut the nickel rod into 1.000 inch pieces.
- 0-13 Trim the O.D of the rod to 0.109 inches except for a 0.032 inch portion of the length. Taper this portion so that the O.D of the rod goes from 0.109 inches to 0.125 inches (see Drawing 104).
- 0-14 Degrease the terminal pin in vapors of hot trichloroethylene.
- 0-15 Cut the magnesium rod into a disc 0.633 inches thick. Face the top and bottom of the disc (see Drawing 106).
- 0-16 Degrease the magnesium disc in vapors of hot trichloroethylene.
- 0-17 Drill a hole in the anode using a number 17 drill. Hole depth = 0.250 inches.
Tap the hole using a 10-24 NC flat bottom tap (see Drawing 106).
Weigh the anode.

- 0-18 Machine the nickel rod per drawing 105. Cut the rod into 2.321 inch pieces. Trim the O.D. as shown. Make sure that the 0.250 inch portion above the threads forms a shoulder against which the anode can be tightened.
- 0-19 Deburr and degrease the connector in vapors of hot trichloroethylene.
- 0-20 Screw the anode connector into the anode. Secure the anode in a vise. Use pliers to tighten the assembly until the surface of the anode is flush with the shoulder of the connector.
- 0-21 Cut three pieces of Varglas sleeving. The sleeving is received in three diameters:

<u>Size No.</u>	<u>Inner Diameter, Inches</u>
5	0.182 - 0.198
6	0.162 - 0.178
7	0.144 - 0.158

Cut a 1.25 inch piece of each size of sleeving.

- 0-22 Form a three-layer single sleeve from the pieces. Slide the No. 7 piece of sleeving over the 0.155" diameter of an anode connector. Then, slide the next two pieces over the connector. Remove the sleeve from the connector.
- 0-23 Insert the anode connector into the anode connector sleeve.
- 0-24 Cut two discs from the roll of Hesson "B" glass tape using a 6 inch diameter template.
- 0-25 Place anode in the center of the separator. Two discs placed on top of one another constitute the separator.
- 0-26 Pull the separator up around the anode. Gather the excess glass tape around the base of the anode connector.
- 0-27 Anneal the Duranickel wire. Put the wire into a cold furnace. Turn on the furnace and allow the temperature to reach 1600^oF. Maintain this temperature for two hours. Shut off the furnace and allow it to cool over-night. Remove the material when the furnace has cooled to room temperature.

- 0-28 Wind the wire into a spring on a lathe using a 0.625 inch O.D. metal rod.
- 0-29 Cut the individual coils of the spring.
- 0-30 Open the coil to the dimensions shown on Drawing 109.
- 0-31 Degrease anode connector retainer ring in vapors of hot trichloroethylene.
- 0-32 Attach the separator to the anode connector using the anode connector retainer ring. Cut off the excess glass tape.
- 0-33 Tighten the anode connector retainer ring around the anode connector using hog ring pliers.
- 0-34 Weigh the anode assembly. Record the weight. This weight is important because it will be used to determine the weight of electrolyte in the separator. Assign a number to each anode assembly.
- 0-35 Insert the anode assembly into the case mold (see Drawings 116 and 119). A cell case is used as a mold for casting the salt block. There is no case cover and the seal is silver soldered to the case.
- 0-36 Insert 1.5 inches of the case mold into the heat sink. (see Drawings 117 and 119).
- 0-37 Wrap the remainder of the case mold with 0.062 inch asbestos sheet (see Drawing 119). This operation and the previous one prevent the surface of the salt from freezing first. The heat sink makes the salt in the bottom of the case freeze first. The asbestos wrap makes the remainder of the salt stay molten long enough to saturate the separator.
- 0-38 Clean the salt crushing box (see Photograph 118) with oxalic acid solution. Rinse the solution from the box with cold water; then dry crushing box in an oven.
- 0-39 Set up the salt crushing box on the Denison Press. Screw the ram of the box into the ram of the press. Line up the edges of the ram with the edge of the box.

- 0-40 Break the glass vial away from the LiCl-CKl eutectic salt. Wear rubber gloves. Make sure all glass is separated from the eutectic. All operations using salt will be done in a dry atmosphere (R.H. < 3%).
- 0-41 Place the salt in the box. Crush the salt at 1300 psi on a 3.250 inch ram. Store the salt in sealed jars in a dry room.
- 0-42 Weigh 500 grams of salt into a Vycor beaker.
- 0-43 Place the beaker in a tube furnace which is pre-heated to 500°C. Melt the salt.
- 0-44 When the salt is molten, remove the beaker from the furnace and pour the salt into the case mold using beaker tongs. Pour the salt between the side of the anode and the case wall to prevent damage to the separator.
- 0-45 Cover the open end of the case with 0.062 inch asbestos sheet (see Drawing 119).
- 0-46 Place the heat sink assembly in a vacuum oven while the electrolyte is still molten. Use beaker tongs. Close the oven door, start the vacuum pump and maintain full vacuum for 90 seconds. Vent the oven and remove the assembly.
- 0-47 Add the remainder of the molten salt to the block. By pouring the same weight of salt into the same size mold for each block, uniform salt block size is insured.
- 0-48 Remove the block from the mold. This is done by tapping the case mold slightly until the block is free.
- 0-49 Use a hack saw to trim the excess salt from the block. Trim the salt from the end of the block opposite from the anode connector. Secure the block in a vise. Cut the block to the dimensions shown in Drawing 110. The acceptable range of salt weight is 355.0g - 355.5g.

- 0-50 Seal each salt block in two plastic bags.
- T-1 Pack the components in the carrying case.
Hand-carry or air freight the components to Fusion Labs,
120 Shoemaker Lane, Agawam, Massachusetts 01001.
- 0-51 Unpack all components. Place the salt block into the dry box immediately to prevent absorption of water by the electrolyte.
- 0-52 Clean the counterbore, terminal seal, terminal pin, and case cover in acetone. Make sure all joint areas (see Drawing 111) are free from dust and dirt to insure optimum welding conditions.
- 0-53 Position the terminal seal in the counterbore. Electron beam weld the terminal seal to the cell case. In this operation, the heat from the beam melts the corner of the counterbore. The metal flows into the joint area (see Drawing 111). This method keeps excess heat from reaching the terminal seal and disturbing the braze.
- 0-54 Position the terminal pin in the 0.109 inch hole in the case as shown in Drawing 111. Electron beam weld the terminal pin to the cell case. The tapered end of the pin holds it in place during welding.
- 0-55 Place all of the cases which pass the leak test into the dry box.
- 0-56 Load the salt block into the case using the rubber gloves in the dry box. Make sure the 0.060 inch portion of the anode connector extends beyond the cap of the terminal seal. Make sure the salt block is all the way up into the cell case.
- 0-57 Take the cases out of the dry box which are to be welded next. If any case is not being welded at a given time, it is kept in the dry box because it now contains the electrolyte.
- 0-58 Electron beam weld the anode connector to the terminal seal as shown in Drawing 111.
- 0-59 Form the nickel rod into rings on a lathe by winding it around a metal rod. Cut it into individual open rings. See Drawing 113.

- 0-60 Degrease the ring in vapors of hot trichloroethylene.
- 0-61 Position the cathode retainer ring in the case using vernier calipers. Match the distance from the counterbore step to the top of the ring with the height of each cathode. See Drawings 112, 114, and 115.
- 0-62 Electron beam weld the cathode retainer ring to the cell case as shown in Drawing 112. The ring is welded in four positions around its circumference.
- 0-63 Strand the copper wire by winding it around a wooden spindle on a drill press. The strands should be 0.25 inches in diameter and 25 inches long. They are made by cutting the wire away from the spindle. The wire is stranded so that the cutting blade will produce more than one needle per cut.
- 0-64 Cut the wire into 0.125 inch needles using an Artos Model M wire cutter (see Photograph 120). Check the length of the needles periodically with a calibrated microscope. Re-adjust the setting of the cutter when necessary.
- 0-65 Measure the length of a random sample of at least 200 needles using a microscope. All needle length distributions should be such that 90% of the sample has a range of 0.090 to 0.170 inches.
- 0-66 Line the glassrock mold with mica. Cut out the mica sleeve and disc as shown in Drawing 121. Fold the mica sleeve. Place the sleeve into the mold as shown in Drawing 125. Place the disc into the sleeve as shown in Drawing 125. The mica makes the cathode easy to remove after sintering.
- 0-67 Position the glassrock mold in the center of the fixture (see Drawings 123 and 125). Insert the die (see Drawing 124) through the top plate of the fixture as shown in Drawing 125. Center the mold and die in the fixture such that the die will rotate in the mold. Tighten the top plate of the fixture against the mold with the wing nuts.

- 0-68 Weigh 72.7 grams of copper needles and pour them into the mold. Make sure that they are evenly distributed in the mold.
- 0-69 Insert the die (see Drawing 124) into the mold and rotate it on the surface of the needles. All of these operations and tools are necessary to make the top of the cathode parallel with the bottom. This in turn insures proper fit against the cathode retainer ring and good contact with the case cover.
- 0-70 Remove the die from the mold. Remove the mold from the fixture by loosening the wing nuts (see Drawing 125).
- 0-71 Place the mold in a preheated muffle furnace for 2 hours at 650°C. During this period, the needles are sintered into a rigid disc.
- 0-72 Remove the mold from the furnace and allow it to cool to room temperature.
- 0-73 Slide the mica sleeve containing the cathode out of the mold. Unwrap the mica from around the cathode (see Drawing 125).
- 0-74 Place the cathode on the furnace shelf. The shelf eliminates handling the cathodes with tongs and saves them from excessive weight loss.
- 0-75 Place the shelf in the furnace pre-heated to 650°C. Connect the air flow and check to see that the flow rate is set at 4 liters/minute. Allow the cathode to oxidize for five days.
- 0-76 Remove the shelf from the furnace. Allow the cathode to cool. Weigh the cathode. (See Drawing 114)
- 0-77 If the cathode is below the weight range shown on Drawing 114, place it back on the shelf. Place the shelf back into the furnace, re-connect the air flow, and re-oxidize the cathode.
- 0-78 Re-weigh the cathode 24 hours later.
- 0-79 Place the cathode on the cathode retainer ring. Center the cathode with respect to the center of the case (see Drawing 115).
- 0-80 Press the cover into the counterbore of the case. Electron beam weld the cover to the case (see Drawing 111).

- T-2 Pack the completed cell into carrying case.
 Hand carry or air freight the cell to Catalyst Research Corp.,
 Baltimore, Md.
- T-3 Hand carry the cell to Penniman and Browne, Inc., Baltimore, Md.
 for X-ray. X-ray the cell such that the view is as shown in
 Drawing 114. Hand carry the cell to Catalyst Research Corp.
- O-81 Weigh the entire cell (Drawing 114). Record the weight.

TESTING PROCEDURES

1. Receive the cell from final assembly. Clean the anode and cathode terminals with steel wool to assure good electrical contact.
2. Locate a chromel-alumel thermocouple at each cell position in the oven and connect to the circuitry.
3. Run two 16 gauge nickel 200 wires insulated with Varglas sleeving, size 16, type H.O., from the cell position in the oven to the circuitry and connect.
4. Screw the connector pin, (see Drawing 126), to the cathode and anode terminals.
5. Place the cell into the Blue M oven (see Photograph 128). Each cell is contained in a 400 ml. beaker which collects any leakage of electrolyte from the cell.
6. Connect the two 16 gauge nickel wires to the terminal pins. Wrap the chromel-alumel thermocouple wire around the pyrex beaker and position the thermocouple junction between the cell case and the inside diameter of the beaker. The maximum number of cells that can be tested simultaneously is four.
7. Close the oven door. (For N_2 atmosphere testing only: Flush the oven chamber with N_2 at a rate of 60 CFH for 30 minutes. Then, reduce the flow to 30 CFH).
8. Set the Blue M temperature controller to the test temperature. Turn on the potential, current, and temperature recorders.
9. Allow the cell to remain on open circuit for 1 hour after it reaches the test temperature.
10. Turn on the cut-off control and the current drain circuit. This completes the "start-up" procedure. After this procedure is completed, the test is completely under the control of the electronic test equipment.

The testing circuitry has the following capabilities:

- a) Record potential (volts of each cell.)

- b) Record current (milli-amperes) of each cell.
- c) Record temperature ($^{\circ}\text{C}$) of each cell.
- d) Induce current drain of 278 ma. drain for 54 minutes and 833 ma. for 6 minutes in a continuous cycle.
- e) Electrically extract, automatically, any cell from the circuit with a potential of 0.5 volts or less under a 278 ma. drain.

The test circuit is shown schematically in Drawing 127 and pictorially in Photograph 128.

11. Manually remove from the Blue M oven each individual cell when the test is completed (voltage drops below 0.5 volts under a 278 ma. drain). Allow the cell to cool to room temperature.

12. Hand carry the spent cell to Penniman & Browne, Baltimore, Md. for X-ray. Return X-ray negative and spent cell to C.R.C.

13. Measure resistance between cathode and anode pins to determine if any shorting occurred.

14. Cut the cell open with a hack saw and retrieve the anode. Re-weigh the anode. This weight is used in the performance calculations (see Appendix II, Sample Calculations). Note the condition of the separator.

15. Cross-section the cell with a hack saw and note the expansion of the cathode and the electrolyte distribution. Note any other unusual conditions present in the spent cell, (swelling of the cell case, displacement of the retainer ring, leakage, etc.).

16. Calculate output, anode efficiency, cathode efficiency, and self-discharge current on each spent cell. Record anode capacity, cathode capacity, and cell life.

Section 2

Quality Plan

Inspection Sequence List For Mg/CuO Cell

<u>Drawing Number</u>	<u>Title</u>	<u>Inspection Sequence No.</u>
100	Cell Case - Nickel 200	1
	Nickel 200 Sheet - 0.050 Inches	2
101	Case Cover, Nickel 200	3
103	Terminal Seal - Alite B-50-1	4
100, 102	Cell Case, Nickel 200	5
	Rod, Nickel 200, 0.125 Inches	6
104	Terminal Pin, Nickel 200	7
	Terminal Pin, Nickel 200	8
	Magnesium Rod	9
106	Magnesium Anode	10
	Nickel 200 Rod, 0.25 Inches	11
105	Anode Connector, Nickel 200	12
	Varglas Sleeving, Type H	13
107	Anode Connector Sleeve	14
	Hesgon "B" Glass Tape 6.0 Inches Wide, 0.005 Inches Thick	15
108	Anode Separator, Hesgon "B" Glass Tape	16
	Wire, Duranickel 301	17
109	Anode Connector Retainer Ring, Duranickel 301	18
	Electrolyte, LiCl-KCl Eutectic	19
110	Anode Assembly and Salt Block	20 & 21
	Case Assembly	22
	Rod, Nickel 200, 0.125 inches	23
113	Cathode Retainer Ring, Nickel 200	24

Inspection Sequence List For Mg/CuO Cell - Continued

<u>Drawing Number</u>	<u>Title</u>	<u>Inspection Sequence No.</u>
111, 112 115	Case Assembly	25
	OFHC Copper Wire, B85 Gauge 38	26
	Cathode, CuO Needles	27
114, 121 122	Cathode, CuO Needles	28
115	Case Assembly	29
116, 115	Thermal Cell, Final Assembly	30

The following abbreviations are used in the inspection sequences:

A.Q.L. - Acceptable Quality Limits per MIL Spec. 105

T.I.R. - True Inner Radius

MC - Magnesium - Copper Oxide Cell

D.E. Plug - Double-End Plug

Quality Control

INSPECTION SEQUENCE

MC #1

PART NAME Cell Case, Nickel 200

INSPECTED AT Receiving Inspection

VENDOR

SEQUENCE
REVISION DATE

DRAWINGS
USED

12-1-68

100

OPER. NO.	USE TOOL OR GAGE NUMBER	INSPECTION OPERATION	INSPECTI LEVEL
1	Visual	Vendor's certification required showing compliance to chemical composition.	A.Q.L. Verify
2	Go-No Go Ring Gauge	O.D. of case per drawing	100%
3	Go-No Go Plug Gauge	I.D. of case per drawing	100%

NOTE: "X" DESIGNATES FIXTURE GAGE - 166 -

REJECTIONS MUST BE RECORDED ON THE REVERSE SIDE OF THIS CARD.
SECURE LATEST DRAWING AS PER PURCHASE ORDER OR RECEIVING REPORT.

Quality Control
 Nickel 200 Sheet
 0.050 Inches

INSPECTION SEQUENCE

MC #2

PART NAME

INSPECTED AT Receiving Inspection

VENDOR

SEQUENCE
 REVISION DATE

DRAWINGS
 USED

12-1-68

PER. NO.	USE TOOL OR GAGE NUMBER	INSPECTION OPERATION	INSPECTION LEVEL
1	Visual	Vendor's certification required showing compliance to chemical composition.	A.Q.L. Verify
2	Micrometer	Check thickness per purchase order	100%
3	Visual	Materials and workmanship	100%

NOTE: "X" DESIGNATES FIXTURE GAGE - 167 -

REJECTIONS MUST BE RECORDED ON THE REVERSE SIDE OF THIS CARD.
 SECURE LATEST DRAWING AS PER PURCHASE ORDER OR RECEIVING REPORT.

Quality Control

INSPECTION SEQUENCE

MC #3

PART NAME Case Cover, Nickel 200 INSPECTED AT Receiving Inspectio

VENDOR

SEQUENCE
REVISION DATE

DRAWINGS
USED

12-1-68

101

OPER. NO.	USE TOOL OR GAGE NUMBER	INSPECTION OPERATION	INSPECT LEVEL
1	Micrometer	Check O.D. per Operation #5	A.Q.L. 100%
2	Micrometer	Check thickness per drawing	100%
3	Visual	Material and workmanship	100%

NOTE: "X" DESIGNATES FIXTURE GAGE - 168 -

REJECTIONS MUST BE RECORDED ON THE REVERSE SIDE OF THIS CARD.
SECURE LATEST DRAWING AS PER PURCHASE ORDER OR RECEIVING REPORT.

Quality Control INSPECTION SEQUENCE MC #4
Terminal Seal,
PART NAME Alite B50-1 INSPECTED AT Receiving Inspection

VENDOR _____ SEQUENCE REVISION DATE 12-1-68 DRAWINGS USED 103

PER. NO.	USE TOOL OR GAGE NUMBER	INSPECTION OPERATION	INSPECTION LEVEL
1	Visual	Vendor's certification showing compliance to chemical composition	A.Q.L. Verify
2	Comparator W/Overlay	Check diameters, length and locations per drawing	100%
3	Visual	Material and workmanship	100%

NOTE: "X" DESIGNATES FIXTURE GAGE -169 -
REJECTIONS MUST BE RECORDED ON THE REVERSE SIDE OF THIS CARD.
SECURE LATEST DRAWING AS PER PURCHASE ORDER OR RECEIVING REPORT.

Quality Control

INSPECTION SEQUENCE

MC #5

PART NAME Cell Case, Nickel 200 INSPECTED AT Receiving Inspection

VENDOR

SEQUENCE
REVISION DATE

DRAWINGS
USED

12-1-68

100, 102

OPER. NO.	USE TOOL OR GAGE NUMBER	INSPECTION OPERATION	INSPECT LEVEL
1	Plug Gauge Go-No Go	Counterbore diameter per drawing 100	A.Q.L. 100%
2	Dial Indicator & "V" Block	T.I.R. per drawing 100	100%
3	Dial Indicator and Plate	Height from the bottom of the case to the counterbore step per drawing 100	100%
4	Height Gauge w/Dial Indica- tor	Overall height per drawing 100	100%
5	D.E. Plug	Hole diameter per drawing 102	100%
6	Receiver Gauge or Overlay	Hole locations per drawing 102	100%
7	Vernier Caliper	Counterbore diameter (terminal seal) per drawing 102	100%
8	Bench Compara- tor w/dial indicator	Counterbore depth (terminal seal) per drawing 102	100%
9	Tube Micrometer	Wall thickness (case cover counterbore), per drawing 100	100%
10	Radius Gauge	Radius per drawing 100	100%
11	Visual	Workmanship, Burrs, Foreign Matter, etc.	100%
12	Visual	Check fit of terminal seals in counterbores by snapping the seal into the counterbore.	100%
13	Visual	Check fit of case cover in counterbore by snapping case cover into counterbore.	100%

NOTE: "X" DESIGNATES FIXTURE GAGE - 170 -

REJECTIONS MUST BE RECORDED ON THE REVERSE SIDE OF THIS CARD.
SECURE LATEST DRAWING AS PER PURCHASE ORDER OR RECEIVING REPORT.

Quality Control

INSPECTION SEQUENCE

MC #6

PART NAME

Rod, Nickel 200,
0.125 Inches O.D.

INSPECTED AT Receiving Inspection

VENDOR

SEQUENCE
REVISION DATE

DRAWINGS
USED

12-1-68

SER. NO.	USE TOOL OR GAGE NUMBER	INSPECTION OPERATION	INSPECTION LEVEL
1	Visual	Vendor's certification required showing compliance to chemical composition	A.Q.L. Verify
2	Micrometer	Check O.D. per purchase order	100%
3	Visual	Materials and workmanship	100%

NOTE: "X" DESIGNATES FIXTURE GAGE - 171 -

REJECTIONS MUST BE RECORDED ON THE REVERSE SIDE OF THIS CARD.
SECURE LATEST DRAWING AS PER PURCHASE ORDER OR RECEIVING REPORT.

Quality Control

INSPECTION SEQUENCE

MC #7

PART NAME Terminal Pin, Nickel 200

INSPECTED AT Receiving Inspector

VENDOR

SEQUENCE REVISION DATE

DRAWINGS USED

12-1-68

104

OPER. NO.	USE TOOL OR GAGE NUMBER	INSPECTION OPERATION	INSPECT LEVEL
			A.Q.L
1	Micrometer	Check length per drawing	100%
2	Chamfer Gauge Go-No Go	Check O.D. and length of taper per drawing	100%
3	Micrometer	Check O.D. of rod which is not tapered per drawing	100%
4	Visual	Material and workmanship	100%

NOTE: "X" DESIGNATES FIXTURE GAGE - 172 -

REJECTIONS MUST BE RECORDED ON THE REVERSE SIDE OF THIS CARD.
SECURE LATEST DRAWING AS PER PURCHASE ORDER OR RECEIVING REPORT.

Quality Control

INSPECTION SEQUENCE

MC #8

PART NAME Terminal Pin, Nickel 200

INSPECTED AT Receiving Inspection

VENDOR

SEQUENCE
REVISION DATE

DRAWINGS
USED

12-1-68

PER. NO.	USE TOOL OR GAGE NUMBER	INSPECTION OPERATION	INSPECTION LEVEL
1	Visual	Check fit of terminal pin in 0.109 inch hole in case	A.Q.L. 100%

NOTE: "X" DESIGNATES FIXTURE GAGE - 173 -

REJECTIONS MUST BE RECORDED ON THE REVERSE SIDE OF THIS CARD.
SECURE LATEST DRAWING AS PER PURCHASE ORDER OR RECEIVING REPORT.

Quality Control

INSPECTION SEQUENCE

MC #9

PART NAME Rod, Magnesium,
1.543 Inches

INSPECTED AT Receiving Inspection

VENDOR

SEQUENCE
REVISION DATE

DRAWINGS
USED

12-1-68

OPER. NO.	USE TOOL OR GAGE NUMBER	INSPECTION OPERATION	INSPECT LEVEL
1	Visual	Vendor's certification required showing compliance to chemical composition	A.Q.L. 100%
2	Balance	Check weight per purchase order	100%
3	Visual	Material and workmanship	100%

NOTE: "X" DESIGNATES FIXTURE GAGE - 174 -

REJECTIONS MUST BE RECORDED ON THE REVERSE SIDE OF THIS CARD.
SECURE LATEST DRAWING AS PER PURCHASE ORDER OR RECEIVING REPORT.

Quality Control

INSPECTION SEQUENCE

MC #10

PART NAME Anode, Magnesium

INSPECTED AT Receiving Inspection

VENDOR

SEQUENCE
REVISION DATE

12-1-68

DRAWINGS
USED

106

PER. NO.	USE TOOL OR GAGE NUMBER	INSPECTION OPERATION	INSPECTION LEVEL
			A.Q.L.
1	Micrometer	Check O.D. per drawing	100%
2	Micrometer	Check thickness per drawing	100%
3	Depth Gauge	Thread depth per drawing	100%
4	Thread Gauge	Check threads per drawing	100%
5	Dial Indicator and "V" Block	T.I.R. per drawing	100%
6	Visual	Material and workmanship	100%
7	Balance	Weight per drawing	100%

NOTE: "X" DESIGNATES FIXTURE GAGE - 175 -

REJECTIONS MUST BE RECORDED ON THE REVERSE SIDE OF THIS CARD.
SECURE LATEST DRAWING AS PER PURCHASE ORDER OR RECEIVING REPORT.

Quality Control

INSPECTION SEQUENCE

MO #11

PART NAME Rod, Nickel 200,
0.25 Inches

INSPECTED AT Receiving Inspection

VENDOR

SEQUENCE
REVISION DATE

DRAWINGS
USED

12-1-68

OPER. NO.	USE TOOL OR GAGE NUMBER	INSPECTION OPERATION	INSPECT LEVEL
1	Visual	Vendor's certification required showing compliance to chemical composition.	A.Q.L. Verify
2	Micrometer and Scale	Check O.D. and length per purchase order	100%
3	Visual	Material and workmanship	100%

NOTE: "X" DESIGNATES FIXTURE GAGE - 176 -

REJECTIONS MUST BE RECORDED ON THE REVERSE SIDE OF THIS CARD.
SECURE LATEST DRAWING AS PER PURCHASE ORDER OR RECEIVING REPORT.

Quality Control

INSPECTION SEQUENCE

MC #12

PART NAME Anode Connector, Nickel 200 INSPECTED AT Receiving Inspection

VENDOR

SEQUENCE
REVISION DATE

DRAWINGS
USED

12-1-68

105

PER. NO.	USE TOOL OR GAGE NUMBER	INSPECTION OPERATION	INSPECTION LEVEL
			A.Q.L.
1	Micrometer	Check O.D. per drawing - 3 places	100%
2	Micrometer	Check overall length per drawing	100%
3	Vernier Caliper	Check thread length per drawing	100%
4	Thread Gauge	Check threads (2 places) per drawing	100%
5	Height Gauge	Inspect height to the shoulder (2 places) per drawing	100%
6	Rockwell Tester	Hardness	100%
7	Visual	Material and workmanship	100%

NOTE: "X" DESIGNATES FIXTURE GAGE - 177 -

REJECTIONS MUST BE RECORDED ON THE REVERSE SIDE OF THIS CARD.
SECURE LATEST DRAWING AS PER PURCHASE ORDER OR RECEIVING REPORT.

Quality Control

INSPECTION SEQUENCE

MC #13

PART NAME Sleeving, Varglas Type H

INSPECTED AT Receiving Inspection

DRAWINGS USED

SEQUENCE REVISION DATE

VENDOR

11-7-69

OPER. NO.	USE TOOL OR GAGE NUMBER	INSPECTION OPERATION	INSPECT LEVEL
1	Visual	Vendor's Certification required showing compliance to chemical composition.	A.Q.L. Verify

NOTE: "X" DESIGNATES FIXTURE GAGE - 178 -

REJECTIONS MUST BE RECORDED ON THE REVERSE SIDE OF THIS CARD.
SECURE LATEST DRAWING AS PER PURCHASE ORDER OR RECEIVING REPORT.

Quality Control

INSPECTION SEQUENCE

MC #14

PART NAME Anode Connector Sleeve

INSPECTED AT

DRAWINGS USED

SEQUENCE REVISION DATE

VENDOR

107

11-7-69

NO.	USE TOOL OR GAGE NUMBER	INSPECTION OPERATION	INSPECTION LEVEL
	Visual Vernier Caliper	Material and workmanship Check dimensions per drawing	A.Q.L. 100% 100%

NOTE: "X" DESIGNATES FIXTURE GAGE - 179 -

REJECTIONS MUST BE RECORDED ON THE REVERSE SIDE OF THIS CARD.
 SECURE LATEST DRAWING AS PER PURCHASE ORDER OR RECEIVING REPORT.

Quality Control

INSPECTION SEQUENCE

MC #15

PART NAME Glass Tape, Hesgon B, 6.0" wide INSPECTED AT Receiving Inspection
0.005" thick

DRAWINGS USED

SEQUENCE REVISION DATE

VENDOR

11-7-69

OPER. NO.	USE TOOL OR GAGE NUMBER	INSPECTION OPERATION	INSPECT LEVEL
1	Visual	Vendor's certification required showing compliance to chemical composition.	A.Q.L. Verify

NOTE: "X" DESIGNATES FIXTURE GAGE - 180 -

REJECTIONS MUST BE RECORDED ON THE REVERSE SIDE OF THIS CARD.
 SECURE LATEST DRAWING AS PER PURCHASE ORDER OR RECEIVING REPORT.

Quality Control

INSPECTION SEQUENCE

MC #16

PART NAME Anode Separator, Hesgon "B"
Glass Tape

INSPECTED AT _____

DRAWINGS USED

SEQUENCE REVISION DATE

VENDOR

108

11-7-69

R.	USE TOOL OR GAGE NUMBER	INSPECTION OPERATION	INSPECTION LEVEL
	Visual Vernier Calipers	Materials and workmanship Check thickness per drawing	A.Q.L. 100% 100%

NOTE: "X" DESIGNATES FIXTURE GAGE - 181 -

REJECTIONS MUST BE RECORDED ON THE REVERSE SIDE OF THIS CARD.
 SECURE LATEST DRAWING AS PER PURCHASE ORDER OR RECEIVING REPORT.

Quality Control

INSPECTION SEQUENCE

MC #17

PART NAME Wire, Duranickel 301
0.062 Inches in Diameter INSPECTED AT Receiving Inspection

VENDOR

SEQUENCE
REVISION DATE

DRAWINGS
USED

12-1-68

OPER. NO.	USE TOOL OR GAGE NUMBER	INSPECTION OPERATION	INSPECT LEVEL
1	Visual	Vendor's certification required showing compliance to chemical composition.	A.Q.L. Verify
2	Micrometer	Check O.D. and length per purchase order	100%
3	Visual	Material and workmanship	100%

NOTE: "X" DESIGNATES FIXTURE GAGE - 162 -

REJECTIONS MUST BE RECORDED ON THE REVERSE SIDE OF THIS CARD.
SECURE LATEST DRAWING AS PER PURCHASE ORDER OR RECEIVING REPORT.

Quality Control

INSPECTION SEQUENCE

MC #18

PART NAME

Anode Connector Retainer Ring
Duranickel 301

INSPECTED AT Receiving Inspection

VENDOR

SEQUENCE
REVISION DATE

12-1-68

DRAWINGS
USED

109

SER. NO.	USE TOOL OR GAGE NUMBER	INSPECTION OPERATION	INSPECTION LEVEL
1	Contour Inspection Gauge	Check length and radius of curvature per drawing	A.Q.L. 100%
2	Micrometer	Check rod O.D. per drawing	100%
3	Visual	Material and workmanship	100%

NOTE: "X" DESIGNATES FIXTURE GAGE - 183 -

REJECTIONS MUST BE RECORDED ON THE REVERSE SIDE OF THIS CARD.
SECURE LATEST DRAWING AS PER PURCHASE ORDER OR RECEIVING REPORT.

Quality Control

INSPECTION SEQUENCE

MC #19

PART NAME

Electrolyte
LiCl-KCl Eutectic

INSPECTED AT Receiving Inspection

VENDOR

SEQUENCE
REVISION DATE

DRAWINGS
USED

12-1-68

OPER. NO.	USE TOOL OR GAGE NUMBER	INSPECTION OPERATION	INSPECTI LEVEL
1	Visual	Vendor's certification required showing compliance to chemical composition	A.Q.L.

NOTE: "X" DESIGNATES FIXTURE GAGE - 184 -

REJECTIONS MUST BE RECORDED ON THE REVERSE SIDE OF THIS CARD.
SECURE LATEST DRAWING AS PER PURCHASE ORDER OR RECEIVING REPORT.

Quality Control INSPECTION SEQUENCE MC #20 & 21

PART NAME Anode Assembly and Salt Block INSPECTED AT Assembly Line

VENDOR

SEQUENCE REVISION DATE

DRAWINGS USED

12-1-68

PER. NO.	USE TOOL OR GAGE NUMBER	INSPECTION OPERATION	INSPECTION LEVEL
			A.Q.L.
1	Balance	Check weight of electrolyte in each block	100%
2	Vernier Caliper	Height of salt block	100%
3	Visual	Fit of anode connector in terminal seal cap	100%
4	Visual	Material and workmanship	100%

NOTE: "X" DESIGNATES FIXTURE GAGE - 185 -
REJECTIONS MUST BE RECORDED ON THE REVERSE SIDE OF THIS CARD.
SECURE LATEST DRAWING AS PER PURCHASE ORDER OR RECEIVING REPORT.

Quality Control

INSPECTION SEQUENCE

MC #22

PART NAME Case Assembly INSPECTED AT Fusion Laboratories

VENDOR

SEQUENCE
REVISION DATE

DRAWINGS
USED

12-1-68

Note: Operations are performed at Fusion Labs, 120 Shoemaker Lane, Agawam, Mass. 01001,
by CRC trained representative.

OPER. NO.	USE TOOL OR GAGE NUMBER	INSPECTION OPERATION	INSPECT LEVEL
1	Receiver Gauge	Check location, perpendicularity and length of terminal pin and seal.	A.Q.L. 100%
2	Visual	Workmanship	100%
3	Mass Spectrometer CEC Model 24-120	Leak check (helium leak detector shall have a sensitivity 10^{-8} cc/sec. or better at room temperature.)	100%
4	Visual	Certification required if leak check is performed by outside vendor.	100%

NOTE: "X" DESIGNATES FIXTURE GAGE - 186 -

REJECTIONS MUST BE RECORDED ON THE REVERSE SIDE OF THIS CARD.
SECURE LATEST DRAWING AS PER PURCHASE ORDER OR RECEIVING REPORT.

Quality Control

INSPECTION SEQUENCE

MC #23

PART NAME

Rod, Nickel,
0.125 inches O.D.

INSPECTED AT Receiving Inspection

VENDOR

SEQUENCE
REVISION DATE

DRAWINGS
USED

12-1-68

SER. NO.	USE TOOL OR GAGE NUMBER	INSPECTION OPERATION	INSPECTION LEVEL
1	Visual	Vendor's certification required showing compliance to chemical composition.	A.Q.L. 100%
2	Micrometer	Check O.D. per purchase order	100%
3	Visual	Material and workmanship	100%

NOTE: "X" DESIGNATES FIXTURE GAGE - 187 -

REJECTIONS MUST BE RECORDED ON THE REVERSE SIDE OF THIS CARD.
SECURE LATEST DRAWING AS PER PURCHASE ORDER OR RECEIVING REPORT.

INSPECTION SEQUENCE

MC #24

Quality Control
Cathode Retainer Ring
Nickel 200

PART NAME

INSPECTED AT Receiving Inspection

VENDOR

SEQUENCE
REVISION DATE

DRAWINGS
USED

12-1-68

OPER. NO.	USE TOOL OR GAGE NUMBER	INSPECTION OPERATION	INSPECTOR LEVEL
1	Micrometer	Check O.D. of rod per drawing	A.Q.L. 100%
2	Vernier Caliper	Check O.D. of ring per drawing	100%
3	Visual	Material and workmanship	100%

NOTE: "X" DESIGNATES FIXTURE GAGE - 188 -

REJECTIONS MUST BE RECORDED ON THE REVERSE SIDE OF THIS CARD.
SECURE LATEST DRAWING AS PER PURCHASE ORDER OR RECEIVING REPORT.

Quality Control

INSPECTION SEQUENCE

MC #25

PART NAME Case Assembly INSPECTED AT Fusion Laboratory

VENDOR

SEQUENCE
REVISION DATE

DRAWINGS
USED

12-1-68

111, 112,
115

Note: Operations are performed at Fusion Laboratories, 120 Shoemaker Lane, Agawam, Mass. 01001, by CRC trained representative.

PER. NO.	USE TOOL OR GAGE NUMBER	INSPECTION OPERATION	INSPECTION LEVEL
1	Visual	Verify that the salt block and cathode retainer ring are positioned in case.	A.Q.L. 100%
2	Vernier Caliper	Check dimensions from counterbore to cathode retainer ring per drawing 115.	100%
3	Visual	Check electron beam weld of terminal seal to anode connector per drawing 111.	100%
4	Visual	Check electron beam weld from cathode ring to case per drawing 112.	100%

NOTE: "X" DESIGNATES FIXTURE GAGE - 189 -

REJECTIONS MUST BE RECORDED ON THE REVERSE SIDE OF THIS CARD.
SECURE LATEST DRAWING AS PER PURCHASE ORDER OR RECEIVING REPORT.

Quality Control

INSPECTION SEQUENCE

MC #26

PART NAME Wire, Copper
B & S Gauge 38

INSPECTED AT Receiving Inspection

VENDOR

SEQUENCE
REVISION DATE

DRAWINGS
USED

12-1-68

OPER. NO.	USE TOOL OR GAGE NUMBER	INSPECTION OPERATION	INSPECTIC LEVEL
1	Visual	Vendor's certification required showing compliance to chemical composition.	A.Q.L. Verify
2	Micrometer	Check O.D. of wire per purchase order	100%
3	Visual	Materials and workmanship	100%

NOTE: "X" DESIGNATES FIXTURE GAGE - 190 -

REJECTIONS MUST BE RECORDED ON THE REVERSE SIDE OF THIS CARD.
SECURE LATEST DRAWING AS PER PURCHASE ORDER OR RECEIVING REPORT.

Quality Control

INSPECTION SEQUENCE

MC #27

PART NAME Cathode, CuO Needles

INSPECTED AT Receiving Inspection

VENDOR

SEQUENCE
REVISION DATE

DRAWINGS
USED

12-1-68

PER. NO.	USE TOOL OR GAGE NUMBER	INSPECTION OPERATION	INSPECTION LEVEL
1	Opaque Microscope	Needle size distribution	A.Q.L. 6.5
2	Visual	Check that top of the cathode is parallel with the bottom and that sides are perpendicular after sintering.	100%

NOTE: "X" DESIGNATES FIXTURE GAGE - 191 -

REJECTIONS MUST BE RECORDED ON THE REVERSE SIDE OF THIS CARD.
SECURE LATEST DRAWING AS PER PURCHASE ORDER OR RECEIVING REPORT.

Quality Control

INSPECTION SEQUENCE

MC #28

PART NAME Cathode, CuO Needles INSPECTED AT Assembly Line

VENDOR

SEQUENCE
REVISION DATE

DRAWINGS
USED

12-1-68

121, 122,
114

OPER. NO.	USE TOOL OR GAGE NUMBER	INSPECTION OPERATION	INSPECT LEVEL
1	Visual	Check dimensions of mica parts and glass rock mold per drawings 121 and 122.	A.Q.L. 100%
2	Visual	Verify oven setting and gas flow	100%
3	Visual	Verify time cathode is in oven	100%
4	Micrometer and Go-No Go Gauge	Check thickness and O.D. per drawing 114.	100%
5	Balance	Weight of cathode per drawing 114.	100%
6	Visual	Workmanship	100%

NOTE: "X" DESIGNATES FIXTURE GAGE - 192 -

REJECTIONS MUST BE RECORDED ON THE REVERSE SIDE OF THIS CARD.
SECURE LATEST DRAWING AS PER PURCHASE ORDER OR RECEIVING REPORT.

Quality Control

INSPECTION SEQUENCE

MC #29

PART NAME Case Assembly INSPECTED AT Fusion Laboratory

VENDOR

SEQUENCE
REVISION DATE

DRAWINGS
USED

12-1-68

115

Note: Operations are performed at Fusion Laboratories, 120 Shoemaker Lane, Agawam, Mass. 01001, by CRC trained representative.

PER. NO.	USE TOOL OR GAGE NUMBER	INSPECTION OPERATION	INSPECTION LEVEL
1	Visual	Verify that cathode is placed in case and is flush against the cathode retainer ring per drawing 115.	AQL 100%
2	Visual	Verify that case cover is in counterbore and is tight against the cathode per drawing 115.	100%

NOTE: "X" DESIGNATES FIXTURE GAGE - 193 -

REJECTIONS MUST BE RECORDED ON THE REVERSE SIDE OF THIS CARD.
SECURE LATEST DRAWING AS PER PURCHASE ORDER OR RECEIVING REPORT.

Quality Control

INSPECTION SEQUENCE

MC #30

PART NAME Thermal Cell,
Final Assembly

INSPECTED AT Assembly Line

VENDOR

SEQUENCE
REVISION DATE

DRAWINGS
USED

12-1-68

115

OPER. NO.	USE TOOL OR GAGE NUMBER	INSPECTION OPERATION	INSPECT LEVEL
1	Go-No Go Ring Gauge	Check O.D. per drawing	A.Q.L. 100%
2	Height Gauge w/dial indicator	Check case height per drawing	100%
3	Height Gauge w/dial indicator	Check length of terminal pin to bottom of case per drawing	100%
4	Height Gauge w/dial indicator	Check length of anode connector to bottom of case per drawing	100%
5	Visual	Material and workmanship	100%
6	Visual	Gross damage due to rough handling	100%
7	Visual	Ceramic seal damage	100%
8	Visual	Check case marking	100%
9	Balance	Weigh each unit and record	100%
10	Ohmmeter	Measure resistance from terminal pin to terminal cap of seal.	100%
11	Visual	Check electrode separation, position of components, and presence of voids in electrolyte (x-ray plate from T-3 on chart).	100%

NOTE: "X" DESIGNATES FIXTURE GAGE - 194 -

REJECTIONS MUST BE RECORDED ON THE REVERSE SIDE OF THIS CARD.
SECURE LATEST DRAWING AS PER PURCHASE ORDER OR RECEIVING REPORT.

MATERIAL SPECIFICATIONS

1. Nickel 200

Ni	99.5%	C	0.05%
Mn	0.25%	Fe	0.15%
S	0.005%	Si	0.05%
Cu	0.05%		

2. Magnesium

Mg	99.8%	Mn	0.15% Max.
Pb	0.01% Max.	Sn	0.01% Max.
Ni	0.001% Max.	Other Impurities	0.05%
Cu	0.02% Max.	Total Impurities	0.2%

3. Nickel Alloy - Duranickel 301

Ni	94.0%	Mn	0.25%
C	0.15%	S	0.005%
Fe	0.15%	Cu	0.05%
Al	4.50%	Ti	0.50%

4. B & S Gauge 38 Standard Copper Wire (Alloy CDA-110)

99.9% pure copper, min.

0.04% O₂, max.

0.06% Trace elements that cannot be determined.

5. Electrolyte

59 mole % LiCl

41 mole % KCl

Glass Tape

Varglas Type H

The material has no polarographic waves less than 2.6 volts versus a 0.1 m. Pt (II)/Pt reference electrode. Residual current less than six micro-amperes at 2.5 volts versus the same reference electrode.

6. Hesgon "B" Glass Tape and Varglas Sleeving Type "H"

Owens-Corning Fiberglas - "E" *

SiO ₂	52% - 56%	Na ₂ O & N ₂ O	0 - 1%
CaO	16% - 25%	MgO	0 - 6%
Al ₂ O ₃	12% - 16%		
B ₂ O ₃	8% - 13%		

*Textile Fiber Materials For Industry, Owens - Corning Fiberglas Corp.,

Pub. No. 1-GT-1375-A, p. 10

MATERIALS AND VENDORS

<u>Material</u>	<u>Vendor</u>
Nickel 200 sheet (0.050")	Whitehead Metals
Nickel 200 rod (0.125" O.D.)	1720 Whitehead Road
Nickel 200 rod (0.250" O.D.)	Baltimore, Md. 21207
Duranickel 301 rod (0.062" O.D.)	
Standard Copper Wire - B & S Gauge 38	
Ceramic Seals	Alite Division of Norton Industries
Alite B-50-1	Box 119 Orville, Ohio 44667
Magnesium Rod (1.543" O.D.)	Dow Chemical Co., Inc. 400 Market St. Camden, New Jersey
Fused LiCl-KCl Electrolyte	Anderson Physics Laboratory 609 S. 6th Street Champaign, Illinois 61824
Nickel 200 Can	Maryland Metal Spinning 5219 Fairlawn Avenue Baltimore, Md. 21215
Varglas Sleeving Type "H"	Varflex Corporation Rome New York 13440
Glass Tape, Hesgon "B"	Hess, Goldsmith, & Company Division of Burlington Industries 1450 Broadway New York, New York 10018